The Role of miR-21 and miR-499 in Head and Neck Cancer

Pamela Alero Ajuyah

This thesis is submitted in fulfilment of the requirements for the degree of Doctor of Philosophy, School of Life Sciences, The University of Technology, Sydney.

August, 2016

Supervisor: Dr. Nham Tran

Associate Supervisor: A/Prof. Gyorgy Hutvagner

Declaration

I hereby state that all the investigations presented in this thesis were carried out under the supervisions of Dr. Nham Tran and A/Prof. Gyorgy Hutvagner. This thesis incorporates original research which has not been previously submitted for a higher degree to any other institution. The experimental investigations and analysis described in this thesis were completed by me, except were assistance has been duly acknowledged and reference has been made in the text.

Pamela Ajuyah **Date:**

Acknowledgements

It has been a long journey. I have learnt so much about myself and strangely enough microRNAs along the way. I have had a unique and interesting PhD experience and I have many people to thank for that. I would like to start off by thanking both my supervisors.

To my primary supervisor Dr. Nham Tran who personally taught me all the basic molecular techniques required to become a versatile scientist. The hours you spent coaching me to become a great presenter paid off too as not only did I lose my fear of public speaking, I actually enjoy it now. I greatly appreciate your time and effort without which I wouldn't be the scientist I am today.

To my co-supervisor A/Prof. Gyorgy Hutvanger whose vast knowledge and experience in the microRNA field was admirable and inspirational to me. Your unwavering support helped me get through the finish line.

I would like to thank a couple of key researchers in UTS whose contributions at certain points of my PhD gave continued momentum to my project. Dr. Michael Johnson for the hours you spent helping me set up and analyse my scratch assays with absolutely nothing expected in return – that is rare in today's world. To Joyce To who sat behind me in the lab so I could always run to you for experimental insight and great conversations – your final piece of advice was what I needed to finish up my proliferation experiments.

I would like to thank the other PhD students at UTS including the students in my office who provided years of laughter and interesting times. I especially thank my now good friends who I met at UTS – Rob, Sam, Elliot, Marty and Peter. You guys served the dual purpose of not only being awesome friends but also sharing great technical advice based on your experiences in the lab.

I have to thank Jimmy and Roxby, past lab members with whom I shared countless 10 pm finishes in the lab with. The companionship made the hours fly by!

A big shout out to my best friends – Alvina, Roro, Jules, Marisa and Loraine. Honestly you girls were such strong emotional pillars of support for me and I have to thank all of you for the endless phone calls, DNMs and being the best type of friends a girl could ask for.

My gratitude to UTS for an APA scholarship and TCRN for an additional scholarship top up, both were essential for survival throughout my PhD and allowed me to focus on my research without worrying about finances.

Finally and most importantly, I thank my family. My sister Josephine and my little brother Hansel for always being supportive no matter what was going on in their lives. My father Asifo for being the ultimate role model not just as a father but also as a scientist. And my mother Pauline for the constant encouragement and almost daily phone calls. Thank you both for being there when I needed you the most.

Abstract

Globally there are more than half a million new cases of head and neck cancer each year [1,2]. More than 90% of head and neck tumours are head and neck squamous cell carcinomas (HNSCCs) which originate in the lip/oral cavity, nasopharynx, oropharynx, hypopharynx and the larynx [1,3].

HNSCCs are inadequately diagnosed and as a result many head and neck cancer patients are diagnosed at the advanced stages of the disease [4]. The lack of biomarkers for HNSCC has resulted in this poor diagnosis of the cancer. Furthermore, a limited understanding of the molecular biology of the cancer has led to few treatment options. The future of HNSCC diagnosis and treatment can lie in the small non-coding RNAs called miRNAs. miRNAs function as gene regulators and have been implicated in the development and progression of various cancers [5-8]. In HNSCC, two miRNAs miR-21 and miR-499 have been found to be upregulated in tumours compared to normal tissues [9]. Furthermore, these miRNAs both regulate the tumour suppressor gene Programmed Cell Death 4 (PDCD4). PDCD4 has been found to be involved in oncogenic pathways including apoptosis, proliferation, angiogenesis and invasion [10,11]. PDCD4 is also downregulated in many HNSCC tumours [12-14]. This thesis endeavoured to determine the role of miR-21 and miR-499 in HNSCC through their regulation of PDCD4.

The first aim was to study the co-regulation of PDCD4 by miR-21 and miR-499. When genes are co-regulated by miRNAs this can lead to heavy regulation of the genes [15]. This is essential for genes critical to cancer initiation and progression [15]. Currently there are limited studies examining the various modes of regulation miRNAs can use to simultaneously regulate a single gene at its 3´ untranslated region (3´UTR). In this project, site mutants for miR-21 and miR-499 at the 3´UTR of PDCD4 were created and ligated to luciferase reporter vectors. Using luciferase assays it was revealed that miR-21 and miR-499 regulate the 3´UTR independently of each other. However,

miR-21 does aid miR-499 interactions with the PDCD4 3´UTR. Furthermore, the last two miR-499 sites are regulated in a co-dependent manner and mutating either site completely abolishes regulation of PDCD4 by miR-499. This is the first study detailing the regulatory dynamics of PDCD4.

The co-regulation of PDCD4 by miR-21 and miR-499 has an extra layer of complexity in that the miRNAs also have a regulatory relationship with each other. Overexpression of miR-21 was found to endogenously upregulate miR-499 expression in cells. There are few studies in the literature on miRNA mediated regulation of another miRNA. These studies show that miRNA mediated regulation usually occurs when a miRNA(s) has a binding site in the primary transcript of another miRNA or at the promoter region of the mature miRNA [16-18]. Further research into miR-21's upregulation of miR-499, found that the regulation was not reciprocal as overexpression of miR-499 did not affect miR-21 levels. A few models were designed and tested to investigate how miR-21 was able to regulate miR-499. Primary levels of miR-499 were unchanged by miR-21 overexpression. Thus regulation of miR-499 by miR-21 occurred post-transcription. The stability of miR-499 was measured when *de novo* synthesis of miRNAs was switched off. miR-499 was found like other miRNAs to degrade over 24 hours. However, if miR-21 was overexpressed in cells then miR-499 levels were stabilised. It was thought that perhaps miR-21 is able to stabilise miR-499 through target-mediated miRNA protection (TMMP). In this model the half-life of a miRNA can be increased by its interactions with a target mRNA [19,20]. It is predicted that through a gene like PDCD4 miR-21 is able to encourage miR-499 interactions with the gene. Perhaps miR-21 binding removes obtrusive secondary structure at the miR-499 binding sites on the 3´UTR. This allows miR-499 to interact with the gene thus protecting it from degradation.

A few studies have found that a single miRNA is able to alter the expression of multiple miRNAs [21,22]. However, the mechanism behind this or even if this is a common occurrence with miRNAs in general is still yet to be understood.

Therefore, the regulation of miR-499 by miR-21 was extended genome-wide to determine if other miRNAs were also affected by miR-21 overexpression. Affymetrix arrays revealed that not only were many miRNAs upregulated by miR-21 overexpression but also downregulated. Furthermore, miR-499 overexpression could also differentially regulate other miRNAs. The miRNAs that were most upregulated by miR-21 were found to have targets that could potentially be co-targeted by several of these miRNAs. miR-21 and miR-499 also had genes that they could potentially co-target together. Therefore, perhaps miRNAs that are regulated by other miRNAs are involved in regulating similar genes leading to an enhanced or differential regulation of these genes.

Finally, the function of miR-21 and miR-499 in HNSCCs were examined. miR-21 is involved in certain oncogenic pathways in HNSCCs [23,24], but no studies have investigated miR-499's role. Considering that miRNAs are at the forefront of gene dysregulation during cancer initiation and development [25-28], it is worth understanding how they are able to affect cancerous processes. This is useful for the identification of new biomarkers for HNSCC but also for the design of miRNA based therapeutics.

Using live cell imaging and scratch assays, it was found that miR-21 and miR-499 were able to promote migration in HNSCCs. It is predicted that this promoted migration most likely occurs through the downregulation of the tumour suppressor genes PDCD4, SRY (Sex Determining Region Y) Box 6 and Forkhead Box Protein 04 (FOXO4). These genes have been shown in other cancers to be directly involved in migration [29-31].

This thesis explores in depth the regulation of the tumour suppressor gene PDCD4 by miR-21 and miR-499 in a HNSCC context. It uncovers the type of regulation this gene undergoes, the relationship between the two miRNAs and other miRNAs and the function of these miRNAs in HNSCC. Studies such as these pave the way for designing new clinical therapeutics by

understanding the molecular aberrations that lead to head and neck cancer development.

Publications and abstracts associated with this thesis

Publications arising from this thesis

P Ajuyah., A Ahadi., J Lu., G Hutvagner., N Tran (2016) The unique co-regulation of the tumour suppressor gene PDCD4 by miR-21 and miR-499. *In Preparation.*

Abstracts associated with this thesis

P Ajuyah., G Hutvanger., N Tran (2015) The unique co-regulation of the tumour suppressor gene PDCD4 by miR-21 and miR-499. ICEI Conference, Shenzhen, China. April 18-20.

P Ajuyah., G Hutvanger., N Tran (2014) The unique co-regulation of the tumour suppressor gene PDCD4 by miR-21 and miR-499. New Horizons Conference. The Kolling Institute of Medical Research, Sydney, Australia. November 17-19.

P Ajuyah., G Hutvanger., N Tran (2014) The unique co-regulation of the tumour suppressor gene PDCD4 by miR-21 and miR-499. JaJRNA Conference. The University of Technology, Sydney, Australia. November 2-5.

P Ajuyah., G Hutvanger., N Tran (2014) The unique co-regulation of the tumour suppressor gene PDCD4 by miR-21 and miR-499. Lorne Genome Conference. Mantra Lorne, Australia. February 16-18.

P Ajuyah., G Hutvanger., N Tran (2014) The unique co-regulation of the tumour suppressor gene PDCD4 by miR-21 and miR-499. RNAUK 2014 Conference. Windermere, UK. January 24-26.

P Ajuyah., G Hutvanger., N Tran (2014) The unique co-regulation of the tumour suppressor gene PDCD4 by miR-21 and miR-499. RNA Silencing Keystone Symposia. Seattle, USA. January 31 – February 5.

P Ajuyah., G Hutvanger., N Tran (2013) The unique co-regulation of the tumour suppressor gene PDCD4 by miR-21 and miR-499. Scientific Research Meeting. The Kolling Institute of Medical Research. Sydney, Australia. November 18-20.

P Ajuyah., G Hutvanger., N Tran (2012) The unique co-regulation of the tumour suppressor gene PDCD4 by miR-21 and miR-499. Scientific Research Meeting. The Kolling Institute of Medical Research. Sydney, Australia. November 20-21.

P Ajuyah., G Hutvanger., N Tran (2012) The unique co-regulation of the tumour suppressor gene PDCD4 by miR-21 and miR-499. Networks in the Life Sciences. 14th International EMBL PhD Symposium. Heidelberg, Germany. October 25-27.

Table of Contents

List of Figures

List of Tables

Abbreviations

actD	actinomycin D
bp	base pair
BOT	base of tongue
CDS	coding sequence
CMM	cooperative miRNA module
DC	double transfection control siRNA
DK	double transfection siAgo2
DMEM	dulbecco's modified eagle medium
DMSO	dimethyl sulfoxide
DNA	deoxyribonucleic acid
dNTPs	deoxynucleotides
ECL	enhanced chemiluminescence
EMT	epithelial-mesenchymal transition
FBS	fetal bovine serum
FOM	floor or mouth
FOXO4	forkhead box protein 04
GAPDH	glyceraldehyde 3-phosphate dehydrogenase
HITS-CLIP	high-throughput sequencing of RNA isolated by crosslinking immunoprecipitation
HNSCC	head and neck squamous cell carcinoma
HPV	human papillomavirus
KD	knock down
KO	knock out
LB	luria-bertani
MAP4K1	mitogen-activated protein kinase kinase kinase kinase 1
miRNA	microRNAs
ncRNA	non-coding RNA
NEB	new england biolabs
nt	nucleotide
oncomiRs	oncogenic miRNAs

ORF	open reading frame
OSCC	oral squamous cell carcinoma
PAR-CLIP	photoactivatable ribonucleoside–enhanced cross-linking and immunoprecipitation
PBS	phosphate buffered saline
PCR	polymerase chain reaction
PDCD4	programmed cell death 4
piRNA	piwi-interacting RNAs
pri-miRNA	primary miRNA
qPCR	quantitative real-time PCR
RISC	RNA induced silencing complex
RNA	ribonucleic acid
RNA pol II	RNA polymerase II
SC	single transfection control siRNA
SDS	sodium dodecyl sulfate
SEER	surveillance, epidemiology and end results
shRNA	short hairpin RNA
siAgo2	ago2 specific targeting siRNA
siRNA	short interfering RNA
SK	single transfection siAgo2
SNP	single nucleotide polymorphism
SOX6	SRY (sex determining region Y) box 6
TMMP	target-mediated miRNA protection
UTR	untranslated region
WT	wild type

Chapter 1: Introduction

1.1. Introduction of head and neck tumours

Worldwide there are about 644,000 cases of head and neck cancer arising each year with two-thirds of these cases emerging from developing countries [1,2]. Head and neck cancer consists of a heterogeneous combination of cancers associated with different sub-sites of the head and neck region [1]. The heterogeneity of the cancer makes determination of an accurate prognosis, treatment and identifying causative genes difficult (as reviewed in Leemans et al., [3]). Prognosis of head and neck cancer patients is poor because of the inconsistencies of tumour biological behaviour across the various sites and an insufficient staging system [32]. Matters are further complicated because of varying classification of these tumours across the literature. Consequently, it is difficult to make consistent comparisons between studies [33,34].

1.1.1. Head and neck squamous cell carcinoma

More than 90% of head and neck cases are head and neck squamous cell carcinomas (HNSCCs) and are found in the lip/oral cavity, nasopharynx, oropharynx, hypopharynx and the larynx as illustrated in Figure 1.1 below [1,3].

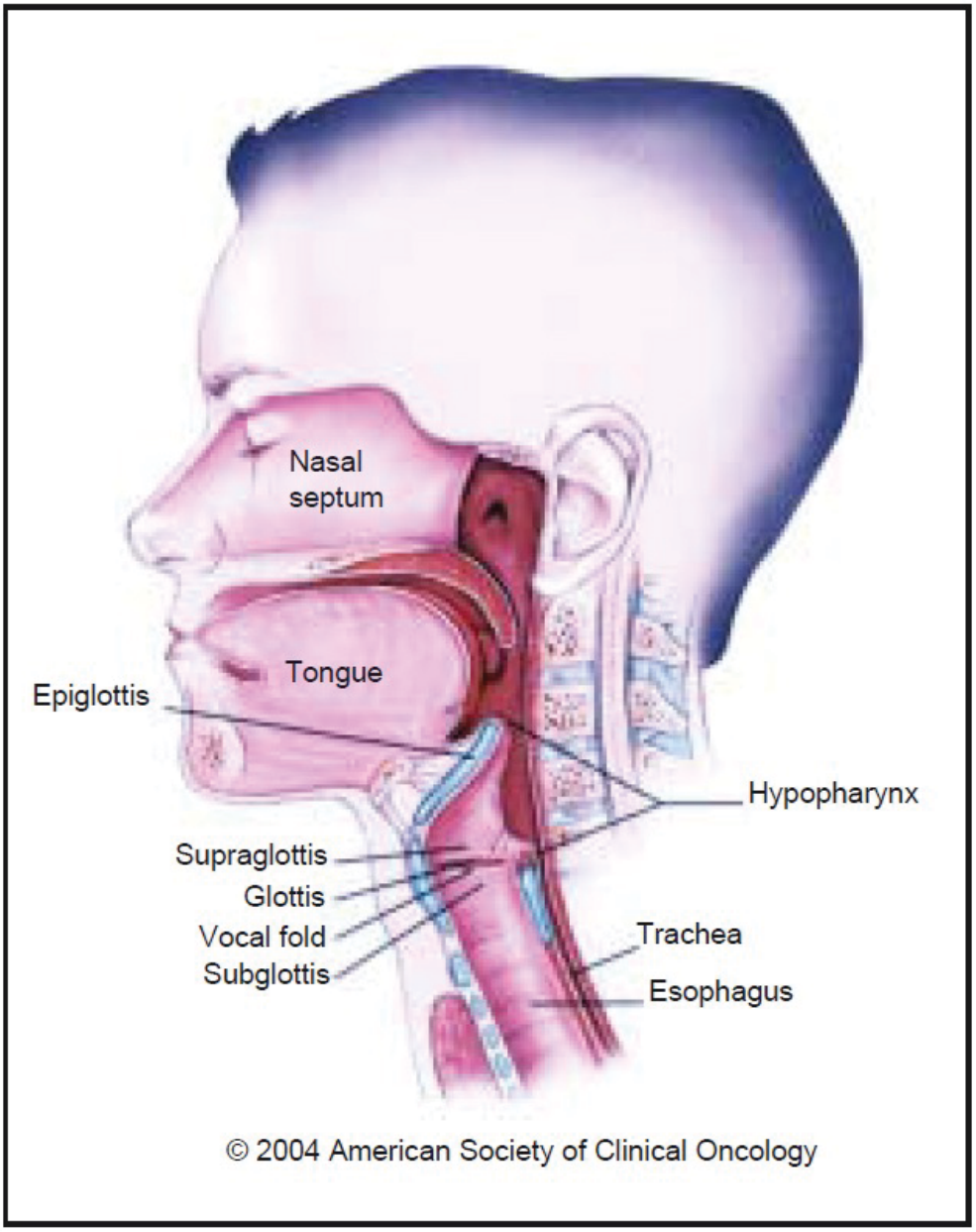

Figure 1.1. Regions of the head and neck which fall under head and neck cancer. Figure from Marur and Forastiere 2008 [1].

The survival rates for the subtypes of HNSCC have not changed much over the last 40 years despite available treatment [32,35]. Five year survival rate estimates for HNSCC patients lie around 40-50% [3]. However, localised tumours which are the least aggressive type, experience the highest rate of survival (83%) (Figure 1.2). Whereas distant, metastasised tumours (the most aggressive) have a lower survival rate of 37.7% (Figure 1.2) [36]. This estimate drops as patients develop tumour recurrence, distant metastases and secondary primary tumours after treatment [3]. Furthermore, HNSCC subtypes have different survival rates. In Australia (2010) the forms of head and neck cancers that caused the most deaths were larynx (255 deaths), tongue (204 deaths), oropharynx (147 deaths) and mouth (121 deaths) [37,38].

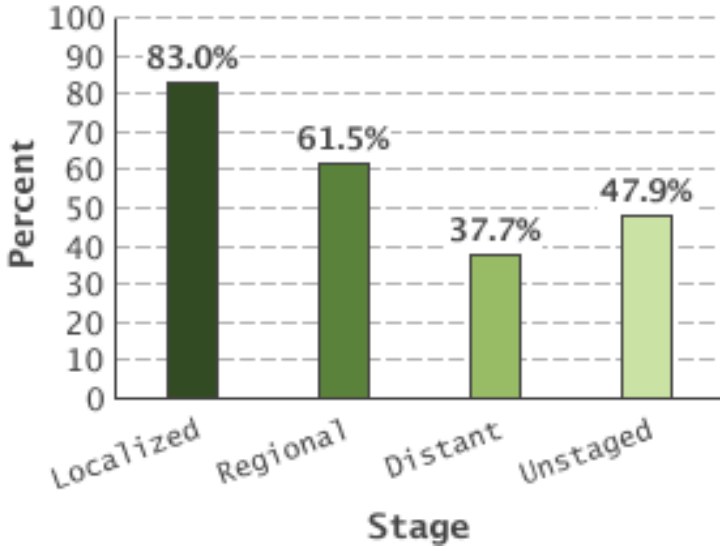

Figure 1.2. Five-year survival rates for different stages of cancer in the US from 2005-2011. Figure taken from Surveillance, Epidemiology and End Results (SEER) including all races and both sexes [36].

1.1.2. Incidence

HNSCC is associated predominantly with an older age group. However, this trend is starting to shift towards a younger age group. From 2008-2012 in the US, predominantly 29% of new cases was from the 55-64 age group. People under 35 formed 2.6% of new cases [36] (Figure 1.3). In Australia (2010) there were 4,134 new cases of HNSCC (3.5% of new cancers diagnosed) and 1045 deaths (2.4% all cancer deaths) [37-39]. The SEER program predicts 45,780 new cases of oral cavity and pharynx cancer and 8,650 deaths in the US this year demonstrating that this cancer is still problematic to public health [36]. Overall the number of new HNSCC cases appear to be rising over time with studies in the US containing 40,250 cases of the oral cavity and pharynx in 2012 compared to 29,370 cases in 2005. Most of these cases are from males (28,540 in 2012 and 19,100 in 2005) whereas female cases are mostly stable (11,710 in 2012 and 10,270 in 2005) [2,40].

Doobaree et al., elucidated that the rate of incidence for each subsite of HNSCC was different [41]. This emphasises the necessity in properly classifying the cancers so that the appropriate treatment can be tailored to the site. A study focusing on global HNSCC incidence rates from 1983-1987 to 1998-2002 was able to determine some interesting trends based on the region, predominant subsite of head and neck tumour and risk factor [42]. It was found that oral cavity tumours increased in numerous European countries but decreased in some Asian countries, United States, Canada and Australia. The main risk factor for oral cavity tumours is tobacco. The researchers thought the decrease in certain countries such as the US was due to smoking becoming less frequent whereas in Europe smoking tobacco is still commonplace [42]. India was found to have the highest rate of oral cavity tumours, most likely due to the consumption of carcinogen containing betel quid. Similar regional trends were observed for laryngeal tumours which also has tobacco as the main risk factor [42].

A different trend was observed with oropharyngeal tumours which are commonly associated with the human papilloma virus (HPV). There was an increase of these tumours in the US, Canada and other economically developed European countries such as Denmark and Sweden [42]. Thus despite the decline in tobacco use, HPV is on the rise in these countries. A study examining cases from 1995-1999 and 2000-2004 in South East England illuminated that the most common HNSCC sites in patients were the intra-oral cavity, larynx and tonsil [41]. The incident rate for tonsillar cancer significantly increased over time in males [41]. This is a general global trend that seems to be associated with people below the age of 45. This is due to the increase in HPV infections which can be associated with HNSCC, oral sex and increase in sexual partners [43]. However people with HPV associated HNSCC do have a better overall survival than people with HPV-negative HNSCC [44].

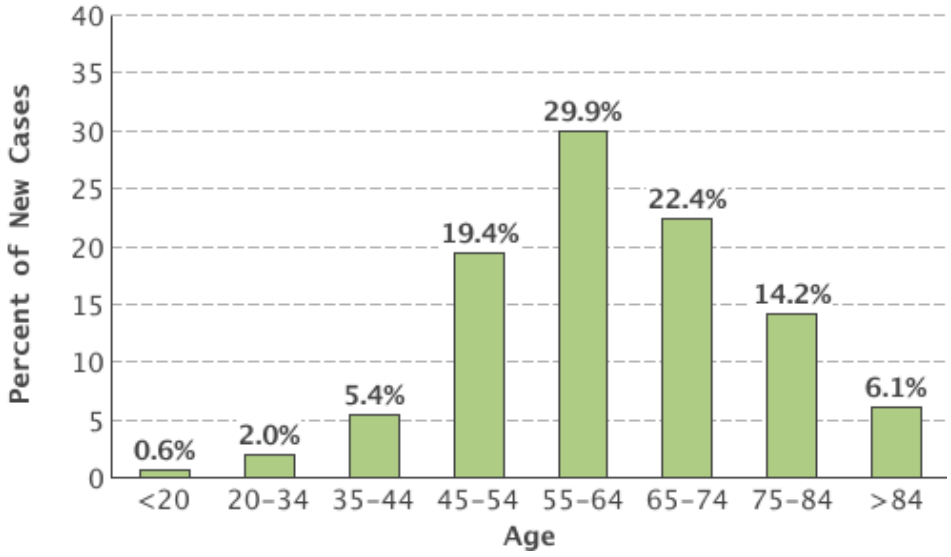

Figure 1.3. Percentage of new HNSCC cases in each age group in the US from 2008-2012. Figure taken from SEER including all races and both sexes [36].

1.1.3. Risk factors

It is now well known that tobacco and alcohol are primarily responsible for HNSCC cases in men [45]. This makes the primary target group for HNSCC, older males with a long history of smoking and alcohol use. People who smoke tobacco have a 5-25 fold chance of developing HNSCC in comparison to non-smokers [46,47]. The tumour suppressor gene p53 is mutated upon long term exposure to alcohol and tobacco. It is believed that the carcinogenic nicotine and polycyclic aromatic hydrocarbons in tobacco may play a role in this [1,48,49]. Within the different head and neck subsites, laryngeal, pharyngeal and oral cancers seem to be attributed to tobacco and alcohol. For women or people below the age of 45 there seems to be other factors such as HPV involved in HNSCC cases [45]. Also genetic disorders such as Fanconi anaemia can make individuals more susceptible to HNSCC [50].

Diet can play a role in development of this cancer. A poor consumption of fruit and vegetables can increase the risk factor for HNSCC [51]. Iron deficiency with the Plummer-Vinson syndrome can also be linked with this cancer [52]. Viruses are also a potential risk factor for HNSCC in particular the Epstein-Barr virus and HPV [53]. Another risk factor is overexposure to chromium, nickel, radium, mustard gas and byproducts of leather tanning and wood-working which have been linked with sinonasal cancers [54,55].

There are some risk factors that appear to be region specific for HNSCC. Nasopharyngeal cancer is very common in Southern China and South East Asia. For this reason, it is thought that Chinese ancestry could be a risk factor for this type of HNSCC. It is also possible that this cancer is rampant in China due to infection with the Epstein-Barr virus which is an established risk factor [56]. Alcohol is a known risk factor for HNSCC but additionally it is thought that the type of alcohol consumed plays a role. In some Eastern European nations the fruity alcohols are thought to have acetaldehyde which may be carcinogenic [57]. Another risk factor for oral cancer in certain parts of

the world is betel quid, which is a substance chewed in parts of South East Asia, the South Pacific islands and migrants around the world. Betel quid contains specific nitrosamines and daily consumption results in 50 times more exposure to this carcinogen than smokers [58].

1.1.4. Genetics

It is not a surprise that genetics plays a role in HNSCC development. One study investigating chromosomal aberrations in HNSCC tumours found that the group of tumours with the most chromosomal aberrations had the worst survival. Whereas the group of tumours with almost no aberrations had the best survival [59]. Anomalies in the chromosome can lead to mutations in genes and changes to signaling pathways which are vital to normal cell function. Currently in HNSCC there are no biomarkers used as frequently as the estrogen receptor or ERK2 in breast cancer or c-KIT for gastrointestinal stromal tumours [60-64]. Research using gene profiling studies have been conducted to identify head and neck markers or genetic clues.

The study of gene expression profiles in other cancers during different stages of tumour progression could aid in deciphering the different pathways of head and neck carcinogenesis. Microarrays on 18 oral tumours revealed a gene set of 116 that could significantly distinguish between metastasised tumours vs non-metastasised [65]. Additionally this profile was similar to a profile developed for pancreatic cancer [65]. Another study examining the expression profile of a head and neck lymph node metastasised subtype found it to be comparable to the expression profile predicting metastasis from breast cancers [66]. This supports the idea of dysregulation of similar pathways in cancer. Another microarray analysis study with 82 primary tumours (with just over half of the samples linked to metastasis) found 102 differentially expressed genes [67]. While many of the genes from the gene metastasis predictor set were related to metastasis, more than half of the identified genes were not linked to cancer development. The gene set was

able to distinguish the potential of metastasis between tumours [67]. These studies clearly emphasise the complexity of HNSCC progression.

A few key candidates of tumour development and progression in HNSCC have been identified. p53 has been shown to be mutated in 50% of HNSCC patients. This mutation is linked with progression from pre-malignancy to invasive disease [68]. Another study revealed that patients with p53 mutations in their primary tumours had early recurrences in comparison to patients without the mutation [69]. There was a reduced number of p53 mutations in patients with HPV-positive tumours and could be the reason as to why HPV-positive patients have a better overall survival [70].

Cyclin D1, which is involved in cell cycle progression, has been shown to be upregulated in many HNSCC patients [71,72]. One of the most common genetic events that occur in the early progression of HNSCC is the deletion of chromosomal region 9p21. This results in loss of the p16 gene, which inhibits cyclin-dependent kinase – a component of the cell cycle [72,73]. In addition mutations in both p53 and p16 in HNSCC patients has been associated with a poorer prognosis [72]. Conversely, the epidermal growth factor receptor has been found to be highly expressed in many HNSCCs and is associated with a poor prognosis and poorer outcome of survival [74].

1.1.5. Treatment

The treatment for HNSCC from 1960-1980 was surgery and radiation therapy [1]. Since then treatment of HNSCC has developed into a multidisciplinary approach consisting of a head and neck surgeon, a radiation oncologist, and a medical oncologist [1]. The stage of the HNSCC tumour dictates the level of treatment required [3]. However it is vital to accurately detect the stage of cancer and the resectability of the tumour [1]. The stage characterisation depends on the size of the tumour, occurrence of lymph-node metastases and distance metastases. Determining the stage of the HNSCC tumour is

done by clinical examination, imaging, cytology of lymph nodes and histopathology of the tumour after surgery [3]. Prognosis of HNSCC patients is dependent mainly on histopathological features such as tumour site, T classification, the presence and extent of nodal metastasis, tumour volume and thickness [32,66].

About two-thirds of HNSCC patients present with an advanced stage tumour with lymph node metastases [4]. Early stage tumours have a more favourable outcome and can be treated by surgery or radiotherapy. Whereas advanced stage tumours require surgery combined with postoperative radiotherapy [3]. Chemotherapy can reduce the chances of recurrence and distant metastasis [75]. Patients with unresectable recurrences usually have to undergo systemic chemotherapy in combination with chemotherapeutic drugs such as cisplatin and methotrexate [1]. A more recent treatment for HNSCC involves the use of the epidermal growth factor receptor-specific antibody cetuximab with radiotherapy [76].

Due to the lack of markers, identifying HNSCC at an early stage is difficult. This results in most patients reaching advanced stages of the cancer [4]. Hence it is imperative to find better markers for this disease. Perhaps focusing on the molecular biology of this complex cancer may reveal more useful prognostic and diagnostic biomarkers than the very few that currently exist.

1.2. Introduction to the microRNA world

The search for molecular biomarkers and treatment options in HNSCC has led to increased focus on the small non-coding RNAs known as microRNAs (miRNAs). However this has only occurred in the last 23 years as researchers were previously unaware of the existence of this type of molecule [77].

It was known for many decades that the amount of protein coding genes remained consistent across eukaryotes regardless of complexity [78]. Humans have approximately 20,000 protein coding genes which is comparable to the nematode *Caenorhabditis elegans* [79]. This was bewildering given the structural and biological complexity of humans compared to other organisms. The discovery of non-coding regions of the genome explained this phenomenon. The number of non-coding intronic and intergenic sequences is positively correlated with developmental complexity [80]. In addition, as the complexity of the organism increases so does the size of the untranslated regions (UTRs) of messenger RNAs (mRNAs) [81,82].

Most of the genome is under pervasive transcription producing stable RNA products [83]. It is believed that less than 2% of the human genome codes for protein and at least half of all transcripts do not code for protein [84,85]. Much is still unknown about these transcripts derived from non-coding regions. Identifying subcellular compartmentalisation, size and genetic modifications can contribute to understanding the function of these RNAs [83].
There are several classes of small non-coding RNAs (ncRNAs) of which three of them are: miRNAs, endogenous short interfering RNAs (siRNAs) and Piwi-interacting RNAs (piRNAs). miRNAs are approximately 20-22 nucleotide (nt) long, single stranded RNA molecules. They do not encode protein and function as gene regulators [5]. miRNAs are implicated in a number of bodily and cellular processes [86]. The cell contains highly abundant RNA species such as ribosomal RNAs, small nuclear RNAs and snoRNAs of which miRNAs are less than 0.5% [87]. siRNAs also have a low abundance in the cell and function to aid against RNA viruses and retrotransposons [88]. siRNAs and

miRNAs are quite alike in their mature state with a similar size and structure. Furthermore they undergo a similar biogenesis pathway and interact with the same proteins [89]. In contrast piRNAs are found in germline cells and are associated with spermatogenesis [90,91].

1.2.1. The history of miRNA

Lin-4 was the first miRNA to be discovered early in 1980 but at the time nothing was known about its structural features or function [92]. It was found in *C. elegans* using a mutational screen for embryonic development [92]. However it was not until 1993 that the uniqueness of this gene in comparison to known genes was revealed [77]. Mutant *lin-4 C. elegans* were unable to proceed to later stages of development. However, expression of *lin-4* in these mutants rescued development. Lee et al., discovered that *lin-4* did not code for a protein. They found it was much smaller than known genes and that it had an antisense complementarity to a sequence located at the 3´ untranslated region (3´UTR) of the *lin-14* gene [77]. This discovery garnered attention to the concept of RNA regulating another RNA via an antisense mechanism.

A second ncRNA *let-7* was uncovered and found to not be homologous to *lin-4* [5]. Since these ncRNAs worked in a temporal manner they were initially named 'small temporal RNAs' [77]. Pasquinelli et al, found that the 21 nt RNA was almost 100% conserved in all animals except jellyfish and sponges [93]. Reinhart et al., established that *let-7* was able to modulate development by binding to the heterochronic genes *lin-14*, *lin-28*, *lin-41*, *lin-42* and *daf-12* [5]. From these studies it was concluded that these two small RNAs mediated the timing of *C. elegans* development. *Lin-4* was required initially for *C. elegans* to develop from the first to the second larval stage. *Let-7* was then responsible for the transition from the late larval to the adult stage [5,77].

1.2.2. miRNAs and cancer

One of the first studies identifying an instrumental link between miRNA and cancer illustrated that most B cell chronic lymphocytic leukemias had a deletion at the chromosomal region 13q14 [94]. Two miRNAs miR-15 and miR-16 are located in this region. These researchers then went on to highlight that more than 50% of miRNAs are located at fragile sites and regions of the genome associated with cancer [27]. These regions are usually deleted, amplified or mutated when the cell is in a cancerous state [27,28]. The aberrant expression of miRNAs can either reduce survival or promote tumour formation [25]. Therefore these miRNAs can either act as tumour suppressors (miRNAs reduced in cancer) or oncogenes (miRNAs overexpressed in cancer) and are named oncomiRs [95].

Many studies have demonstrated the role miRNAs play in cancer. Usually their expression is dysregulated leading to alterations in gene regulation [26]. There is a strong correlation between miRNA expression and the progression of a cancer. A study analysing the downregulation of 90 different miRNAs in HeLa and A549 cells found that multiple miRNAs were involved in cell proliferation and apoptosis [96]. Another study assessed the expression profile of 228 miRNAs in six different solid cancers and found 21 miRNAs which were differentially expressed in most of the cancers [97].

Different cancer types appear to have a unique miRNA profile with miR-21 being the only commonly upregulated miRNA across many cancers including breast, glioblastoma and pancreatic cancers [8,23,97-102]. This miRNA affects multiple pathways unique to different cancers and pathway/s common to most cancers. It is well documented that miR-21 is involved in cell proliferation, invasion and metastasis [103]. One of the targets of oncogenic miR-21 is the tumour suppressor gene PTEN [104]. This phosphatase mediates the PI-3 kinase-Akt signaling pathway and when miR-21 is overexpressed this pathway is unrestrained leading to cell proliferation [104].

Researchers view the epithelial-mesenchymal transition (EMT) (reviewed in Kalluri et al., and Acloque et al., [105,106]) as one of the first steps in cancer development. In this process epithelial cells which are normally attached to each other and the basal membrane via various junctions and adhesion complexes are transformed into mesenchymal cells [106]. These cells have the ability to move independently throughout the extracellular matrix. During this conversion the cell gains the ability to migrate, invade and resist apoptosis [107]. Changes in specific miRNAs is linked with EMT [105] (Figure 1.4). Activation of EMT in adults is normally for wound healing and tissue repair and abnormal activation of EMT usually leads to tumourigenesis [106].

Cell proliferation is a component of tumourigenesis that occurs when cells divide at a rate greater than the baseline level due to external or internal stimuli [108]. miRNAs have been shown to be directly involved in promoting proliferation in cancer. An example is the miR-17-92 cluster which is overexpressed in lung carcinomas [109]. When the miR-17-92 cluster was artificially overexpressed in lung cells there was an increase in cell proliferation [109]. Whereas *let-7* prevented cell proliferation by regulating genes involved in cell cycle and cell division [110].
miRNAs are also involved in another facet of tumourigenesis known as cell invasion. Cell invasion occurs when cells release proteases and glycosidases which degrade the extracellular matrix allowing the tumour cells to push through and move to a new location [111]. For instance miR-21 is known to promote invasion in non-small cell lung cancer and inhibiting miR-21 results in a reduction in the invasion capability of cells [112]. Whereas miR-141 and miR-200c inhibit ZEB1, a protein involved in EMT and this suppresses invasion of tumour cells [113].

Migration is another component of tumour progression. When cells gain mobility this allows for cell migration, which is critical for metastasis. Various signaling molecules are activated which leads to remodeling of the actin

cytoskeleton and this process provides the physical force needed for cell migration to occur [114]. Overexpression of miR-101 was shown to significantly inhibit migration but also cellular proliferation and invasion of gastric cancer cells by targeting EZH2, Cox-2, Mcl-1 and Fos [115]. On the contrary, there is a significant correlation between miR-10b levels and the invasiveness of various esophageal squamous cell carcinoma cell lines [116]. Overexpressing miR-10b results in promotion of migration via the tumour suppressor gene KLF4 [116].

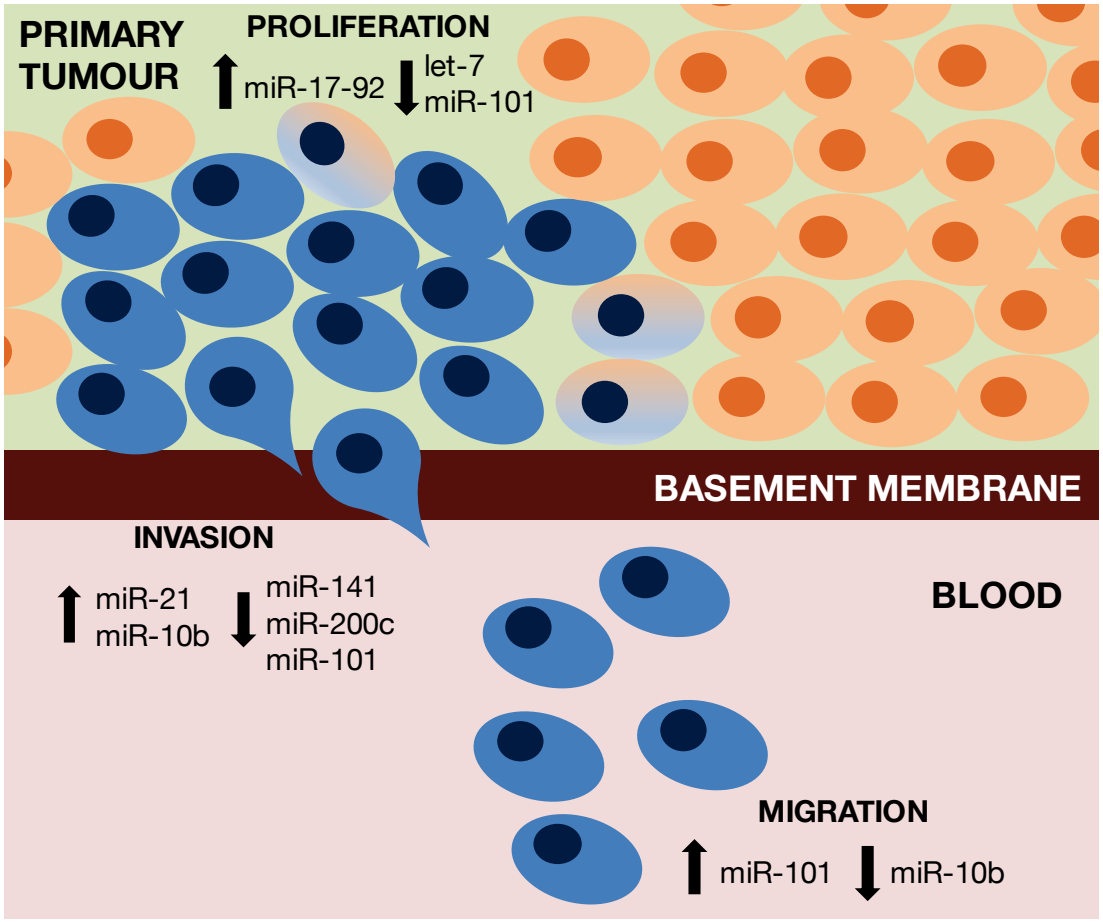

Figure 1.4. The development of a primary tumour and its progression into the blood stream facilitating the spread to other tissues.

Proliferation, migration and invasion – processes involved in cancer initiation and development are highlighted with examples of dysregulated miRNAs.

1.2.2.1. miRNAs in the clinic

It is clear from these studies that the expression profiles of miRNAs can be used as a specific prognostic [97,117] and diagnostic tool [118] for many tumours. In fact miRNA profiling could provide a better diagnosis than mRNA profiling as exemplified by the Lu et al., study [117]. They found that classifying poorly differentiated tumours using a miRNA profile of 200 miRNAs was more effective than a mRNA profile consisting of 16,000 coding genes [117]. Moreover, several studies have correlated miRNA expression with poor patient survival, presence of metastases and high progression risk in numerous cancers [101,119,120]. Another enticing use of miRNAs in the clinic is utilising them as either therapeutic targets (in the case of oncogenic miRNAs) or therapeutics agents (with tumour suppressor miRNAs). Krutzfeldt et al., demonstrated that endogenous oncogenic miRNAs could be inhibited *in vivo* with mice [121]. This was achieved by intravenous injection of chemically engineered, single stranded RNA molecules complementary to the mature miRNA (antagomirs) [121]. A cholesterol group was attached to the 3´ end of these antagomirs to increase stability, half-life in serum and cellular uptake. miR-16 was inhibited and this inhibition was effective in all tissues except the brain. This indicates that antagomirs are unable to travel through the blood-brain barrier [121].

It is important to have a comprehensive understanding of the biology of miRNAs and the pathways they target and interact with in order to fully grasp the implications of inhibiting/overexpressing miRNAs. This is necessary to minimise off-target effects.

1.2.3. miRNAs in HNSCC

Determining differentially and specifically expressed miRNAs in HNSCC can be of enormous value in finding molecular biomarkers for this disease. This would also contribute to understanding the mechanisms behind the development of this complex malignancy.

Using aberrant miRNAs as biomarkers may be indicative of early stages of HNSCC since it is possible that miRNA dysregulation is one of the initial steps of the disease [122,123]. He et al., found an upregulation of miR-221 in normal tissue adjacent to thyroid tumour tissue [122]. This indicates that this miRNA's dysregulation was occurring before the malignant phenotype appeared [122]. Another study wanted to determine the predictive potential for dysregulated miRNAs in HNSCC to identify if it was possible to distinguish tumourigenic tissue from healthy tissue [123]. Out of four miRNAs (miR-21, miR-18a, miR-221, miR-375) the miR-221:miR-375 ratio was the most clinically informative with a sensitivity of 92% and specificity of 93% in separating tumours from healthy tissue [123].

As previously mentioned different cancers have a unique miRNA profile whereas squamous cell cancers from the larynx, oropharynx, hypopharynx, tongue and oropharyngeal appear to be similar [98,124]. Hui et al., analysed 51 HNSCC patient samples from the larynx, oropharynx, and hypopharynx and found that the miRNA profiles from all three subsites were similar [98]. This can add to the complexity of tumour classification in HNSCCs due to the similarity in the molecular biology of the different subsites.

It is now known that the dysregulation of most miRNAs is not random and are usually located in fragile sites and parts of the genome associated with cancer [27,98]. Hui et al., found in their HNSCC study that a cluster of dysregulated miRNAs were present in parts of the genome that were either amplified or deleted in HNSCC [98]. This appears to be a mechanism leading to alteration of miRNA levels in HNSCC. Another study found in their HNSCC samples that downregulated miRNAs such as miR-100 and miR-99a were in two frequently deleted chromosomal regions 11q24.1 and 21q21.1 [98,125,126]. Upregulated miRNAs from this study were associated with chromosomal regions that are customarily amplified in HNSCC [98].

1.2.3.1. miR-21 in cancer and HNSCC

miR-21 is one of the most highly expressed miRNAs [127,128] and thus unsurprisingly is associated with various cancers such as malignant melanoma [129], liver [130], glioblastoma [102], gastric [131], breast [132] and kidney cancer [133].

There are numerous studies on the role of miR-21 in HNSCC. Hui et al., illustrated that miR-21 was overexpressed by more than 3.5-fold in 78% of their HNSCC patient samples [98]. Tran et al., also found an overexpression of miR-21 in all their HNSCC cell lines [124]. Another study examining HNSCC found 13 significantly overexpressed miRNAs including miR-21 [134]. Researchers analysing 169 HNSCC tumours showed that high miR-21 expression was linked with a significant decrease in five year survival rates [135]. miR-21 has also been associated with a functional role in HNSCC [23]. It was found that miR-21 miRNA mimics when transfected into cells increased cell growth, whereas transfected miR-21 inhibitors suppressed cell growth [23]. Studies such as this unveil the possibility of using small ncRNAs as therapeutic agents in cancer. A major area of concern would be off target effects of this application since miR-21 has many targets.

1.2.3.2. miR-499 in cancer and HNSCC

miR-499 is a cardiac specific miRNA found predominantly in the heart [136]. It has been shown to be involved in cardiac differentiation of human embryonic stem cells [137]. miR-499 inhibits cardiomyocyte apoptosis and is downregulated under pathological conditions. Thus it is involved in maintaining healthy cardiac cells [138].

It is thought that polymorphisms in pre-miRNA may prevent/alter binding of the miRNA machinery. This can lead to altered or suppressed processing of the miRNA and its function therefore increasing cancer susceptibility [139,140]. A miR-499 polymorphism (rs3746444 T>C or A>G) has been associated with many cancers though the conclusions vary between studies [140-147]. The miR-

499 polymorphism is significantly associated with prostate cancer in an Indian population [140], gastric cancer in a Japanese study [141] and cervical squamous cell carcinoma in a Chinese population [142]. Another study found no statistically significant results between the miR-499 polymorphism and increased breast cancer risk in Italians and Germans. Thus contradicting Hu et al., study conducted with a Han Chinese population [143,144]. The contradiction highlights other variables which may affect these studies such as genetic background, environment and study size [144]. Other studies that also found no association between the miR-499 polymorphism include a gallbladder cancer study [145], non-small cell lung cancer and primary liver cancer in Chinese populations [146,148], and non-small cell lung cancer in Caucasians [147].

There are very few studies exploring the role of miR-499 in HNSCC. A Taiwanese study examining 895 males found that the miR-499 polymorphism is associated with an increased risk of oral squamous cell carcinoma (OSCC) [149]. Whereas a study assessing a Caucasian population revealed that the miR-499 AG and GG genotypes were associated with a reduced risk of HNSCC [150]. A meta-analysis study seeking to understand the miR-499 polymorphism in various cancers addressed this contradiction. They noted how in various meta-analyses the cancer risks between Asians and Caucasians differed and they suggested that this could be due to genetic diversities, different life style risk factors and environmental factors [151]. Therefore, more studies need to be conducted into the miR-499 polymorphism and its association with HNSCC with ethnicity taken into consideration.

1.2.4. The regulation of tumour suppressor genes by miRNAs

miRNAs that are overexpressed in cancers typically downregulate genes known as tumour suppressor genes. These genes are involved in pathways critical to normal cell vitality, homeostasis and cell repair. Repressing one or more of these genes is critical to cancer development and progression. A

multitude of factors dictate the extent of repression of a tumour suppressor gene including developmental stage, cell and tissue type and endogenous levels of the gene. As a result, a tumour suppressor gene which may be a strong candidate for tumour prevention in one cancer may be a poor candidate for another. Therefore, studies need to examine each cancer individually for tumour suppressor genes and the oncomiRs that suppress these genes. Examples of tumour suppressor genes and the miRNAs that regulate them in HNSCC are listed below.

Well known tumour suppressor genes in HNSCC include p57, transforming growth factor-β (TGF-β) and FANCG. p57 also known as cyclin-dependent kinase inhibitor 1C is a cell cycle inhibitor that arrests the cell cycle in G1 phase. The tumour suppressor gene is known to negatively regulate cell proliferation [152,153]. A study found that miR-24 targets the tumour suppressor p57. Western blotting revealed a downregulation of p57 when miR-24 was overexpressed [154]. miR-24 was regularly upregulated in HNSCC tumour tissue and plasma samples compared to control tissues and samples. Overexpressing miR-24 alters the growth rate of HNSCC cells and promotes proliferation [154].

The chewing of areca nut extracts is a major factor in oral cell carcinogenesis and causes overexpression of miR-23a [155]. The overexpression or knock down (KD) of miR-23a regulates FANCG levels [155].The FANCG gene is one of six known human Fanconi anemia genes [156,157]. The gene forms a complex with the other members and regulates monoubiquitination of the FANCD2 protein [158]. When DNA damaging agents that can cause double stranded DNA breaks are introduced to cells, the complex monoubiquitinates FANDC2 which leads to repair of the DNA [156]. This prevents chromosomal aberrations which lead to cancer development.

A study examining HNSCC tissues found that miR-106b had the highest overexpression in tumour tissues compared to normal tissues [159]. Knocking

down miR-106b reduced proliferation and clonogenicity of HNSCC cells. The gene targets of miR-106b in HNSCC have not been studied extensively, however in other cancers this miRNA has been involved in inactivating the TGF-β tumour suppressor pathway [160]. The tumour suppressor gene TGF-β is known to inhibit cell growth by arresting the cell cycle in middle to late G1 phase [161,162].

1.2.4.1. PDCD4 in cancer and HNSCC

One of the more recently discovered targets of the highly expressed miR-21 is the tumour suppressor gene programmed cell death 4 (PDCD4) [24]. PDCD4 is a proinflammatory protein that promotes activation of the transcription factor NF-κB and suppresses interleukin 10 in lipopolysaccharide signaling [163]. Yang et al., found with the yeast two hybrid technique that PDCD4 interacted with the two eukaryotic translation initiation factors eIF4A and the eIF4F complex (consisting of eIF4A, eIF4E and eIF4G) [164,165]. The eIF4A protein is an RNA helicase that is involved in translation initiation by unwinding the secondary structure of mRNA at the 5´UTR leading to ribosome binding [166]. By inhibiting the helicase activity of eIF4A, PDCD4 is able to impede the translation machinery [165]. PDCD4 has also been shown to decrease benign and malignant tumour progression *in vivo* [167]. PDCD4 is shown to inhibit activation of the transcription factor AP-1 when it binds to eIF4A and this prevents cell transformation [165,168]. PDCD4 has been shown in a mouse model to promote apoptosis, prevent cell proliferation and tumour angiogenesis [10]. Furthermore, miR-21 is able to cause cell transformation by downregulating PDCD4 [24]. In various cancers such as lung, breast and colorectal, PDCD4 has been shown to promote invasion, proliferation and tumour progression [132,169].

Several studies have also examined PDCD4 in HNSCC and found the gene to be underexpressed in tumourigenic HNSCC tissues compared to their normal counterpart [12-14,103]. PDCD4 mRNA was underexpressed in 86% of OSCCs and the protein was absent/underexpressed in 89% of OSCCs illustrating the

diagnostic capability of PDCD4 [11]. PDCD4 was shown to be prognostic as patients with a more advanced tumour stage had lower levels of PDCD4 and worse survival. PDCD4 prevented invasion in oral carcinoma cells and the KD of PDCD4 reversed this process [11]. miR-21 can be linked with PDCD4 regulation as tumours with low levels of PDCD4 had high levels of miR-21. Furthermore when miR-21 was overexpressed in cell lines PDCD4 levels were decreased and the reciprocal was observed when miR-21 was inhibited [11].

1.2.5. miRNAs and non-cancerous disease

miRNAs are known to be involved in cellular and biological processes such as cell growth [96,170], cell differentiation [171,172], cell proliferation [109,173], apoptosis [96,174], metabolism [175,176], hematopoiesis [177,178] and oncogenesis [179,180]. It is thought that inherited changes in the genome to a miRNA sequence (usually in the pri- or pre-miRNA) such as a single nucleotide polymorphism (SNP) is likely an indicator of disease [143,181]. miRNAs have been found to be tissue and function specific and hence are implicated with different diseases [182].

Cardiovascular disease is commonly associated with miRNA. miR-499 is predominantly produced in the heart compared to other tissues and high plasma levels of miR-499 is associated with acute myocardial infarction [136]. miR-21 is one of the most upregulated miRNAs in rat hearts after ischemic preconditioning and is protective against cardiac cell apoptosis [183]. Overexpressing miR-1 and miR-133 has been shown to suppress cardiac hypertrophy [184].

miRNAs also play a role in autoimmune diseases. One study found a polymorphism at the miR-499 pre-miRNA to be associated with increased risk of rheumatoid arthritis [185]. Whereas, miR-21 was upregulated and strongly associated with systemic lupus erythematous disease activity. Additionally the upregulation of miR-21 was found to cause aberrant T cell responses in this disease [186].

Dysregulation of miRNAs is also commonly linked with neurological diseases [187]. This is unsurprising as out of all human tissues, the nervous system has the highest number of miRNAs with the brain containing about 70% of total detectable miRNAs [182,188]. A study found miR-146a, miR-149, miR-196a2 and miR-499 polymorphisms to be linked with patients with stroke and silent brain infarctions [189].

1.2.6. MicroRNA biogenesis: the canonical model

In the current literature the significance of miRNAs is accentuated with the prediction that more than 60% of mRNAs in humans are regulated by miRNAs [190]. The importance of miRNAs in the cell is also evident by their dysregulation in diseases such as cancer [98,100,191]. It has been shown that gene regulation by miRNAs is altered by decreasing the miRNA machinery and consequently miRNA levels [192,193]. The widespread gene silencing by miRNAs is a highly regulated process that can even be quantitated [194,195]. A single miRNA can regulate the expression of multiple genes [23,84]. Most miRNAs are found in the cytoplasm and only a small number in the nucleus [196]. The miRNA biogenesis pathway is summarised in Figure 1.5.

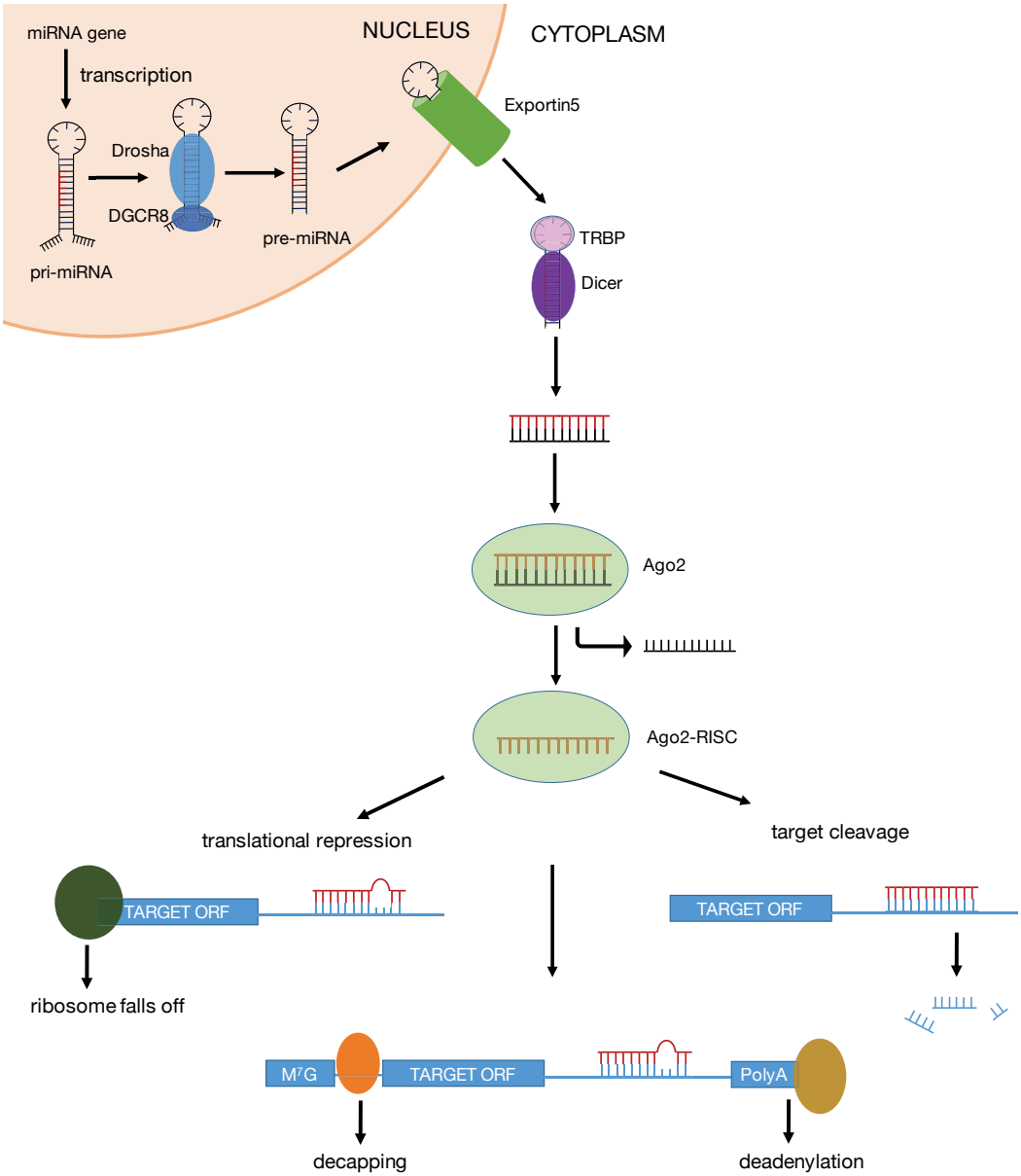

Figure 1.5. The miRNA biogenesis pathway. RNA polymerase II transcribes a miRNA gene producing the stem-loop structure of a primary miRNA (pri-miRNA). Drosha and DGCR8 cleave the pri-miRNA forming the pre-miRNA. The pre-miRNA is exported out of the nucleus with Exportin5 and is bound by Dicer and TBRP. This results in further cleavage of the pre-miRNA resulting in an 18-22 nt double stranded miRNA. This RNA duplex is bound by Argonaute 2 (Ago2) and one of the strands removed. The Ago2 and bound miRNA combination known as the RNA silencing complex (Ago2-RISC) is then able to cause downregulation of a target mRNA. This occurs either by target cleavage or target degradation by translational repression or decapping and deadenylation.

1.2.6.1. miRNA transcription

Most miRNA genes are found in non-coding regions of the genome and in the introns of protein coding genes [197,198]. They are often transcribed by RNA polymerase II (RNA pol II) [199,200]. Upon transcription the primary miRNA transcript (pri-miRNA) forms an ~80 nt hairpin stem-loop structure. Additionally the pri-miRNAs have a 5´ cap and polyadenylated tail similar to mRNAs [201].

1.2.6.2. pri-miRNA and pre-miRNA processing

The biogenesis of miRNAs begins with the formation of the Microprocessor complex in the nucleus consisting of the RNase III endonuclease Drosha, and its protein partner DGCR8 [202]. The short hairpin structure of the pri-miRNA is recognised by the Microprocessor complex and both strands of the pri-miRNA are asymmetrically cleaved at the stem. The resulting 60-80 nt hairpin is known as a pre-miRNA which is exported out into the cytoplasm of the cell by Exportin5 [5,93,203]. In the cytoplasm the RNase III enzyme Dicer along with its protein partners TRBP or PACT, recognises the pre-miRNA and cleaves off the loop resulting in an 18-22 nt mature double stranded miRNA [204-206].

1.2.6.3. Strand selection

In the cytoplasm the RNA duplex is loaded onto the protein Argonaute (Ago) where dissociation occurs between the two strands. One strand known as the star or passenger strand is usually degraded (though recently star strands have been found to have regulatory potential [207,208]), while the other strand known as the guide strand is retained. The guide strand bound within the Ago protein forms a complex known as the RNA induced silencing complex (RISC) [209].

The decision as to which strand becomes the passenger or guide strand is due to the inherent asymmetric nature of the RNA duplex which is based on

thermodynamic stability [206,210]. Schwarz et al., found that the strand with the uracil at the 5´ end rather than cytosine is kept [206]. This 5´ end is thermodynamically more unstable (U:A has two hydrogen bonds compared to C:G with 3 hydrogen bonds). The stability is also based on the first four nucleotides from the 5´ end. Other factors that influence the choice of guide strand include the 5´ nucleotide and structure of the RNA duplex (but not if the miRNA originally resided in the 5´ or 3´ arm of the pre-miRNA) [209]. It is generally accepted that RISC assembly then occurs when the RNA duplex is loaded onto the Ago protein and the strands separate within Ago [206].

1.2.6.4. Argonaute family

In the current literature there is a concerted effort to elucidate the interactions between the Ago proteins and miRNAs. This information may reveal why certain miRNAs target specific mRNAs, their tissue type specificity or why they respond to different stimuli. In humans there are four Ago proteins: Ago 1-4 [211,212].

1.2.6.4.1. Structure of Argonautes

Agos have four distinct domains: N-terminal, PAZ, MID and PIWI (as reviewed in Hutvagner and Simard [213]) . Crystallography has illuminated that the 3D structure of Ago consists of a crescent like shape formed by the N-terminal, MID and PIWI domains [214]. The PAZ domain sits above the crescent, creating a pocket for miRNAs and siRNAs to enter through [214]. The PAZ domain of Agos (also found in Dicer) is a globular domain that has a β barrel fold with two α helices on one side of the barrel and a cleft inbetween facing the crescent [214]. This domain has a oligonucleotide/oligosaccharide-binding fold that binds to the 3´ end of miRNAs [214]. The PIWI domain is at the C-terminal of Ago [214]. It sits in the middle of the crescent and below the PAZ domain [214]. It has a central five stranded β sheet with α helices on either side. A smaller β sheet connects the PIWI domain to the N-terminal domain [214]. The PIWI domain has an RNase-H-like fold which is essential for catalytic

activity [213]. The PIWI domain has 'slicer' activity because it is capable of cleaving mRNA complementary to the bound small RNA [214]. The 5´ end of miRNAs at the phosphate is captured by a divalent cation between the PIWI and MID domains [213]. The surface of this 'pocket' inside Ago is filled with positive charges which is complementary to the negatively charged phosphate backbone and 2´ hydroxyl portion of RNA [214].

1.2.6.4.2. Role of Argonautes

The four mammalian Agos are structurally very similar but only Ago2 has slicer activity [212]. Removing Ago2 in a mice model causes embryonic lethality [215]. However, the existence of multiple Agos suggests an evolutionary need to have four variants. Ago1 is involved in heterochromatin silencing via the association of Ago1 and TRBP2 with endogenous Polycomb target promoters in human cells [216]. Ago1 also plays a role in angiogenesis as it is targeted specifically by hypoxia-responsive miRNAs and KD of Ago1 increases angiogenesis *in vivo* [217]. Ago3 may have a role in interacting with the passenger strands of miRNAs [218]. The inhibition of Ago3 specifically reduces *let-7a-3p* expression [218]. Whereas Ago4 has been shown to regulate meiosis in germ cells in Ago4 KO mice [219]. These Agos are all capable of loading miRNAs and thus may have a role in gene silencing that is yet to be established.

1.2.6.5. RISC assembly

The miRNA-Ago combination is essential for RISC activity as the miRNA contributes specificity while the Ago is required for silencing [220]. There are two steps in the RISC assembly process: loading and removal of the passenger strand. Several models have been proposed explaining RISC assembly. Kawamata and Tomari., suggested a 'rubber band' model in which chaperone proteins aid Ago in undergoing a conformational change. This allows for the RNA duplex to be loaded onto the protein. Then as the Ago protein starts to fold back to its initial closed conformation, this releases

energy which is used for unwinding of the RNA duplex and removal of the passenger strand [209]. However, this model has recently been revised [221]. Crystallography reveals unloaded Ago in a flexible and unstable form [222-224]. It is thought that when chaperone proteins interact with Ago, the protein maintains a conformation that is able to receive the rigid RNA duplex [221]. Once the guide strand binds to the pocket at the 5´end of the PIWI domain in Ago this begins stabilisation of the Ago protein. The domains move closer to each other which stabilises the protein further but eventually the movement closes up the space within Ago forcing removal of the passenger strand [221].

It was originally thought that Dicer was also essential for RISC assembly. Liu et al., found that mature RISC in mouse embryonic fibroblasts was formed with an Ago and a single stranded miRNA. KO of Dicer prevented formation of RISC and it was concluded that Dicer is required for the loaded Ago to process the miRNA [225]. However, Kanellopoulou et al., found that the addition of exogenous siRNAs in embryonic stem cells had comparable gene silencing between the WT and Dicer KO. This implied that the Dicer protein was superfluous to small RNA biogenesis and activity [226]. Other studies have since found that Dicer is not required for the loading of the RNA duplex onto Ago [227-231].

The final step of mature RISC formation is removal of the passenger strand. A recent model proposes ‘wedging’ as the most likely method of passenger strand removal [232]. In this model the N domain of Ago opens up the RNA duplex at the 3´ end of the guide strand [232]. The 5´ end of the guide strand is tightly held by the Ago pocket (by the cation at the PIWI domain) [231,233] and the 3´ end of the guide strand is bound by the PAZ domain [234]. The passenger strand as a result can be easily ejected as it is not held as tightly as the guide strand by Ago. The protein can then proceed to separate the two strands [232].

1.2.6.6. mRNA regulation

After RISC assembly the RISC complex interacts with the 3´UTR of a target mRNA complementary to the loaded guide strand. There is also a subset of mRNAs which can be regulated from their 5´UTR [235-237]. When regulating a gene, the miRNA specifically binds to nts at position 2-8 of the complementary miRNA site on the mRNA. Nucleotides 2-8 on the miRNA is known as the 'seed' region [238,239]. More recently a mechanism for how RISC identifies target mRNA has been elucidated [240]. In this model RISC scans along the 3´UTR using lateral diffusion. It searches initially for nts matching positions 2-4 of the loaded guide strand and forms weak interactions at this site [240]. The interactions become stronger if the next few nts are also complementary to the guide seed. With RISC docked on the target site downregulation of the mRNA can then occur.

Downregulation of the target mRNA can occur by either degradation of the mRNA transcript or inhibition of translation [241]. RISC is able to induce deadenylation and decapping of the target mRNA resulting in an unprotected mRNA that is degraded. Alternatively, the RISC complex can cause the ribosome to drop off the target mRNA therefore preventing the recruitment of translational machinery and causing translation inhibition [241,242]. However if the miRNA has perfect complementarity to the miRNA site this will result in cleavage of the mRNA [242].

1.2.6.6.1. miRNA sites on target mRNAs

There are two main types of miRNA sites. The first type is "5´ dominant" sites which have strong base pairing to the 5´ end of the miRNA. Within this category are two subtypes, the first being "canonical sites" which have strong base pairing at the 5´ and 3´ end of the miRNA. The second subtype are "seed" sites which base pair (bp) poorly or not at all to the 3´ end of the miRNA [238]. The other main type of miRNA site is "3´ compensatory" sites which have pairing to the 5´ end of the miRNA and also to the 3´ end.

Further complicating miRNA regulation is the length of the seed of which there are three main lengths. The first is the 6mer seed (miRNA positions 2-7) which is the least effective site [243]. The higher efficacy seed lengths for binding are the 8mer seed (miRNA positions 1-8 with an A at position 1) and the 7mer seed (positions 2-8) (Figure 1.6) [238]. The 7mer seed can further be broken into the 7mer-m8 seed (positions 2-8) and 7mer-A1 seed (positions 2-7 with an A at position 1) [243,244].

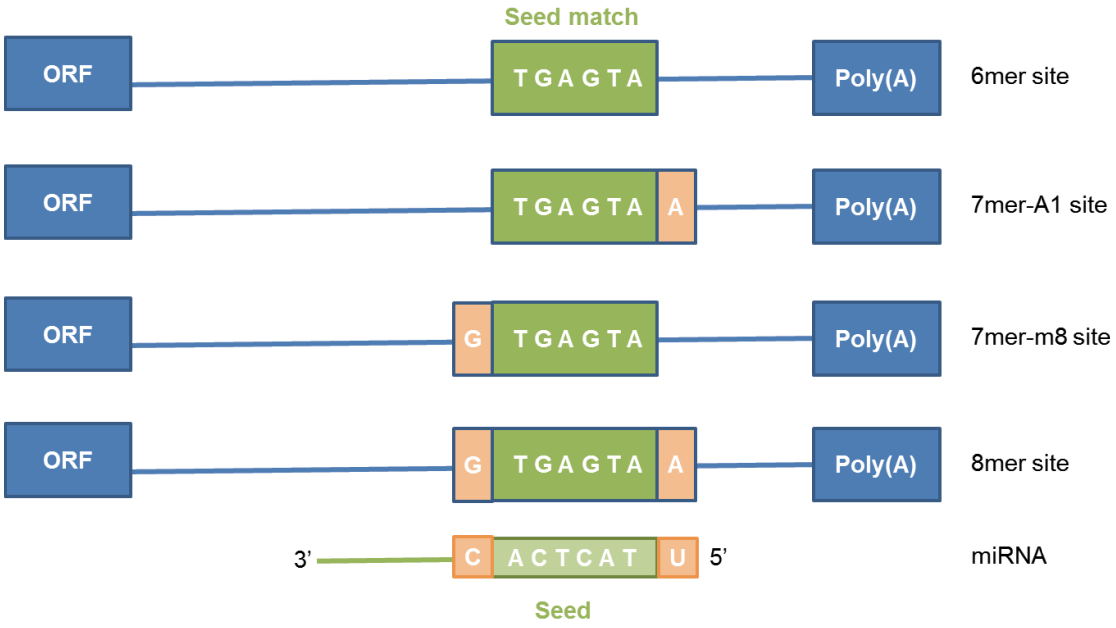

Figure 1.6. The different types of seed site matches found at the 3´UTR. The 8mer site is complementary to nts 1 – 8 of the miRNA seed. The 7mer-m8 site is complementary to nts 2 – 8 of the miRNA seed. The 7mer-A1 site is complementary to nts 2 – 7 with a complementary A at position 1. The 6mer sites is complementary to nts 2 – 7 of the miRNA seed.

1.2.7. miRNA machinery in cancer

There are a few studies in the literature that affiliate the miRNA machinery with cancer. Humans with Wilm's tumours customarily have a low expression of Agos 1, 3 and 4 because the chromosomal region they are located in (1p34-35) is usually deleted [245,246]. Another study highlighted a correlation between low levels of Dicer and a poor prognosis in non-small cell lung carcinomas [247]. The reciprocal was seen with prostate adenocarcinomas which are associated with an upregulation of Dicer [248]. Chiosea et al., found a link between upregulated Dicer, clinical stage and lymph node status. They also thought the increase in Dicer was the reason behind the overall global upregulation of miRNAs in the cancer [248]. In breast cancer, ovarian cancer and melanomas, copy number irregularities of Dicer1 and Ago2 have been identified [249].

1.3. Co-regulation of genes by multiple miRNAs

The identification in *C. elegans* of the seven *lin-4* sites in the *lin-14* 3´UTR prompted researchers to consider gene regulation across multiple sites as opposed to a single miRNA site [250]. The type of regulation where either a single miRNA is regulating multiple sites or different miRNAs are regulating the target mRNA is known as combinatorial regulation or co-regulation [251]. Many studies have identified that mRNA have multiple miRNA binding sites [190,252-254]. Additionally it is estimated that each miRNA has about 100 mRNA targets and this was observed when miR-1 or miR-124 were transfected into cells [238,255]. Multiplicity of targets from one miRNA and cooperativity of multiple miRNA on the one target are the hallmarks of miRNA function [256]. Despite evidence of interactions between multiple miRNAs or miRNA complexes leading to RNA silencing, combinatorial regulation has not been extensively studied.

About 50% of miRNA targeted mRNA 3´UTRs have two or more different miRNA sites [257]. Hon and Zhang., found that of the 6123 human miRNAs they examined, an average of 7.3 miRNAs theoretically target a single gene. Some genes were targeted by as many as 65 putative miRNAs and 12.3% of genes were targeted by more than 15 miRNAs [15]. Stark et al., found that the combination of miRNA sites on a 3´UTR can confer tissue specificity to a gene. For instance, the transcription factor Nerfin-1 can only be found in the nervous system. It is thought that the 15 seed sites on its 3´UTR for 10 different miRNAs is behind this location specificity [257]. *In silico* predictions indicate that genes regulated by multiple miRNA are involved in pathways that result in disease states if the regulation is disrupted [15]. Therefore, heavy regulation of these genes allows for cell homeostasis.

When seeking to understand combinatorial regulation of an mRNA by miRNAs there are two main types of regulation. There is independent regulation at multiple binding sites which can lead to an additive effect or

synergistic, cooperative regulation at multiple binding sites which leads to a more enhanced regulation of the gene [257]. The various types of regulation are as follows and illustrated in Figure 1.7.

i) Non-additive regulation: The miRNA sites on the 3´UTR are too close to each other and this prevents regulation of either site.

ii) Independent or additive target regulation: A single miRNA is able to sufficiently downregulate the target 3´UTR. Adding multiple miRNA leads to a downregulation that is equal to the sum of the regulation by the individual miRNAs.

iii) Interdependent/co-dependent target regulation: The combination of miRNAs is required for downregulation of the 3´UTR to occur. Lai et al., mentioned how this could be the case for some miRNAs that have a very limited repressive effect on a target mRNA when expressed alone [258].

iv) Synergistic or cooperative target regulation: Regulation by the group of miRNAs leads to a greater than expected downregulation of the 3´UTR. This is achieved with a modest upregulation of all the miRNAs.

a) non-additive

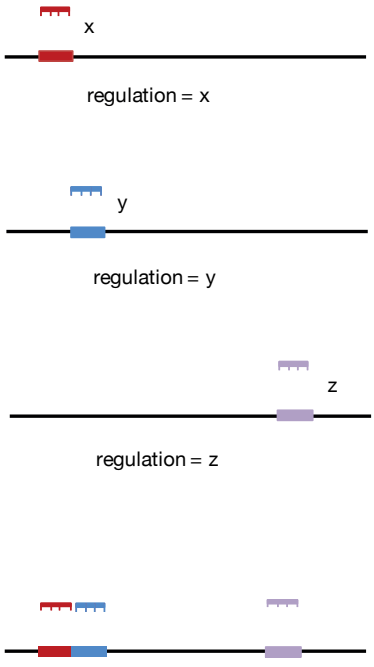

$\sum x + y + z$ **< (x + y) + z**

b) independent/ additive

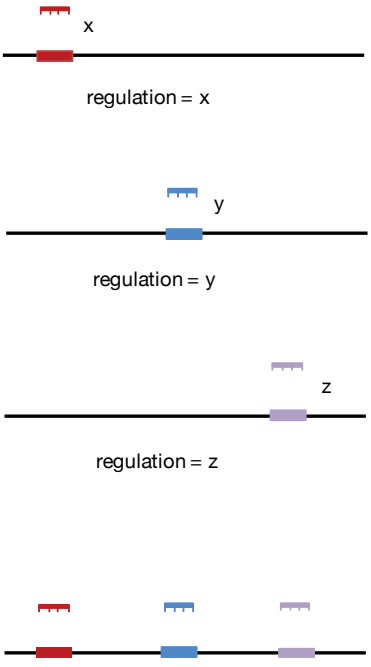

$\sum x + y + z$ **= x + y + z**

c) interdependent/ co-dependent

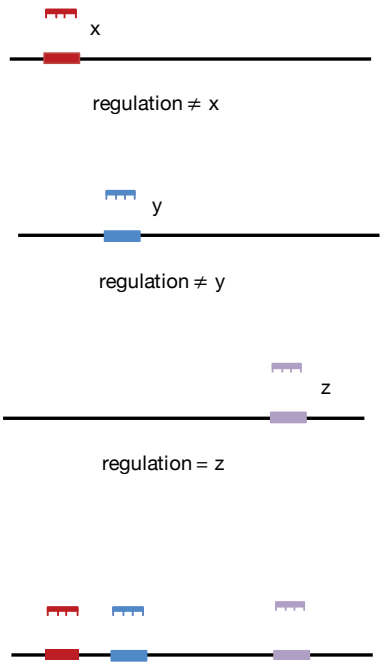

$\sum x + y + z$ **= (x + y) + z**

d) cooperative/ synergistic

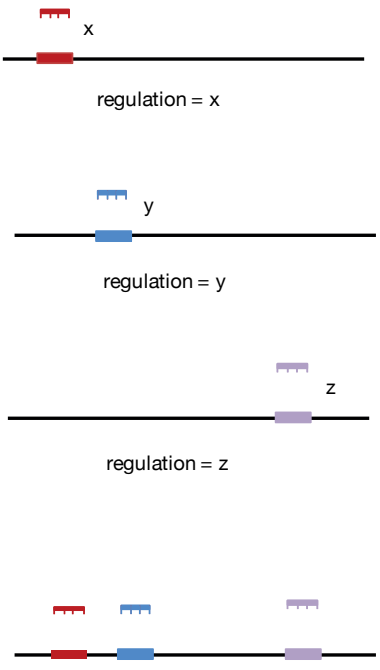

$\sum x + y + z$ **> (x + y) + z**

Figure 1.7. Various modes of combinatorial regulation at the 3´UTR of genes by multiple miRNAs. (a) Non-additive regulation. In this type of regulation, the miRNA binding sites (x and y) are too close causing steric hindrance between adjacent miRNA complexes. Therefore, regulation at these two sites tend to equal to that of one site or less. The total sum (Σ) of the regulation of x, y and z would be less than the sum of each site regulated independently. **(b)** Independent/additive regulation. In this type of regulation, the miRNA binding sites are far enough that the sum of regulation at the 3´UTR is equal to the combined regulation at the individual sites. **(c)** Interdependent downregulation. The presence of a single miRNA binding site alone (x or y) at the 3´UTR is too weak to cause sufficient downregulation. Both sites are required for regulation. **(d)** Cooperative/synergistic downregulation. The distance between two miRNA binding sites (x and y) is at an optimal proximity allowing for an enhanced regulation that is greater than the individual sum of its parts.

1.3.1. Our current understanding of combinatorial regulation

Technology has limited advances into uncovering combinatorial regulation by miRNAs. Until there is an improvement in computational methods, reporter assays and arrays are still the main ways to identify and validate co-regulation by miRNAs. More recent methods however include High-throughput sequencing of RNA isolated by crosslinking immunoprecipitation (HITS-CLIP) [259], photoactivatable ribonucleoside–enhanced cross-linking and immunoprecipitation (PAR-CLIP) [260] and individual-nucleotide resolution CLIP [261]. These techniques by crosslinking mRNA bound by miRNA loaded RISC allow for the identification of miRNAs and their binding sites. Similarly, the pull down of biotinylated miRNA can also be used to find miRNA binding sites [262].

1.3.1.1. Correlation between repression and the number of miRNA sites on the 3´UTR

Doench et al., (2003) conducted the early experiments revealing the cooperative nature of multiple miRNAs [250]. During this period, only two miRNAs *lin-4* and *let-7* had known functions [263]. The *lin-14* 3´UTR has seven putative *lin-4* miRNA sites and the *lin-41* 3´UTR has one *lin-4* and two *let-7* miRNA sites. Due to the numerous sites it was theorised that the quantity of sites could dictate the efficacy of translational repression [250].

This theory was tested with a seed site for the CXCR4 siRNA containing a central bulge to mimic miRNAs and was ligated to luciferase reporters containing zero, two, four or six sites. Cells transfected with the reporters revealed that the level of repression became amplified with increasing number of sites [250]. Furthermore, it was observed that with the four to six CXCR4 seed sites there was an enhanced regulation which showed cooperation between the miRNA-like sites. Conversely, a perfectly complementary seed site (representing a standard siRNA site) with increasing number of sites showed additive repression. Therefore it was concluded that

siRNAs bind to multiple sites in an independent manner whereas miRNAs bind cooperatively [250].

Later studies highlighted that more miRNA binding sites lead to greater repression. Pillai et al., demonstrated that with a reporter containing three bulged sites to *let-7*, there was a greater repression (20%) compared to no repression with the single site [264]. Brennecke et al., also found increased regulation with two copies of either an 8mer or 7mer miRNA seed site compared to a single site [238]. Broderick et al., found with their miRNA-like siRNA sites that at least three sites were required for reasonable silencing. Moreover, this silencing increased with additional sites in a cooperative manner [265]. These studies primarily focused on increased copies of the same seed site, which is not reflective of natural 3´UTRs with different types of seed sites.

Krek et al., found that the three most highly expressed miRNAs (miR-124, *let-7b* and miR-375) in a murine pancreatic cell line MIN6 targeted the Mtpn gene cooperatively [266]. The co-transfection of all three miRNAs most effectively decreased Mtpn levels compared to individual transfections [266]. This was one of the first studies to show co-regulation by different miRNAs on a 3´UTR with the natural sites. Wu et al., found that up to 28 miRNAs were able to regulate the CDKN1A 3´UTR [267]. It was observed that eight of these miRNAs were located on the same chromosome suggesting an association between location and miRNAs that target the same gene. It was hypothesised that these miRNA may regulate the gene in a spatial and temporal manner in different tissues and developmental stages [267].

1.3.1.2. Weak sites are factors in combinatorial regulation

Brennecke et al., claimed that combinatorial regulation occurs with weaker miRNA sites that cannot be regulated independently. Thus giving the cell a mechanism to fine-tune regulation of genes using different miRNAs to co-regulate the 3´UTR [238]. The 3´UTR of the Drosophila gene *grim* was examined which has a single weak 6mer site to miR-2, miR-4 and miR-11. With a single site only miR-2 was able to downregulate *grim* due to additional 3´ base pair binding between the miRNA and its site [238]. The *sickle* 3´UTR was then

examined which contains a 6mer site to miR-2, miR-6, two 6mer sites for miR-11 and a second 7mer site to miR-2 and miR-6 [238]. It was found that miR-2 had the strongest downregulation of the gene because it had additional 3´ base pairing to the *sickle* 3´UTR. miR-6 was also able to downregulate the 3´UTR but to a lesser extent and miR-11 had no downregulation with the two weak sites [238] (Figure 1.8). This study along with others illuminate that weak sites are involved in cooperative regulation but a strong site that can be independently regulated is required as well [238,257].

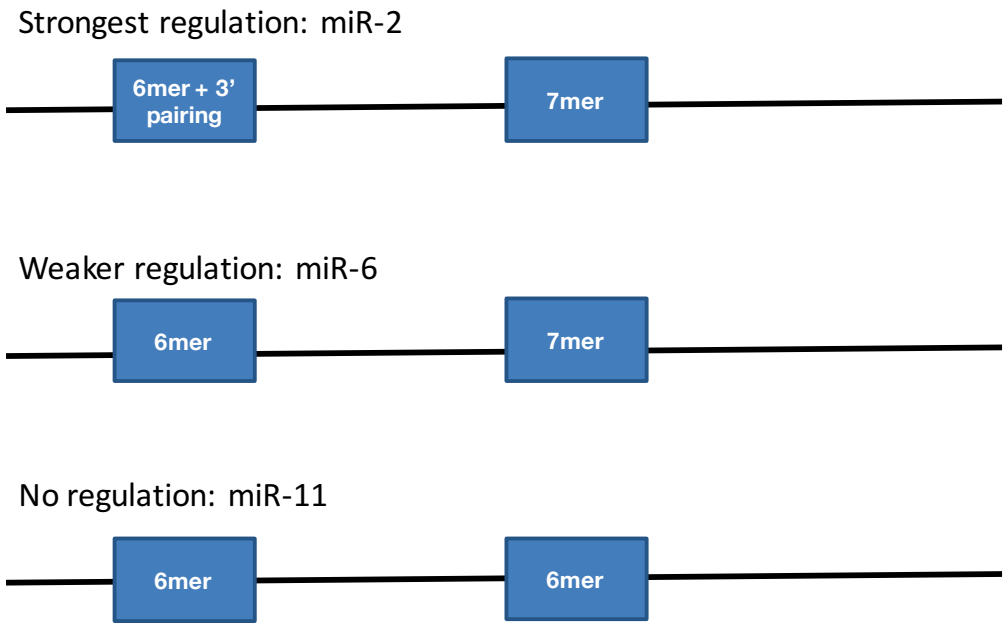

Figure 1.8. Strength of regulation at 6mer and 7mer sites for miR-2, miR-6 and miR-11 on the *sickle* 3´UTR (based on the findings by Brennecke et al.,) [238]. The strongest regulation occurs with miR-2 which has the strongest seed matches (6mer site with additional 3´ pairing and a 7mer site), weaker regulation occurs with the miR-6 sites and there is no regulation with the two miR-11 6mer sites.

1.3.1.3. The distance between miRNA sites determine cooperativity

The aforementioned studies demonstrated the possibility of cooperative regulation between multiple seeds by miRNAs. The next question was the distant requirements for cooperative regulation of the 3´UTR. Saetrom et al., upon examining the distance between identical miRNA seed matches compared to control shuffled seed matches in 3´UTRs from the University of California, Santa Cruz Genome Browser observed a trend. miRNA seed matches with distances less than 13 nt were underrepresented in the database whereas seed matches with distances between 16-20 nt were overrepresented. This revealed distance dependent conservation between identical miRNA seed matches [268].

Furthermore, miRNA seed matches with a distance of more than 130 nt had no form of conservation and this was the same with seed matches that were too close. Therefore it appeared that identical miRNA seed matches had to be within an optimal distance for conservation [268]. It was hypothesised that if the conserved distance between sites is biologically significant then an enhanced, cooperative binding should be observed with these sites. Using a reporter vector, *let-7* sites were artificially created with distances varying from 9-70 nts between seed match pairs. Conducting *let-7* overexpression and KDs in different cell lines demonstrated enhanced cooperativity between seed matches with an optimal distance of 16-20 nts [268]. In addition, a triple seed site with optimal distances of 17 nt between sites minimally increased regulation. This could be due to steric hindrance with multiple miRNA complexes [268].

Distance dependent regulation was also validated with a naturally occurring 3´UTR containing different miRNA sites [268]. The BMPR2 3´UTR was selected which has miR-25 (position 508-515), miR-106b (positions 206-212, 1523-1529) and miR-93 (positions 206-212, 1523-1529) sites. In the initial reporter assay no KD was observed, however when they moved the sites within 17 nts of each other a 30% reduction occurred. This illustrated that enhanced

cooperativity between optimally placed sites is maintained even with different miRNAs [268].

Grimson et al., found an enrichment for proximally spaced miRNA sites when assessing the conservation of sites in 3´UTRs of human, mouse, rat and dog [254]. This implies a biological selection for short intervening sequences between miRNA seed matches. Two miR-124 sites with a distance of 19 nt interacted in a cooperative manner and this was lost when changed to 50 nt but regained at 34 nt. Furthermore, when the miR-124 sites were switched to miR-1 sites, cooperativity was maintained illustrating that this regulatory mechanism is miRNA identity independent [254]. Proximally located dual miRNA sites of different identities (miR-1 and miR-33) on an artificial reporter also experienced cooperative downregulation of the 3´UTR. Spacing was essential as optimal repression occurred with a distance of 8 to approximately 40 nt between sites. Less than 8 nt prevented cooperative repression. It was concluded that cooperative miRNA sites leads to augmented sensitivity to small changes in miRNA expression [254].

Doench and Sharp., also examined distance constraints using a construct with four of the miRNA-like siRNA CXCR4 sites. The two internal sites were spaced by 0 and 4 nt and equivalent levels of repression was witnessed when CXCR4 was overexpressed [269]. When the distance was reduced even further so that there was an overlap between the seed match sites, it was not until there was a 9 nt overlap that repression was reduced to that of a single seed match site [269]. These findings contradict later studies which demonstrate that a distance of less than 8 nt results in negligible repression [254,268].

Broderick et al., focused on the roles of Agos and the type of regulation perfect and bulged siRNAs had on an artificial 3´UTR [265]. The distance and the nature of the Ago that bound the small RNA dictated whether silencing of the 3´UTR occurred in an independent or cooperative manner [265].

Cooperative regulation occurred with adjacent sites and this was disrupted at a distance of 19 nt or more. RISC formed with Ago 1, 3 or 4 allowed for cooperative regulation whereas Ago2-RISC resulted in independent downregulation of the mRNA target.

1.3.1.4. The functional relationship between genes involved in co-regulation

A few studies illuminated that not only were mRNAs regulated by multiple miRNAs but that these miRNAs also regulated genes with similar functions. This introduces the concept of a group of miRNAs that together can control specific processes and pathways in the cell.

Hua et al., demonstrated that miRNAs that co-regulated the angiogenic gene VEGF, also regulated other angiogenic related genes [270]. Different combinations of miRNAs therefore can possibility switch on and off angiogenesis. Hon and Zhang., examined the link between function and mRNAs containing multiple miRNA sites that were possibly subjected to co-regulation [15]. There was an enrichment for mRNAs with multiple miRNA sites (highly regulated genes). Gene Ontology analysis revealed that one-third of these mRNAs were involved in transcriptional regulation, almost half were nuclear proteins and 25% developmental genes. In contrast when they analysed genes targeted by five miRNAs or less there was no common association with function. Thus the functional relatedness of highly regulated genes appears to be real [15]. Exploring microarray data revealed that genes targeted by five or more miRNAs have lower expression on average. Consequently, dysregulation of these genes could lead to cancer [15]. Examination of the Cancer Gene Census revealed an over four-fold enrichment for cancer genes targeted by more than 30 miRNAs [271]. It was investigated whether cancer genes were especially targeted by multiple miRNAs and calculations revealed that on average 5.6 miRNAs targeted cancer genes[15]. This is higher than expected by chance.

These studies imply that the miRNA seed sites on an mRNA are not random but rather allow for differential regulation by miRNAs with similar functions. Furthermore, a portion of these genes are involved in cancer related pathways which indicates that co-regulation is essential for cell survival.

1.3.2. Genome-wide analysis of co-regulation by miRNAs

With the explosion of bioinformatics more studies began exploring *in silico* predictions of combinatorial miRNA targeting [272]. A computationally predicted seed is an indication of miRNA targeting. However, there may be other factors that contribute to regulation that should also be taken into consideration. Brennecke et al., found computationally an overrepresentation of seed matches suggesting that two-thirds of predicted 8mer seed matches and half of 7mer seed matches are functional [238]. Therefore, prediction tools for miRNA targets have a certain degree of accuracy. Computational analysis has sped up progress on revealing the nature and kinetics of miRNA-mRNA interactions and delivering valuable insights into the regulatory world of miRNAs. *In silico* research however still requires experimental validation as the output is still limited by algorithm design and bias, and our understanding of miRNA targeting.

1.3.2.1. Correlation between repression and the number of miRNA sites

With advances in computational analysis combinatorial regulation was expanded to hub genes - genes that are regulated by a large number of miRNAs [258]. Lai et al., decided to focus on the 3′UTR of p21 which has numerous miRNA binding sites. They investigated miR-572 and miR-93 which according to the regulatory map they built should cooperatively regulate p21 [258]. Individually the miRNAs could repress p21 to different extents due to site efficacy. Together though they had an enhanced repression of p21, which is reflective of miRNAs synergistically downregulating the 3′UTR.

Nielsen et al., computationally found a linear relationship between mRNA fold change and the number of seed matches present on the mRNA for up to five seed matches [273]. Conversely their results did not suggest a cooperative binding but rather that RISC was binding independently to each site resulting in an increased repression proportional to the number of sites [273].

1.3.2.2. Computational method to determine common pool of mRNA targets for miRNAs

Krek et al., using the computational algorithm PicTar were able to predict and identify common targets between miRNAs. They found by examining *lin-4* and *let-7* together that there is a shared pool of common mRNA targets which is indicative of potential co-regulation [266].

Tsang et al., used the computational method mirBridge to create a miRNA-miRNA co-targeting network [274]. There was an enrichment for co-targeting by 25% for clustered co-expressed miRNAs (polycistronic miRNAs), compared to 3% by non-clustered miRNAs. By assessing the networks formed Tsang et al., were able to identify different miRNAs with similar functions and pathways (and thus most likely target the same genes) that were previously unknown [274]. Xu et al., found computationally that miRNA from different families could be co-expressed and regulate a gene together [275]. Using the miRNA clusters, miR-17-92 and miR-106b-25 they found a synergistic regulation of genes in the oncogenesis pathway. Moreover they found an extra level of regulation where synergistic miRNA were regulated by common transcription factors [275]. This study illustrated the potential of combinatorial regulation by multiple miRNA on genes, in particular cancer genes.

Using the p21 regulatory map, Lai et al., computationally examined p21 levels when regulated by putative cooperative or non-cooperative miRNAs [258]. With cellular functions such as DNA repair and cell migration, p21 levels did not change between cooperative or non-cooperative regulation by miRNAs. Whereas with functions such as senescence and immune response

there was a difference in p21 levels between cooperative and non-cooperative miRNAs. It was suggested that in these conditions only miRNAs within a cooperativity permitting distance on 3´UTRs must be expressed [258]. To complement this study, analysis of the expression of cooperative and non-cooperative miRNAs in these different circumstances would validate the conclusions of the study.

Na and Kim., developed a miRNA association network computationally by combining miRNA-miRNA binding information and miRNA-miRNA co-expression profiles [276]. Using an algorithm they grouped miRNAs into cooperative miRNA modules (CMM) based on shared transcription factors and target genes [276]. They found that miRNAs within a CMM had a significantly similar seed match sequence but not mature or precursor sequence. Additionally, an association was found with the secondary structure of the precursor miRNA [276]. Na and Kim., noted that though CMMs contained many miRNA families this could not explain secondary structure as the miRNAs usually have different precursors. They suggested that perhaps pre-miRNA secondary structure may be a reflection of the mature miRNA's function [276]. Further research however is needed to validate this finding.

1.3.2.3. Estimating cooperative distance using computational approaches

Hon and Zhang examining datasets found that dense seed match site 3´UTRs (many binding sites and short 3´UTRs) had greater repression. When the distance between the 5´ end of miRNA site pairs was assessed, it was found that distances between 16-30 bp had optimal repression [15]. It was noted that even though proximally closer sites had reduced repression, when exploring the datasets there was a much higher than expected number of overlapping miRNA binding site pairs in the genome. These tandem overlapping sites (up to seven in some cases) resulted in greater repression than a single overlapping pair (Figure 1.9). This was most likely due to the increased potential of sites for RISC to bind which results in a higher

probability of repression [15]. Furthermore, a single overlapping miRNA site pair would experience steric hindrance which multiple overlapping sites can potentially overcome.

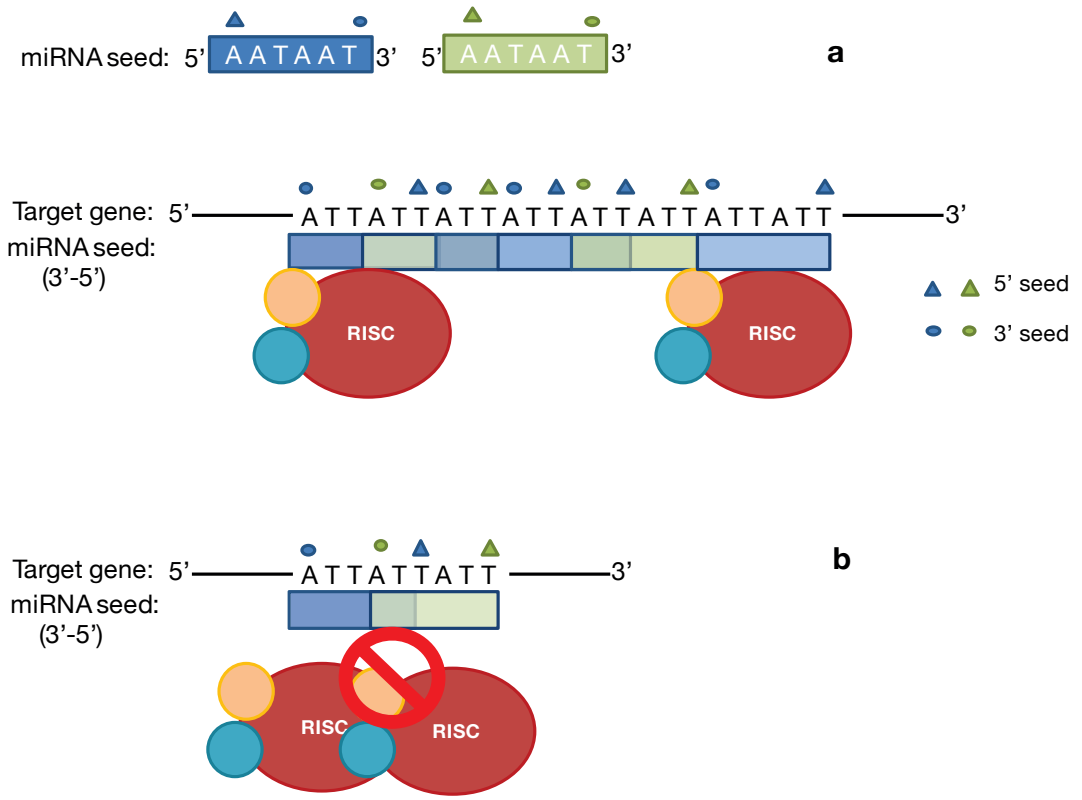

Figure 1.9. Overlapping sites have increased repression based on the Hon and Zhang study [15]. A region with multiple overlapping identical sites has enhanced repression most likely due to RISC being able to bind multiple places. Whereas two overlapping identical sites have no repression due to two RISCs clashing with each other spacially. The triangle represents the 5´ end of the miRNA seed and the circle represents the 3´ end of the seed.

Rinck et al., suggested based on their findings and other findings in the literature that the optimal cooperative distance from the 5´-5´ ends of two adjacent miRNA binding sites was 15-26 nts which is roughly the length of a miRNA [277]. It was thought that any cooperative regulation that occurred outside of this distance was probably due to secondary structure bringing the sites closer together spatially. Using computational methods and analysing the distance between sites of a single miRNA, and groups of two or five miRNAs, they found a peak enrichment for a distance of approximately 21 nt [277]. With experimental data from previous HITS-CLIP [259] and PAR-CLIP [260] studies along with TargetScan and miRanda they found the greatest enrichment for cooperative distance with groups of five different miRNAs [277]. Therefore, cooperative regulation is more likely to occur at a 3´UTR with different miRNAs as opposed to a 3´UTR with identical miRNA seeds.

Despite disparities on the exact distance for cooperative regulation, a peak distance of 21 nt is within most studies and is probably the best distance for cooperative regulation.

1.3.3. Co-dependent regulation in the literature

Most studies examining co-regulation focus on cooperative or independent target regulation. Only a couple of studies thus far have identified examples of co-dependent target regulation. The hallmarks of co-dependent regulation are that both seed sites on a target mRNA need to be functional and regulated simultaneously or sequentially by the miRNAs. This is exemplified in the study by Kloosterman et al., which focused on the regulation of the *lin-41* gene by *let-7* in zebrafish embryos [278]. The two biologically active *let-7* sites are separated by 57 nt however when the distance was reduced to 5 nt, downregulation of the *lin-41* gene still occurred [278]. *Let-7* can regulate both sites at the 3´UTR to the same extent. If either site is mutated to prevent regulation, then regulation is lost altogether. However, when the second *let-7* site is changed to a miR-221 site, regulation of the 3´UTR still occurs. Therefore, both miRNAs have to be overexpressed simultaneously for

regulation to occur. Individual overexpression of the miRNAs results in an absence of regulation [278].

Jopling et al., found that distance was not the only requirement for co-regulation [279]. The RNA virus, hepatitis C virus (HCV) has two miR-122 sites at the 5´UTR of the virus. miR-122 binding to the sites causes an upregulation of the virus. However if the miR-122 site is artificially inserted into the 3´UTR this causes a 50% downregulation of the virus RNA [279,280]. Single and double mutants of the miR-122 seed matches at the 5´UTR revealed that both sites were essential to accumulation of the HCV RNA [279]. Mutating the miR-122 sites with distinguishing mutations revealed that HCV RNA accumulation would only occur when both miR-122 mutants was overexpressed in cells. It was concluded that miR-122 needed to bind either sequentially or concurrently to both miR-122 seeds in order for them to be functionally active. Furthermore, Jopling et al., found that mutating the highly conserved 14 nt intervening sequence between the two miRNA sites resulted in a twofold decrease of RNA accumulation compared to the wildtype. Therefore the sequence between the two miR-122 sites is critical [279].

This study further complicates the type of regulation that occurs with two proximally located seed sites. The distance between the two co-dependent miR-122 sites was 14 nt which other studies have linked with cooperative regulation. Could the nature of the seed match sites determine the type of regulation? Or perhaps as claimed by Jopling et al., it is dependent on the sequence between seed matches [279]. Nachmani et al., found that a 24 nt distance between a viral miRNA and cellular miRNA resulted in synergistic downregulation of the gene MICB [281]. However, the binding sites of cellular miRNAs miR-373 and miR-376a are also separated by a distance of 24 nt and these two miRNAs antagonise each other in the regulation of MICB. Therefore, site proximity appears to not be the sole factor leading to cooperative downregulation [281].

1.3.4. Possible mechanisms of co-regulation by miRNAs

In the binding cooperativity model, binding of mature RISC stabilises the loaded miRNA's interaction with its target and increases the likelihood of the next seed site being bound [277]. Ago2-RISC spends more time on a target with two adjacent seed matches compared to a single seed match [240]. It is predicted that with the extra time a greater suppression of the target mRNA can occur [240].

The functional cooperativity model describes binding by RISC that leads to the recruitment of other proteins or enhancers which promote further binding of the 3´UTR [277]. Sites that are too close would suffer from steric hindrance from the RISC complexes. Whereas sites that are too far would not allow for the RISC complexes and possibly bound proteins to interact with each other [277]. Furthermore, two silencing complexes in close proximity to each other could allow for displacement of secondary mRNA structure to occur [254,268].

Saito and Saetrom., suggested an interesting model for the co-regulation of mRNA by examining the miRNA sites present in the coding sequence (CDS) [282]. When miRNAs downregulate a gene by translational suppression, this is a slow process that Saito and Saetrom., thought could be sped up by the proximal binding of multiple RISC complexes [282,283]. Hence why miRNA targets in the 3´UTR are favoured because at the CDS ribosomes would push off RISC complexes before completion of translational suppression [282]. Further evidence for this theory was that when rare codons, which slow down the processing speed of the ribosome, were moved in front of a previously non-functional miRNA site in the CDS, that site became functional [284]. Another line of evidence is that sites in the CDS that are functional usually have a very strong site [285,286] or multiple, proximally spaced sites [172,282,287].

1.3.5. Co-regulation of the tumour suppressor PDCD4

The theoretical and experimental studies in the literature illuminate the possibility of global gene co-regulation by multiple miRNAs. There is limited information on the regulation of the tumour suppressor gene PDCD4 but there are approximately 100 miRNA binding sites on its 3´UTR. However, the experimental evidence for the direct interaction of a miRNA with the PDCD4 3´UTR is available only for a selected number of these sites. miRNAs that have been shown to regulate the 3´UTR of PDCD4 include miR-9 [288], miR-182 [289], miR-183 [290], miR-320a [291], miR-141 [292], miR-21[103] and miR-499 [293]. There is no current information as to whether these miRNAs undergo combinatorial regulation to regulate the PDCD4 3´UTR. Examining the distance between the 5´ ends of neighbouring seeds (calculated in Figure 1.10) and basing optimal distance to be 8 – 40 nts [254], cooperative regulation could occur between miR-21 and miR-183 (17 nt) and miR-141 with miR-320a or miR-9 (36 nt).

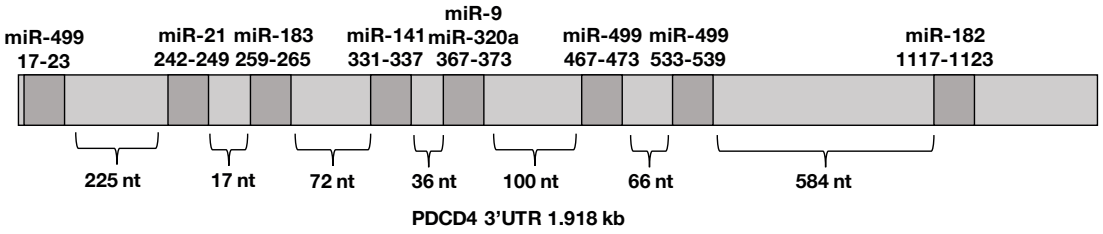

Figure 1.10. Schematic of PDCD4 3´UTR with sites of the seven miRNAs known to downregulate the gene.

1.4. Aims and Objectives

This thesis focuses on the tumour suppressor gene PDCD4 and the possibility of co-regulation by miRNAs. PDCD4 is downregulated in most HNSCC tumours and yet little is known about its regulation in HNSCC. Multiple miRNAs are overexpressed in HNSCC tumours but we focus on the two upregulated oncomiRs, miR-21 and miR-499. These miRNAs both target PDCD4 thus introducing the possibility of co-regulation.
We hypothesis that miR-21 and miR-499 co-regulate PDCD4 which leads to the activation of cancer pathways in HNSCC such as proliferation, metastasis and invasion.

Our first aim is to investigate the co-regulation of PDCD4 by miR-21 and miR-499 (Chapter 3). This is achieved using PDCD4 3´UTR site mutants for miR-21 and miR-499. Using luciferase assays we determine the regulatory dynamics of PDCD4 between miR-21 and miR-499. Specifically, if miR-21 and miR-499 use different modes of silencing (independent, co-dependent and cooperative) to regulate the 3´UTR. Finally, we investigate the role of Agos in regulating PDCD4.

The second aim is to examine the regulatory relationship between miR-21 and miR-499 (Chapter 4). In particular, we want to determine the underlying mechanism behind miR-21 directed upregulation of miR-499. Various models are created to explain the miRNA-miRNA regulation phenomena and experiments implemented to validate the most likely model.

The third aim is to assess miRNA-miRNA regulatory relationships on a genome-wide scale using RNA from a HEK293 cell line (Chapter 5). We want to elucidate if miR-21 could regulate other miRNAs besides miR-499 and identify common factors between the upregulated miRNAs.

The final aim is to examine the function of miR-21 and miR-499 in HNSCC (Chapter 6). Specifically, we investigate if these miRNAs are involved in the tumourigenic processes proliferation and migration. This is achieved through the use of HNSCC cell lines at various stages of cancer.

Chapter 2: Materials and Methods

2.1. Materials

List of reagents, commercially available kits, TaqMan probes and antibodies used in this study including the catalogue number and manufacturer.

Table 2.1. Reagents used in this study.

Item	Catalogue Number	Manufacturer
4-bromoanisole	104-92-7	Sigma-Aldrich, Australia
Actinomycin D (actD)	11805017	ThermoFisher Scientific, Australia
Ampicillin	A0166-5G	Sigma-Aldrich, Australia
BamHI	R3136S	NEB, USA
Blasticidin	A1113902	ThermoFisher Scientific, Australia
CellLytic M Cell Lysis Reagent	C2978	Sigma-Aldrich, Australia
DH5α*E. coli* cells	18258-012	ThermoFisher Scientific, Australia
Dimethyl Sulfoxide (DMSO)	67-68-5	Sigma-Aldrich, Australia
Dulbecco's Modified Eagle Medium (DMEM)	11965-092	ThermoFisher Scientific, Australia
EagI	R0505L	NEB, USA
ECL plus reagent	RPN2133	GE Healthcare Life Sciences, Australia
Ethanol	64-17-5	Sigma-Aldrich, Australia
Fetal Bovine Serum (FBS)	10437028	Gibco, Thermofisher Scientific Australia
Glycine	G8898	Sigma-Aldrich, Australia
Glycogen	AM9510	ThermoFisher Scientific, Australia
Hyperladder 1 KB	BIO-33053	Bioline, UK
Isopropanol	190764	Sigma-Aldrich, Australia
Lipofectamine 2000	11668500	ThermoFisher Scientific, Australia
Lipofectamine 3000	L3000-001	ThermoFisher Scientific, Australia
Lipofectamine RNAiMAX	3778030	ThermoFisher Scientific, Australia

Item	Catalogue Number	Manufacturer
Luria-Bertani (LB)	J106-1KG	Amresco, USA
Methanol	5005-10L	ThermoFisher Scientific, Australia
NotI	R3189S	NEB, USA
NuPAGE (4-12%) Bis-Tris Gel	NP0321BOX	ThermoFisher Scientific, Australia
NuPAGE MES SDS Running buffer	NP0002	ThermoFisher Scientific, Australia
NuPAGE Transfer Buffer	NP0006	ThermoFisher Scientific, Australia
Opti-MEM	31985070	ThermoFisher Scientific, Australia
PBS Tween 20	28352	ThermoFisher Scientific, Australia
Phosphate Buffered Saline (PBS)	P4417-50TAB	Sigma-Aldrich, Australia
Puromycin	A1113803	ThermoFisher Scientific, Australia
RNAase-free water	10977015	ThermoFisher Scientific, Australia
RNAzol RT	RN190-200ML	Astral Scientific, Australia
Serine protease inhibitor	A6664-10MG	Sigma-Aldrich, USA
Tetracycline	T7660-5G	Sigma-Aldrich, Australia
TrypLE	12563029	Gibco, ThermoFisher Scientific Australia

Table 2.2. Commercially available kits and related reagents used in this study.

Kit/Reagents	Catalogue Number	Manufacturer
BSA Assay	5000002	BioRad, USA
CellTiter 96 Aqueous One Solution	G3582	Promega, Australia
Deoxynucleotides (dNTPs)	AM8200	ThermoFisher Scientific, Australia
Dual-Luciferase Reporter Assay System	E1910	Promega, Australia
High-Capacity cDNA Reverse Transcription	4374966	ThermoFisher Scientific, USA
Multiscribe Reverse Transcriptase	4311235	ThermoFisher Scientific, USA
PureLink Quick Plasmid Miniprep	K210010	ThermoFisher Scientific, Australia
Qiagen HiSpeed Plasmid Maxi	12662	Qiagen, Australia
Quick Ligation	M2200S	NEB, Australia
Random Primer	48190011	ThermoFisher Scientific, USA
TaqMan Universal PCR Master Mix	4324018	ThermoFisher Scientific, Australia

Table 2.3. TaqMan probes used in this study (Applied Biosystems, ThermoFisher Scientific, USA).

miRNA	Catalogue Number
18S	Hs99999901_s1
ACTB	Hs01060665_g1
AGO2	Hs01085579_m1
B2M	Hs00187842_m1
Cy3 Dye-Labeled Negative Control	AM17120
FAM Dye-Labeled Negative Control	AM17012
FOXO4	Hs00936217_g1
hsa-let-7a-5p	478575_mir
hsa-let-7g-5p	478580_mir
hsa-miR-17-5p	478447_mir
hsa-miR-21-5p	477975_mir
hsa-miR-21(TaqMan® Pri-miRNA Assay)	Hs03302625_pri
hsa-miR-499a (TaqMan® Pri-miRNA Assay)	Hs03304133_pri
hsa-miR-499a-5p	478139_mir
MYC	Hs00153408_m1
PDCD4	Hs00377253_m1
RNU44	001094
RNU6B	001093
Scrambled/Negative Control	AM17111
SOX6	Hs00264525_m1
TP53	Hs01034249_m1
U75	001219

Table 2.4. Antibodies used in this study for western blotting.

Antibody	Catalogue Number	Manufacturer
Ago1	ab5070	Abcam, USA
Ago2	SAB4200085-25UL	Sigma-Aldrich, Australia
anti-mouse	ab97046	Abcam, USA
anti-rabbit	ab6721	Abcam, USA
anti-rat	ab6734	Abcam, USA
GAPDH	ab9385	Abcam, USA
PDCD4	ab51495	Abcam, USA
Tubulin	3873	Cell Signaling Technology, USA

2.2. Methods

2.2.1. Tissue culture

Cells were cultured at 37°C, 5% CO_2 in 75 cm^2 tissue culture flasks in Dulbecco's Modified Eagle Medium ((DMEM) with 4.5g/L glucose, 4mM L-glutamine, and 110mg/L sodium pyruvate) (ThermoFisher Scientific, Australia) supplemented with 10% Fetal Bovine Serum (FBS) (Gibco ThermoFisher Scientific, Australia). They were harvested as described. First, the growth media was removed and the cells washed with 1X Phosphate Buffered Saline (PBS) (Sigma-Aldrich, Australia) solution at room temperature. Cells were dissociated from the flask surface using TrypLE™ (Gibco ThermoFisher, Australia) and growth media with FBS was added to neutralise the TrypLE. Cells were then pelleted by centrifugation at 1200 rpm in an Eppendorf 5702 (Eppendorf, USA) for 5 minutes at room temperature. The supernatant was decanted and the pellet resuspended in the appropriate growth media.

2.2.2. Transfection of mammalian cells

Cells were either plated onto 6 or 24 well plates (BD Falcon, Australia) and transfected with 30 or 6 pmol respectively of artificially modified miRNA mimics/inhibitors (Ambion, USA) unless stated otherwise. Transfections were performed in triplicates at a cell confluence of 80-90%. The volume of transfection reagent or opti-MEM (ThermoFisher Scientific, Australia) varied per experiment depending on the size of the well and the number of the cells according to the manufacturer's instructions. Several delivery reagents/kits were used for different types of mammalian transfections.

2.2.2.1. Forward transfection

Cells at varying seeding densities were plated overnight in DMEM. The next day, the transfection reagents (lipofectamine RNAiMAX, lipofectamine 2000 or lipofectamine 3000) were added in combination with the miRNA mimics, inhibitors and/or plasmids to the cells without media. After an hour, media

was added and the cells incubated at 37°C and 5% CO_2 prior to further experimentation.

2.2.2.1.1. DNA plasmid and miRNA mimic co-transfection

Lipofectamine™ 2000 (ThermoFisher Scientific, Australia) was used to transfect DNA (200 ng) and miRNA mimics (30 nM) together into cells. According to manufacturer's instructions, before transfection, 2×10^5 cells were seeded into each well of a 24-well plate. DNA was diluted with opti-MEM and 1.5-4 µl Lipofectamine™ 2000 was diluted with opti-MEM for 5 minutes before they were added together. The mixture was incubated for 20 minutes at room temperature, and added to each well of a 24-well plate. Luciferase assay (See Chapter 4.2) was conducted after a 24-hour incubation to determine miRNA interaction with the 3´UTR of PDCD4 WT and mutants.

2.2.2.2. Reverse transfection

This modality of transfection yields a higher efficiency, is more high-throughput and maximises KD of target in comparison to the traditional forward transfection protocol [294]. In this format, the lipofectamine and chemically modified miRNA complexes were prepared and plated, after which cells and media were added. All reverse transfections were performed using Lipofectamine™ RNAiMAX (ThermoFisher Scientific, Australia) as per manufacturer's instructions.

2.2.2.2.1. RNA only transfection (quantitative polymerase chain reaction)

Lipofectamine RNAiMAX was used to transfect miRNA mimics. Briefly, 1×10^5 cells were seeded into wells of a 6-well plate unless stated otherwise. miRNA mimics and 3 µl Lipofectamine RNAiMAX were diluted with opti-MEM separately for 5 minutes and then incubated together for 20 minutes before addition to cells. Total RNA was collected 24 hours after transfection and used for downstream polymerase chain reactions (PCRs).

2.2.3. RNA isolation

RNA isolation was followed according to manufacturer's instructions of RNAzol RT (Astral Scientific, Australia) with several modifications. 1 ml of RNAzol was added to each well post transfection but this volume could be scaled down. In brief, 400 μl of water was added to each well and stored at room temperature for 15 minutes. This was followed by centrifugation at 15,000 rpm for 15 minutes at 4°C. 5 μl of 4-bromoanisole (Sigma-Aldrich, Australia) was added to a 1 ml aliquot of supernatant, shaken and left for 3-5 minutes at room temperature. This was centrifuged at 15,000 rpm for 15 minutes at 4°C. 600-750 μl of supernatant was collected and an equivalent amount of isopropanol (Sigma-Aldrich, Australia) was added with 25 μg of glycogen (ThermoFisher Scientific, Australia).

The RNA samples were left overnight at -20°C. These samples were then centrifuged at 15,000 rpm at 4°C and the supernatant decanted. The pellet was resuspended in 75% ethanol (Sigma-Aldrich, Australia) and centrifuged at 15,000 rpm for 10 minutes at 4°C rather than the 4000 g for 3 minutes in the original protocol. This was repeated, the supernatant decanted and the pellet left to air dry. The RNA pellet was resuspended in 20 μl of RNAase-free water and the Nanodrop ND-1000 spectrophotometer (ThermoFisher Scientific, USA) was used to determine RNA concentration and to normalise the RNA samples to 100-200 ng/μl for cDNA synthesis. The nanodrop was blanked with 2 μl of water and 2 μl of RNA sample was measured. Samples with 260/280 ratios of 1.7-2.1 were used subsequently.

2.2.4. Quantitative Real-Time PCR (qPCR)

To determine the expression of both miRNA and normal coding genes, a two-step qPCR TaqMan Assay (ThermoFisher Scientific, Australia) was utilised. The Vapoprotect (Eppendorf, USA) was used for cDNA synthesis and

the 7500 machine Real Time PCR System or StepOnePlus™ (Life Technologies, USA) was used for qPCR.

2.2.5. cDNA synthesis

The enzyme Multiscribe Reverse Transcriptase (ThermoFisher Scientific, USA) was used for all cDNA synthesis. Individual miRNA primers were used in the cDNA synthesis of miRNA genes (Table 2.5) and random primer (ThermoFisher Scientific, USA) was used for cDNA synthesis of non-miRNA genes (Table 2.6). Reactions were set up according to manufacturer's instructions for the cDNA synthesis kit (ThermoFisher Scientific, USA) as detailed below. The cycle conditions as suggested by the manufacturer were: 1) 25°C for 10 minutes, 2) 37°C for 120 minutes, 3) 65°C for 5 seconds and 4) hold at 4°C. The resulting cDNA product was diluted at a 1:4 ratio in nuclease-free water and stored at -20°C for subsequent qPCRs.

Table 2.5. cDNA synthesis set up for miRNA.

Components	1x Reaction (µl)
Specific Primers	6
10X RT Buffer	1.5
100 mM dNTPs	0.6
Rnase Inhibitor	0.2
Reverse Transcriptase	1
RNA (100ng)	1
Water	4.7
Total Volume	15

Table 2.6. cDNA synthesis set up for mRNA.

Components	1x Reaction (µl)
10X RT Buffer	2
100 mM dNTPS	0.8
Rnase Inhibitor	1
10X Random Primers	2
Reverse Transcriptase	0.5
RNA (100 ng)	1
Water	12.7
Total Volume	20

2.2.6. TaqMan hydrolysis probes for qPCR

RNA expression was quantified using the TaqMan gene assay. All target gene probes were FAM-labelled and reference gene controls were VIC-labelled. This combination of dyes permitted multiplexing of both gene target and reference genes in a single reaction well. However, miRNA target genes and reference genes were FAM labelled. As a result, all miRNA reactions were performed as singleplex mixtures. Table 2.7 shows the volumes of each component used in either singleplex reactions or multiplex reactions. The gene probes used in this study are listed in Table 2.8. All reactions were conducted in triplicate and a non-template control was included.

Relative expression of a gene was calculated as described. In order for downstream analysis to occur PCRs must have similar efficiencies and this was determined by the similarity of their amplification plots [295]. The fold expression and statistical significance were calculated using the $2^{-\Delta\Delta Ct}$ method [295]. Ct values were normalised using RNU44, U75 or U6B for miRNA genes and 18S, B2M or ACTB for non-miRNA genes and indicated as fold (Δ). To give the final relative expression of the gene of interest the fold change (calculated by $2^{-\Delta\Delta Ct}$) of the control sample was normalised to one and the gene fold change in the test samples made relative to the control [295]. Alternatively, the gene fold change in the test samples was only made relative to the control sample.

Table 2.7. Single and multiplex probe qPCR reaction set up.

Component	Singleplex (µl)	Multiplex (µl)
Applied Biosystems mix	2	2
Target Probe	0.25	0.25
Control Probe	-	0.25
Water	0.75	0.5
cDNA	1	1
Total Volume	4	4

Table 2.8. Target genes studied in this thesis and the reference genes used in qPCR reactions.

	miRNA	non-miRNA genes
Target gene	hsa-miR-21-5p hsa-miR-499a-5p hsa-let-7a-5p hsa-miR-17-5p hsa-let-7g-5p	PDCD4 SOX6 FOXO4 MYC AGO2 TP53 hsa-miR-21 (TaqMan® Pri-miRNA Assay) hsa-miR-499a (TaqMan® Pri-miRNA Assay)
Reference Gene	U75 RNU6B RNU44	ACTB 18S B2M

2.2.7. Protein methodology

Cells were harvested at either 24, 48, 72 or 96 hours. Protein lysis was achieved in each well using 200 μl CellLytic M Cell Lysis Reagent (Sigma-Aldrich, Australia) supplemented with 0.1% serine protease inhibitor (Sigma-Aldrich, USA). A plate scraper was used to remove cells from the surface of the well and to promote the physical disruption of the cells. The resulting mixture was placed on ice for 10 minutes, vortexed for 15 seconds and this process was repeated twice more. The samples were then spun for 20 minutes, 15,000 rpm at 4°C. Approximately half the supernatant was stored and kept at -20°C. Alternatively, if harvesting a larger cell pellet, then 1 ml of CellLytic M Cell Lysis Reagent was required.

Protein concentration was determined using the BSA assay (BioRad, USA) or the Qubit 2.0 Fluorometer (Life Technologies, Australia) according to manufacturer's instructions. The quantitated proteins were then loaded at 20 μg per lane onto a precast NuPAGE (4-12%) Bis-Tris Gel (ThermoFisher Scientific, Australia) in NuPAGE MES Sodium Dodecyl Sulfate (SDS) Running buffer (ThermoFisher Scientific, Australia). The electrophoresis was performed at 150 V for an hour after which the proteins were transferred onto a PDVDF membrane (Pierce, Australia) using NuPAGE Transfer Buffer (ThermoFisher Scientific, Australia). This was run for an hour at 25 V. The membrane was then either blocked with 5% skim milk or fetal calf serum for an hour. The membrane was incubated with primary antibody (see Table 2.5) for an hour at room temperature or overnight at 4°C. The membrane was then washed with 0.05% PBS-Tween 20 (ThermoFisher Scientific, Australia) and conjugated with secondary antibody containing HRP for an hour at room temperature or 2-3 hours at 4°C. Enhanced chemiluminescence (ECL) plus reagent (GE Healthcare Life Sciences, Australia) was used to detect the specific protein bands. The image capture was processed using the Intelligent Dark Box LAS-3000 (FUJIFILM, USA). For repeated immunodetection, antibodies were removed from the membrane by soaking

in a mild stripping buffer (1.5% glycine, 0.1% SDS, 1% Tween 20, pH 2.2) three times, 15 minutes per wash.

Table 2.9. Antibodies used in this thesis for protein detection.

Primary Antibody	Dilution	Secondary Antibody	Dilution
PDCD4	1:5000	anti-rabbit	1:3000
Ago1	1:1000	anti-rabbit	1:3000
Ago2	1:1000	anti-rat	1:5000
Tubulin	1:1000	anti-mouse	1:5000
GAPDH	1:5000	HRP	-

Chapter 3: Understanding the co-regulation of PDCD4 by miR-21 and miR-499

3.1. Introduction

It is estimated that each year there will be half a million cases of head and neck cancer worldwide [296]. This has remained unchanged in the past several decades due to our poor understanding of the molecular events causing this disease. Genetics and aberrant gene expression play a significant role in the onset of HNSCC. A few gene candidates involved in HNSCC development have been identified [71,72,74]. However further studies are required to gain sufficient knowledge in HNSCC genetics. Investigating miRNA can hold the key to understanding the molecular aberrations that lead to HNSCC development. Previous work from our group has shown that the tumour suppressor gene, Programmed Cell Death 4 (PDCD4) is downregulated in oral cancers[9]. We showed that miR-21 and miR-499 can regulate PDCD4 in a time dependent manner but the exact mechanism for this regulation remains elusive [9].

PDCD4 a gene inhibitor for translation initiation [164,297] is a known tumour suppressor in many cancers including head and neck [11,14,103,132,169]. PDCD4 is downregulated in head and neck tumours compared to normal tissues in patients [12-14]. PDCD4 indirectly stops activation of the AP-1 transcription factor preventing cell transformation [165,168]. A therapeutic study showed that PDCD4 promoted apoptosis, prevented cell proliferation and tumour angiogenesis [10]. Furthermore increasing PDCD4 levels stopped invasion in oral cancer cells whereas reducing PDCD4 levels increased invasion [11]. Thus

studying the regulation of PDCD4 in HNSCC may aid towards developing an efficient therapeutic against this tumour type.

Many studies focus on the direct interaction between miRNA-mRNA interactions and the resulting loss of function. However, the numerous binding sites on the 3´UTRs of mRNAs deem it possible that miRNA regulate genes in a concerted fashion. miR-21 and other miRNA such as miR-330-3p [298], miR-499 [293], miR-106a [299], miR-182 [300], and miR-183 [301] are known to directly regulate PDCD4 in other cancers. The caveat with all these *in vitro* studies is the delivery of a single miRNA mimic which binds to the 3´UTR of PDCD4 to induce silencing of a luciferase reporter. Given that the PDCD4 3´UTR is approximately 1900 nucleotides in length and harbours approximately 100 conserved miRNA binding sites, there is the likelihood of co-regulation by more than a single miRNA [243]. We speculate that interdependent target regulation may be involved in the regulation of PDCD4.

Several computational studies have documented the possibility of co-regulation between miRNAs to perform gene silencing [15,190,252-254,257]. Studies using synthetic constructs and targets have revealed the cooperative nature of miRNA-mediated gene regulation and this has led to a better understanding of miRNA regulation [244,265,302]. This chapter will significantly add to the understanding of miRNA co-regulation by presenting data from a naturally occurring system.

3.2. Methods

3.2.1. Tissue samples

Six head and neck tumour and normal tissue samples were used in qPCR analysis (Table 3.A). The tumour and normal tissue samples were obtained from the tissue procurement facility at Royal Prince Alfred Hospital.

3.2.2. Microscopy

HEK293 cells were transfected with 10 pmol of Cy3 or FAM labelled siRNAs (Ambion, USA) to determine transfection efficiency. The 6-well plate containing the transfected cells was viewed using the Olympus BX51 upright epifluorescence microscope with DIC objectives and DP70 CCD camera (Olympus, Australia). The cells were imaged through a red filter (Cy3 label) and green filter (FAM label), viewed at 10X and 20X magnification and analysed with the imaging program ImageJ [303].

3.2.3. Argonaute short hairpin RNA inducible cell lines

The approach to study Ago2 interactions with miR-21 and miR-499 involved employing siRNA KD of the Ago. This was achieved with Ago short hairpin RNA (shRNA) HEK293 inducible cell lines (a gift from Gyorgy Hutvagner and originally produced by Schimtter et al., [304]). Under drug selection these cells produce a shRNA targeting specific Ago family members. The inducible HEK293 cell lines were put under drug selection three passages prior to transfection. The Ago1 and Ago2 shRNA cell lines were selected with 2 µg/ml of puromycin (ThermoFisher Scientific, Australia) and 10 µg/ml of blasticidin (ThermoFisher Scientific, Australia) (Table 3.B).

Table 3.A. Clinic-pathological information of patient tissue samples used in study. BOT (base of tongue), FOM (floor of mouth).

Sample Name	Gender	Age	Site
HN31/02	M	43	Tonsil left
HN30/02	M	66	BOT
HN25/03	F	68	FOM
HN38/02T	M	N/A	Tongue
HN19/04T	M	76	FOM
HN34/02T	F	65	Oral Cavity

Table 3.B. Drugs required for expression of the shRNA in the drug inducible shRNA HEK293 cell lines.

Antisense hairpin	shRNA induction	Selection	Reference
Ago2	Tetracycline (10 μg/ml)	Blasticidin (10 μg/ml) & Puromycin (2 μg/ml)	Schimtter et al 2006

Five days prior to transfection cells were induced for shRNA production to maximise KD of the target. The cells were then transfected in combination with 30 nM miR-21, miR-499 or a scrambled control miRNA. Four hours after transfection cells were induced with tetracycline (Sigma-Aldrich, Australia) to switch on expression of the Ago2 shRNA. The RNA and protein was collected 24, 48, 72 and 96 hours post induction and the levels of PDCD4 determined at the RNA and protein level. Table 3.C shows the five different experimental conditions, what miRNA(s) were transfected in the condition and the expected levels of Ago in the cell after drug induction (+) or no drug induction (-).

Table 3.C. Transfection strategy with the Ago shRNA inducible cell lines and miRNAs.

Conditions	Transfected miRNA	Induced (+) or not induced (-)	Expected levels of Ago2
Cells	None	+	Low
		-	High
Control	Scrambled	+	Low
		-	High
Both	miR-21 & miR-499	+	Low
		-	High
miR-21	miR-21	+	Low
		-	High
miR-499	miR-499	+	Low
		-	High

3.2.4. Preparing 3´UTR mutants

To evaluate the role of the single miR-21 and three miR-499 binding sites on the 3´UTR of PDCD4, the sites were mutated at the third, fifth and seventh nt of the seed sequence (Figure 3.A). Previous studies have shown that mutation of these nucleotides at the site complementary to the seed region of the miRNA was sufficient to disrupt binding without causing unwanted effects such as change to the tertiary structure [59,305-307]. These mutant sequences were synthesised at GeneArt with the restriction sites EagI (CGGCCG) and NotI (GCGGCCGC) added on either side of the sequence to allow for subcloning [308]. The wildtype gene insert contained the partial 3´UTR unaltered PDCD4 sequence (positions 1-789 of the 3´UTR or 1697-2485 of the full transcript) and with the addition of the EagI and NotI sites the total size of the insert was 803 bp. The miR-21 site mutant contained the 3´UTR PDCD4 sequence with single nt mutations at the miR-21 sequence (242-249). This same principle was applied to the first miR-499 site (17-23), the second miR-499 site (467-473) and the last miR-499 site (533-539). The wildtype and four PDCD4 3´UTR mutant sequences were ordered with the pMA plasmid backbone (GeneArt, Invitrogen) and reconstituted to a stock concentration of 100 ng/µl with nuclease free water and subjugated to bacterial transformation.

ATATAAGAACTCTTGCAGTCTTAGATGTTATAAAAATATATATCTGAATTGTAAGAGTTGTTAGCACAAGTTTTTTTTT
TTTTTTTTTTAAGCACTTGTTTTGGGTACAAGGCATTTCTGACATTTTATAAACCTACATTTAAGGGGAATTTTTAAA
GGAAATGTTTTTTCTTTTTTTTTTGTTTTTCGAGGGGGCAAGGAGGGACAGAAAAGTAACCTCTTCTTAAGTGGAATA
TTCTAATAAGCTACCTTTTGTAAGTGCCATGTTTATTATCTAATCATTCCAAGTTTTGCATTGATGTCTGACTGCCACTC
CTTTCTTTCAAGGACAGTGTTTTTTGTAGTAAAATCACTGGTTTATACAAAGCTTTATTTAGGGGGTAAAGTTAAGCT
GCTAAAACCCCATGTTGGCTGCTGCTGTTGAGATACTGTGCTTTGGGAGTAAAAAAAGAAAGTTATTTCTTTGTCTTA
AAGAATTTTTAAAAAATTAGTCATGAGACTTATTCATCTTTCCAGGGAACATACTGATTGGTCTTAAAAGACTAGACA
GTTAAGTAAAAGGTGGCTGGAACATCTATTTTTCTACAAAACTGGAAAAATGAACCTGGTTCTAGAAGAATGTACAC
CAAAATAAAACATGTGAAGCAGTATTGATTCTTTATTGGGAGTACATTTTTTTAGGTCTCTTAAACTTTAATTTCACAC
AGTAAATTTTGAATCTCATAAGGAAGCATATTTGAACCTAGTCAATTTAATCTTAGTGTTCCCTTGAAAACTTTTTTTC
CCTA

Figure 3.A. 789 bp sequence of the PDCD4 3´UTR highlighting the positions of miR-21 and miR-499. The red sequence shows the first miR-499 site, blue the miR-21 site, green the second miR-499 site and purple the third miR-499 site.

3.2.5. Cloning: bacterial transformation

The four 3´UTR mutant sequences ligated to pMa plasmids (GeneArt, Invitrogen) were reconstituted and stored at -20°C when not in use. 1-5 µl of plasmid was added to 50 µl of DH5α *E. coli* cells (ThermoFisher Scientific, Australia). The cells and DNA suspension was then incubated on ice for 30 minutes, and placed in a 42°C water bath for 30-45 seconds. The suspension was placed on ice for 2 minutes and added to 1 ml of Luria-Bertani (LB) (Amresco, Australia). The solution was left in a shaker at 250 rpm for an hour at 37°C. 200-500 µl of transformed cells were then spread onto LB agar plates containing 100 µg/ml ampicillin (Sigma-Aldrich, Australia) and left overnight at 37°C.

3.2.6. DNA preparation: minipreps

To isolate DNA from screen clones, colonies were picked from the agar plate and used to inoculate 2 ml of LB containing 50 µg/ml ampicillin. These were left overnight at 37°C and plasmid isolation performed using the PureLink Quick Plasmid Miniprep Kit (ThermoFisher Scientific, Australia) according to the manufacturer's instructions. The inoculate was decanted and centrifuged at 15,000 rpm for 2 minutes. The pellet was resuspended with resuspension buffer and lysis buffer. This was left for 5 minutes and precipitation buffer added. Samples were spun for 10 minutes at 15,000 rpm and the supernatant decanted into preparation columns and spun for 2 minutes. The supernatant was removed and wash buffer added. This was spun for 5 minutes and the supernatant decanted. A recovery tube was used to collect the resultant DNA when 75 µl of water was added and spun for 2 minutes. The Nanodrop ND-1000 Spectrophotometer (ThermoFisher Scientific, USA) was used to determine DNA concentration and the DNA samples stored at -20°C when not in use.

3.2.7. Restriction digests

Restriction digest of the four mutant PDCD4 3´UTR sequences from the pMa plasmid backbone involved using 1 µg/µl of PDCD4 and 10 U/µl of the restriction digest enzymes EagI and NotI (NEB, USA). Also added to the mixture was 1XB3 and water to a final volume of 10 µl. The samples were then left at 37°C for 2-3 hours. A 1% agarose gel was run for 2 hours at 70 V to confirm the efficiency of the digest. The isolated mutant sequences were amplified with the PureLink Quick Plasmid Miniprep Kit after bacterial transformation in preparation for gel extraction.

3.2.8. Ligation of PDCD4 3´UTR gene inserts to luciferase reporter psiCHECK2

The PDCD4 3´UTR inserts were cloned into the psiCHECK^{TM-}2 reporter plasmid (Promega, USA). These inserts were ligated into the multiple cloning region downstream of the SV40 driven Renilla luciferase gene (Figure 3.B).

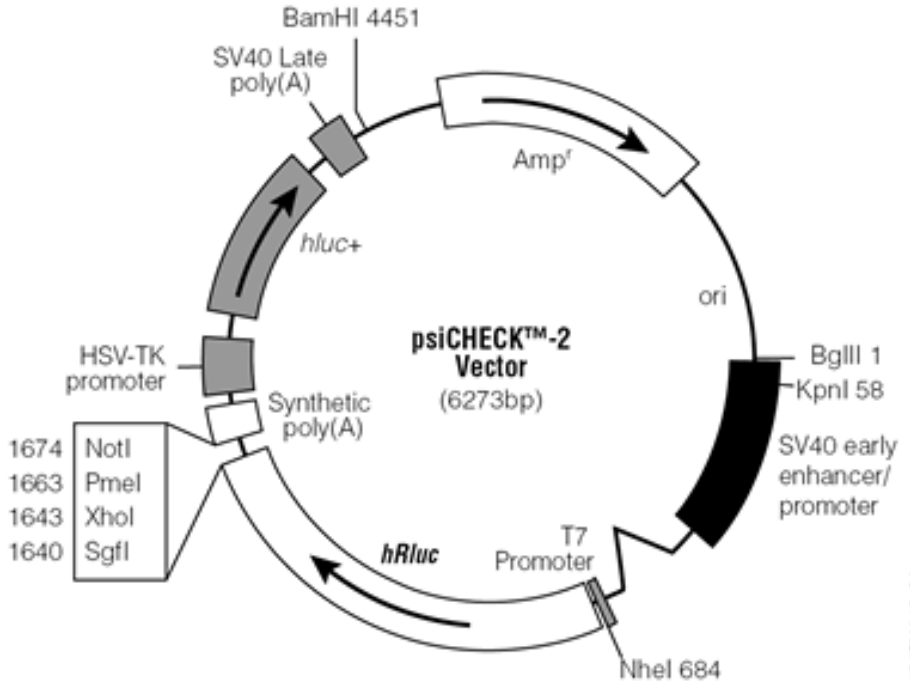

Figure 3.B. Schematic of the psiCHECK™-2 vector. The schematic shows the multiple cloning site, promoters and poly(A) tail on the vector. This vector was used as a reporter in the luciferase assays after the PDCD4 3´UTR inserts were subcloned into the multiple cloning site.

The following reagents from the Quick Ligation Kit (NEB, Australia), 1X T4 DNA Ligase Buffer, 0.5 µl of vector DNA (psiCHECK^{TM}-2), and insert DNA (3´UTR gene inserts) were added at approximately 10X the amount of vector. 1 µl of Quick T4 DNA Ligase and water was added to a final volume of 10 µl. This mixture was left overnight at 16°C in the PCR cycler - VapoProtect (Eppendorf, Germany). The ligation product was then transformed into DH5α bacterial cells and maxipreps conducted to generate psiCHECK-2 reporter plasmids used for transfection studies.

3.2.9. DNA preparation: maxiprep

To obtain a higher quantity of DNA for downstream transfections, plasmids were isolated using the Qiagen HiSpeed Plasmid Maxi kit (Qiagen, Australia) according to manufacturer's instructions. A single colony was selected from a freshly streaked plate and a starter culture inoculated containing 2 ml LB and incubated for 8 hours at 37°C, 250 rpm. 500 µl of starter culture was transferred to a 250 ml LB containing 100 mg/ml ampicillin and incubated for 12-16 hours at 37°C, 250 rpm. The bacterial cells were harvested at 6500 rpm for 15 minutes at 4°C in the Hitachi CR22 Super Speed centrifuge. The cells were resuspended in 10 ml Buffer P1 and mixed thoroughly with 10 ml Buffer P2 and left for 5 minutes at room temperature. 10 ml of chilled Buffer P3 was added to the solution and the entire mixture was poured into the barrel of the QIAfilter cartridge. This was incubated at room temperature for 10 minutes and a plunger inserted into the cartridge to filter the cell lysate into the HiSpeed Tip. The HiSpeed Tip was washed with 60 ml of Buffer QC and the DNA eluted with 15 ml Buffer QF. The eluted DNA was precipitated by adding 10.5 ml of isopropanol at room temperature and incubated for 5 minutes. The eluate/isopropanol mixture was transferred into the QIAprecipitator and a plunger inserted to remove the waste. 2 ml of 70% ethanol was added to the QIAprecipitator to wash the DNA. The DNA was air dried twice with the QIAprecipator. The QIAprecipator was placed over a 1.5 ml collection tube and the DNA eluted with 1 ml of water and stored at -20°C.

3.2.10. Luciferase assay

The Dual-Luciferase Reporter Assay System (Promega, Australia) was used to measure luciferase activity of cells co-transfected with target 3´UTR and miRNA mimics. The luciferase assay was conducted according to manufacturer's instructions. Firefly and luciferase activities from psiCHECK-2 were measured 24 and 48 hours after transfections. The expression of the Renilla gene was used to determine the regulation of the PDCD4 3´UTR. The Firefly luciferase gene was used for normalising transfections due to its constitutive expression.

Luciferase assay was conducted after 24 hours post transfection to determine miRNA interaction between the 3´UTR of PDCD4 WT and mutants. The cells were washed with PBS and lysed with 100 µl of passive lysis buffer (Promega, Australia) for 15 minutes with steady rocking at room temperature. The contents of each well were freeze thawed to complete lysis. 20 µl of lysate was added in triplicate to wells of an opaque 96-well plate (PerkinElmer, USA), which was followed by the addition of 100 µl of LARII (Promega, Australia) to all wells. The plate was transferred to the Tecan Infinite®200 PRO spectrophotometer (Tecan, Switzerland) which was set up to measure Firefly activity. 100 µl of Stop & Glo (Promega, Australia) reagent was added to each well and the plate read for Renilla activity. For each luminescence reading, after injector dispensing assay reagents into each well, there would be a 2 second pre-measurement delay, followed by a 10 second measurement period. Luciferase assays were analysed based on the ratio of Renilla/Firefly to normalise cell number and transfection efficiency.

3.2.11. Transfections

Increasing amounts of miR-499 was transfected into HEK293 cells to determine the efficacy of the miR-21 and miR-499 binding sites on the 3´UTR of PDCD4. This was achieved by creating a serial dilution of the miR-499

mimic with concentrations of 0.0012, 0.012, 0.12, 1.2 and 12 nM. The dilutions were added to a transfection set-up consisting of 50 ng 3´UTR PDCD4 vector and $4x10^4$ seeded HEK293 cells. The cells were then harvested at 24 hours and measured for luciferase activity. IC_{50} was calculated using the Hill equation [309] and propagated error and the graphs created with the Igor Pro Carbon Program [310].

3.3. Results

3.3.1. PDCD4 is a direct target of miR-21 and miR-499.

A previous study from our group (Zhang et al.,[9]) showed that PDCD4 was regulated by miR-21 and miR-499 (Figure 3.1). However, the underlying mechanism remained unclear. We decided to investigate this action further using a luciferase reporter system.

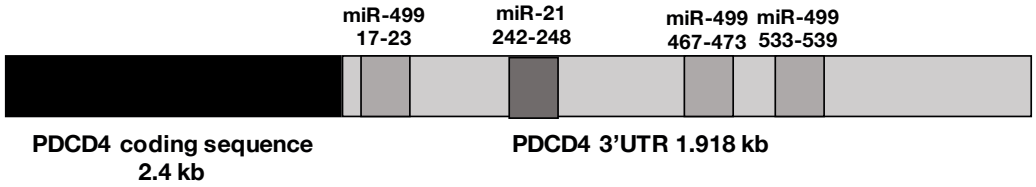

Figure 3.1. Schematic of the PDCD4 gene. The schematic shows the coding sequence and 3´UTR containing the miR-21 binding site (nts 242-248) and three miR-499 sites (first site nts 17-23, second site nts 467-473, third site nts 533-539).

3.3.2. Cells are successfully transfected with miRNA mimics

To study miR-21 and miR-499 regulation of PDCD4, cells were subjected to transfection. Transfection of chemically synthesised miRNA mimics into cells is a fundamental technique into studying miRNA function and gene regulation. To ensure that the miRNAs were successfully transfected into cells, transfection efficacy was measured. Cy3 and FAM labelled siRNAs were transfected into cells using the RNAiMAX protocol and imaged under a fluorescent microscope. The red filter (CY3 label) and green filter (FAM label) proved qualitatively that the rate of transfection was high as most of the dye labelled siRNAs appeared in the cells rather than in the surrounding media (Figure 3.2a, b).

Transfection success could also be determined quantitatively by measuring transfected miRNA mimic levels by qPCR. The cell lines Hela and HEK293 were transfected with chemically designed miRNA mimics (double stranded RNA molecules that imitate biological mature miRNAs). They are very similar to siRNAs but not pre-miRNAs because they do not contain a hairpin. These miRNA mimics when transfected into cells are loaded onto RISC-complexes and using the guide strand are brought over to complementary target sites on the 3´UTR causing downregulation of the gene.

The Hela and HEK293 cell lines were transfected with miR-21 and miR-499 mature miRNA mimics, the miRNAs under investigation in this study. RNA was extracted from the cells and qPCR analysis performed. The transfected levels of miR-21 and miR-499 was measured in these cells compared to the endogenous levels of the miRNAs. Transfected HEK293 cells had a value 15 Cts lower of miR-21 expression than endogenous miR-21 in the untransfected HEK293 cells (Figure 3.2c). Thus transfecting the cells resulted in a 225-fold increase in miR-21 RNA. The endogenous expression of miR-499 was too low to be detected in both Hela and HEK293. However, upon transfection with 30 nM miR-499, miR-499 levels became detectable (Figure

3.2d). These qPCRs display how well the transfection worked as the target miRNA levels successfully increased upon transfection of the mimics.

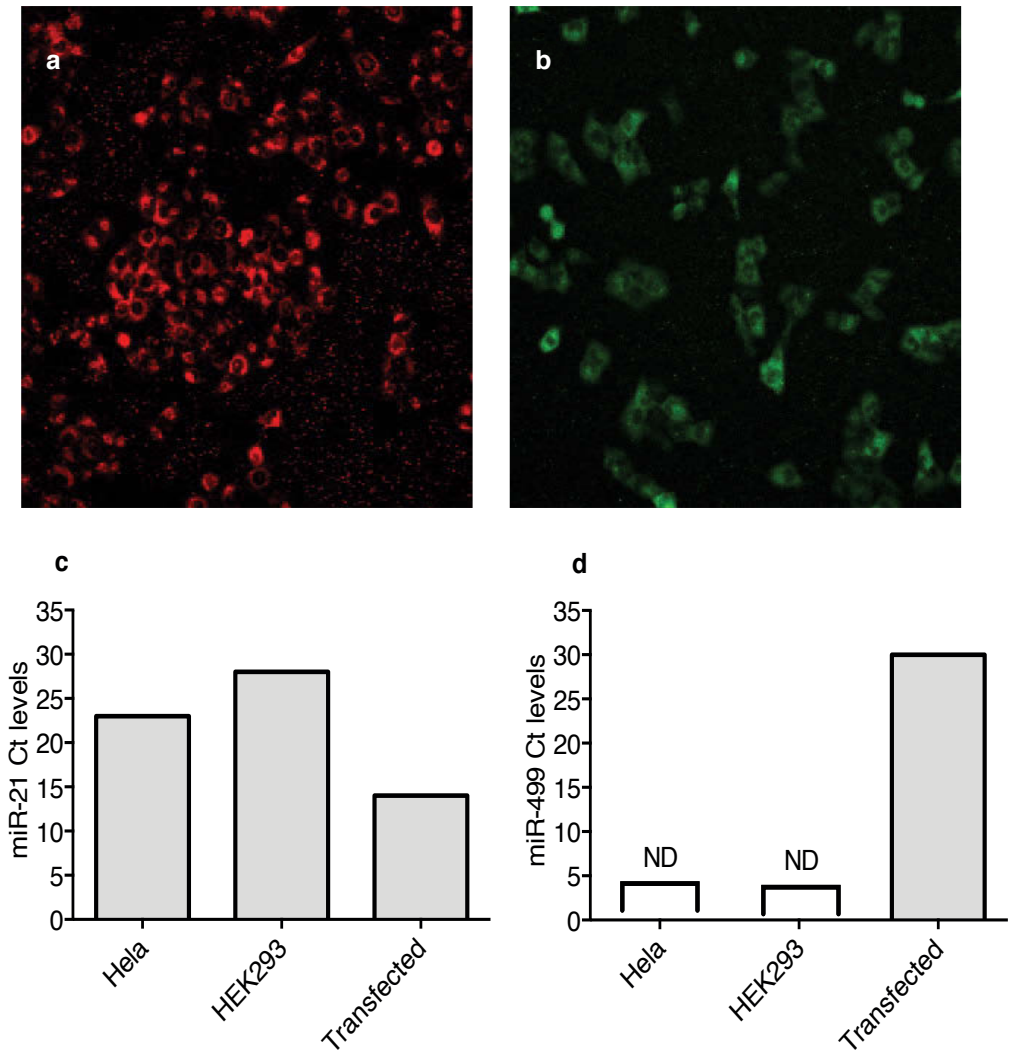

Figure 3.2. Cell lines are successfully transfected with miR-21 and miR-499 miRNA mimics. HEK293 cells were either transfected with 30 nM dye labelled scrambled miRNA mimics, miR-21 miRNA mimic or miR-499 miRNA mimic and imaged under a fluorescent microscope. RNA was harvested from the cells 24 hours post transfection and qPCR conducted to measure the subsequent levels of miRNA in cells. **(a)** Image of HEK293 cells transfected with CY3 tagged miRNA mimic at 20X magnification. **(b)** Image of HEK293 cells transfected with FAM tagged miRNA mimic at 10X magnification. **(c)** Endogenous miR-21 Ct levels in Hela and HEK293 cells and miR-21 Ct levels in miR-21 transfected HEK293 cells. **(d)** Endogenous miR-499 Ct levels in Hela and HEK293 cells and miR-499 Ct levels in miR-499 transfected HEK293 cells.

qPCR examining the levels of PDCD4 revealed the downregulation of this gene by miR-21 and miR-499. The qPCR was conducted on head and neck cancer patient tumour and normal tissues (Refer to Table 3.A) to determine if there was an inverse correlation between PDCD4 levels in normal vs cancerous tissues. PDCD4 was revealed to be downregulated in tumours supporting its functionality as a tumour suppressor in head and neck cancer (Figure 3.3).

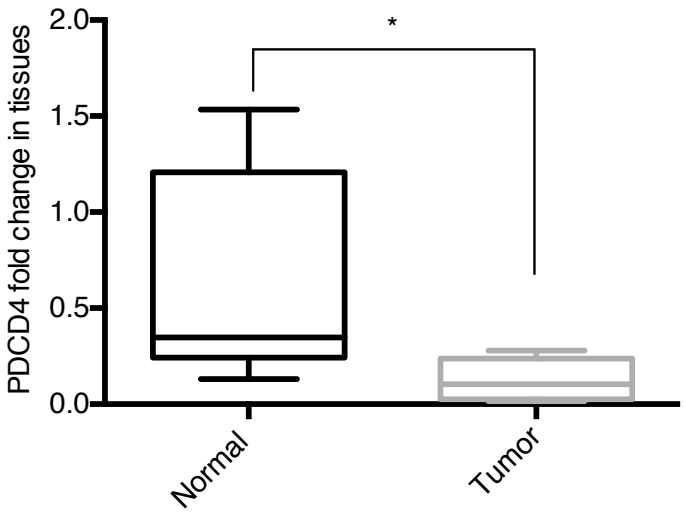

Figure 3.3. The tumour suppressor gene PDCD4 is downregulated in tumour tissues from head and neck cancer patients compared to their corresponding normal tissues. Box plot of PDCD4 level from the normal and tumourigenic tissues of six head and neck cancer patients. The box represents the interquartile range and the line across the box indicates the median value. The PDCD4 fold change was normalised to GAPDH (Error bars are s.e.m. *$p<0.05$, student t test, n=6).

To confirm a direct link between PDCD4 and its regulation by miR-21 and miR-499, a transfection was performed in HEK293 cells. These miRNAs were overexpressed and the resulting PDCD4 expression examined. Ectopic expression of miR-21 caused PDCD4 RNA to be downregulated by about 40% compared to cells transfected with a scrambled miRNA mimic control. miR-499 overexpression caused an approximate 30% decrease compared to the control transfection and both miRNA together decreased PDCD4 RNA by half (Figure 3.4). Protein analysis revealed a 50-60% of PDCD4 in cells overexpressing both miR-21 and miR-499 compared to the transfected miRNA control (Figure 3.5). Therefore, miR-21 and miR-499 decrease PDCD4 expression.

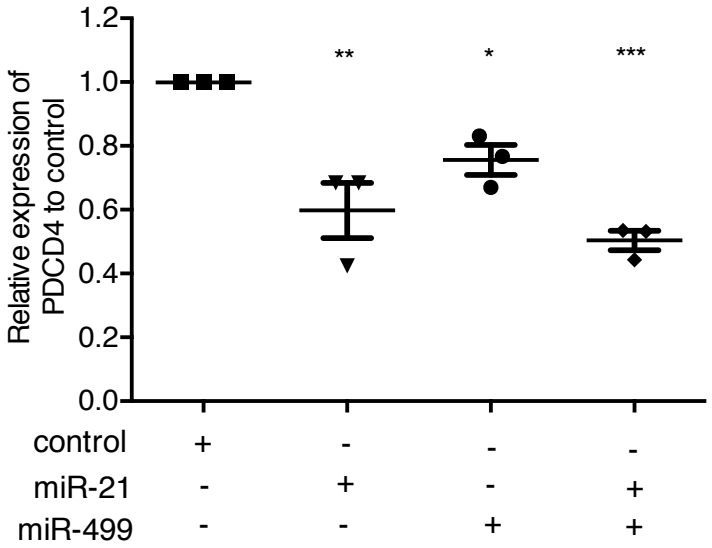

Figure 3.4. PDCD4 is downregulated when miR-21 and miR-499 are overexpressed in cells. HEK293 cells were transfected with 30 nM scrambled control, miR-21 and miR-499 mimics individually and together. qPCR was conducted to measure the levels of PDCD4 relative to the scrambled control (*p<0.05, **p<0.01, ***p<0.005. One-way anova, Dunnett test).

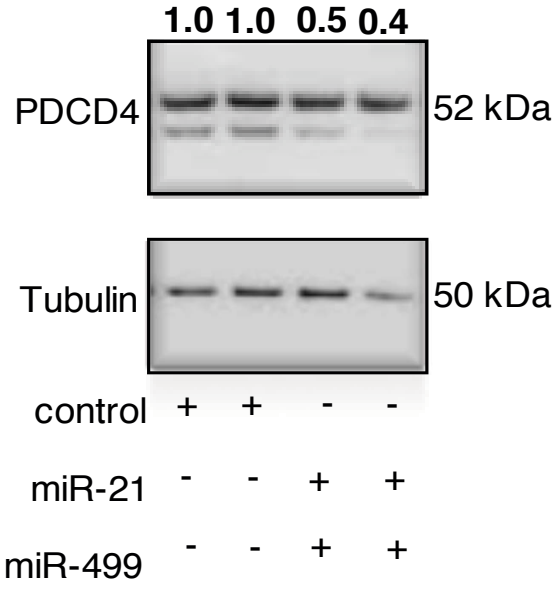

Figure 3.5. PDCD4 is reduced at the protein level when both miR-21 and miR-499 are overexpressed in cells. Protein was harvested from cells transfected with 30 nM scrambled control mimic, miR-21 and miR-499 mimics. Western blot was performed to examine PDCD4 (52 kDa) and Tubulin (50 kDa). The bottom PDCD4 band was normalised to the corresponding tubulin band using ImageJ densitometry. The PDCD4 bands corresponding to miR-21 and miR-499 overexpression were then normalised to the control overexpression bands. The resulting values were plotted above the gel.

3.3.3. The generation of PDCD4 3´UTR WT and mutant vectors

It is currently unknown how PDCD4 is regulated by miR-21 and miR-499, and whether this occurs in a cooperative or independent manner. To determine the mechanism of miRNA regulation of PDCD4, we synthesised 3´UTR mutants of PDCD4 with mutations at the seed sites for miR-21 and miR-499. The second, fifth and seventh nt of the complementary sequence of each miR-21 and miR-499 site on the 3´UTR was mutated to prevent binding by the miRNA (Figure 3.6). The process of cloning is described and summarised in Figure 3.6.

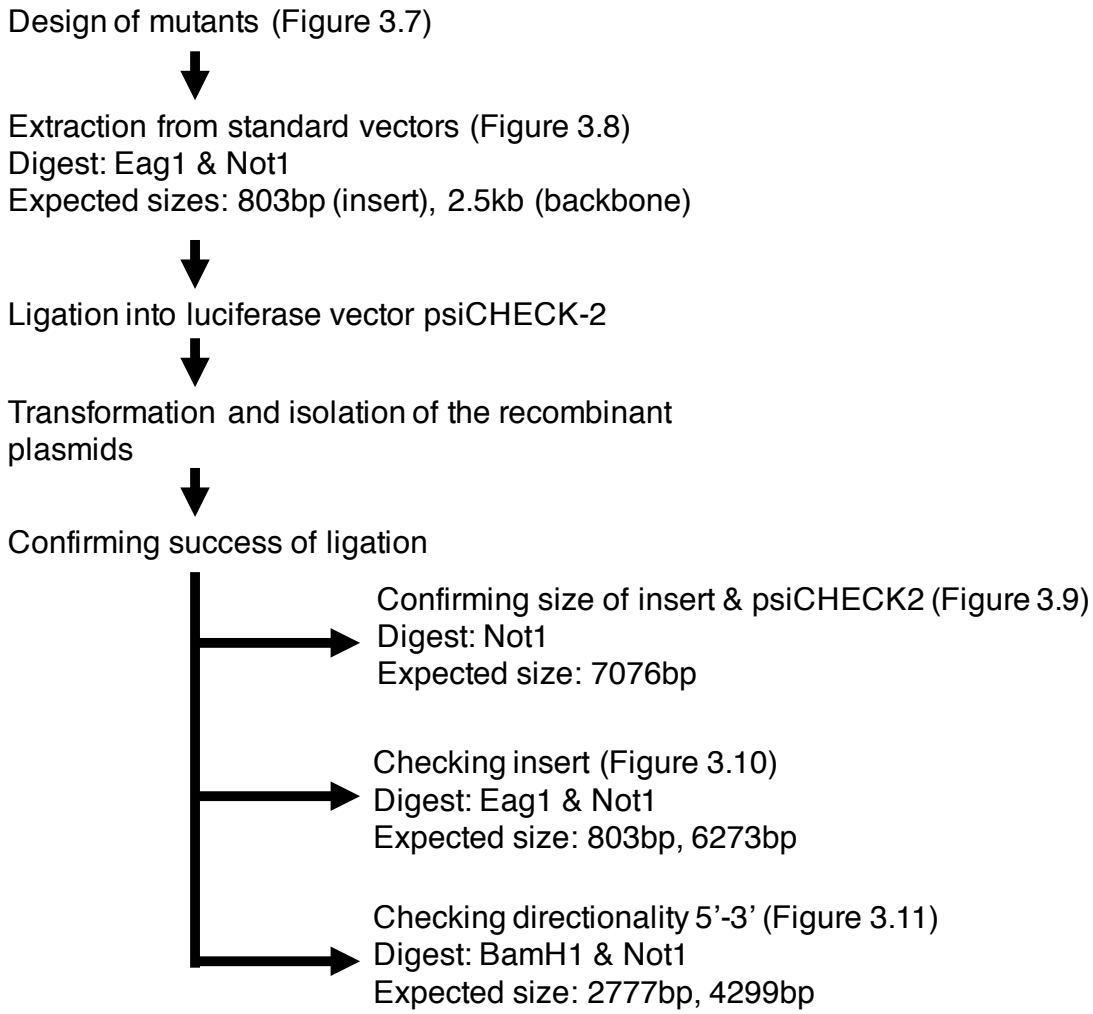

Figure 3.6. Cloning flowchart of PDCD4 WT and mutant 3´UTRs into the luciferase vector psiCHECK-2.

This resulted in five constructs with a psiCHECK-2 backbone harbouring either the PDCD4 3´UTR – pWT, p499/M1 – referring to mutation of the first miR-499 binding site, p21/M2 – referring to mutation of the miR-21 binding site, p499/M3 – referring to mutation of the second miR-499 binding site and p499/M4 – referring to mutation of the third miR-499 binding site (Figure 3.7).

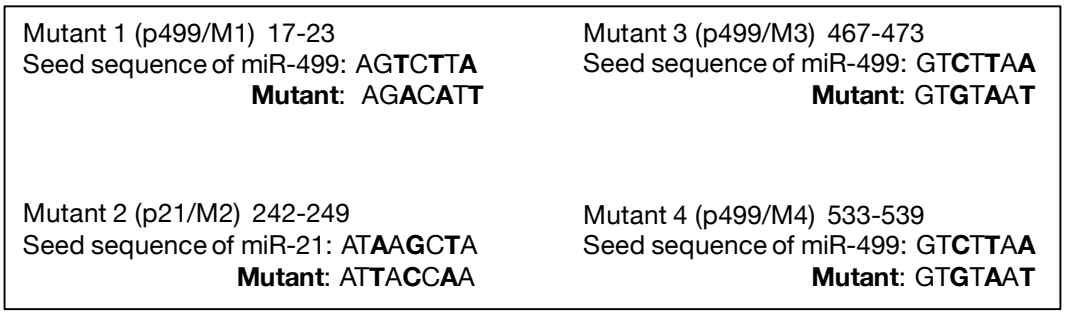

Figure 3.7. miR-21 and miR-499 binding sites on the 3´UTR of PDCD4 showing mutations at the 3rd, 5th and 7th nucleotides. The first miR-499 site is located at nucleotides 17-23 of the PDCD4 3´UTR (p499/M1). The miR-21 site is nucleotides 242-249 (p21/M2), the second miR-499 site is at nucleotides 467-473 (p499/M3) and the third miR-499 site is at nucleotides 533-539 (p499/M4).

3.3.4. Subcloning the miR-21 and miR-499 mutants into psiCHECK-2

The PDCD4 3´UTRs were digested from the pMA backbone with EagI and NotI restriction enzymes into the reporter vector. A 1% agarose gel electrophoresis was performed of the digests and an expected band of 803 bp was detected for each of the PDCD4 3´UTRs (Figure 3.8).

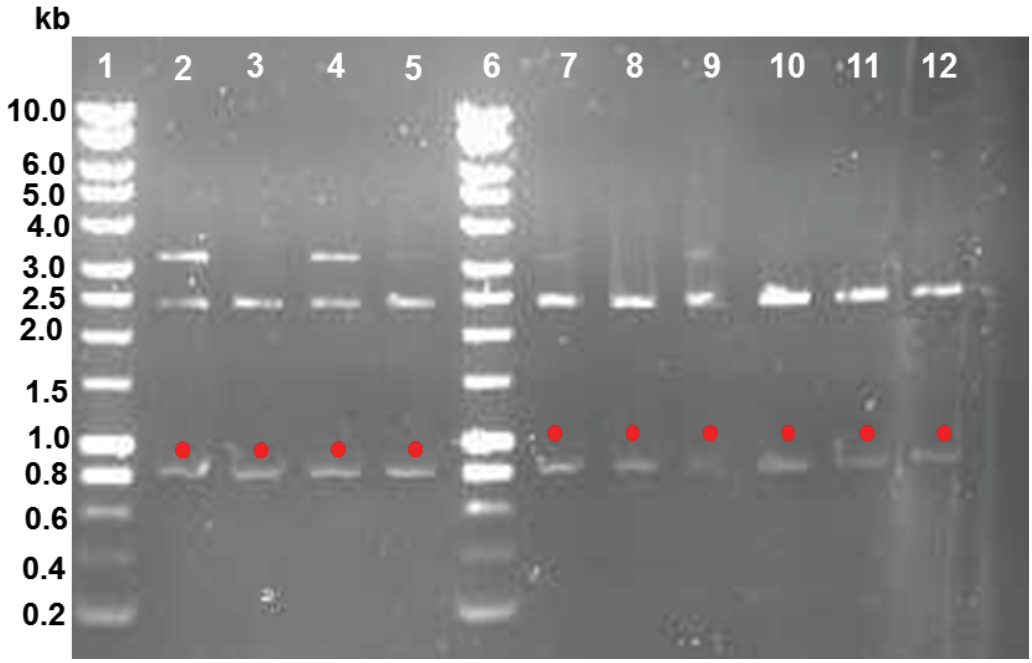

Figure 3.8. Restriction endonuclease digests for PDCD4 3´UTR inserts from the original vector. Lane 1: hyperladder 1 kb (Bioline, Australia), Lane 2-3: clones of pWT, Lane 4-5: clones of p499/M1 (EagI), Lane 6: hyperladder 1 kb (Bioline, Australia), Lane 7-8: clones of p21/M2 (EagI), Lane 9-10: clones of p499/M3 (EagI), Lane 11-12: clones of p499/M4 (EagI). PCR products showing the insert (803 bp) is marked with red dots.

The PDCD4 3´UTR inserts were then subcloned into the psiCHECK-2 backbone containing two luciferase genes – Firefly and Renilla. To screen positive clones, single digests with NotI revealed expected sizes of approximately 7082 bp - the combined size of the 3´UTR (803 bp) and psiCHECK-2 (6273 bp) (Figure 3.9). Further single digest with EagI would drop out the insert but also digest another part of the vector resulting in three bands. This restriction endonuclease digest pattern would indicate a successful ligation of the insert to the luciferase vector (Figure 3.9).

Figure 3.9. Restriction digests of mutants confirming PDCD4 insert. Lane 1-2: Hyperladder 1 kb), Lane 3-4: clones of p21/M2 (NotI), Lane 5-6: clones of p499/M1 (NotI), Lane 7-8 clones of p499/M4 (NotI), Lane 9-10: clones of p499/M3 (NotI), Lane 11: clone of pWT (NotI), Lane 12-13: clones of p21/M2 (EagI), Lane 14-15: clones of p499/M1 (EagI), Lane 16-17: clones of p499/M4 (EagI). Lane 18-19: clones of p499/M3 (EagI), Lane 20: pWT (EagI). PCR products showing the insert (803 bp) are marked with red dots.

To determine orientation of the 3´UTR, due to the compatible NotI (5´-GC^GGCCGC-3´) and EagI (5´-C^GGCCG-3´) sites, the plasmid was digested with BamHI (NEB, USA). An antisense configuration would give two bands of approximately 3.5 kb whereas a sense orientation would yield two bands of approximately 2.8 and 4.3 kb (Figure 3.10a,b).

This resulted in five PDCD4 3´UTR recombinant vectors that could now be used in luciferase assays to measure the silencing activity of miR-21 and miR-499 at their binding sites on the 3´UTR (Figure 3.11).

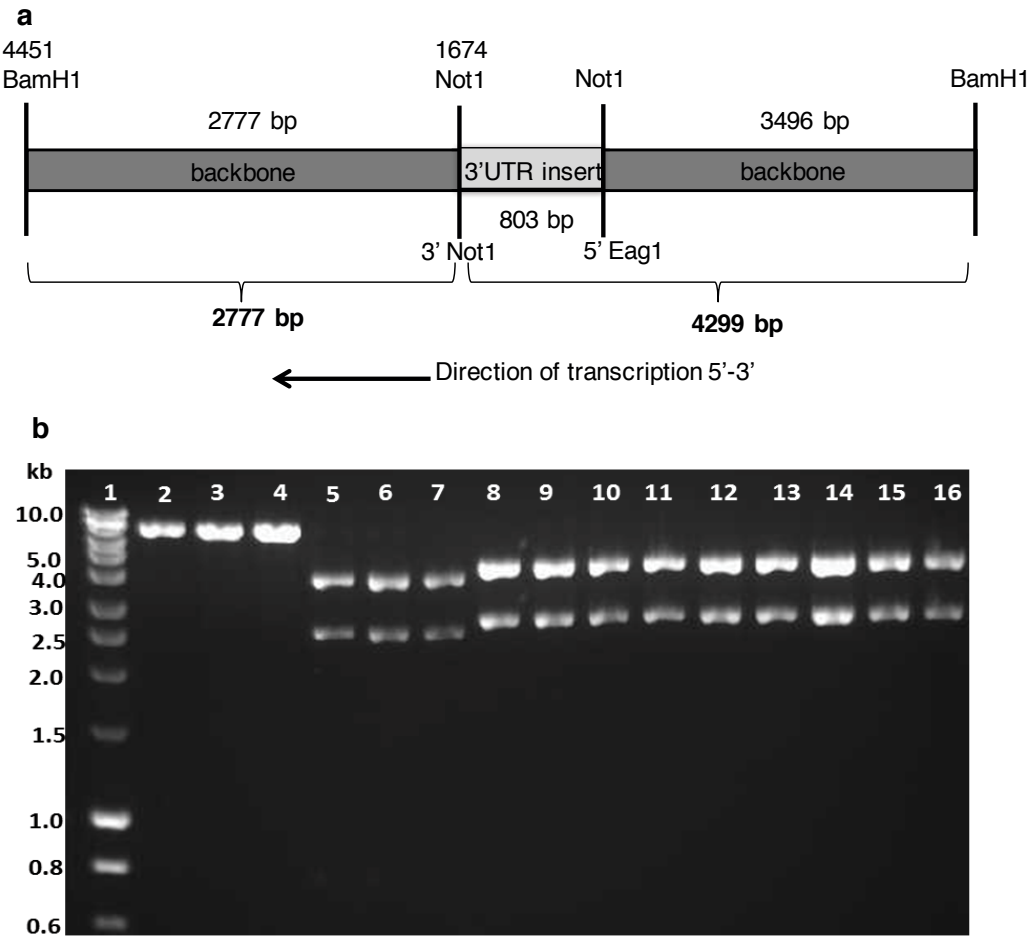

Figure 3.10. Checking directionality of the 3´UTR PDCD4 inserts into psiCHECK-2. (a) Schematic of the directionality of BamHI and NotI double digests with the PDCD4 3´UTR and psiCHECK-2 backbone ligations. **(b)** Restriction digests of mutants determining directionality. Lane 1: Hyperladder 1 kb, Lane 2-4: clones of p499/M3 (NotI), Lane 5-7: products of unrelated project, Lane 8-9: clones of p499/M4 (BamHI & NotI), Lane 10: p499/M3 (BamH1 & Not1), Lane 11-12: clones of p21/M2 (BamHI & NotI), Lane 13-14: clones of p499/M1 (BamH1 & Not1), Lane 15-16: clones of pWT (BamHI & NotI).

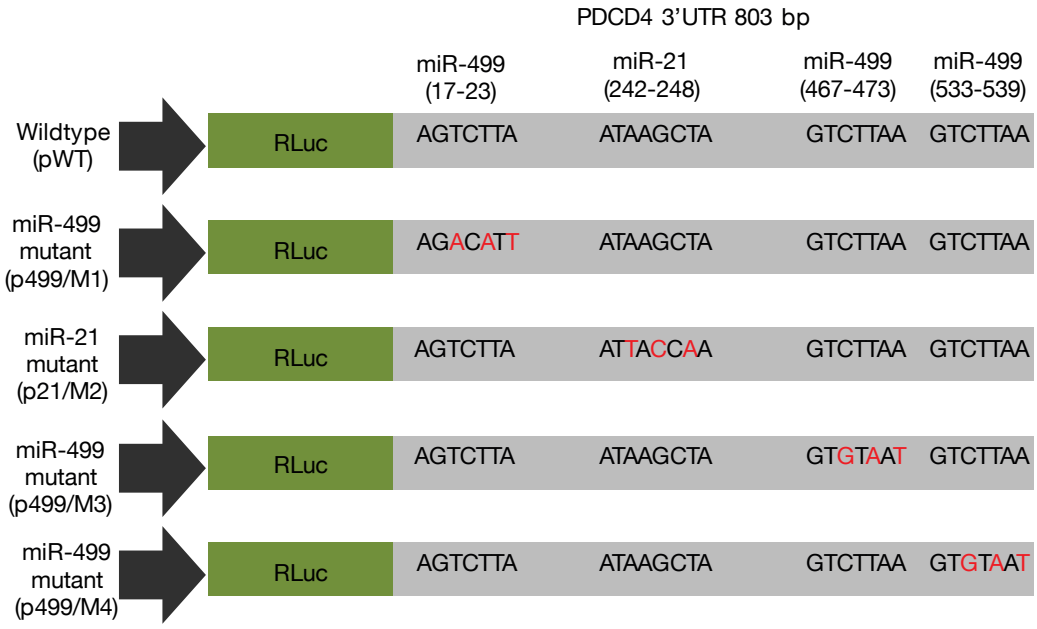

Figure 3.11. Schematic of WT and the four miR-21 and miR-499 binding sites mutants used in this study. Each construct was synthesised using Invitrogen GeneArt and then subcloned into psiCHECK-2 luciferase expression vectors.

3.3.5. miR-21 and miR-499 regulate the luciferase reporter ligated to the PDCD4 3´UTR in luciferase assays

Dual luciferase assays were conducted to determine the contribution of each miR-21 and miR-499 site to the regulation of PDCD4. Two concentrations (20 and 30 nM) of miRNA mimics - the scrambled control and miR-21 were used to determine which concentration gave optimal regulation of the WT PDCD4 3´UTR vector (pWT). At a concentration of 20 nM scrambled control and miR-21 there was no difference in the relative luciferase activity (expression of firefly/renilla) between the control and miR-21 transfected cells (Figure 3.12). The 30 nM concentration of miRNA mimics resulted in a 30% decrease of luciferase activity between the control and miR-21 transfected cells (Figure 3.12). Hence 30 nM was selected as the optimal concentration for transfection of the miRNA mimics into cells.

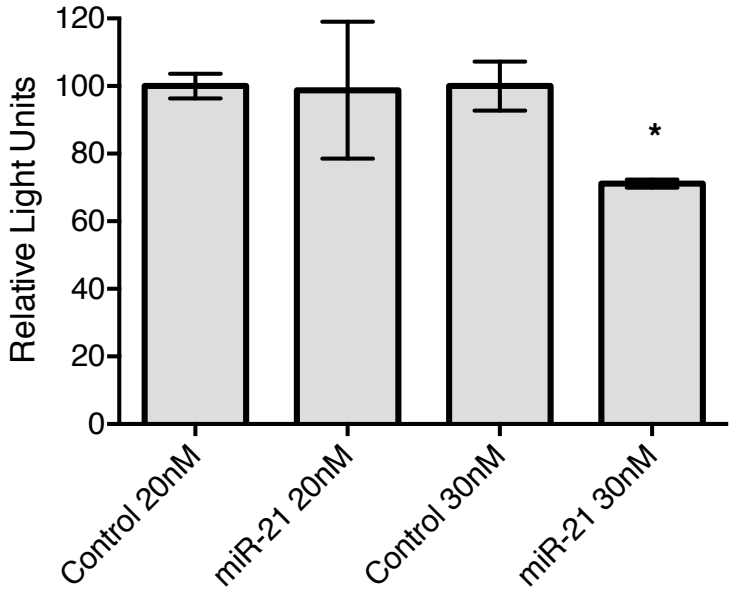

Figure 3.12. Optimising miRNA concentration for luciferase activity. HEK293 cells were co-transfected with either a miR-21 mimic or miRNA control in combination with the psiCHECK-2 vector harbouring the WT PDCD4 3′UTR pWT. The data indicates the relative repression of firefly luciferase expression standardised to the internal control, Renilla luciferase. (Error bars are s.e.m. n=3. *p<0.05. One-way anova, Dunnett test).

We experienced some inconsistency while using the miRNA mimic between luciferase assays. Thus an alternative miRNA that did not bind to the 3´UTR of PDCD4 was sought using TargetScan (Appendix 1, Figure A1). *Let-7a* was chosen and evaluated as a substitute for the miRNA/negative control (Figure 3.13a).

Two time points, 24 and 48 hours were examined to reveal if a difference in regulation of the chimeric PDCD4 3´UTR vectors was noticeable by miR-21 and miR-499. Co-transfection of pWT (WT 3´UTR) and the miRNA mimics at 30 nM revealed an approximate 30% decrease of luciferase activity with the miR-21 and miR-499 transfected cells compared to the *let-7a* transfected cells (Figure 3.13b,c). With the miR-21 site mutated plasmid, p21/M2 there was a minimal decrease of luciferase activity when miR-21 was overexpressed compared to the *let-7a* control (Figure 3.13b,c). However, there was about a 50% decrease of luciferase activity with the p21/M2 vector with an overexpression of miR-499 in cells (Figure 3.13b,c). Similar results were obtained at 24 and 48 hours and thus regulation of the vectors by miR-21 and miR-499 remained the same up to 48 hours (Figure 3.13b,c). Based on these results, *let-7a* was utilised as a suitable control for all following transfections.

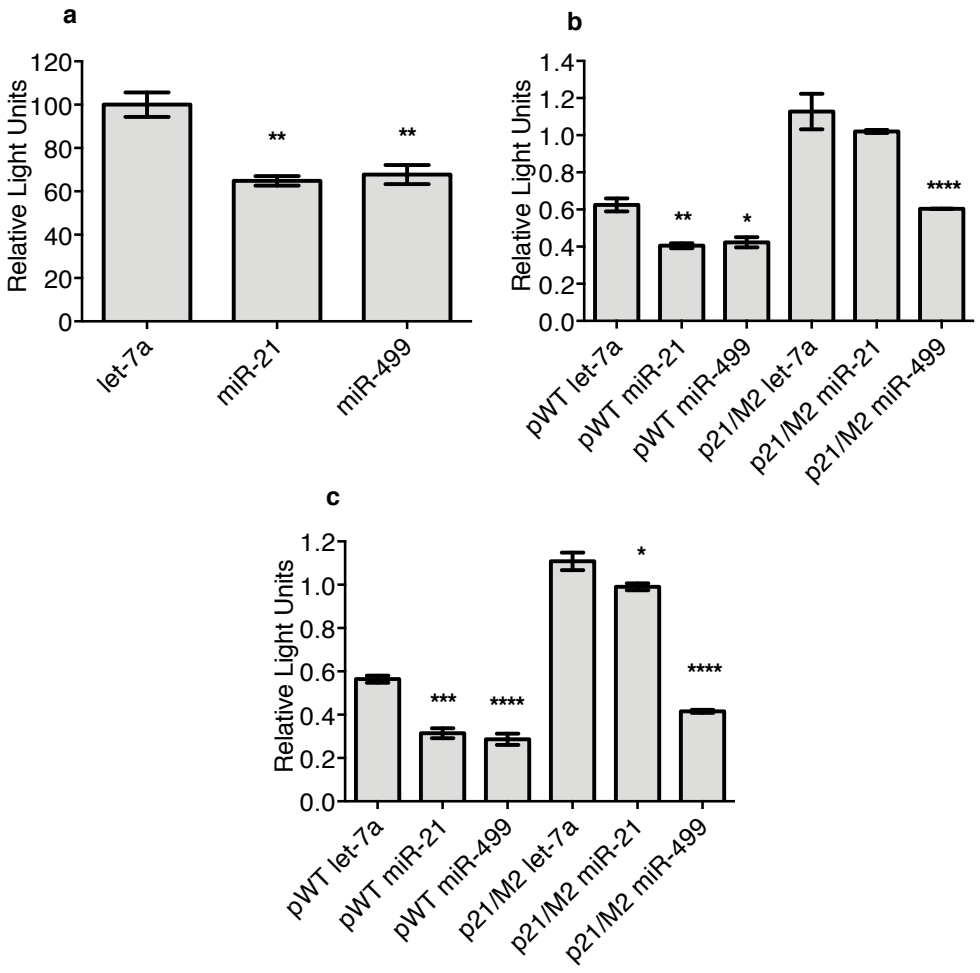

Figure 3.13. Optimising *let-7a* as a control for miRNA mimic overexpression. HEK293 cells were co-transfected with 30 nM of *let*-7a, miR-21 or miR-499 in combination with the WT PDCD4 3´UTR, pWT or miR-21 site mutant, p21/M2. **(a)** Luciferase activity at 24 hours of miRNA transfected HEK293 cells in combination with the pWT plasmid **(b)** Luciferase activity at 24 hours of miRNA transfected HEK293 cells with the vectors pWT or p21/M2. **(c)** Luciferase activity at 48 hours of miRNA transfected HEK293 cells with the vectors pWT or p21/M2. The data indicates the relative repression of firefly luciferase expression standardised to the internal control, Renilla luciferase. (Error bars are s.e.m. n=3. *p<0.05, **p<0.01, ***p<0.001, ****p<0.0001. One-way anova, Dunnett test).

3.3.6. The first miR-499 site on the PDCD4 3´UTR is redundant

The WT PDCD4 3´UTR and mutant constructs were then used to determine miRNA interaction at the PDCD4 3´UTR. Cells expressing the pWT vector in combination with either miR-21 or miR-499 resulted in an approximate 40% reduction in luciferase expression (Figure 3.14a). Cells transfected with the miR-21 site mutant vector p21/M2 and miR-21 showed an impaired regulation of the 3´UTR. However in cells harbouring p21/M2 and miR-499 mimic there was still a notable reduction in luciferase activity of ~60% (Figure 3.14b). Thus miR-499 was able to downregulate the 3´UTR without miR-21.

In cells overexpressing the first miR-499 site mutated vector p499/M1, we observed downregulation of 50% by miR-21 and 40% by miR-499 for the luciferase reporter. This suggested that the first miR-499 site was redundant. We then sought to understand the contribution of the remaining miR-499 sites.

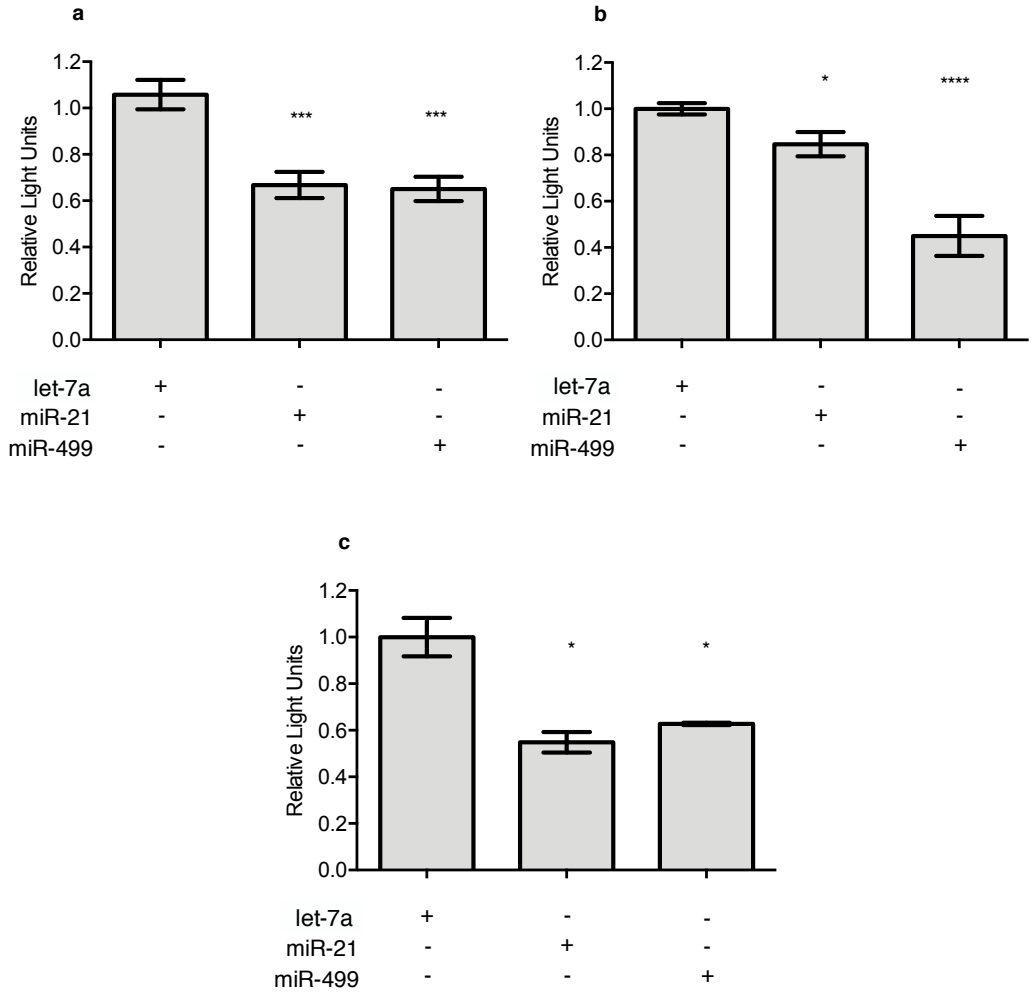

Figure 3.14. Measuring the silencing contribution of the first miR-499 site. HEK293 cells were co-transfected with 30 nM of *let*-7a, miR-21 or miR-499 in combination with the WT PDCD4 3´UTR, pWT, miR-21 site mutant, p21/M2 or first miR-499 site mutant, p499/M1. **(a)** Luciferase activity of the miRNA transfected HEK293 cells in combination with the pWT vector. **(b)** Luciferase activity of the miRNA transfected HEK293 cells in combination with the p21/M2 vector. **(c)** Luciferase activity of the miRNA transfected HEK293 cells in combination with the p499/M1 vector. (Error bars represent s.e.m. n=3. *p<0.05, **p<0.01, ***p<0.005. One-way anova, Dunnett test).

To further examine the potential redundancy of the first miR-499 site, we transfected HEK293 cells with miR-499 at varying concentrations to determine silencing efficacy. This was achieved by calculating the IC_{50} value in cells transfected with pWT compared to the first miR-499 site mutated vector, p499/M1. It was shown that the suppression of the target in p499/M1 and pWT by miR-499 was overlapping (IC_{50} 0.139±0.06 vs 0.081±0.052). Therefore, the first miR-499 site on the PDCD4 3´UTR is not an active site for miRNA mediated regulation (Figure 3.15).

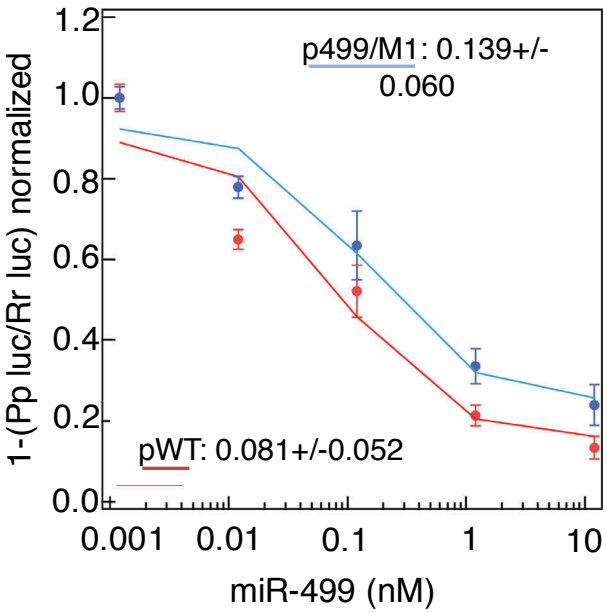

Figure 3.15. Silencing efficacy of the first miR-499 site. HEK293 cells were transfected with a concentration range of 0.0012-12nM miR-499 mimic in combination with either pWT or p499/M1. Cells were harvested at 24 hours and luciferase assays were performed to measure the firefly and renilla activities which were then normalised. The IC_{50} and propagated error were determined. The lines denote p499/M1 (blue) vs pWT (red). (Error bars are propagated error, n=2).

3.3.7. The last two miR-499 sites are co-dependent

Luciferase assays were also conducted to examine the regulation of the last two miR-499 sites on the PDCD4 3′UTR. In this instance we transfected the p499/M3 vector which harbours the second mutated miR-499 site in combination with miR-21 and miR-499. To our surprise, we observed no suppression of the reporter in cells overexpressing miR-499. Cells overexpressing miR-21 and p499/M3 were still able to elicit significant silencing (Figure 3.16a). This exact observation also occurred with mutant p499/M4 where miR-499 overexpression was not able to mediate suppression of the 3′UTR (Figure 3.16b). Therefore, it seems that the last two miR-499 sites are co-dependent as both sites are necessary to inhibit expression of the PDCD4 3′UTR reporter by miR-499. Moreover, miR-21 does not require miR-499 for regulation of the reporter.

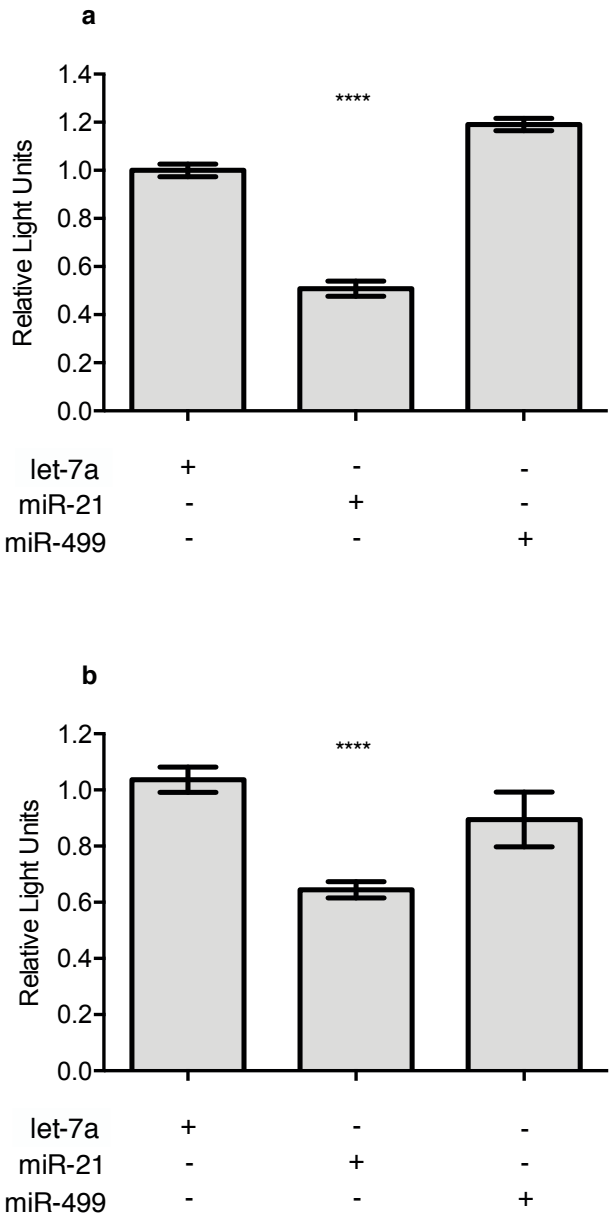

Figure 3.16. The regulatory function of adjacent miR-499 target sites is co-dependent. HEK293 cells were co-transfected with 30 nM of *let*-7a, miR-21 or miR-499 in combination with the PDCD4 3´UTR miR-499 site mutant vectors – p499/M3 and p499/M4. **(a)** Luciferase activity of the miRNA transfected HEK293 cells in combination with the second miR-499 site mutant vector, p499/M3. **(b)** Luciferase activity of the miRNA transfected HEK293 cells in combination with the third miR-499 site mutant vector, p499/M4 vector. (Error bars are s.e.m. n=3. ****p<0.0001. One-way anova, Dunnett test).

3.3.8. miR-21 contributes to miR-499 silencing efficacy

Although miR-499 can act independently of miR-21 there is a possibility that overall silencing of PDCD4 by miR-499 may be reliant on miR-21. To further dissect this regulation, cells were transfected with pWT and the miR-21 site mutated vector, p21/M2 in combination with increasing amounts of the miR-499 mimic. The results indicated that the cells with p21/M2 had an approximately ten-fold increase in the IC_{50} when compared to cells with pWT (0.176 vs 0.0175). This implies that the available miR-21 site enhances the efficacy of miR-499 suppression by ten-fold (Figure 3.17a).

To further investigate this regulation, we then transfected cells with pWT in combination with miR-21 (30 nM) and *let-7a* (30 nM) with increasing levels of miR-499. Cells overexpressing miR-21 had a lower IC_{50} value than the control transfection cells (0.0043±0.003 vs 0.093±0.1). This illustrated that miR-21 promotes through an unknown mechanism miR-499 silencing efficacy of the target PDCD4 (Figure 3.17).

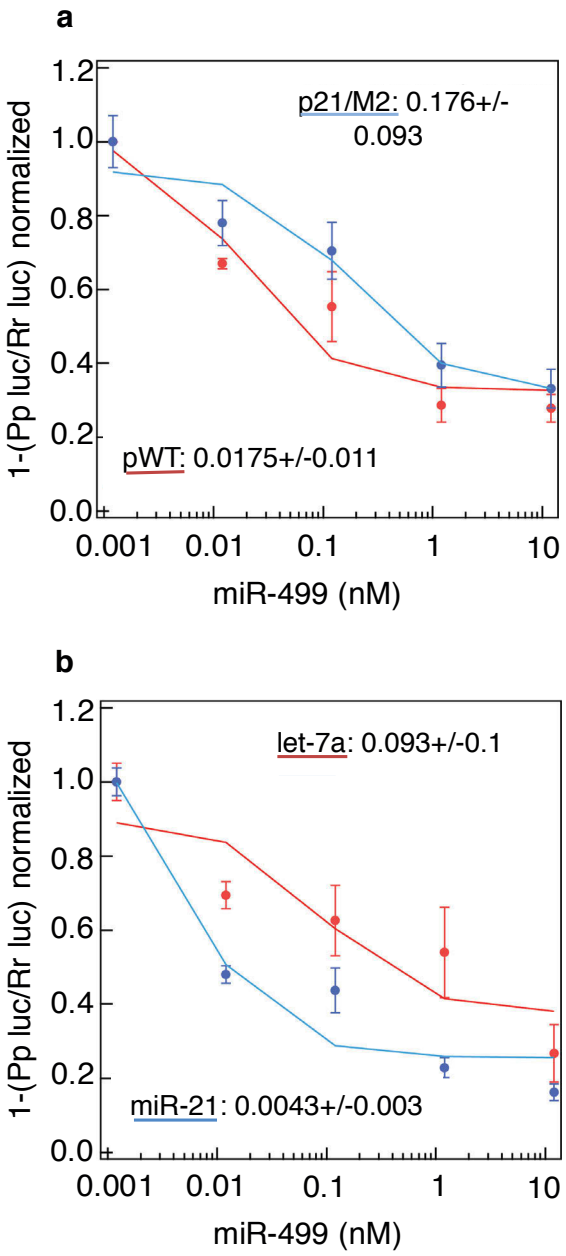

Figure 3.17. miR-21 contributes to miR-499 mediated downregulation of PDCD4. (a) Assay of p21/M2 (blue) vs pWT (red) with miR-499 concentrations of 0.0012-12nM. **(b)** Assay of pWT with *let-7a* miRNA overexpressed (red) vs miR-21 overexpressed (blue) with different miR-499 concentrations. (Error bars are propagated error. n=2).

The co-regulation of PDCD4 by miR-21 and miR-499 as shown in this results chapter is summarised in Figure 3.18. The first miR-499 site is redundant. In contrast miR-21 regulates the 3´UTR independently and can also aid regulation of the last two miR-499 sites. The last two miR-499 sites require co-dependent regulation by miR-499 but can interact with the 3´UTR independently of the miR-21 miRNA and binding site.

Figure 3.18. Schematic of PDCD4 3´UTR summarising the role and different types of regulation of the miR-21 and miR-499 sites. The miR-21 site is regulated in an independent manner, however miR-21 interaction with this site aids miR-499 interactions with the last two miR-499 sites. The first miR-499 site is redundant and the last two miR-499 sites are regulated in a co-dependent manner but are still functionally independent of miR-21.

3.3.9. Is Ago2 the primary Argonaute involved in mediating miR-21 and miR-499 targeting of the PDCD4 3´UTR?

Broderick et al., showed that the RISC complex formed with Ago1, 3 or 4 tended to regulate sites on the 3´UTR in a cooperative manner. Whereas Ago2-RISC targets the 3´UTR in an independent manner from other target sites on the 3´UTR [265]. This led to the idea that perhaps miR-21 is loaded onto Ago2-RISC complexes and miR-499 is loaded onto another Ago. Hence there would be different mechanisms towards inhibiting the PDCD4 3´UTR (Figure 3.19). The main caveat with this approach was that it was not certain if miR-499 which is involved in co-dependent regulation would necessarily be loaded by Ago1, 3 or 4 like cooperative miRNAs are.

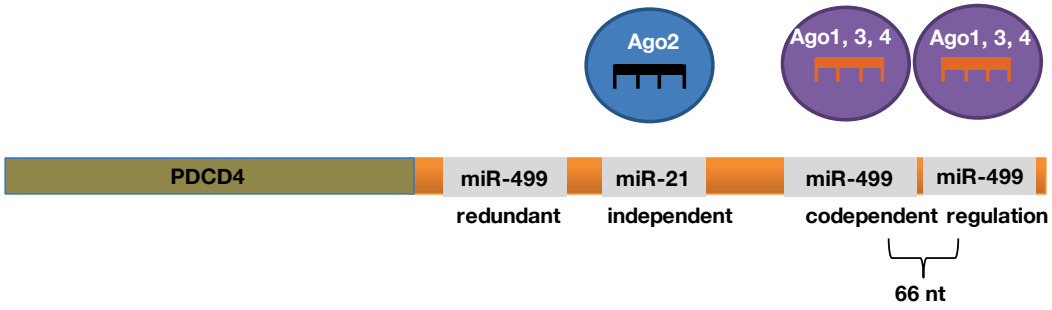

Figure 3.19. Differential Ago loading model. Schematic of the PDCD4 gene and the 3´UTR showing the miR-21 and miR-499 seed sites and their different modes of regulation. Ago2 carries miR-21 to its site for independent downregulation of the 3´UTR whereas Ago1, 3 or 4 carry miR-499 over for co-dependent downregulation.

3.3.9.1. Differential loading of miRNAs by Ago2 using an inducible Ago2 knock down shRNA cell line

In order to examine whether Ago2 was differentially loading miR-21 and miR-499, Western blots were conducted using protein from a tetracycline inducible Ago2 KD shRNA HEK293 cell line [304]. The cells were transfected with 30 nM of scrambled control, miR-21 and miR-499 miRNA mimics. Tetracycline (10 μg/ml) was added four hours later to induce (+) cells or otherwise left non-induced (-). Protein was harvested from the cells at 96 hours post-transfection (optimal KD of Ago2 was achieved at this time point – see Appendix 2, Figures A2-5), Western blotting was then performed and stained with Ago2, PDCD4 and tubulin (loading control) specific antibodies. The KDs gave variable results when compared to the non-induced cells (Figure 3.20). Thus an alternative method was utilised to examine differential loading of miR-21 and miR-499 by Ago2.

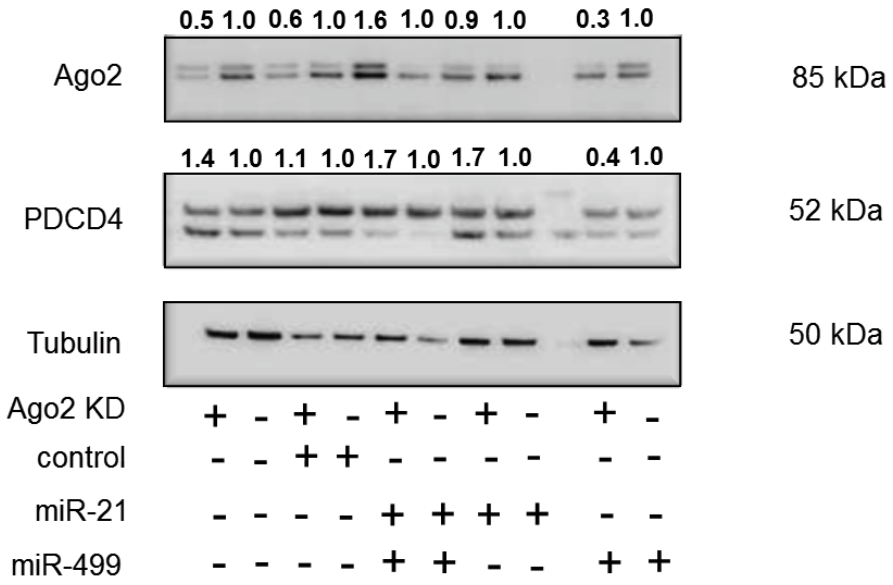

Figure 3.20. Protein levels of PDCD4 is reduced when Ago2 is KD at 96 hours. Inducible Ago2 shRNA cells were induced with tetracyline (+) or not induced (-), transfected with control, miR-21 and miR-499 and protein harvested at 96 hours. Ago2 and PDCD4 bands were normalised to tubulin bands using ImageJ densitometry and the inducible KD (+) normalised to the corresponding non-induced band (-). **(a)** Ago2 levels were measured on the Western blots and imaged for a band at 85 kDa. **(b)** PDCD4 levels were measured on the westerns and imaged for a band at 52 kDa. **(c)** Tubulin levels were measured on the western and imaged for a band at 50 kDa.

3.3.9.2. Testing differential loading of miRNAs with Ago2 targeting siRNAs reveals that both miRNAs appear to be loaded by Ago2

To determine whether Ago2 was loading either miR-21 and/or miR-499, we depleted Ago2 in the cell using an siRNA. This involved transfecting HEK293 cells with 40 nM of Ago2 specific targeting siRNA (siAgo2) or a scrambled control siRNA (single transfection) or transfecting the siRNA again 24 hours later (double transfection). This approach would ensure maximum KD of Ago2 by doubling the amount of siRNA with reduced toxicity to the cells. The cells were then harvested 48 hours after transfection and RNA expression of Ago2 measured. The transfection was efficient with an 80% reduction in the amount of Ago2 RNA with both the single and double transfections (Figure 3.21).

The efficacy of the KD was also measured at the protein level, which confirmed approximately 70-80% of Ago2 levels were reduced in both the single and double transfections when comparing the siAgo2 transfected samples to the control (Figure 3.22).

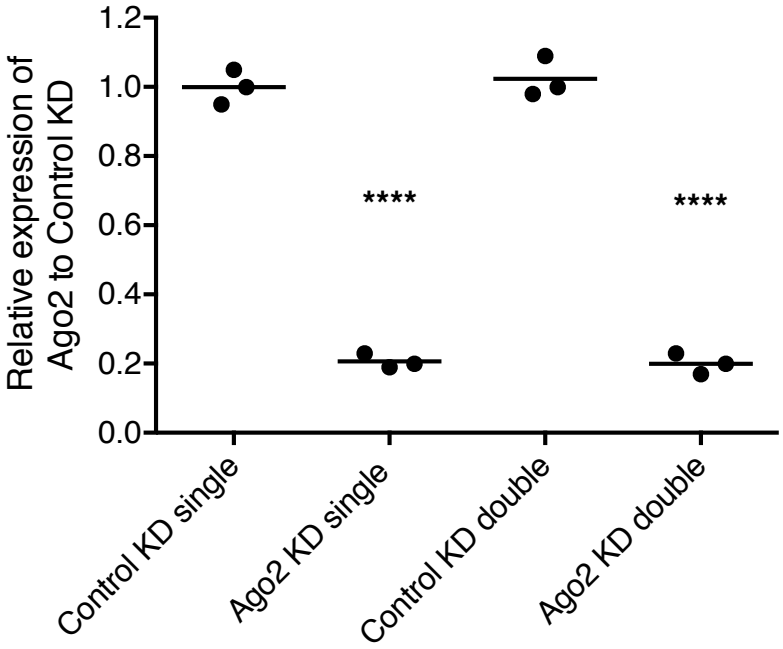

Figure 3.21. Ago2 is reduced when siAgo2 is transfected into cells.
HEK293 cells were transfected with siAgo2 and a control siRNA at 30 nM (single)**.** A secondary transfection was repeated 24 hours later with the siRNAs (double). RNA was harvested 24 hours later and qPCR conducted to measure Ago2 levels. RNA was normalised to the housekeeping gene Glyceraldehyde 3-phosphate dehydrogenase (GAPDH) and fold change made relative to control KD to give relative expression of Ago2. (Error bars are s.e.m. n=3. ****p<0.0001, One-way anova, Dunnett test).

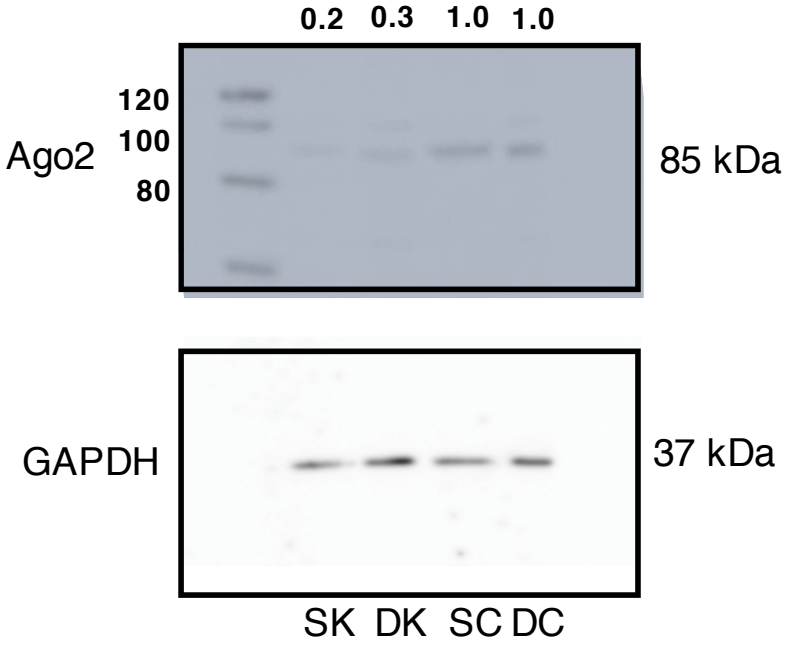

Figure 3.22. Ago2 expression is reduced at the protein level when siAgo2 is transfected into cells. Protein was harvested from cells with a single transfection (siAgo2 SK, control siRNA SC) and a double transfection (siAgo2 DK, control siRNA DC). Western blot was performed to examine Ago2 (85 kDa) and GAPDH (37 kDa). Densitometry was performed with ImageJ and the Ago2 bands were normalised against the GAPDH bands. The Ago2 KDs were normalised to the control bands and the resulting values plotted above the blots.

Analysis of the RNA and protein from the siAgo2 transfected cells showed efficient KD of Ago2. A luciferase assay was conducted in this depleted background to determine whether the wild type PDCD4 3´UTR, pWT could be regulated when miR-21 and miR-499 was overexpressed in cells. The RNA expression of Ago2 was measured from the luciferase wells and shown to be effectively reduced by about 80% between the siAgo2 and control transfected cells (Figure 3.23). The amount of miR-21 RNA was measured to test the outcome of the Ago2 KD and found to be reduced by 60% in cells transfected with siAgo2 (Figure 3.23).

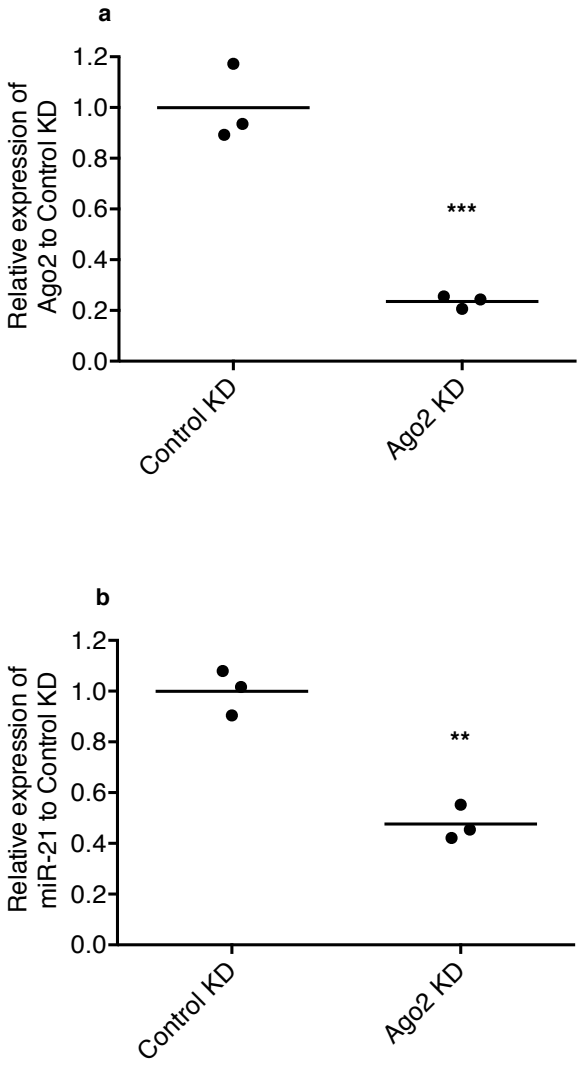

Figure 3.23. Reduction of Ago2 RNA levels by targeting siRNAs. HEK293 cells were transfected with siAgo2 and a control siRNA at 30 nM and the RNA harvested 24 hours later. RNA was harvested from cells and qPCR conducted. The expression of genes was normalised to reference gene GAPDH and then normalised to control KD to give relative expression **(a)** relative expression of Ago2 **(b)** relative expression of miR-21. (Error bars are s.e.m. n=3. **p<0.01, ***p<0.001. One-way anova, Dunnett test).

After confirming the KD status of Ago2, HEK293 cells were transfected with either a control siRNA or siAgo2 and then co-transfected with *let-7a*, miR-21, miR-499 or both miRNA. Cells transfected with miR-21 and/or miR-499 had similar suppression of luciferase activity with or without Ago2. The results suggest that even when Ago2 levels are decreased by about 80% and miRNA expression is reduced by half, miR-21 and miR-499 are still capable of regulating the 3´UTR PDCD4 reporter in these conditions (Figure 3.24).

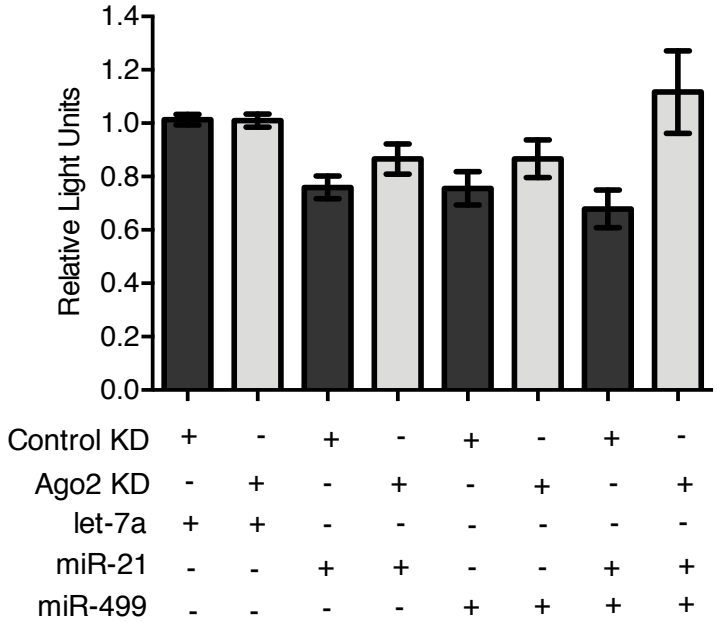

Figure 3.24. miR-21 and miR-499 downregulate the activity of the PDCD4 3´UTR reporter even in Ago2 reduced conditions. HEK293 cells were co-transfected with the chimeric psiCHECK-2 vector ligated to the WT PDCD4 3´UTR and control siRNA, siAgo2, *let-7a*, miR-21 and/or miR-499. The data presents the relative repression of firefly luciferase expression standardised to an internal control, renilla luciferase. Luciferase activity was measured to determine the extent of regulation of the PDCD4 3´UTR by the miRNAs. (Error bars are s.e.m. n=3).

3.4. Discussion

There is an abundance of literature on the role and function of PDCD4 in various cancers. Despite PDCD4 being a known tumour suppressor, the regulation of this gene is poorly understood. Here we investigated the regulation of this crucial tumour suppressor in head and neck cancer and uncovered an interdependent target regulation of the gene by miRNAs. It was found that the 3´UTR of PDCD4 was subjected to different modes of regulation by miR-21 and miR-499.

The luciferase assays revealed that the 3´UTR of PDCD4 is differentially regulated by the oncomiRs miR-21 and miR-499 via three possible mechanisms. The first miR-499 site was proven redundant as the downstream sites of miR-21 and miR-499 were still able to induce silencing at the same efficiency. The redundancy of the first miR-499 site is not surprising due to its proximity to the 5´ end of the 3´UTR (17-23 nts). It is known that during translation the ribosome moves through the mRNA past the stop codon into approximately the first 15 nt of the 3´UTR. The presence of the ribosome would remove any bound RISC complexes and prevent binding until ribosomal drop off [254,311]. This only occurs when translation is inhibited at the elongation step by miRNA bound RISC rather than initiation [264,312-315]. However, the presence and conservation of the first miR-499 site would suggest that it has some role. Perhaps under different circumstances there is an alternative polyA site which places the first miR-499 site further away from the open reading frame (ORF) hence restoring functionality.

Investigation into the last two miR-499 sites revealed that a disruption to either of these sites prevented miR-499 targeting which would suggest a co-dependency between the sites. Broderick et al., 2011 reported that the distance between miRNA binding sites could determine if the miRNA silences the 3´UTR in either an independent or cooperative manner [265]. In this instance the distance between the last two miR-499 sites on PDCD4 is

greater than the 19 nt reported for cooperative binding. The last two miR-499 sites have a distance of 66 nt from the first nt of the second miR-499 site to the first nt of the third miR-499 site. There are contradictions in the literature to the agreed range between two miRNA binding sites that leads to cooperative binding with the general consensus being 13-40 nts [254,277]. However, the last two miR-499 sites of PDCD4 show co-dependence as opposed to cooperativity. This could be why the distance required for co-dependence in our system is greater than 40 nt.

One mode by which miR-21 could be regulating the 3´UTR in a different manner from miR-499 can be through accessory proteins bound to RISC. There are many accessory proteins associated with RISC including fragile X mental retardation protein, vasa intronic gene, the arginine methyltransferase, PRMT5, Dicer and TRBP (as reviewed in Nilsen [316]). These additional proteins interact with the core Ago complex differentially and in different contexts [316]. It is possible that the accessory proteins on the miR-21:Ago complex is different from the miR-499:Ago complex which is how they could regulate the PDCD4 3´UTR differently.

The luciferase assays based on the miR-21 mutated site suggest that miR-499 suppresses its site independent of a functional miR-21 site. However, further investigation of the miR-21 site mutant revealed that miR-21 provides a contribution to the regulation of the PDCD4 3´UTR by miR-499. This suggests that miR-21 facilitates the silencing potential of miR-499. This enhanced cooperative regulation could either be due to a conformational change or recruitment of other proteins. The location of the miR-21 binding site in the PDCD4 3´UTR is important for optimal Ago:miRNA binding.

Perhaps binding of the Ago:miR-21 complex changes the conformation of the PDCD4 3´UTR allowing the miR-499 complex to bind. In this scenario the accessibility of the binding sites determines which miRNAs interact first with PDCD4. With this reasoning miR-21 would be located at an optimal site

on the 3´UTR for the Ago:miRNA complex to dock on. Despite miR-499 having three sites along the 3´UTR these sites may be less accessible for binding. Thermodynamic studies have shown that the miR-21 site has the lowest free energy (ΔG -2.69) and thus is the most energy efficient site for RISC to access [9]. Whereas the first miR-499 site has the highest free energy (ΔG 6.04) making it the least accessible and the last two miR-499 sites are in the middle (ΔG -1.57 and -1.58) [9].

A study investigated the role of site accessibility in miRNA mediated repression of a target 3´UTR [317]. They found that when the target was converted to a closed stem structure, miRNA mediated repression was reduced due to lack of accessibility. Furthermore, the sequences surrounding the target site could affect repression. If the flanking nucleotides around the site showed strong base-paring interactions within the mRNA then site accessibility was also reduced [317]. Additionally it was established that if there was no secondary structure 17 nts upstream and 13 nts downstream of the miRNA target site then there was unrestrained access to the site [317].

On this basis, we used RNAstructure to analyse the secondary structure of the PDCD4 3´UTR [318]. Focusing on the last two miR-499 sites it seemed that the 17 nts upstream of the second miR-499 site (nts 467-473) is subjected to extensive secondary structure. Therefore it can be postulated that miR-21:RISC needs to bind to open up the miR-499 sites. This could be how miR-21 aids miR-499 regulation of the 3´UTR. Furthermore we noted that spacially the last two miR-499 sites have close proximity and thus it may be possible to engage in interdependent target regulation (Figure 3.25).

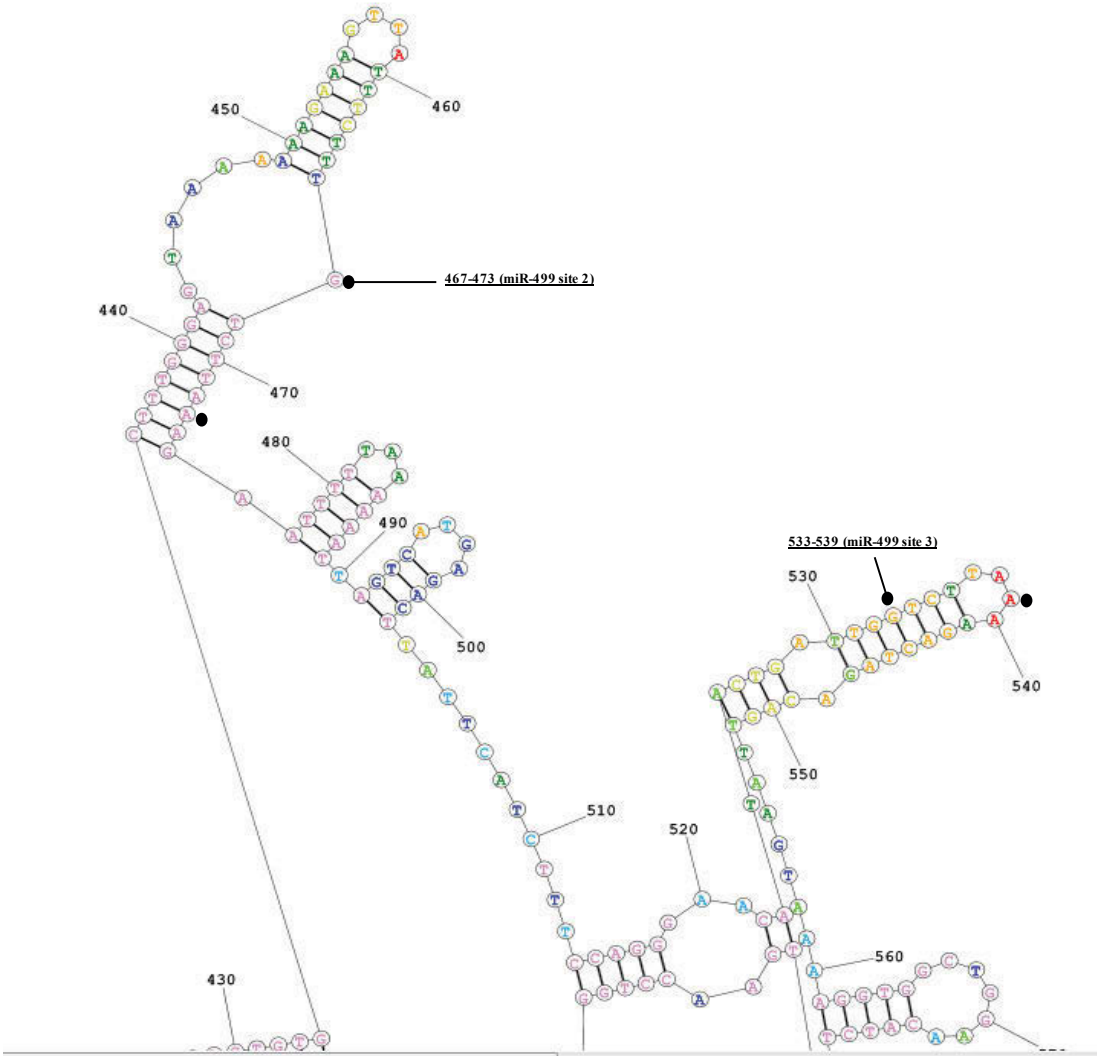

Figure 3.25. Secondary structure of the 3´UTR of PDCD4 based on prediction program RNAstructure [318]. The black dots highlight the beginning and end of the last two miR-499 sites on the 3´UTR.

Broderick et al., found in their study that the regulation of the target 3´UTR by ncRNAs was dependent on the Ago protein [265]. It was theorised that Ago2 was bringing miR-21 over for independent regulation and miR-499 was being brought over by one of the other Agos. Luciferase activity showed that both miRNAs were able to downregulate the reporter to the same extent even in Ago2 reduced conditions. Most likely the residual Ago2 in the KD cells is able to carry the miRNAs over to the 3´UTR or otherwise another Ago is able to take over the miRNA mediated regulation. Wang et al*.,* demonstrated that ablation of one Ago resulted in an upregulation of the other Agos [319]. However initial experiments found no change in Ago1 expression when Ago2 was KD (Appendix 3, Figure A5).

Alternatively, since miR-21 does aid in miR-499's regulation of the 3´UTR, miR-21 is not exclusively involved in independent regulation and thus could be carried by other Agos involved in cooperative regulation. This could be another reason as to why miR-21 regulation was not altered in Ago2 KD conditions.

This data sheds new light on the complex regulation of the tumour suppressor gene PDCD4 by multiple miRNAs. It is one of the first examples on an endogenous target and may represent a more common form of regulation beyond the one miRNA regulating one target scenario.

Chapter 4: Characterisation of miR-499 regulation by miR-21

4.1. Introduction

In the previous section we addressed the co-regulation of PDCD4 by miR-21 and miR-499. It was found that miR-21 regulated the 3´UTR in an independent manner whereas the last two miR-499 sites required co-dependent interaction by miR-499. On this basis, we decided to further investigate if a regulatory relationship between miR-21 and miR-499 existed.

There are a few studies on miRNA mediated regulation of another miRNA in the literature. Forrest et al., showed that the anti-differentiative miR-9 was downregulated when pro-differentiative miR-424 and miR-503 were overexpressed [16]. They postulated that this regulation occurred by either miR-424 or miR-503 binding to a target site in the primary transcript, pri-miR-9-3 [16]. Hatziapostolou et al., revealed that miR-24 and miR-629 indirectly regulate miR-124 [17]. The researchers found that the gene HNF4α is directly regulated by miR-24 and miR-629. Furthermore there is a HNF4α binding site on the promoter of miR-124. Therefore the inhibition of HNF4α (by siRNA or miR-24 and miR-629) resulted in a significant decrease in miR-124. This reveals another miRNA regulatory relationship whereby the overexpression of miR-24 and miR-629 resulted in a reduction of miR-124 [17].

Kato et al., found another set of miRNA-miRNA mediated regulation but via a different mechanism. They examined the indirect upregulation of miR-216a and miR-217 by miR-192 [18]. The ncRNA RP23 encodes the two miRNAs miR-216a and miR-217, and upstream the promoter region of RP23 are E-boxes (DNA response elements). miR-192 is known to inhibit Zeb1/2 which are E-box repressors and upregulate Tfe3 an E-box activator. Therefore it was

predicted that miR-192 stimulates miR-216a and miR-217 expression by activating the E-boxes on the RP23 gene containing the two miRNAs [18].

Studies have investigated miRNA-miRNA mediated relationships and identified a few biological mechanisms for this type of regulation. This chapter will examine the regulatory relationship between miR-21 and miR-499 and proposes mechanisms to explain this type of regulation.

4.2. Methods

4.2.1. Transfection

Lipofectamine™ 2000 and Lipofectamine™ 3000 were used to transfect the PDCD4 3´UTR WT and mutant vectors into cells. 250, 500, 750 and 1250 ng of vector was transfected into cells with the appropriate amount of lipofectamine in a 6-well plate. 4×10^5 cells were seeded onto each well of a 6-well plate. The appropriate amount of opti-MEM was added to lipofectamine and DNA vector separately and incubated for 5 minutes at room temperature before being combined together and incubated for 20 minutes at room temperature. The mixture was then added to each well containing cells. Cells were incubated at 37°C and 5% CO_2 for 24 hours before RNA extraction for qPCR.

4.2.2. Actinomycin D (actD) treatment

A total of 4×10^5 cells were seeded in a 6-well plate. After 24 hours, cells were transfected with RNAiMAX, control miRNA and miR-21 mimics at 30 nM, left for 3 hours and actD (5 µg/ml) (ThermoFisher Scientific, Australia) or Dimethyl Sulfoxide (DMSO) (Sigma-Aldrich, Australia) added. After the addition of actD, cells were incubated at 37°C and 5% CO_2 for 0, 1, 3, 8, 12 and 24 hours. Cells were then lysed using RNAzol and RNA isolated for subsequent qPCRs measuring miRNA stability.

4.3. Results

4.3.1. miR-21 increases the expression of miR-499

miR-21 is a major oncomiR in most cancer types and it has a role in the downregulation of target genes. While studying the regulation of the tumour suppressor PDCD4 by the oncomiRs miR-21 and miR-499, an interesting observation became apparent. It appeared that miR-21 was able to influence the expression of miR-499. To investigate this notion, we delivered a scrambled control and miR-21 mimic (1, 10 and 30 nM) into HEK293 cells. Overexpression of miR-21 was confirmed by qPCR at all concentrations (Figure 4.1a). Surprisingly there was also a substantial increase of miR-499 levels in cells overexpressing miR-21 suggesting a possible “positive feedback” for the expression of miR-499 (Figure 4.1b).

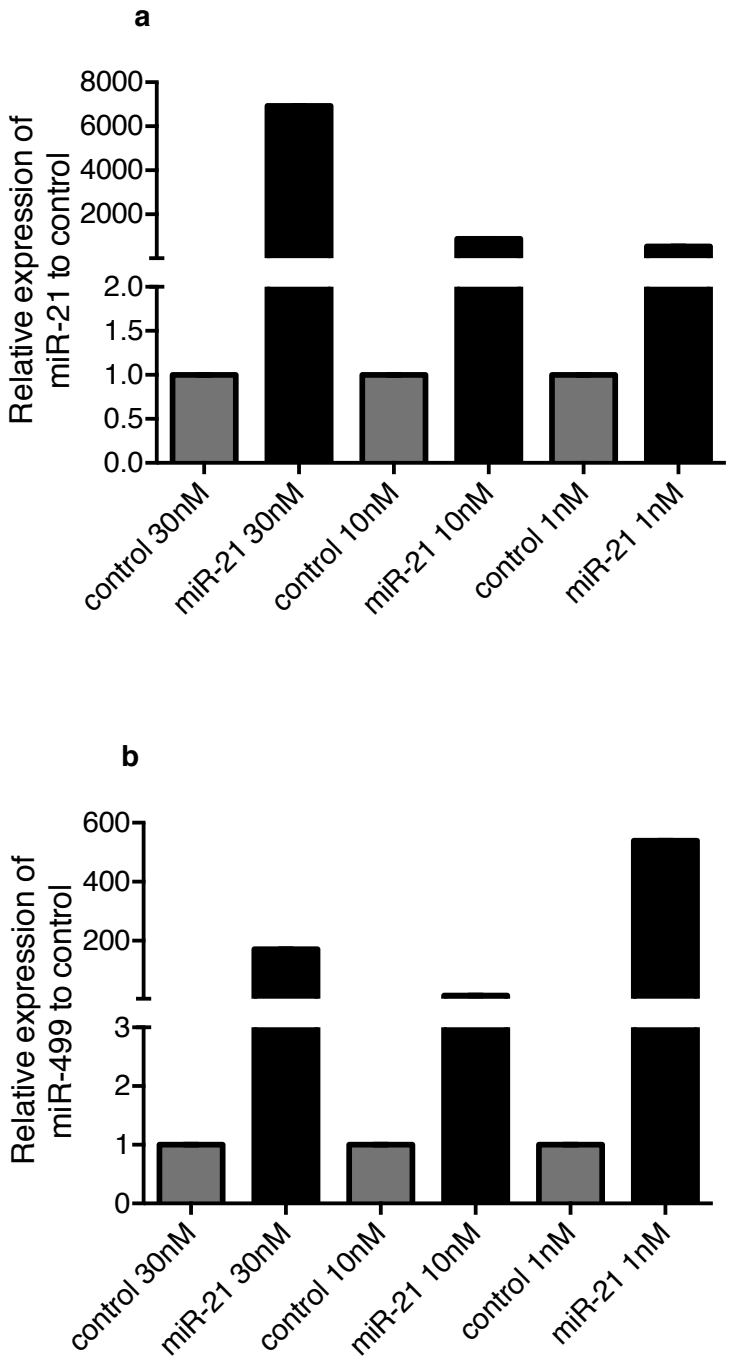

Figure 4.1. miR-21 upregulates miR-499. HEK293 cells were transfected with 1, 10 and 30 nM of scrambled control and miR-21. RNA was harvested from cells and qPCR conducted. The expression of genes was normalised to reference gene RNU6B and then normalised to scrambled control at 1, 10 and 30 nM to give relative expression. **(a)** qPCR analysis of miR-21 levels in transfected cells. **(b)** miR-499 levels in transfected cells. (n=1).

In order to determine whether this was a specific phenomenon, other miRNAs were also studied. We noted that overexpression of miR-21 resulted in decreased *let-7a* levels (the opposite trend to miR-499) (Figure 4.2a). Quantifying the amount of miR-17 in the cell at 30 nM revealed no change when miR-21 was overexpressed (Figure 4.2b).

To determine whether miR-21 overexpression had any functional consequences, we assessed the expression of target genes for both miR-21 and miR-499 (Figure 4.3). PDCD4 and SRY Box 6 (SOX6), gene targets for both miR-21 and miR-499 were decreased in miR-21 transfected cells compared to the scrambled control cells (Figure 4.4). Surprisingly, Forkhead box protein 04 (FOXO4) which only has miR-499 target sites was also decreased in miR-21 transfected cells (Figure 4.4). These results suggest that the increased miR-499 due to miR-21 overexpression is functionally capable of downregulating target genes specific for miR-499.

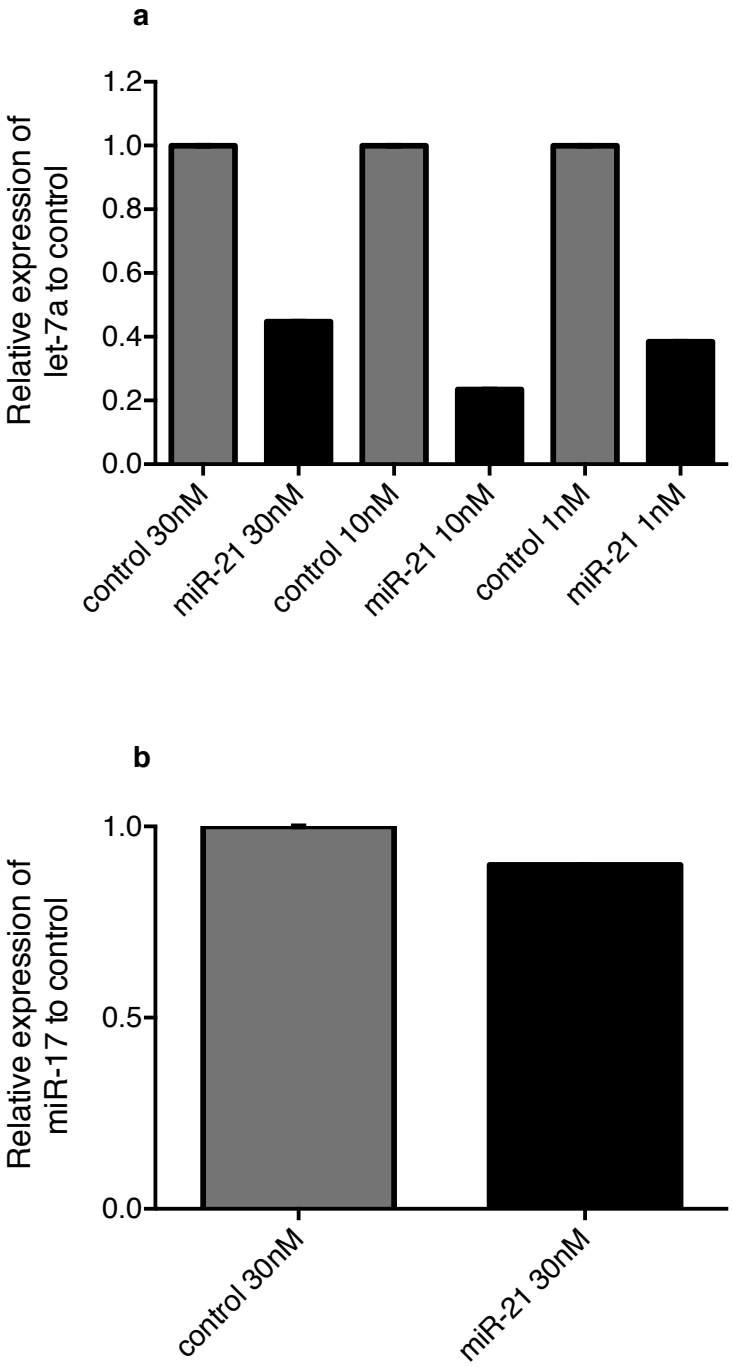

Figure 4.2. Steady state levels of other miRNA are not elevated in response to miR-21. HEK293 cells were transfected with 1, 10 and 30 nM of scrambled control and miR-21. RNA was harvested from cells and qPCR conducted. The expression of genes was normalised to reference gene RNU6B and then normalised to control to give relative expression. **(a)** *let-7a* levels in transfected cells. **(b)** miR-17 levels in transfected cells. (n=1).

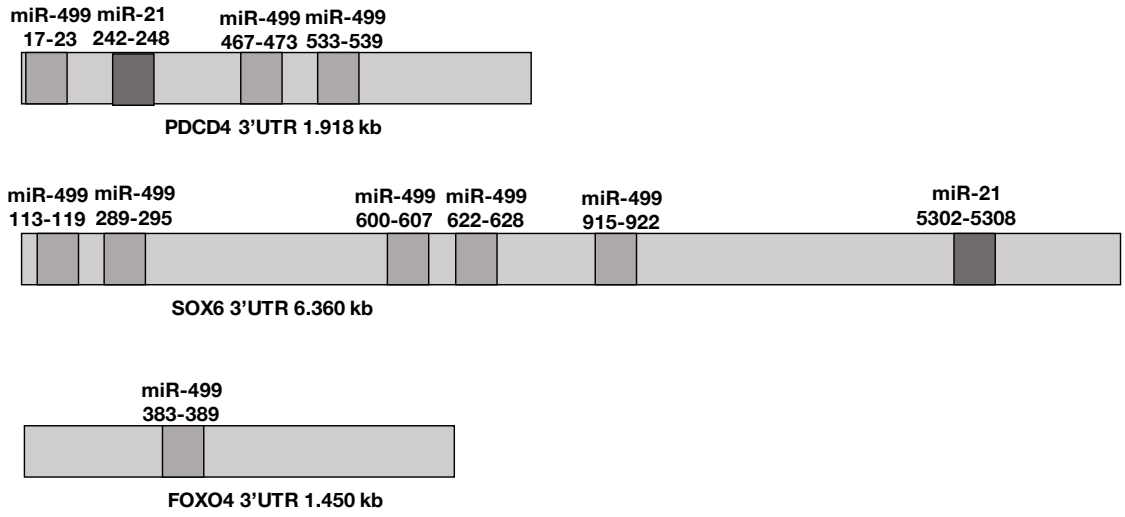

Figure 4.3. Schematic of the 3´UTRs of genes targeted by miR-21 and/or miR-499. Light grey boxes indicate the miR-499 sites and the dark grey boxes indicate the miR-21 sites on the 3´UTR based on the TargetScan algorithm.

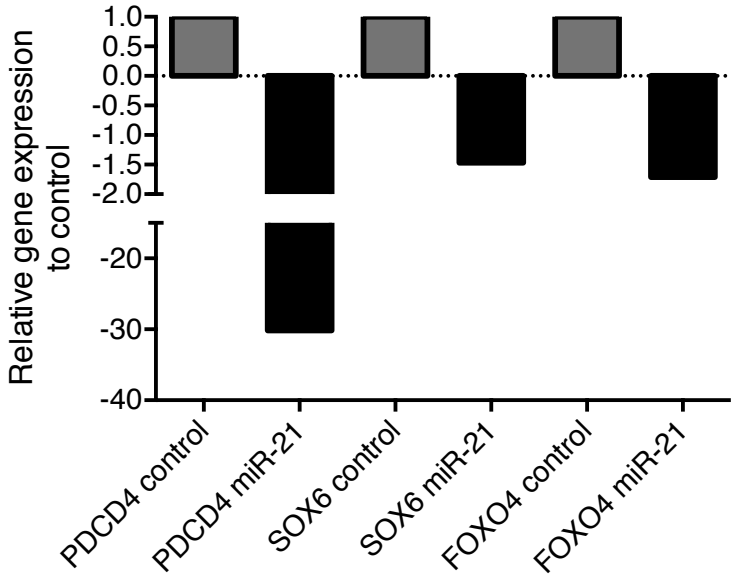

Figure 4.4. The expression of candidate gene targets of miR-21 decreases with miR-21 overexpression in cells. HEK293 cells were transfected with 30 nM of scrambled control or miR-21. RNA was harvested from cells and qPCR conducted. The expression of genes was normalised to reference gene ACTB and then normalised to the scrambled control to give relative expression (n=1).

Our initial observations revealed a regulatory relationship between miR-21 and miR-499, but we did not know if this effect was reciprocated in miR-499 overexpressing cells. As shown by qPCR, the same pattern was repeated when overexpression of miR-21 led to an increase in the amount of miR-499 (Figure 4.5b,d). However overexpressing miR-499 did not increase the amount of endogenous miR-21 (Figure 4.5a,c). Therefore, this relationship is not reciprocated and only miR-21 is able to promote an increase in miR-499 expression.

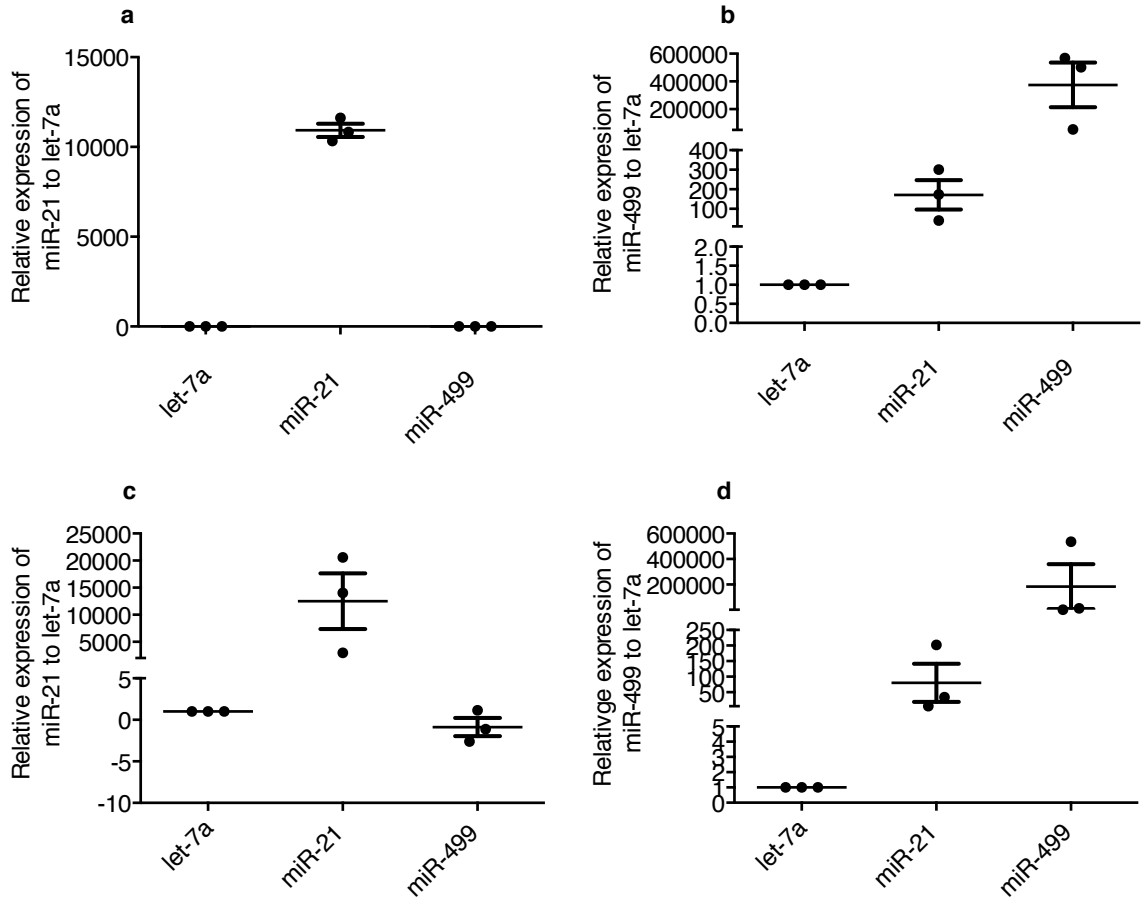

Figure 4.5. miR-21 upregulates miR-499. HEK293 cells were transfected with 10 or 30 nM of *let-7a*, miR-21 or miR-499. RNA was harvested from cells and qPCR conducted. The expression of genes was normalised to reference gene RNU6B and then normalised to *let-7a* to give relative expression. **(a)** miR-21 levels in cells transfected with 30 nM miRNA mimics. **(b)** miR-499 levels in cells transfected with 30 nM miRNA mimics. **(c)** miR-21 levels in cells transfected with 10 nM miRNA mimics. **(d)** miR-499 levels in cells transfected with 10 nM miRNA mimics. (Error bars represent s.e.m. n=3).

As a control, miR-17 was also quantified in this experiment and the change observed in miR-17 expression when miR-21 is overexpressed was minimal (1.3 fold). Therefore, miR-21 upregulation of miR-499 was miRNA specific (Figure 4.6).

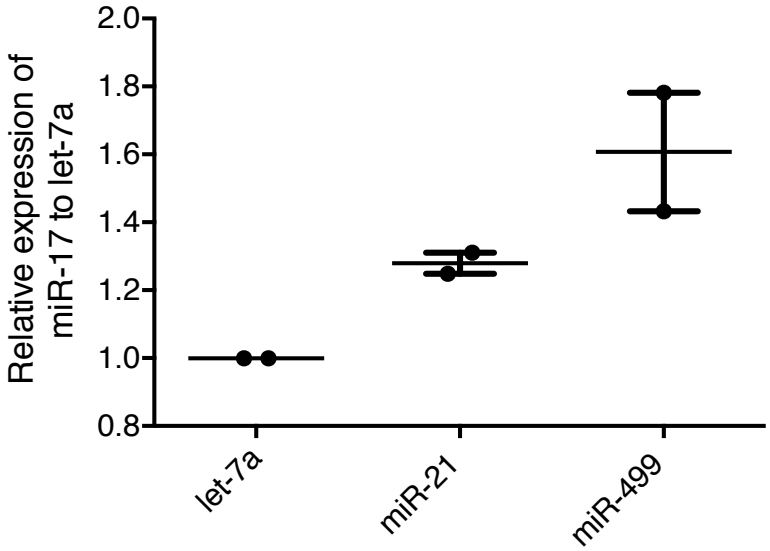

Figure 4.6. miR-17 levels are slightly altered by overexpression of transfected miR-21 and miR-499 miRNA mimics. HEK293 cells were transfected with 30 nM of *let-7a*, miR-21 or miR-499. RNA was harvested from cells and qPCR conducted. The expression of genes was normalised to reference gene RNU6B and then normalised to *let-7a* to give relative expression of miR-17. (Error bars are s.e.m. n=2).

4.3.2. Inhibiting miR-21 and miR-499 reveals the same regulatory relationship between the two miRNA

The evidence so far has suggested that overexpression of miR-21 regulates miR-499 steady state levels. We wanted to know if we would still observe this type of regulation if miR-21 and miR-499 were inhibited in cells instead. To achieve this, UMSCC22B cells were transfected with miR-21 and miR-499 inhibitors. This cell line was chosen as the endogenous concentration of miR-499 was higher than in HEK293 cells as measured by qPCR (Figure 4.7a). First we examined the amount of miR-21 in cells with reduced amounts of miR-21 or miR-499. As expected, miR-21 levels were reduced in cells transfected with anti-miR-21 (30 nM and 40 nM) and miR-499 levels were reduced in cells transfected with anti-miR-499 (30 nM) (Figure 4.7b,c). To our surprise, when miR-499 was decreased by the inhibitor, we witnessed a marked increase between four to seven fold for miR-21 RNA expression. Therefore, the reduction of miR-499 in cells saw an increase of endogenous miR-21 over 24 hours. To add further complexity to the interaction between these two miRNAs, when miR-21 is reduced by the miR-21 inhibitor, there is a concomitant decrease in miR-499 levels (Figure 4.7c). In brief, miR-499 expression is positively correlated to miR-21 but miR-21 levels are negatively regulated by miR-499 levels.

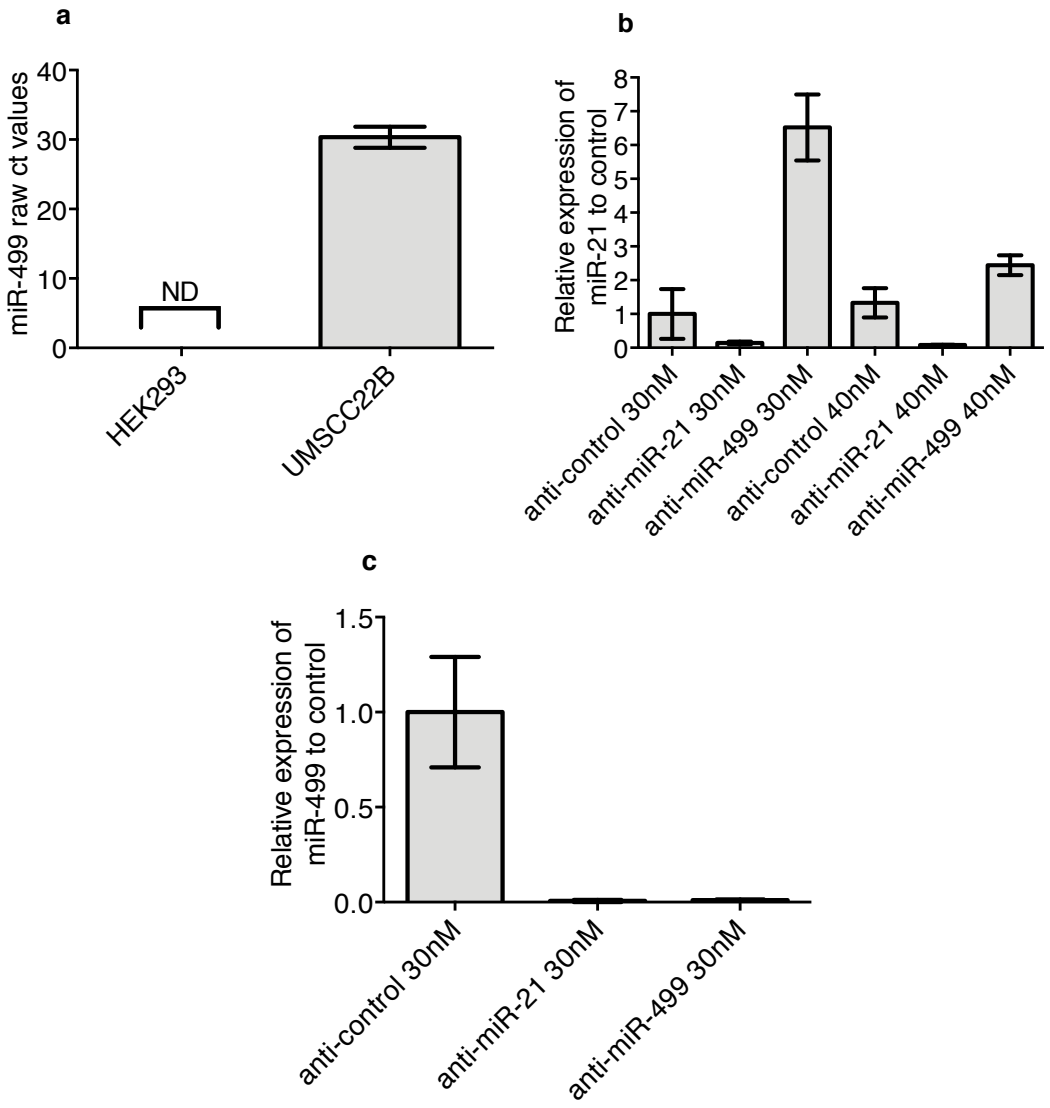

Figure 4.7. The levels of miR-499 are positively correlated with miR-21 levels. RNA was isolated from HEK293 and UMSCC22B cells and the quantity of endogenous miR-21 and miR-499 measured by qPCR. **(a)** qPCR analysis of raw miR-499 Ct values in HEK293 and UMSCC22B cells. UMSCC22B cells were transfected with 30 or 40 nM of antisense inhibitors to miR-21 (anti-miR-21), miR-499 (anti-miR-499) or a scrambled control (anti-control). RNA was harvested from cells and qPCR conducted. The expression of genes was normalised to reference gene RNU6B and then normalised to anti-control to give relative expression. miR-21 levels in cells transfected with 30 and 40 nM anti-control, anti-miR-21 and anti-miR-499. **(c)** miR-499 levels in cells transfected with 30 nM anti-control, anti-miR-21 and anti-miR-499. (Error bars are s.e.m. n=3).

4.3.3. Potential mechanisms for miR-21 regulation of miR-499

We propose two miR-21-miR-499 models, which could explain this interesting interaction (Figure 4.8). The first model was that miR-21 increases pri-miR-499 leading to increased mature miR-499 levels. The second model proposed that miR-21 promoted miR-499's interactions with a miR-499 target gene, which would therefore result in a slower turnover of miR-499. The first model proposed that this regulation occurred during transcription whereas the second model suggested this regulation was a post-transcriptional process. We explore these themes in the following sections.

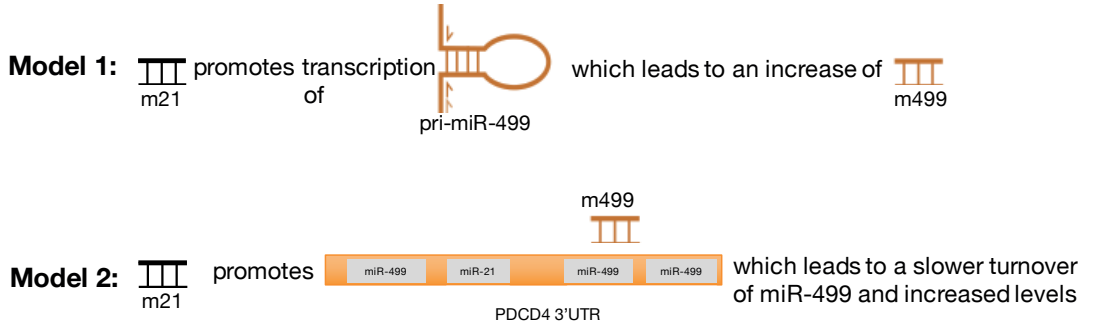

Figure 4.8. Models proposing mechanisms for miR-21's regulation of miR-499. Model one proposes that miR-21 is able to increase the expression of pri-miR-499 and that leads to an increase of miR-499. Whereas model two proposes that miR-21 promotes miR-499 interaction with the 3´UTR of PDCD4 and this reduces the turnover of miR-499.

4.3.3.1. Transcriptional model: miR-21 does not promote the production of pri-miR-499

To test this idea, HEK293 cells were transfected with 30 nM *let-7a*, miR-21 or miR-499 mimics and the amount of pri-miR-499, the precursor to mature miR-499 was measured using qPCR. It was found that overexpressing miR-21 did not change the primary amounts of miR-499 compared to the control transfected cells (Figure 4.9). Therefore, it seems that miR-21 does not promote the production of excess pri-miR-499 leading to increased miR-499 levels.

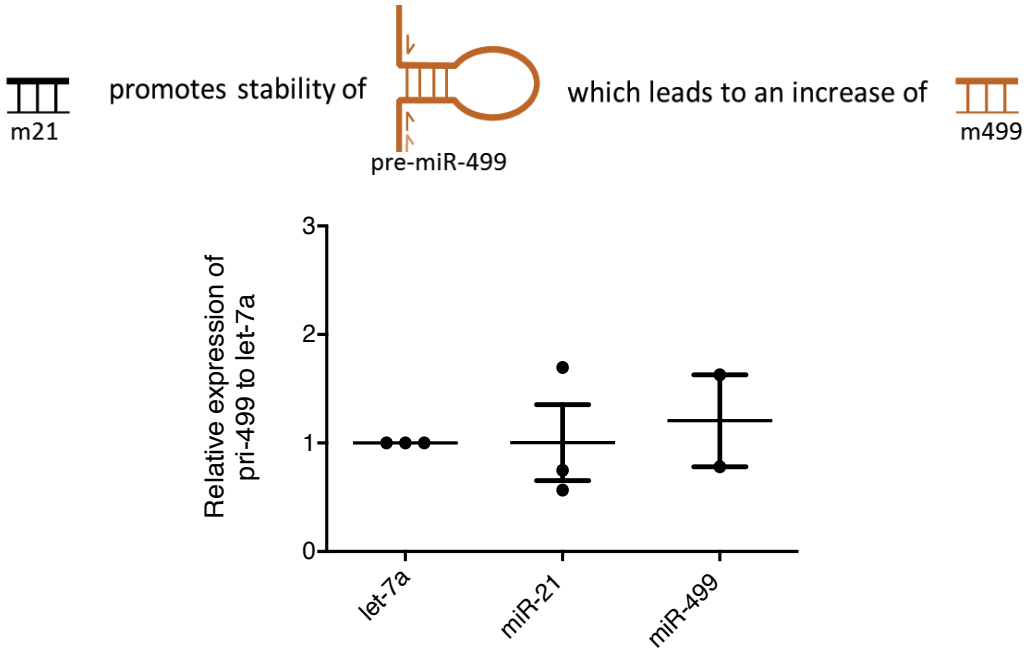

Figure 4.9. Primary levels of miR-499 are unchanged by the overexpression of miR-21 or miR-499. HEK293 cells were transfected with 30 nM *let-7a*, miR-21 or miR-499 miRNA mimics. RNA was harvested from the cells and qPCR conducted. The expression of genes was normalised to reference gene RNU6B and then normalised to *let-7a* to give relative expression of pri-miR-499. (Error bars are s.e.m. n=3).

4.3.3.2. miR-21 stabilises mature miR-499 levels

We observed that primary miR-499 levels were consistent suggesting a post-transcriptional intervention. Thus we postulate that miR-499 levels may be affected by the turnover rate of miR-499. To investigate this notion, we inhibited RNA Pol II by using actD therefore preventing further transcription of any nascent mRNA species. HEK293 cells were transfected with *let-7a* or miR-21 mimic and harvested at 0 and 4 hours. Either actD or a DMSO vehicle control was also added to transfected cells. In this optimisation approach, DMSO treated cells were comparable to actD treated cells (Figure 4.10a,b). The primary levels of miR-499 did not change under miR-21 overexpression conditions compared to the *let-7a* control (Figure 4.10a). However, the concentration of mature miR-499 was upregulated at 4 hours by miR-21 (Figure 4.10b). This suggests that miR-21 is able to affect mature miR-499 by 4 hours.

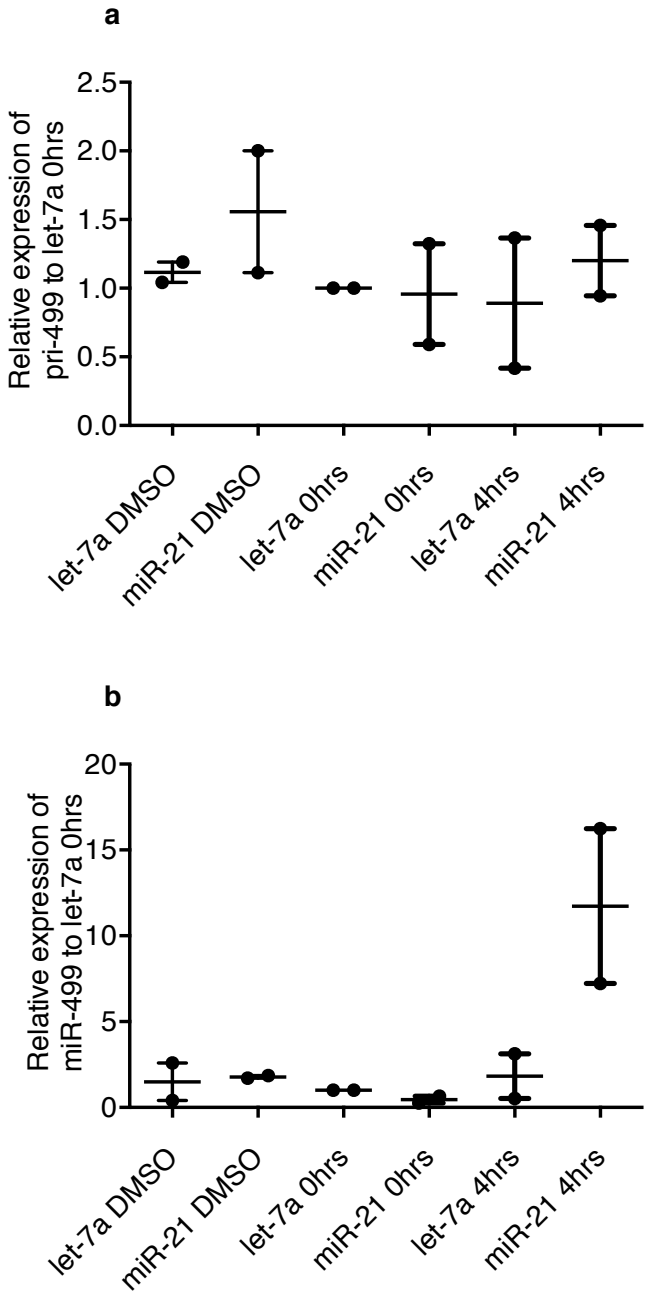

Figure 4.10. Initial optimisation of actD experiment. HEK293 cells were transfected with 30 nM of *let-7a* or miR-21. DMSO or 5 μg/ml actD was added to wells containing transfected cells 3 hours post transfection. Cells were harvested at 0 and 4 hours for qPCR analysis. RNA was harvested from the cells and qPCR conducted. The expression of genes was normalised to reference gene RNU6B and then normalised to *let-7a* at 0 hours to give relative expression. **(a)** pri-miR-499 expression in transfected cells. **(b)** miR-499 expression in transfected cells. (Error bars are s.e.m. n=2).

Based on these initial observations we extended the actD treatment to longer time points. To confirm actD was switching off cellular transcription, we measured cmyc which has a half-life of approximately 30 minutes [320]. Figure 4.11 shows that cymc levels decrease by 3 hours post actD treatment and this was maintained up to 24 hours.

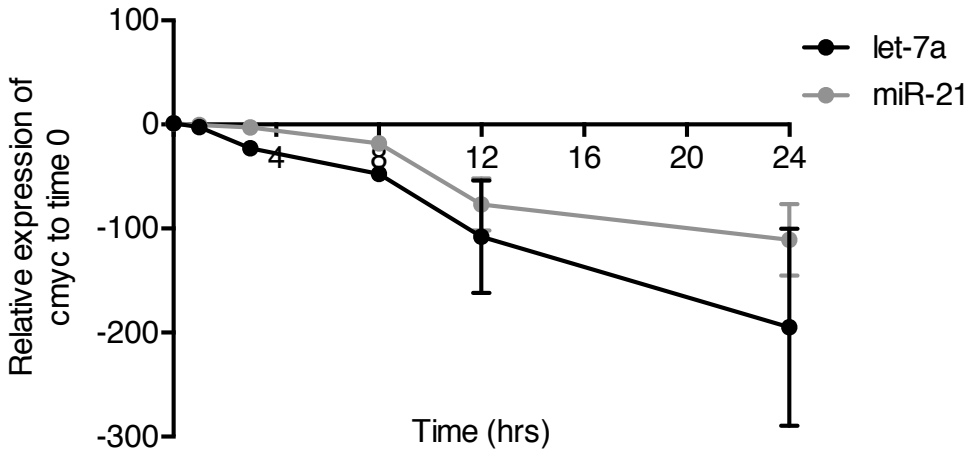

Figure 4.11. Cmyc levels are reduced over a time course of 0, 1, 3, 8, 12 and 24 hours. HEK293 cells were harvested at 0, 1, 3, 8, 12 and 24 hours post transfection with *let-7a* or miR-21 and post treatment with actD for qPCR analysis. RNA was harvested from the cells and qPCR conducted. The expression of genes was normalised to reference gene ACTB and then normalised to *let-7a* or miR-21 at 0 hours to give relative expression of cmyc. (Error bars are s.e.m. n=3).

The primary levels of miR-21 and miR-499 were then measured in actD treated and DMSO vehicle transfected cells to determine if miR-21 can stabilise miR-499 levels. We observed a rapid decrease in the primary transcripts for both miR-21 and miR-499 (Figure 4.12a,b). This result suggests that miR-21 does not affect the endogenous amount of pri-miR-499 confirming the results from the first model (Figure 4.9).

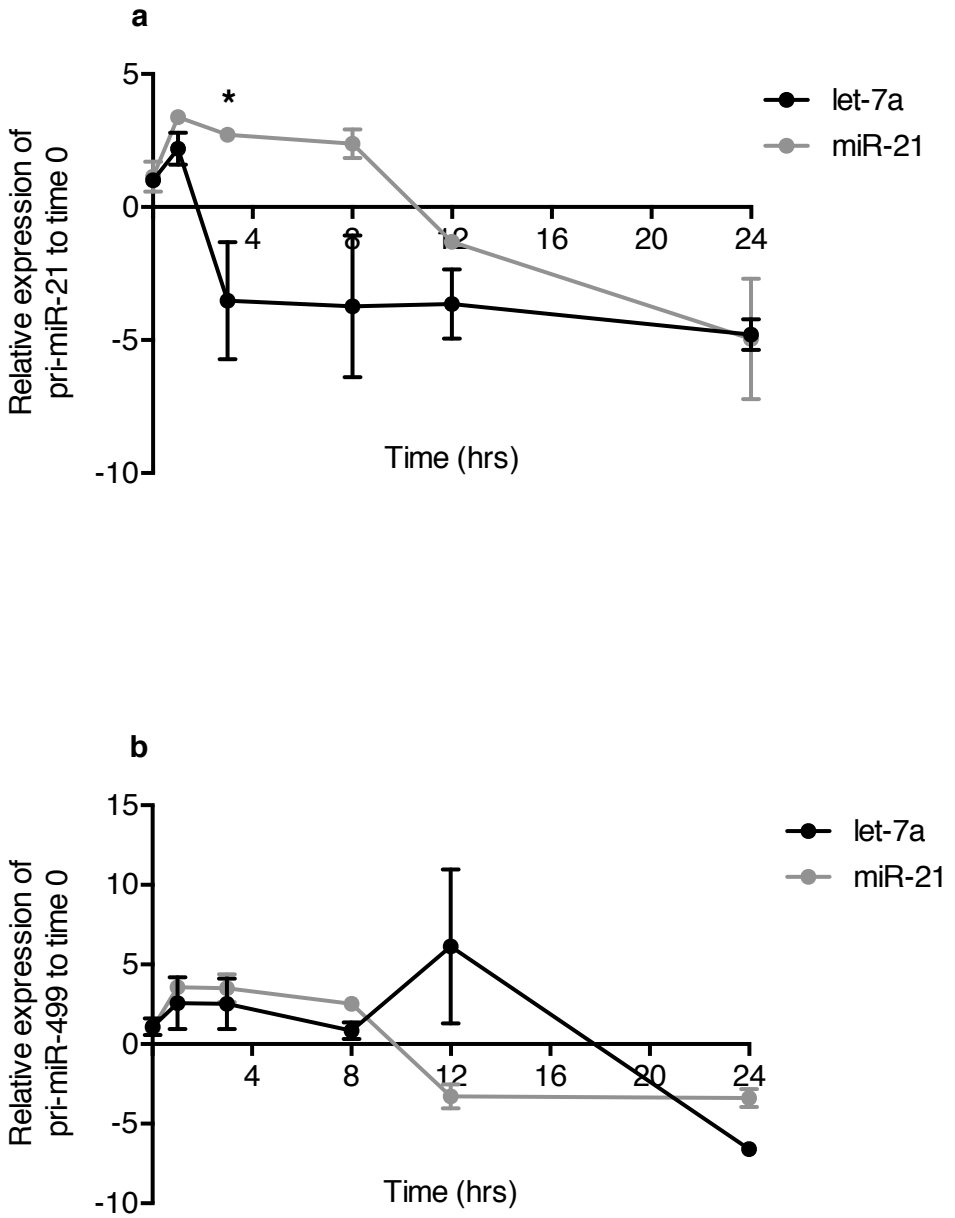

Figure 4.12. The primary levels of miR-21 and miR-499 decrease over time. HEK293 cells were harvested at 0, 1, 3, 8, 12 and 24 hours post transfection with *let-7a* or miR-21 and post treatment with actD for qPCR analysis. RNA was harvested from the cells and qPCR conducted. The expression of genes was normalised to reference gene ACTB and then normalised to control to *let-7a* or miR-21 at 0 hours to give relative expression. (**a**) pri-miR-21 levels over time when either a *let-7a* or miR-21 mimic is overexpressed. (**b**) pri-miR-499 levels over time when either a *let-7a* or miR-21 mimic is overexpressed. (Error bars are s.e.m n=3).

Given the previous finding, we then focused on post-transcriptional regulation of miR-499. We wanted to determine if miR-21 could stabilise the steady state amounts of mature miR-499. To address this, we measured miR-21 and miR-499 expression over the actD treatment time course. As expected, cells overexpressing miR-21 showed a high amount of miR-21 consistent with overexpressing a miRNA mimic. Interestingly, these miR-21 overexpressing cells also had an increase in the mature levels of miR-499 by 24 hours (Figure 4.13a,b). These cells had not been transfected with miR-499 yet there was more than 100 times the amount of miR-499 in the miR-21 overexpressing cells compared to the *let-7a* overexpressing cells by 24 hours. This data supports miR-21 regulation of miR-499.

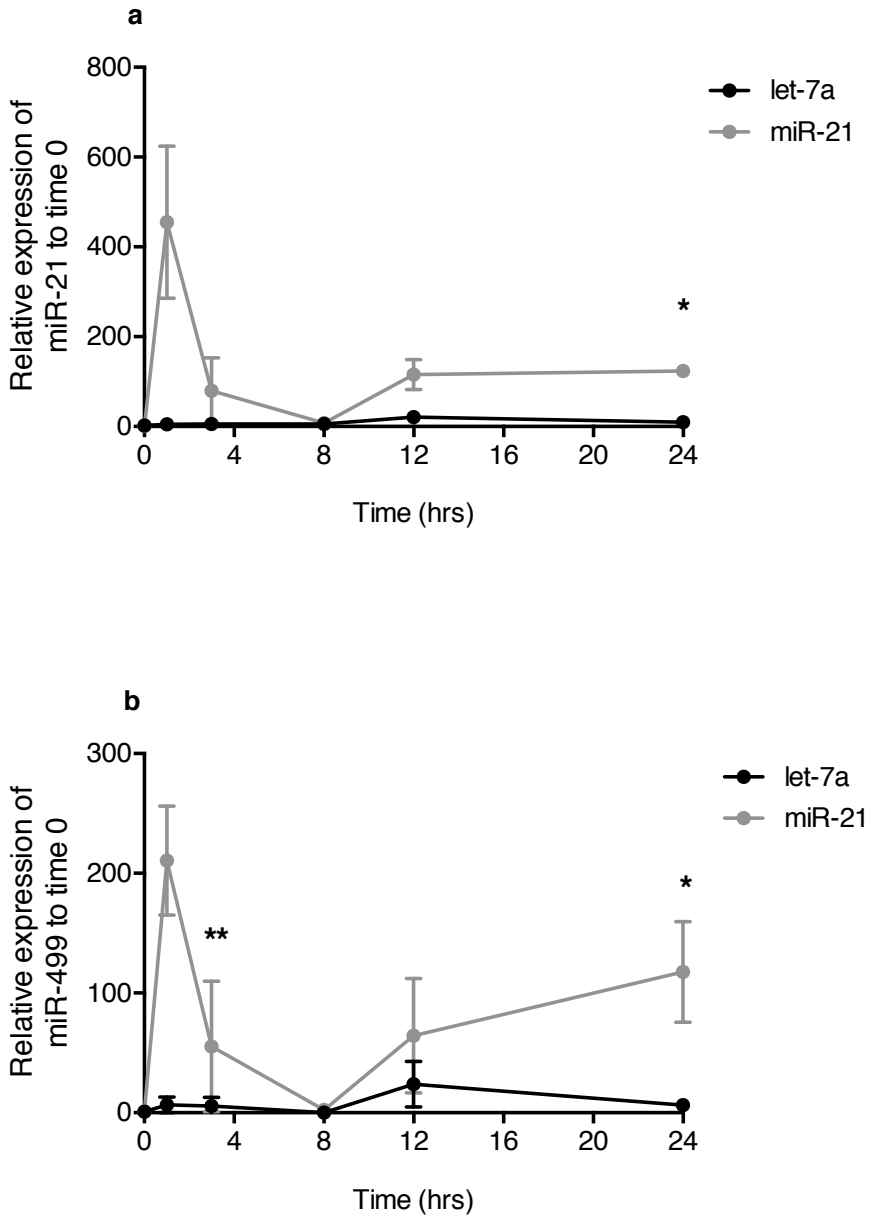

Figure 4.13. miR-21 stabilises miR-499 levels during transcription inhibition with actD. HEK293 cells were harvested at 0, 1, 3, 8, 12 and 24 hours post transfection with *let-7a* or miR-21 and post treatment with actD for qPCR analysis. RNA was harvested from the cells and qPCR conducted. The expression of genes was normalised to reference gene RNU6B and then normalised to *let-7a* or miR-21 at 0 hours to give relative expression. (**a**) miR-21 levels over time when either a *let-7a* or miR-21 mimic is overexpressed. (**b**) miR-499 levels over time when either a *let-7a* or miR-21 mimic is overexpressed (Error bars are s.e.m. n=3. *p<0.05, **p<0.01. Two-sided unpaired T-test).

To assess whether this was specific to miR-499, we examined the levels of *let-7g*. The results indicate that the amount of *let-7g* in miR-21 overexpressing cells were similar to the control cells. (Figure 4.14). This indicates that the presence of miR-21 is stabilising the mature levels for miR-499 but not *let-7g*.

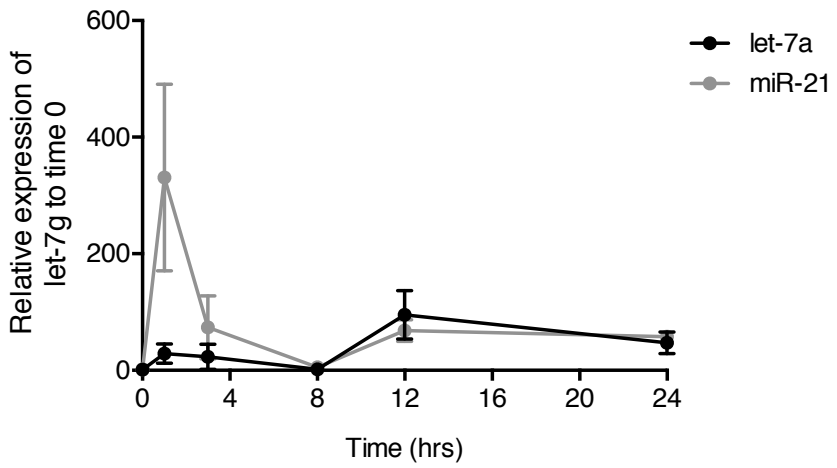

Figure 4.14. *Let-7g* levels decrease over 24 hours. HEK293 cells were harvested at 0, 1, 3, 8, 12 and 24 hours post transfection with *let-7a* or miR-21 and post treatment with actD for qPCR analysis. RNA was harvested from the cells and qPCR conducted. The expression of genes was normalised to reference gene RNU6B and then normalised to *let-7a* or miR-21 at 0 hours to give relative expression of *let-7g*. (Error bars are s.e.m. n=3).

4.3.4. miRNA binding to excess target sites may reduce turnover of specific miRNA.

The results thus far suggest that miR-21 is able to stabilise mature miR-499 but the mechanism behind this remained unknown. In the literature it has been found that the pairing of a miRNA with its RNA target results in stabilisation of the miRNA [19,20]. This model known as target-mediated miRNA protection (TMMP) is believed to act as a counterbalance to miRNA decay in cells. This allows for the fine-tuning of the steady state of cellular miRNA levels.

We wanted to determine if the miR-499 increase by miR-21 was due to interactions with target sites on a gene. A titration of PDCD4 vectors was conducted and the endogenous expression of the miRNAs measured to determine if there was a change to miR-499 levels. To our immediate surprise it was found that increasing the PDCD4 WT vector led to an increase and plateau of miR-21 at 500 ng vector (Figure 4.15a). This was not reflected with miR-499 which showed no change possibly due to a low endogenous amount of miR-499 in HEK293 cells (Figure 4.15b).

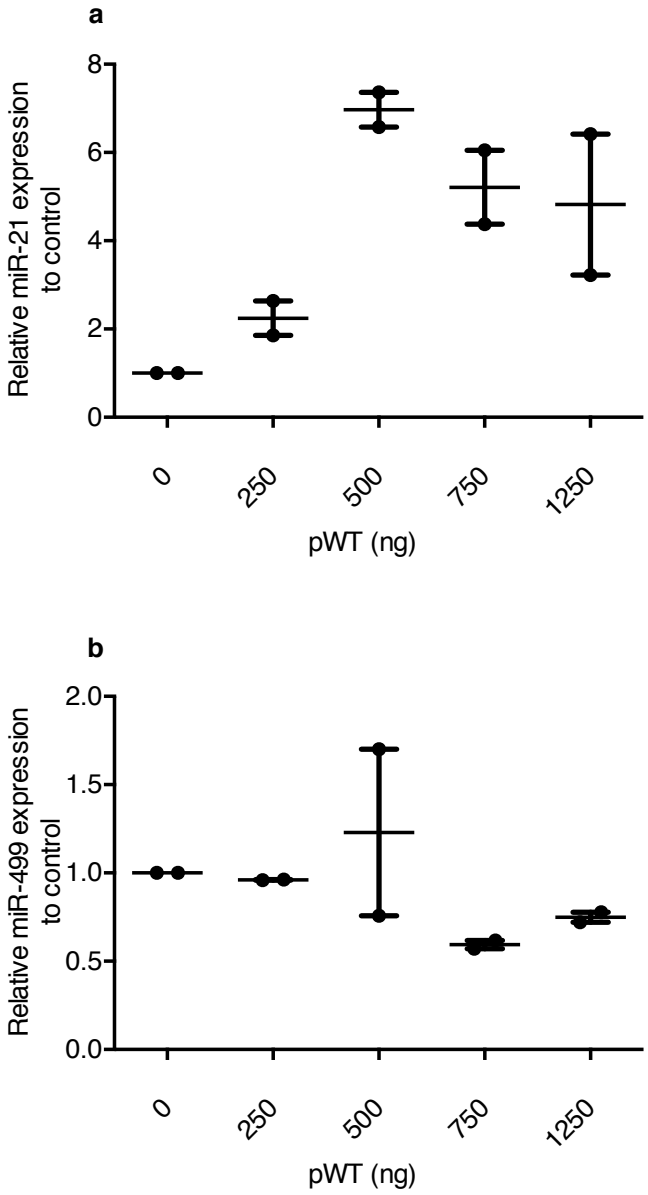

Figure 4.15. miR-21 levels increase with increasing levels of target. HEK293 cells were transfected with 0, 250, 500, 750 and 1250 ng of the PDCD4 WT vector, pWT. RNA was harvested from cells and qPCR conducted. The expression of genes was normalised to reference gene RNU6B and then normalised to control (no pWT) to give relative expression. **(a)** miR-21 levels in transfected cells. **(b)** miR-499 levels in transfected cells. (Error bars are s.e.m. n=2).

The primary levels of miR-21 and miR-499 were investigated and did not change with increasing amounts of pWT. In fact there was a decrease of both primary levels at 250 ng which was maintained up to 1250 ng of pWT (Figure 4.16a,b).

Other miRNAs were quantitated as well to determine if the specificity of miRNA target stabilisation was only specific to miRNA with binding sites present in the target. miR-17 and *let-7g* do not contain binding sites in the PDCD4 3´UTR, yet despite this the amount of miR-17 and *let-7g* appeared to increase with increasing concentration of the WT vector (Figure 4.17a,b).

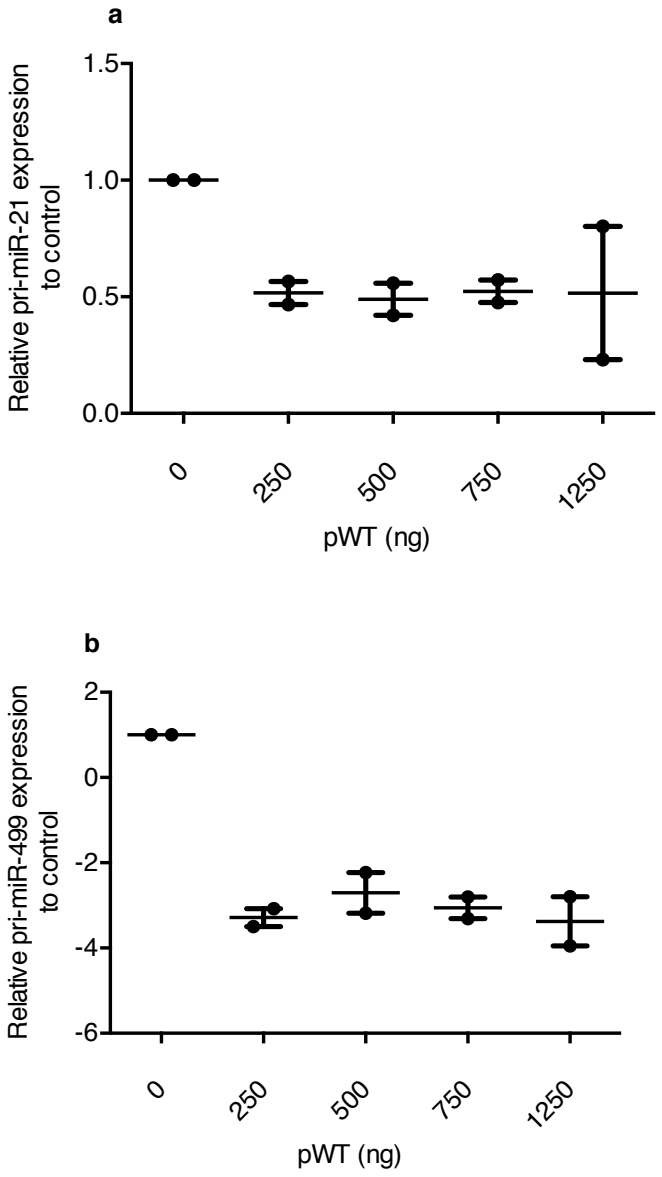

Figure 4.16. Primary levels of miR-21 and miR-499 decrease and remain constant with increasing levels of target. HEK293 cells were transfected with 0, 250, 500, 750 and 1250 ng of the PDCD4 WT vector, pWT. RNA was harvested from the cells and qPCR conducted. The expression of genes was normalised to reference gene GAPDH and then normalised to control (no pWT) to give relative expression. **(a)** pri-miR-21 levels in transfected cells. **(b)** pri-miR-499 levels in transfected cells.

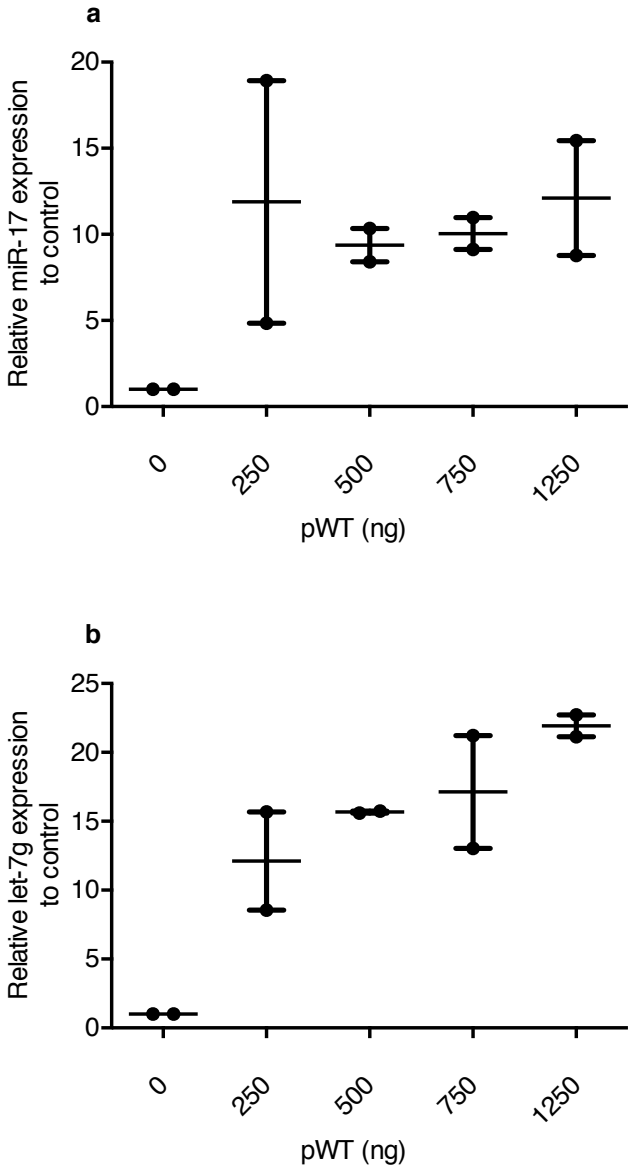

Figure 4.17. miRNAs without a seed site on PDCD4 3´UTR are upregulated with increasing levels of target. HEK293 cells were transfected with 0, 250, 500, 750 and 1250 ng of the PDCD4 WT vector, pWT. RNA was harvested from the cells and qPCR conducted. The expression of genes was normalised to reference gene RNU6B and then normalised to control (no pWT) to give relative expression. **(a)** miR-17 expression in transfected cells. **(b)** *let-7g* expression in transfected cells. (Error bars are s.e.m. n=2).

Due to the upregulation of miR-17 and *let-7g* with increasing pWT, we evaluated the potential artificial effect of the backbone vector psiCHECK-2. The vector was titrated as described previously and there was no discernible change in the amount of miR-21 at increasing concentrations of psiCHECK-2 (Figure 4.18a).

It was of interest to examine if removing the miR-21 site would change the observed miR-21 trend (Figure 4.16a). Increasing the concentration of the miR-21 site mutant recombinant vector, p21/M2 found no change to the expression of miR-21 (Figure 4.18b) which meant that a miR-21 target site needed to be present in order for miR-21 levels to increase with target.

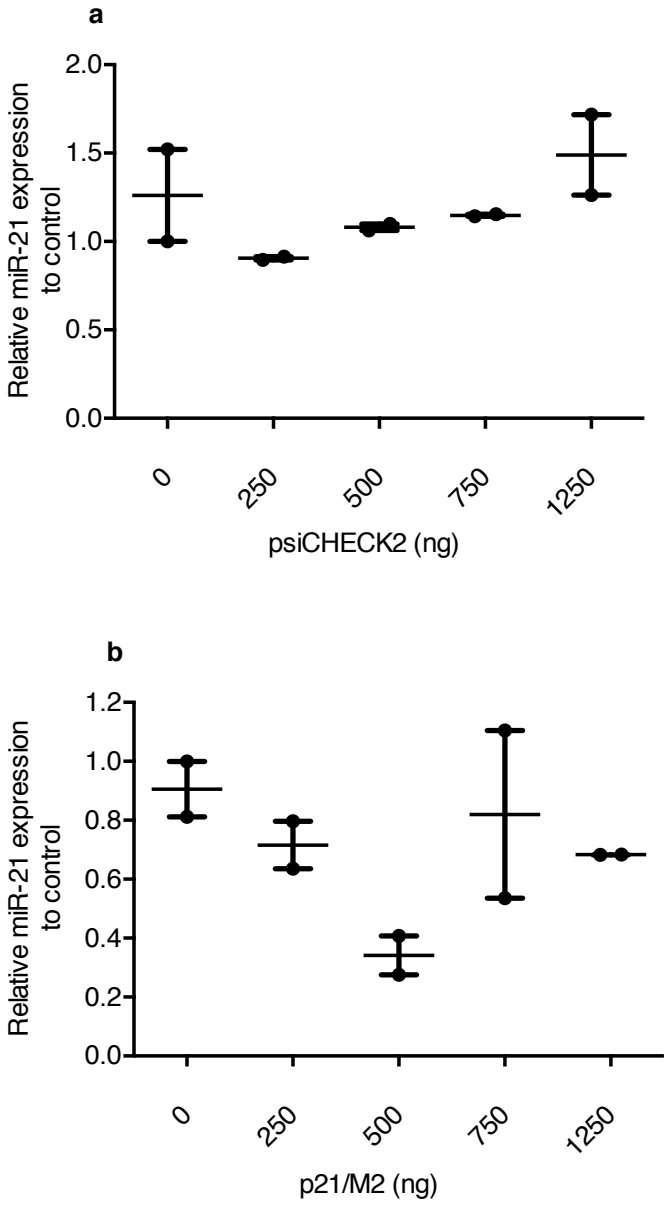

Figure 4.18. miR-21 requires a target site to be upregulated with increasing target. HEK293 cells were transfected with 0, 250, 500, 750 and 1250 ng of the PDCD4 miR-21 site mutant – p21/M2 or empty reporter psiCHECK-2. RNA was harvested from the cells and qPCR conducted. The expression of genes was normalised to reference gene RNU6B and then normalised to control (no psiCHECK-2 or p21/M2) to give relative expression of miR-21. **(a)** miR-21 expression with increasing amounts of psiCHECK-2 in vector transfected cells. **(b)** miR-21 expression with increasing amounts of p21/M2 in vector transfected cells. (Error bars are s.e.m. n=2).

4.3.5. The regulation of miR-499 by miR-21 appears not to be due to shared transcription factors

The results demonstrated that the regulation of miR-499 by miR-21 occurred at the mature state of miR-499. However, another theory was that the relationship between miR-21 and miR-499 was overseen by a common set of transcription factors. Transcription factors are known to be a common link between cooperative miRNAs [321]. Using the resource ChIPBase the transcription factors for the miRNAs were identified and then crosschecked for common factors [322]. From this database miR-499 shared 64% of its transcription factors with miR-21 (Figure 4.19, Table 4.1).

To put this percentage into context the transcription factors of two other miRNAs were identified and compared to miR-21 and miR-499. miR-125b, a miRNA linked with cardiovascular activity just like miR-499 would be expected to have a common pair of transcription factors. miR-128 was selected because it is a miRNA associated with the brain and should not have many similarities with miR-21 or miR-499. miR-21 shared 65% of its transcription factors with miR-499, 63% with miR-128 and 67% with miR-125b (Table 4.1). miR-499 shared 67% of its transcription factors with miR-21, 81% with miR-128 and 80% with miR-125b (Table 4.1). miR-21 had a similar level of shared transcription factors with all the miRNAs and miR-499 actually had a higher shared percentage with miR-128 and miR-125b than with miR-21. Therefore, this would suggest that shared transcription factors do not play a role in the miR-21 and miR-499 relationship.

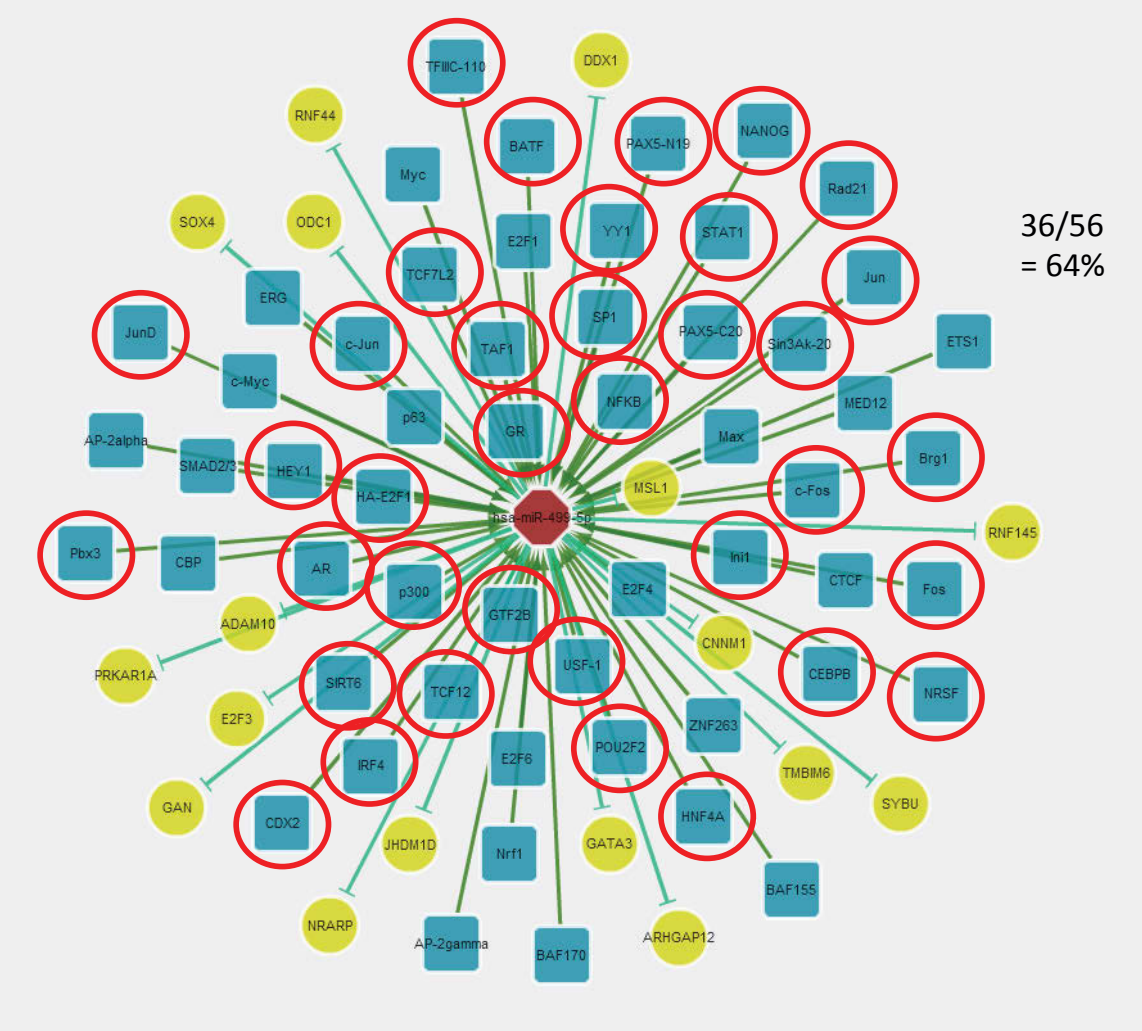

Figure 4.19. Common transcription factors between miR-21 and miR-499. Green squares represent transcription factors, yellow circles are genes that are repressed by miR-499 and the red circles are around transcription factors that target both miR-21 and miR-499. Figure obtained and adapted from ChIPBase [322].

Table 4.1. Shared transcription factors between miR-21, miR-499, brain linked miR-128 and cardio miRNA miR-125b along with their percentage similarity to miR-21 and miR-499.

	miR-21	miR-499	miR-128	miR-125b
miR-21 %	100	65	63	67
miR-499 %	67	100	81	80
	AR	AR	AP-2alpha	AR
	BATF	AP-2alpha	AP-2gamma	CEBPA
	BCL3	AP-2gamma	BAF155	CDX2
	BCL11A	BAF155	BAF170	c-Jun
	BDPI	BAF170	Brg1	CTCF
	BRF1	BATF	CBP	HNF4A
	BRF2	Brg1	CDX2	JunD
	Brg1	CBP	CEBPB	NFKB
	CDX2	CDX2	c-Fos	Nrfl
	CEBPA	CEBPB	c-Myc	NRSF
	CEBPB	c-Fos	E2F4	Rad21
	c-Fos	c-Jun	E2F6	STAT1
	c-Jun	CTCF	EBF	TCF7L2
	EBF	c-Myc	ETSI	ZNF263
	ER	E2F4	ERG	ZNF11
	ERalpha	E2F6	Fos	
	Erbeta	E2FI	FOSL2	
	Egr-1	ETSI	GABP	
	Fos	ERG	GATA6	
	FOSL2	Fos	GTF2B	
	GATA6	GTF2B	HA-E2F1	
	GTF2B	GR	HEY1	
	GR	HA-E2F1	HNF4A	
	HA-E2F1	HEY1	Inil	
	HEY1	HNF4A	IRF4	
	HNF4A	Inil	Jun	
	Inil	IRF4	JunD	
	IRF4	Jun	Max	
	Jun	JunD	Myc	
	JunD	Max	NANOG	
	NANOG	MED12	NFKB	
	NFKB	Myc	NF-YB	
	NRSF	NANOG	NF-YS	
	OCT4.	NFKB	NRSF	
	p300	Nrfl	PAX5-C20	
	PAX5-C20	NRSF	PAX5-N19	
	PAX5-N19	p300	Pbx3	
	Pbx3	p63	POU2F2	
	PU. 1	PAX5-C20	PU. 1	
	POU2F2	PAX5-N19	Rad21	
	Rad21	Pbx3	RPC155	
	RXRA	POU2F2	Sin3Ak-2D	
	Sin3Ak-2D	Rad21	SIX5	
	SIRT6	Sin3Ak-2D	Spl	
	Spl	SIRT6	STAT2	
	SRF	SMAD2/3	STAT1	
	STAT2	Spl	TAF1	
	STAT1	STAT1	TCF12	
	TAF1	TAF1	TCF7L2	
	TCF12	TCF12	TFIIIC-110	
	TCF7L2	TCF7L2	USF-1	
	TFIIIC-110	TFIIIC-110	YY1	
	USF-1	USF-1	ZNF263	
	YY1	YY1	ZBTB33	
		ZNF263		

Colour legend
miR-21
miR-499
both

4.4. Discussion

This chapter examined the miR-21 and miR-499 relationship and revealed the regulatory dynamic between the two miRNAs. Studies were conducted to determine how this regulation was occurring. Our data suggested several mechanisms for miR-499 expression. Firstly, miR-21 stabilises the mature levels of miR-499 and excess target sites further contributed to this possible stabilisation.

We noted that overexpressing miR-21 led to a significant increase in the levels of miR-499 but this was not reciprocated by miR-499. The mechanism behind the miR-21-miR-499 regulation occurs post-transcriptionally. Measuring the stability of miR-499 while inhibiting RNA Pol II revealed that miR-21 was able to increase miR-499 expression by stabilising the mature miRNA (Figure 4.13b). It was thought that miR-21 was able to stabilise the mature miR-499 by enabling interactions with a target gene 3´UTR.

When a miRNA is efficiently processed the pre-miRNA and pri-miRNA levels usually decrease as more mature miRNA is produced [323,324]. However, even though mature miR-499 expression increased, it seemed that the miR-21 interaction with pWT did not affect miR-21 and miR-499 processing. It is instead possible that the miR-21 interaction with a common target would make the more elusive miR-499 sites available for access by RISC and slow down miR-499 turnover rate. The decrease of a miRNA's turnover rate by interactions with a target site has been shown in other studies. Chatterjee et al., found in *C. elegans* that a single site mutation in the seed of *pre-let-7* reduced the amount of mature *let-7(n2853)* compared to wild type *let-7* levels *in vivo* [19]. However, the processing of mutant *let-7* was as efficient as the WT *let-7*. Therefore, they believed it was diminished target binding that caused degradation of *let-7(n2583)*. This was further proven when the overexpression of a *let-7(n2853)* target in cells rescued mutant *let-7* levels [19]. Chatterjee et al., showed that this was a specific increase as overexpressing

a target without *let-7(n2853)* sites did not change the amount of *let-7(n2853)* in cells. These findings contradict the Baccarini et al., study in which increasing RNA target expression resulted in decreased miRNA levels by accelerating the rate of miRNA decay in mammalian cells [325]. Whereas findings by Kuchen et al., supports both studies as they found in mammalian cells that overexpression of complementary target sequences to miR-744 and miR-191 caused an upregulation of miR-744 and downregulation of miR-191 [20]. Overall there is evidence for the TMMP model but further studies are required to explore the underlying mechanism for this model further.

In this chapter the amount of miR-499 was too low to be detected in the HEK293 cells but endogenous miR-21 expression was upregulated with increasing levels of the WT PDCD4 3´UTR, pWT in transfected cells (Figure 4.16a). This supports the hypothesis that increasing the number of available miR-21 sites results in a stabilisation of miR-21. This occurs as the interaction of the miRNA with the gene slows down the turnover rate of the miRNA. However, *let-7g* levels also increased with increasing PDCD4 input despite not having a binding site on the 3´UTR (Figure 4.17b). An explanation for this could be that the formation of the complex of miR-21 with Ago2 carries other miRNAs as well. This could be resolved with immunoprecipitation of the Ago2 complex in cells overexpressing miR-21 and qPCR to identify bound miRNAs.

Another possible type of miRNA-miRNA regulation is duplex formation of miRNA pairs. With this type of regulation, miR-21 would bind to miR-499 forming a duplex leading to stabilisation of miR-499. Examining the database miRWalk 2.0 provided evidence for this theory [326]. miRWalk 2.0 highlights putative miRNA-miRNA interactions. When miR-21 was used as the input in a search for miRNA binding partners the only human miRNA that was a matching binding partner from 1880 miRNAs was miR-499-3p (Figure 4.20) [327]. Thus it appears at least theoretically that the 5p arm of miR-21 interacts with the 3p arm of miR-499 leading to an increase of miR-499. This

provides theoretical evidence for the duplex theory however duplex formation of human miRNAs has yet to be proven experimentally. Lai et al., investigated miRNA-miRNA pairs and found two families of Drosophila miRNAs with a high potential to form miRNA duplexes with each other [328]. The researchers established that complementarity was not the sole reason for these miRNAs pairing together [328]. They found that there were other miRNAs with higher complementarity (which is the same situation for miR-21 and miR-499). However, this hypothesis requires further verification with human miRNAs.

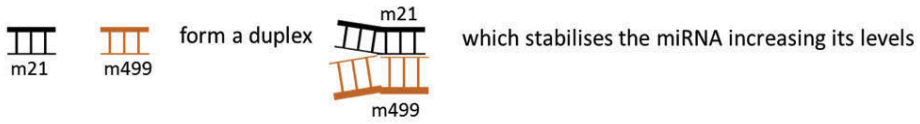

miRNA targeting	Target miRSeq	SPMS	Input miRNA	SL	SeedS	Input miRSeq	SeedE	pvalue
mmu-miR-3569-3p	UCAGUCUGCGCUCCUCUCCAGC	1	hsa-miR-21-5p	8	16	UAGCUUAUCAGACUGAUGUUGA	9	0.0003
hsa-miR-499a-3p	AACAUCACAGCAAGUCUGUGCU	1	hsa-miR-21-5p	7	20	UAGCUUAUCAGACUGAUGUUGA	14	0.0013
hsa-miR-499b-3p	AACAUCACUGCAAGUCUUAACA	1	hsa-miR-21-5p	7	20	UAGCUUAUCAGACUGAUGUUGA	14	0.0013
mmu-miR-217-3p	CAUCAGUUCCUAAUGCAUUGCCU	1	hsa-miR-21-5p	7	18	UAGCUUAUCAGACUGAUGUUGA	12	0.0013
mmu-miR-452-3p	UCAGUCUCAUCUGCAAAGAGGU	1	hsa-miR-21-5p	7	16	UAGCUUAUCAGACUGAUGUUGA	10	0.0013
rno-miR-499-3p	AACAUCACAGCAAGUCUGUGCU	1	hsa-miR-21-5p	7	20	UAGCUUAUCAGACUGAUGUUGA	14	0.0013
ptr-miR-499	AACAUCACAGCAAGUCUGUGCU	1	hsa-miR-21-5p	7	20	UAGCUUAUCAGACUGAUGUUGA	14	0.0013
ppy-miR-499-3p	AACAUCACAGCAAGUCUGUGCU	1	hsa-miR-21-5p	7	20	UAGCUUAUCAGACUGAUGUUGA	14	0.0013
mmi-miR-499-3p	AACAUCACAGCAAGUCUGUGCU	1	hsa-miR-21-5p	7	20	UAGCUUAUCAGACUGAUGUUGA	14	0.0013
ssc-miR-499-3p	AACAUCACAGCAAGUCUGUGCU	1	hsa-miR-21-5p	7	20	UAGCUUAUCAGACUGAUGUUGA	14	0.0013
gga-miR-499-3p	AACAUCACUUUAAGUCUGUGCU	1	hsa-miR-21-5p	7	20	UAGCUUAUCAGACUGAUGUUGA	14	0.0013

Figure 4.20. miR-21 may potentially form a duplex with miR-499.
Screenshot from miRWalk2.0. Dweep, H et al. miRWalk2.0: a comprehensive atlas of microRNA-target interactions, Nature Methods, 12(8): 697-697 (2015) [326].

Overall it seems that the endogenous upregulation of miR-499 when miR-21 is overexpressed in cells is not due to nascent transcription but stabilisation of the mature miRNA by miR-21. This stabilisation could possibly occur by miR-21 binding to the 3′UTR of a gene causing conformational changes which allows the miR-499 site to be accessible by RISC.

This chapter unveils an additional layer of regulation between miRNAs. The regulation of miR-499 by miR-21 may occur through interactions with target genes. Therefore, target site abundance in the cell may not only affect genes in downstream pathways but also miRNA concentration. The miRNA-miRNA regulation observed between miR-21 and miR-499 is studied further in Chapter 5 but on a genome-wide scale to determine if this is a specific phenomenon or more widespread.

Chapter 5: Exploring miR-21 and miR-499 regulation of other miRNAs and target genes

5.1. Introduction

Transcription factor-miRNA-mRNA networks play an important role in cellular biology [329-331]. These extensive networks reveal the complex regulation by miRNAs to fine-tune their control of molecular pathways. This interdependent regulation of different molecular factors is known as regulatory circuits. Molecular regulatory circuits are usually made up of transcription factors which regulate a miRNA and together they can regulate several genes [332].

An example involving miRNA circuitry is the differentiation of human granulocytes [333]. Fazi et al., showed that two transcription factors NFI-A and C/EBPα compete for binding to the miR-223 promoter. Binding of NFI-A to this promoter decreases the amount of miR-233 whereas C/EBPα upregulates miR-223. Furthermore, the interaction between miR-233 and NFI-A introduces a negative feedback loop whereby miR-233 suppresses NFI-A [333]. This highlights the complexity of regulatory circuitry and the different types of positive and negative interactions that occurs between these components leading to different responses in the cell.

Studying regulatory circuitry is important as it can reveal how modulating a single miRNA can affect a cascade of other miRNAs. This is exemplified by Tuccoli et al., who showed that decreasing miR-221 and miR-222 levels in mouse models resulted in nine other miRNAs being upregulated and 23

miRNAs downregulated [21]. Unravelling miRNA circuitry may aid in reducing side effects with the design of therapeutic miRNAs.

Chapter 4 revealed the regulatory relationship between the two miRNAs, miR-21 and miR-499. In this chapter we focus on miR-21 and miR-499 as a regulatory circuit. We identify the potential miRNAs and genes regulated by either miR-21 or miR-499. Furthermore, a bioinformatic approach was used to determine if the co-regulation by miR-21 and miR-499 was a widespread regulatory phenomenon in mammalian cells.

5.2. Methods

5.2.1. miRNA expression analysis

Total RNA extraction and purification were followed using RNAzol according to manufacturer's instructions. miRNA expression profiles were generated from HEK293 cells overexpressing 30 nM of scrambled control mimic, miR-21 or miR-499 mimic. Samples were sent to the Ramciotti centre at UNSW for Affymetrix oligonucleotide miRNA arrays.

5.2.2. Databases and programs used for analysis of microarray data

The following databases were used for analysing the array data:

TargetScan [243]

CIMminer [334]

miRWalk 2.0 [326]

miRGator [335]

miRBase [336]

5.3. Results

5.3.1. The expanding regulatory network for miR-21 and miR-499

In previous chapters we demonstrated that miR-21 and miR-499 regulated the specific tumour suppressor PDCD4 and this occurred in an interdependent manner. Furthermore, miR-21 amplified miR-499 silencing potency. Therefore, this raised the possibility of other miR-21 and miR-499 co-regulated targets. To investigate the co-targeting by miR-21 and miR-499 on a wider spectrum, TargetScan was used to find potentially co-regulated targets.

To this end, a list of target genes containing miR-21 and miR-499 sites was obtained (Table 5.1). Sixteen genes were found containing both sites with five of these genes (PDCD4, SOX5, MEIS1, SOX6, WDR3) containing more than one miR-499 site. This allows for the possibility of co-dependent regulation between these miR-499 sites. Furthermore, this would suggest that the interdependent regulation of PDCD4 by miR-21 and miR-499 is not just restricted to this gene but may extend to other targets. However, it should be noted that the distance between most of the miR-499 sites was greater than the consensus 13-40 nts for cooperative binding [254,277]. Therefore, it is likely that miR-499 sites may impart a regulation on the 3´UTR that is either co-dependent or independent.

Table 5.1. TargetScan predictions of conserved and poorly conserved genes co-targeted by miR-21 and miR-499. The location of the miR-21 and miR-499 sites along with the distance between miR-499 sites.

Conserved			
Gene	miRNA sites on 3'UTR (nt)		Distance between predicted binding sites for miR-499
	miR-21	miR-499	
SOX6	5302-5308	113-119 289-295 600-607 622-628 915-922	170 305 15 287 290
PDCD4	242-249	17-23 467-473 533-539	444 60
SOX5	226-233	115-122 280-286	158
MEIS1	1500-1507	1138-1144 1605-1611	461
SATB1	887-893 933-939	804-810	-
FOXP2	2804-2810	1327-1334	-
ZNF438	165-171	200-206	-
TESK2	378-385	636-643	-
PBRM1	155-162	2615-2621	-
PPP3CA	1129-1135	540-547	-
ACBD5	332-338	2017-2023	-
JPH1	2054-2060	560-566	-
Poorly Conserved			
WDR3	905-911	826-833 7030-7036	6197
ARHGAP24	16-22	51-58	-
NR0B1	261-268	342-348	-
BSPRY	87-93	1069-1075	-

5.3.2. miR-21 and miR-499 regulate other miRNA

Based on the previous results whereby the overexpression of miR-21 in HEK293 cells resulted in the increased expression of miR-499 levels, we investigated if miR-21 could regulate the expression of other miRNAs beside miR-499.

Using the Affymetrix miRNA array, we characterised the expression of other miRNAs from cells overexpressing 30 nM of miR-21, miR-499 and a scrambled control miRNA mimic. The results revealed that both miR-21 and miR-499 were able to modulate the expression of specific miRNAs (Table 5.2, refer to electronic data). It must be noted that the upregulation of miR-499 by miR-21 was not as pronounced as previously measured by qPCR. This can due to the different detection sensitivity which is inherent to oligonucleotide arrays and qPCR [337,338].

An interesting observation was that miR-499 upregulated other miRNAs to a greater extent than miR-21. The ten most upregulated miRNAs by miR-499 had an average fold change of 90 compared to a mean fold change of 17 for miR-21. miR-21 and miR-499 were also observed to downregulate miRNAs (Figure 5.1, Refer to electronic data).

Table 5.2. Microarray data of the top ten upregulated miRNAs in cells overexpressing miR-21 or miR-499. The fold change is expressed relative to a scrambled control miRNA mimic. The yellow highlighted miRNA is upregulated by both miR-21 and miR-499.

miR-21 overexpression	Fold	miR-499 overexpression	Fold
hsa-miR-3613-5p	66.101	hsa-miR-873-5p	348.459
hsa-miR-19a-3p	18.843	hsa-miR-224-5p	111.300
hsa-miR-339-3p	13.293	hsa-miR-3613-5p	105.589
hsa-miR-183-5p	12.652	hsa-miR-3148	85.502
hsa-miR-187-3p	11.464	hsa-miR-548a-3p	44.710
hsa-miR-196a-5p	10.500	hsa-miR-5009-3p	42.789
hsa-miR-503-5p	9.618	hsa-miR-1298-3p	42.479
hsa-miR-15a-5p	9.408	hsa-miR-1468-3p	42.134
hsa-miR-378g	8.111	hsa-mir-335	36.102
hsa-miR-192-5p	8.111	hsa-mir-548y	36.097

Clustering of these miRNAs using hierarchic clustering (two matrix) and the resulting heat map based on some of the miRNAs gave a visualisation of the array data (Figure 5.1). It showed the similar regulation of miRNAs by both miR-21 and miR-499. miRNAs that were upregulated by both miR-21 and miR-499 overexpression included miR-19a-3p, miR-3613-5p, miR-503-5p, miR-15a-5p. Whereas miRNAs downregulated by both miR-21 and miR-499 overexpression were miR-3663-3p, miR-3195, miR-6778-5p and miR-6831-5p. There was also differential regulation of miRNAs for example miR-225-5p which is upregulated by miR-499 but downregulated by miR-21 (Figure 5.1).

Figure 5.1. CIMminer heat map of a small group of randomly selected miRNAs altered in the miR-21 and miR-499 overexpression array. Red refers to miRNAs that are upregulated and blue to miRNAs that are downregulated.

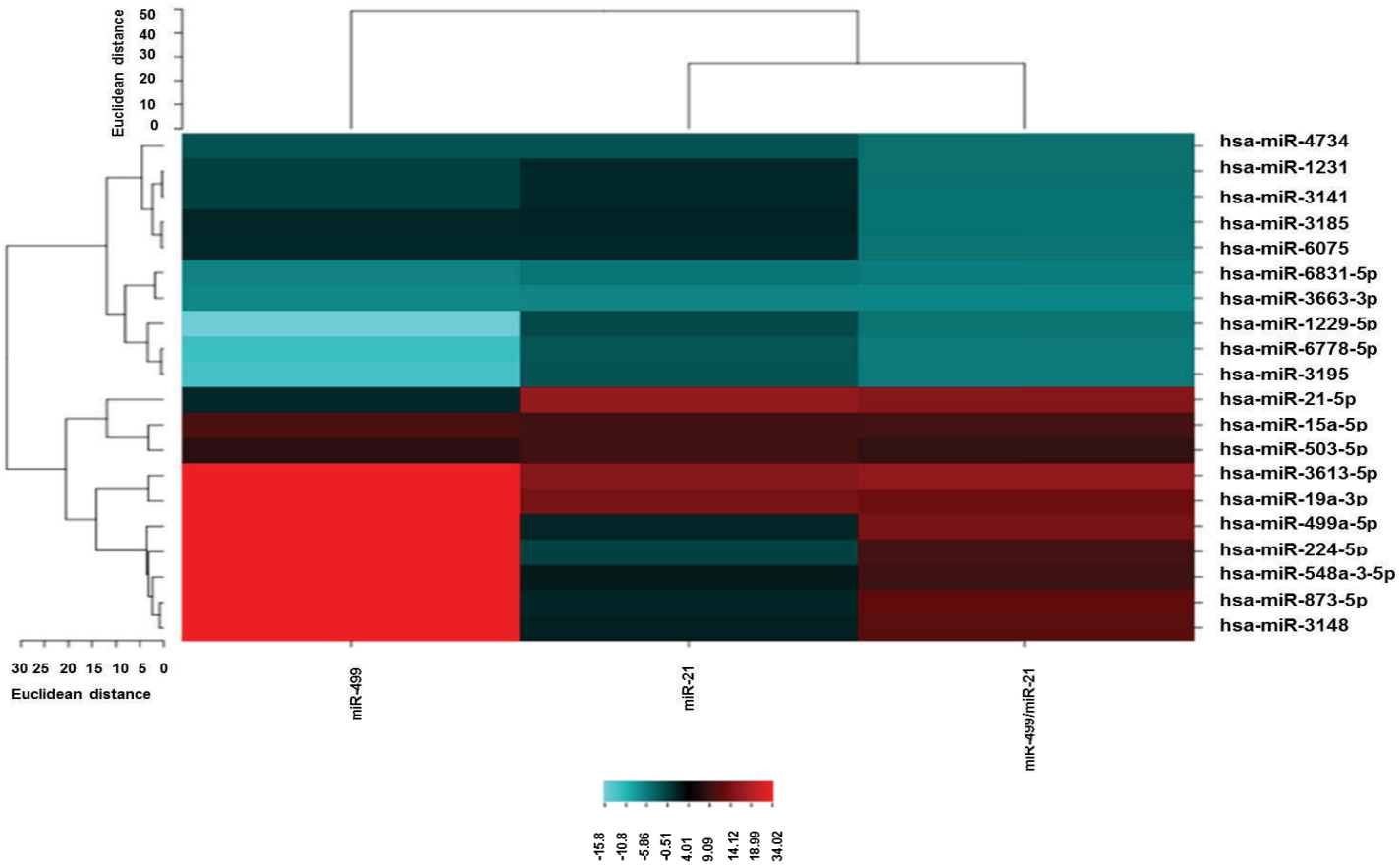

5.3.3 Relationship between miR-21 and the top upregulated miRNAs

We then assessed if there was a relationship in the miRNAs upregulated by miR-21 or miR-499. However, we noted that most of the miRNAs upregulated by miR-499 were recently discovered and there is limited information regarding their function and expression in cancer. In contrast most of the miRNAs regulated by miR-21 are well characterised and could be further explored.

The genomic loci of these regulated miRNAs were examined using miRBase. This was to determine if these miRNAs were derived from a common transcript or were proximally located near each other. The locations of these miR-21 upregulated miRNAs were found to be randomly distributed throughout the genome and thus there is no common genomic trend linking these miRNAs (Table 5.3).

Table 5.3. Location of the top most upregulated miRNAs in miR-21 overexpressing cells.

miRNA	Chromosome location
miR-21	17q23.1
miR-499	20q11.22
miR-19a	13q31.3
miR-339	7p22.3
miR-183	7q32.2
miR-187	18q12.2
miR-196a	17q21.32
miR-503	Xq26.3
miR-15a	13q14.2
miR-378g	1
miR-192	11q13.1

In this genome-wide analysis we wanted to determine if there was a relationship between the seeds of the top upregulated miRNAs by miR-21. If these miRNAs shared a similar seed sequence it would suggest that regulation by miR-21 is influenced by the seed. Table 5.4 shows that the miRNAs all had different seed sequences except for miR-15a and miR-503. This implies that the increase of these miRNAs in cells overexpressing miR-21 is not due to their seed sequence. However further studies would be required to determine if the promoters or motifs within these miRNAs could be related.

Table 5.4. Mature miRNA sequences (5´-3´) of the top upregulated miRNAs by miR-21 overexpression. The seed sequences are bolded and identical seed sites are highlighted in green.

miRNAs	Mature miRNA Sequence (5'-3')
hsa-miR-3613-5p	U**GUUGUAC**UUUUUUUUUUGUUC
hsa-miR-19a	U**GUGCAAA**UCUAUGCAAAACUGA
hsa-miR-339-3p	U**GAGCGCC**UCGACGACAGAGCCG
hsa-miR-183-5p	U**AUGGCAC**UGGUAGAAUUCACU
hsa-miR-187-3p	U**CGUGUCU**UGUGUUGCAGCCGG
hsa-miR-196a-5p	U**AGGUAGU**UUCAUGUUGUUGGG
hsa-miR-503-5p	U**AGCAGC**GGGAACAGUUCUGCAG
hsa-miR-15a-5p	U**AGCAGC**ACAUAAUGGUUUGUG
hsa-miR-378g	A**CUGGGCU**UGGAGUCAGAAG
hsa-miR-192-5p	C**UGACCUA**UGAAUUGACAGCC

5.3.4. Involvement of miR-21 and upregulated miRNAs in HNSCC

Furthermore, we wanted to explore the miR-21 upregulated miRNAs in a head and neck cancer context. Examination of the literature revealed that indeed all the miRNAs upregulated by miR-21 are differentially expressed in various head and neck cancers (Table 5.5). Most of the miRNAs were oncomiRs like miR-21 and were overexpressed in HNSCC tumours. The only exceptions were miR-503 and miR-378g which were downregulated in tumour tissue.

The miRNAs linked with laryngeal cancer included the upregulated miRNAs miR-3613-5p [339], miR-19a [340], miR-183 [341], miR-187 [341,342], and miR-196a-5p [341,343]. Oral cavity tumours were associated with the upregulated miR-19a-3p [340,341], upregulated miR-183-5p [341], upregulated miR-187-3p [341], upregulated miR-196a-5p [343,344], downregulated miR-503 [345] and upregulated miR-15a [346].

Oropharyngeal cancers were linked with the upregulated miRNAs miR-19a-3p [340,341] and miR-196a-5p [341,343,344]. Cancers affecting the tongue correlated with changes in the expression of upregulated miR-339 [343], upregulated miR-196a-5p 5p [343,344] and downregulated miR-503 [342,345]. Floor of the mouth tumours were linked with upregulated miR-339 [343] and upregulated miR-196a-5p [341,343,344]. Nasopharyngeal cancers were associated with upregulated miR-183-5p [341], upregulated miR-187-3p [341], downregulated miR-378g [347] and upregulated miR-192 [348].

Therefore, the overexpression of miR-21 in head and neck cancers may lead to further regulation of other oncogenic miRNAs and activation of multiple cancer related pathways.

Table 5.5. The dysregulation of the ten most upregulated miRNAs in the miR-21 overexpression array in various HNSCC tumours.

miRNA	Head and neck tumor location	References
hsa-miR-3613-5p	larynx	Huang et al 2013
hsa-miR-19a-3p	larynx, oral cavity, oropharynx, oral cavity	Wu et al 2014, Harris et al 2012, Hebert et al 2007
hsa-miR-339-3p	tongue and floor of mouth	Severino et al 2013
hsa-miR-183-5p	larynx, oral cavity, nasopharynx	Harris et al 2012
hsa-miR-187-3p	larynx, oral cavity, nasopharynx	Harris et al 2012, Lajer et al 2011
hsa-miR-196a-5p	oral cavity, oropharynx, hypopharynx, larynx, tongue and floor of the mouth	Liu et al 2010, Severino et al 2013, Harris et al 2012
hsa-miR-503-5p	oral cavity, tongue	Lajer et al 2011, Lu et al 2012
hsa-miR-15a-5p	oral cavity	Hebert et al 2007
hsa-miR-378g	nasopharynx	Lin et al 2015
hsa-miR-192-5p	nasopharynx	Sengupta et al 2008

5.3.5. Co-targeted genes between miR-21 and upregulated miRNAs

If these miRNAs are all involved in HNSCC they potentially could regulate the same genes forming a regulatory circuitry. Identifying miRNAs that are upregulated by overexpression of another miRNA could lead to the identification of co-regulated targets. Our hypothesis from the previous chapter was that miR-21 was stabilising miR-499 through possible interactions with a common target. This would suggest that these upregulated miRNAs from the microarray should also have similar targets to miR-21.

Using the miRGator database with the Miranda algorithm, genes that were potentially co-regulated between miR-21 and eight of the upregulated miRNAs were analysed. miR-3613-5p and miR-378g were excluded as these miRNAs were not present in the miRGator database. All the miRNAs had co-targeted genes with miR-21 and in some instances up to three miRNAs targeted the same gene (Table 5.6).

Table 5.6. Genes targeted by miR-21 and the upregulated miRNAs in the miR-21 overexpression array. In green are genes with more than one site for the upregulated miRNA and in bold are genes which are targeted by more than two miRNAs including miR-21.

miR-21/miR-339	miR-21/miR-19a	miR-21/miR-187	miR-21/miR-15a	miR-21/miR-183	miR-21/miR-196a	miR-21/miR-503	miR-21/miR-192
AGXT	ARMCX1	HFE2	GUCA1C	PTGER3	IGFBP7	**RAGE**	**DCTN3**
GPR6	**CCPG1**	**AGXT2L1**	IQCA	**WHSC1L1**	MELK	ACTA1	VSX1
NUSAP1	**DCTN3**	**ARMC4**	**MYO6**	AKAP12	**RHCE**	**BNIP1**	**ASB3**
SPAG11	DDX24	CACNG1	ARL6	APEH	ADFP	HERPUD1	CBX8
TRIM29	DNAJA2	GBAS	**CSE1L**	ARMCX5	**AGXT2L1**	**HTN1**	CHRNB1
VMD2L1	FBXO4	IL13RA2	HMGCS2	**CALCB**	ALS2CR19	LATS1	CHST2
ZNF575	METTL3	ITGB1BP1	**HTN1**	CART1	ANXA1	RNF32	CLNS1A
	PRKAA1	MRPL43	IL15	CCKAR	AP1M2	**SNRPA1**	CTCF
	RHCE	**PRKAA1**	INSR	**CCL18**	APOB	**SPTBN4**	EXOSC3
	ARMC4	RNF103	**PDCD6**	CLEC4A	**ASB3**	**VMD2L1**	**EXT2**
	BANK1	SARDH	**RAGE**	**EBNA1BP2**	**CALCB**	**WHSC1L1**	FARS2
	BNIP1	SCAP1	RIT2	**EXT2**	CDR2		HIST1H2BF
	CCL18	**SRP19**	**SNRPA1**	HS3ST1	**EBNA1BP2**		LNX
	CD69	STATH	**SPTBN4**	**ING3**	FYB		LZTFL1
	CNTFR	TEX14	VRK3	LPA	HSPH1		PIK3R4
	CR2	UCHL1	**WHSC1L1**	MPHOSPH10	**HTN1**		RNF6
	CSE1L	VGLL1	ZNF142	**NUSAP1**	INSL3		SMARCA5
	DNAJB11		ZNHIT1	**PDCD6**	LRRC3B		WFDC13
	FOSL1			**PLK1**	**MYO6**		
	FUNDC1			POT1	NIN		
	HERC1			RNF123	POLI		
	ING3			SLC10A1	SALL3		
	MASS1			SLC35B3	SLC16A10		
	MID1IP1			SPRY2	SMCR8		
	PADI4			SURB7	**SPTBN4**		
	PLK1			**TUSC3**	STK25		
	RASA1				**WHSC1L1**		
	RNF34						
	SPOCK						
	SRP19						
	THBS1						
	TMEM45A						
	TUSC3						
	UBE3B						
	USMG5						
	ZNF219						

5.3.6. The miRNAs in the miR-17-92 cluster are differentially regulated by miR-21

Further analysis of the miRNA array results revealed that the six members of the miR-17-92 polycistronic cluster were differentially regulated by miR-21 (Table 5.7). Given the differential expression between members of this cluster when miR-21 is overexpressed suggests that the miRNA increase is not due to transcriptional activation. Otherwise all the members which are regulated by the same promoter would have been affected by miR-21 overexpression [349,350]. This provides support that miR-21 may by stabilising the other miRNAs perhaps by interactions with a co-targeting gene.

Table 5.7. Fold change of miRNAs in the miR-17-92 cluster in HEK293 cells containing miR-21 or miR-499 overexpression.

	Fold Change	
	miR-21 Overexpression	miR-499 Overexpression
hsa-miR-17-5p	2.288	3.690
hsa-miR-17-3p	1.904	1.904
hsa-miR-18a	1.000	1.000
hsa-miR-18a-5p	3.241	6.529
hsa-miR-18a-3p	1.160	0.576
hsa-mirR-19a	1.106	1.106
hsa-miR-19a-5p	1.179	1.000
hsa-miR-19a-3p	18.843	35.466
hsa-miR-20a	1.250	1.250
hsa-miR-20a-5p	2.827	5.284
hsa-miR-20a-3p	0.904	1.000
hsa-miR-19b-1	1.000	1.140
hsa-miR-19b-1-5p	1.000	1.000
hsa-miR-92a-1	1.000	0.940
hsa-miR-92a-1-5p	1.021	0.940

Previously examining the seed sequences of the most upregulated miRNAs by miR-21 revealed no commonality. The seed sequences of the miR-17-92 cluster are related and thus also examined. The miRNA pair miR-17 and miR-20a have identical seeds and are upregulated with miR-21 overexpression (Table 5.8). Conversely miR-18a and miR-19a-3p have different seed sequences and yet are also upregulated with miR-21 overexpression. This reaffirms the earlier conclusion that miR-21 regulates multiple miRNAs independent of their seed sequence.

Table 5.8. Seed sequences of miRNAs in the miR-17-92 cluster.

Upregulated miRNAs from miR-21 overexpression are highlighted yellow and seed sequences are bolded. Identical seed sequences are highlighted green or light blue.

miRNAs	Mature miRNA Sequence (5'-3')
hsa-miR-17-5p	C**AAAGUG**CUUACAGUGCAGGUAG
hsa-miR-17-3p	A**CUGCAG**UGAAGGCACUUGUAG
hsa-miR-18a-5p	U**AAGGUG**CAUCUAGUGCAGAUAG
hsa-miR-18a-3p	A**CUGCCC**UAAGUGCUCCUUCUGG
hsa-miR-19a-5p	A**GUUUUGC**AUAGUUGCACUACA
hsa-miR-19a-3p	U**GUGCAA**AUCUAUGCAAAACUGA
hsa-miR-20a-5p	U**AAAGUG**CUUAUAGUGCAGGUAG
hsa-miR-20a-3p	A**CUGCAU**UAUGAGCACUUAAAG
hsa-miR-19b-1-5p	A**GUUUUGC**AGGUUUGCAUCCAGC
hsa-miR-92a-1-5p	A**GGUUGGG**AUCGGUUGCAAUGCU

5.4. Discussion

In this chapter we explored the co-targeting of genes by miR-21, miR-499 and miR-21 upregulated miRNAs. We identified other possible targets for miR-21 and miR-499 and noted that these targets were perhaps regulated in the same interdependent manner as the PDCD4 3´UTR. Analysis of the miRNA array revealed that miR-21 and miR-499 were able to stimulate the expression of other miRNAs and there was some overlap between the miRNAs they regulated. Further examination of the miR-21 upregulated miRNAs found that they were altered in HNSCC but they did not have any sequence similarities and were distributed randomly throughout the genome.

Investigating TargetScan revealed several genes that were regulated by both miR-21 and miR-499. A few studies have concluded that weak sites are a prerequisite of interdependent regulation [238,257]. These sites cannot be regulated on their own such as the last two miR-499 sites on the PDCD4 3´ UTR, which are also regulated by a miRNA lowly expressed in most cells. These weak sites require a strong site (sites which can downregulate the 3´UTR on their own) such as miR-21 in the PDCD4 3´UTR which is optimally located and is also the site of a highly expressed miRNA. Thus while this could be the situation in the five miR-21, miR-499 regulated genes (PDCD4, SOX5, MEIS1, SOX6, WDR3) with multiple miR-499 sites, there are other genes with just a single site of miR-499. This would suggest that the interdependent regulation by miR-499 is only required in certain contexts (PDCD4) and the miRNA is capable of regulating a single site. Alternatively, the single miR-499 sites in these other genes could be inactive/redundant, similar to the first miR-499 site in PDCD4.

This study determined the specificity of the miR-21-miR-499 regulation. Analysis of the miRNA array revealed that the miRNA-miRNA regulation appeared to be a pervasive occurrence with miR-21 and also miR-499 being

able to regulate many miRNAs. miR-499 appears to be a more potent activator of miRNAs than miR-21. This reveals an interesting observation where the overexpression of an endogenously lowly expressed miRNA causes a significant upregulation of other lowly expressed miRNAs. However, the array would need to be repeated with two more independent miR-21 and miR-499 transfected samples to draw significant conclusions.

It is known that not all miRNAs are capable of regulating other miRNA. As Matkovich et al., discovered, the overexpression of miR-143 did not change the miRNA environment in their mouse models whilst miR-378 and miR-499 did [22]. An interesting question is how miRNAs dictate which specific miRNAs they will regulate in a cell. From this chapter we know that it is most likely not due to the location or the seed sites of the miRNAs. This contradicts the study by Na and Kim who found that miRNAs that co-targeted genes had significantly similar seeds [276].

The miRNAs upregulated by miR-21 are involved in HNSCC and potentially co-target genes. This would indicate that miR-21 is regulating miRNAs that participate in similar pathways. This combinatorial regulation by multiple miRNAs can then lead to a stronger suppression or more complex fine-tuning of miR-21 based pathways. The identification of pathways regulated in a novel manner in HNSCC carcinogenesis would greatly expand our molecular understanding of this disease. To date, there are no publications which explore the miRNA-miRNA interaction as a driver for HNSCC development.

In summary this chapter highlights the relationships between miRNA pairs, groups and common genes. These miRNAs and genes are indirectly and directly regulating each other forming a complex network of miRNA-miRNA-mRNA interactions that can allow for the refinement and activation of different pathways in different cellular contexts spanning both normal and disease biology.

Chapter 6: miR-21 and miR-499 promote migration in Head and Neck Cancers

6.1. Introduction

The development of cancer consists of a series of key events including proliferation, migration, invasion and metastasis to lymph nodes and to secondary sites. HNSCC cells when migrating from their primary site to a distant site first undergo regional metastasis [351]. This is when, tumour cells enter microvessels surrounding the primary site which provides access to the lymphatic channels. From these channels, the cells migrate to regional lymph nodes in the neck where they settle and proliferate [351]. A tumour that has progressed to the regional nodes is usually considered aggressive as the tumour is more likely to recur after treatment [352]. Distant metastasis to a secondary organ occurs during a series of processes including, degradation of the extracellular matrix, tumour migration, angiogenesis and invasion into the vascular system and blood circulation of the tumour cells to the secondary site [351].

In patients with lymph nodes metastasis survival is reduced by 50% [353,354]. Once these tumour cells reached the nodes they now have access to blood vessels and serosal surfaces and can migrate to distal parts of the body [353,354]. The most common sites for metastasis are the lung, bone and liver [355]. Different subtypes of HNSCC have different rates of metastasis [356]. In a study involving 992 patients, patients with cancers originating from the hypopharynx and base of tongue had the highest rate of metastasis with more than 50% having distant metastasis (80% of these distant metastases

being in the lung). Furthermore, Stage IV patients had the highest incidence of distant metastases.

The overall survival for patients with recurrent or metastatic cancer is less than a year. The standard treatment for HNSCC patients with metastatic cancer is palliative systemic therapy with a chemotherapeutic agent and/or EGFR inhibitor [355]. Since the 1980s platinum-based chemotherapeutic agents such as cisplatin has been the standard treatment for metastatic cancer [355,357]. The only targeted therapy used currently is the drug Cetuximab which is a monoclonal antibody to EGFR [355]. Emerging therapies involve targeting the PI3K/AKT/mTOR pathway. Some potential drug targets include MET which is upstream of the pathway [358] and mTOR a serine/threonine kinase downstream of PI3K/AKT [355].

Cell proliferation is a component of tumourigenesis that occurs when cells divide at a rate greater than the baseline level due to external or internal stimuli [108]. There is a direct link between miRNAs and proliferation in head and neck cancer cells. A study investigating the levels of miRNAs in HNSCC tissues found miR-874 to be downregulated in most tissues. Using the head and neck cell lines SAS and FaDu it was found that overexpressing miR-874 inhibited cell proliferation, induced G2/M arrest in the cell cycle and caused cell apoptosis [359]. Another study showed that restoring miR-133a expression in HNSCC cells suppressed proliferation, most likely through the moesin gene which is involved in cross-linking the plasma membrane to the actin cytoskeleton [360]. In contrast overexpression of miR-205 has the opposite effect in HNSCC cells by stimulating proliferation [361]. Another study showed that two miRNAs, miR-196a and miR-10b which are part of the miR-17-92 cluster were dysregulated in carcinogenic tissue samples [343]. Gain-of-function experiments also revealed a disruption of proliferative pathways by these miRNAs [343].

Migration is another component of tumour progression. Cell migration occurs when cells gain the ability to be mobile which is essential for cell metastasis. In order for cell migration to occur specific signaling molecules are activated leading to remodeling of the actin cytoskeleton [114]. Several miRNAs are known to either promote migration or suppress it such as miR-101[115] and miR-10b [116].

There are few studies regarding the functional role of the oncomiRs, miR-21 and miR-499 in HNSCC. Studies from other cancers show that inhibiting miR-21 suppresses proliferation in cervical cancer cells [362] and reduces lung metastasis in colorectal cancer [103]. miR-21 has been linked with the migratory capacity of hepatocellular carcinoma cells and miR-21 inhibition repressed cell migration [363]. Furthermore, miR-21 in breast cancer cells has been found to promote proliferation and cell growth *in vitro* and *in vivo* [132,364].
The function of miR-499 in cancer is less well-documented and there is no functional data in HNSCC. Low serum expression levels of miR-499 has been linked with poor survival in non-small-cell lung cancer [365]. Another study has shown that overexpressing miR-499 increased migration *in vitro* and promoted lung and liver metastasis *in vivo* [293].

In previous chapters miR-21 and miR-499 were found to be upregulated in HNSCCs indicating that they may be involved in promoting and/or maintaining tumourigenesis. No study has described the functionality of both miR-21 and miR-499 in HNSCC. This chapter aims to uncover their functionality through the use of the proliferation assay, scratch assay and live cell imaging. This allows for the analysis and visualisation of changes to HNSCC cell lines upon transfection with miR-21 and miR-499. Overall this chapter will focus on the role of these miRNAs in HNSCC in terms of proliferation and migration – key pathways in cancer development.

6.2. Methods

6.2.1. Scratch Assays

6.2.1.1. Manual Scratch

HNSCC cell lines were seeded into 24-well culture plates and grown until 80-90% confluency (Table 6.A). The cells were then transfected with 30 pmol of miR-21, miR-499 and *let-7a* mimics. At 24 hours post-transfection cells were at 100% confluency and a p200 pipette tip was used to create a vertical scratch through the confluent cells. The scratched cells were viewed with a standard microscope with a mounted camera. Images were taken of the scratch either at 4X or 10X and the cells placed at 37°C, 5% CO_2 for 18-24 hours. The cells were then photographed at the end of the time point at the same location as the initial scratch. The images were analysed with ImageJ to determine the width of the scratch using the line tool [303] (Figure 6.A).

Table 6.A. Seeding densities of the various head and neck cancer cell lines used in the scratch assay to reach 100% confluency at the same time.

Cell line	Cells seeded/24-well	Cells/ml
Hela	$5X10^4$	$1X10^5$
SCC099	$1.8X10^5$	$3.6X10^5$
SCC4	$7X10^4$	$1.4X10^5$
SCC089	$1X10^5$	$2X10^5$
UMSCC22B	$9X10^4$	$1.8X10^5$

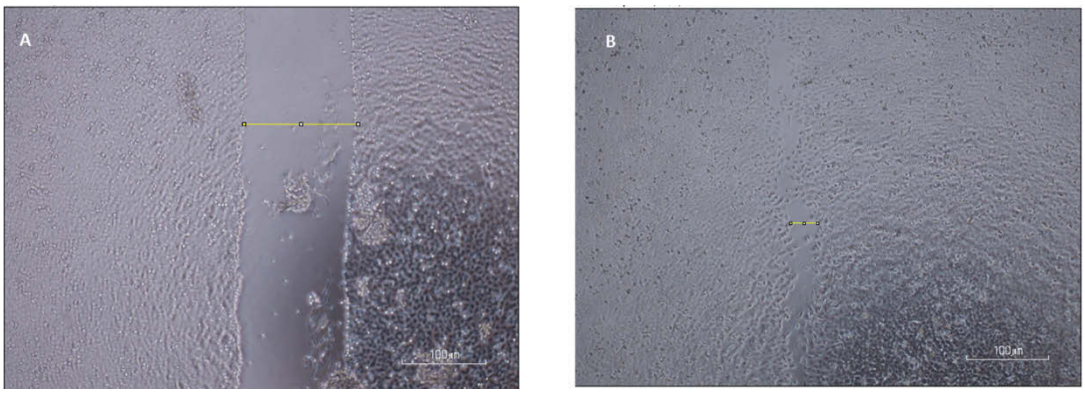

Figure 6.A. Manual quantification of the scratch under 10X magnification. (a) The initial scratch with the line tool superimposed over the scratch using ImageJ. **(b)** The scratch area 18 hours later showing closure of the gap.

6.2.1.2. Live Cell Imaging

Cells were seeded into 24-well plates, transfected and scratched accordingly. The scratched cells were taken to the Nikon Ti inverted epifluorescent microscope which also had a mounted 37°C, 5% CO_2 chamber. The microscope was programmed to capture an image every 30 minutes over 23 hours at the same spot in each well. Three independent areas of each scratch was captured with duplicate wells per condition. The image analysis program Fiji [366] was used to determine percentage area of the wound over the total area over time. These values were used to calculate the rate of migration. RNA was isolated at the end of the scratch assay from each well by adding 0.5 ml of RNAzol to the wells. The RNA isolation procedure and qPCR were then conducted as described previously.

6.2.1.2.1. Image analysis

Analysing the scratch image through Fiji involved a series of steps modified from the Fiji Training Manual [366]. Prior to image analysis, the images had to be converted into pseudo fluorescent images. This was achieved by opening the stack of images (representing a single area of the scratch consisting of the 46 images taken over 23 hours) in Fiji and defining the edges of the cells. This required selection of the Process tab followed by Find Edges. To sharpen the image, the Process tab was selected then Sharpen. The Process tab was then selected followed by Filters then Gaussian Blur. In the Gaussian Blur dialog, a value of 5 was entered into Sigma (Radius) box which made the cells white and contrasts against the dark scratch area. All of this was performed on the initial image and then the program would automatically process all images in the stack accordingly.

6.2.1.2.2. Thresholding the scratch

The images required a threshold to separate the scratch margin from the cells. This was done by opening the Image tab selecting Adjust then selecting Threshold. The Threshold dialog box was configured to a dark

background and the area of the scratch was made red. Areas that are not part of the scratch were selected as well and these areas were removed from analysis via size exclusion.

6.2.1.2.3. Eliminating unwanted areas from the scratch

Size exclusion was achieved by opening the Analyse tab, selecting Set Measurements followed by Area, Limit to threshold and Display Label in the dialog box. The Analyse tab was selected followed by Analyse particles. The Analyse Particles dialog box was configured so that Size ($pixel^2$) was usually 500-Infinity (but this was dependent on each scratch and the size of the gaps that needed to be excluded), Circularity was 0.00-1.00 and Show was Masks. Clear results and Summarize were also selected in the dialog box. After accepting this all planes were processed so that the size exclusion was applied to each image captured in a stack of 23 hours' worth of images. Each image showed the outline of the scratch and the number of gaps excluded and their size. This was also summarised in a table for all the planes (images in a stack). This table was used to determine whether the size exclusion settings needed to be altered.

6.2.1.2.4. Creating an outline of the scratch

The next step was to create an outline of the scratch which could be placed over the original image to confirm proper separation of the cells and scratch prior to measurement of the scratch area. This was achieved by first duplicating the image through the Image tab and Duplicate option. The second image needed to be thresholded (Refer to Section 6.2.1.2.2) and the size exclusion applied (Refer to Section 6.2.1.2.3).

This resulted in a binary mask of the analysed area with the scratch area in black and the cells in white. If this was not the case, the image could be inverted by selecting the Edit tab followed by Invert. The next step was to open the Process tab followed by Binary and then Outline and the image inverted so that the image was black with a white outline representing the

edges of the scratch. All planes were then processed so that the mask was applied to all images in the scratch. The original and duplicate images were required to have the same bit depth so that the outlined image could be merged over its original image. To execute this function, the original image was selected, the Image tab opened, followed by Type and 8 bit. To merge the images, the Image tab was selected followed by Colour, and Merge Channels. The Merge Channels dialog was configured so that C2 (green): Mask of image, C4 (gray): Original image and the remaining C1, C3, C5-7 was None. Create composite and Keep source images were selected in the dialog box as well. This resulted in a composite (two channels in a stack) image which was then converted to RGB so that it would be compatible with Powerpoint. The composite video was selected and the Image tab opened, followed by Color then Stack to RGB. The video was saved as an AVI file with Compression set to JPEG and Frame Rate at 5 fps.

6.2.1.2.5. Measuring the rate of migration

To retrieve the area of the scratch from the video for each plane/frame/image, the Analyse tab was selected followed by Set Measurements, the options Area Fraction and Limit to Threshold to get a summary table with area and percentage area of the scratch for each image in a stack. These values were transferred to Excel and divided by time (hours) to calculate the rate of migration at each time point.

6.2.2. Proliferation

Cells were seeded at $4X10^4$ into each well of a 24-well plate and left overnight in a 37°C, 5% CO_2 incubator. The cells were transfected with 6 pmol miRNA mimics and left for 30 hours in a total volume of 500 μl per well. 50 μl of CellTiter 96 Aqueous One Solution (Promega, Australia) was then added into each well. After 5 minutes and 40 minutes incubation at 37°C and 5% CO^2, 100 μl of culture medium from each well were transferred to a clear

bottom 96 well plate for absorbance measurement at 490 nM with the Tecan spectrophotometer.

6.3. Results

6.3.1. The expression of tumour suppressor genes in head and neck cancer cell lines of different tumourigenicity

To understand the functional contribution of miR-21 and miR-499 in HNSCC, two aspects of tumour development – proliferation and migration were studied. Several HNSCC cell lines of varying tumourigenicity were acquired (Table 6.1). They represented the various stages of cancer including primary, recurrence and metastasis. These cells acted as an ideal model for functional studies as they are easily manipulated and the resulting changes in cell behaviour quantifiable.

SCC099 is a recurrent stage I cell line originating from the floor of mouth and was the least aggressive cell type [367]. This was empirically observable as these cells demonstrated slow migration and reduced proliferative rates over 24 hours compared to the other head and neck cancer cell lines. SCC4 is a stage III, primary cell line originating from the tongue of a patient treated with radiotherapy and chemotherapy. SCC089, a stage IV primary cell line was isolated from the tonsil, is distinctively shaped and moved aggressively when viewed under the microscope [367]. UMSCC22B is a stage III, metastatic cell line originating from the hypopharynx which has migrated from the lymph nodes [368]. Hela cells are derived from a cervical cancer patient and were used as a control for a non-head and neck cancer cell line (Table 6.1).

Table 6.1. Characteristics of Hela and the four HNSCC cell lines used in this study.

Name	Cell line	Stage	Specimen site	Type of lesion	Primary site	Previous treatment
Control	HeLa	-	N/A	-	Cervix	Radiation
Stage I, Recurrence	SCC099	I	Floor of mouth	Recurrence	Floor of mouth	None
Stage III, Primary	SCC4	III	Tongue	Primary	Middle of tongue	Radiotherapy, chemotherapy
Stage III, Metastatic	UMSCC22B	III	Lymph node	Metastasis	Hypopharnyx	None
Stage IV, Primary	SCC089	IV	Tonsil	Primary	Tonsil	None

6.3.2. miR-21 and miR-499 do not promote proliferation in HNSCC cell lines

miRNAs are involved in multiple pathways relating to cancer [103,109,369-372]. An early pathway in tumourigenesis is proliferation and we reasoned that miR-21 and miR-499 may be able to promote proliferation in HNSCC cells. Proliferation was tested in cell lines Stage III metastatic UMSCC22B, Stage IV primary SCC089 and Stage III primary SCC4. These cells were transfected with 30 nM of control mimic, miR-21 or miR-499. At 30 hours post transfection CellTiter96 Aqueous One Solution reagent was added to the cells and proliferation measured 5 minutes and 40 minutes post administration.

There was no difference in the proliferation of cells transfected with either miR-21 and miR-499 compared to the control miRNA mimic at both time points in either UMSCC22B, SCC089 or SCC4 (Figure 6.1a, b). Manual cell counts were also conducted and the UMSCC22B and SCC4 cell lines were shown to have no difference in cell numbers thus corroborating the proliferation results (Figure 6.2). The SCC089 cells could not be counted manually due to their tendency to aggregate. In summary, miR-21 and miR-499 overexpression in these HNSCC cell lines did not promote cellular proliferation.

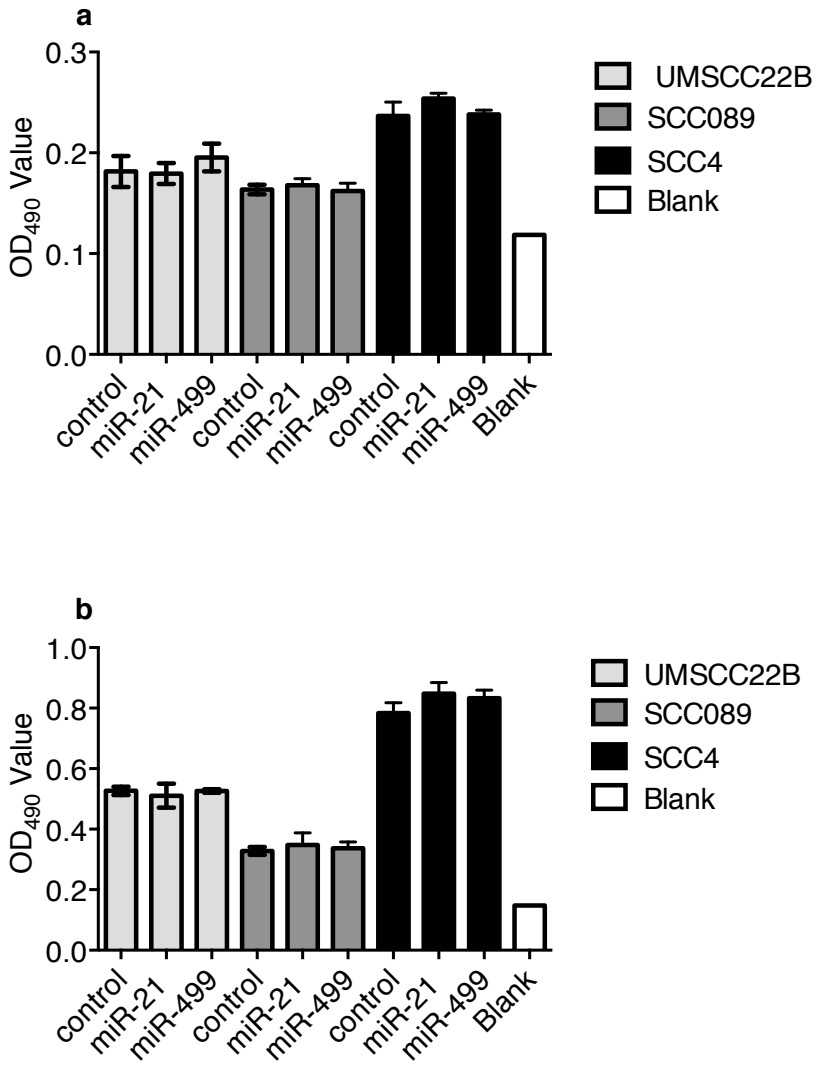

Figure 6.1. miR-21 and miR-499 do not promote cell proliferation. Head and neck cancer cells were transfected with 30 nM of control, miR-21 and miR-499, left for 30 hours and CellTiter96 Aqueous One Solution reagent added into each well. The plates were left in the incubator for a further 5 and 40 minutes and the media in the wells transferred to a clear bottom 96 well plate for reading by the Tecan spectrophotometer. **(a)** OD values from cells containing the CellTiter96 Aqueous One Solution reagent and measured 5 minutes after addition. **(b)** OD values from cells containing the CellTiter96 Aqueous One Solution reagent and measured 40 minutes after addition.

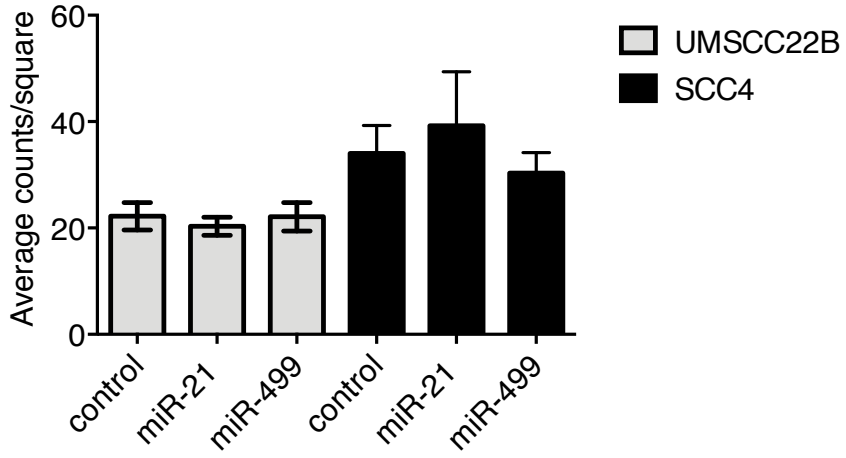

Figure 6.2. Manual counts of cell lines show no change in cell proliferation. Manual counts of control, miR-21 and miR-499 transfected UMSCC22B and SCC4 cell lines after addition of the CellTiter96 Aqueous One Solution reagent.

6.3.3. Measuring the migratory capacity of cancer cells.

During cell migration the levels of miRNAs and genes within the cell fluctuate. Identifying these changes will develop our understanding of tumour development. Thus, by using different HNSCC cell lines, it will provide a useful model for studying changes which may be indicative of cancer progression. We wanted to investigate how miR-21 and miR-499 which are involved in downregulating tumour suppressor genes are able to cause tumourigenesis. To move forward, we utilised the HNSCC cell lines to examine migration, a vital process that leads to metastasis and spreading of the tumour to secondary tissues.

The scratch assay is a well-defined method to measure cell migration [373]. Firstly, a scratch using a pipette tip was created in a confluent well containing Hela, SCC4 or UMSCC22B cells. An image was captured at the initial scratch and 18 hours later based on methodology described by Liang et al., [373]. The cells had migrated into the gap created by the scratch during the 18 hours (Figure 6.2, Table 6.3). These results demonstrated that the scratch assay could be used to quantify migration in HNSCC cells.

The assay while a simple technique does have several caveats and limitations. The two main concerns being; it is difficult to detect a difference with slower moving cells as noted with the SCC4 cells which had not migrated into the opening (Figure 6.3). The other technical concern was locating the exact same spot where the initial image was taken. A slight directional change from the initial scratch would significantly affect the interpretation of the migratory cells. To address these issues, the scratch assay was extended by several hours and the magnification was decreased to 4X.

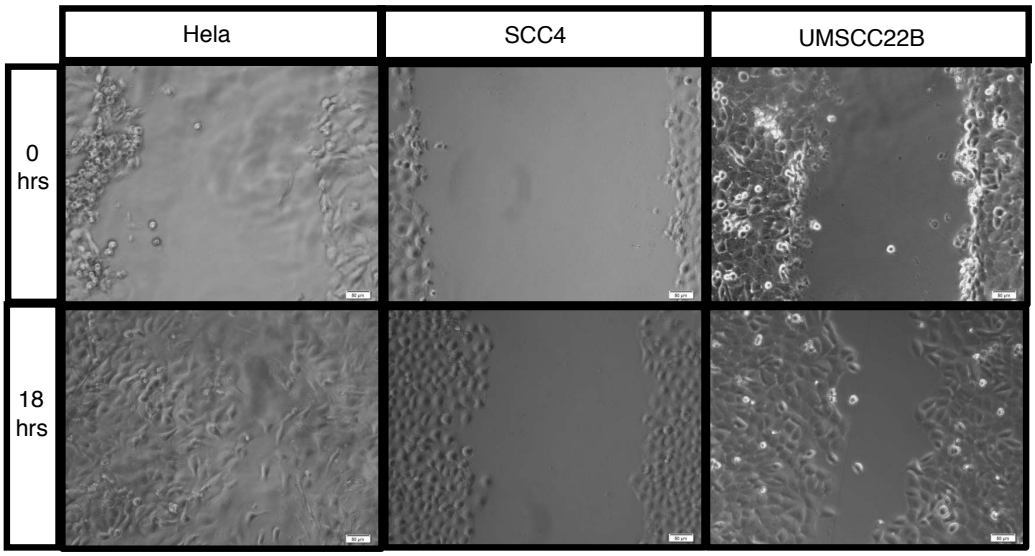

Figure 6.3. Optimisation of the scratch assay protocol. Hela, Stage III, primary SCC4 and Stage III, metastatic UMSCC22B cells were plated and grown to confluency and the cell monolayer was scratched with a 200 µL tip. Migration of the cells towards the "wound" was visualised with images taken at 0 and 18 hours after the scratch. The software program ImageJ was used to determine the migration distance. The images were visualised at 10X magnification.

Table 6.2. Migration of Hela, stage III, primary SCC4 and stage III, metastatic UMSCC22B cell lines over 18 hours. Percentage closure determined by the width of scratch at 18 hours over the initial width of the scratch. The width was calculated with ImageJ and distance units is the number of pixels across the image.

	Hela	SCC4	UMSCC22B
0 hours	299	388	225
18 hours	95	268	135
% closure	32	69	60

6.3.4. Optimisation of the scratch assay for HNSCC cells

To further refine the scratch assay, we extended the post scratch time to 23 hours with still images recorded at 4X at time 0 and 23. Cells were also transfected with either 30 nM scrambled control, miR-21 or miR-499 miRNA mimics to ascertain their effects on cell migration.

The images taken of the Hela cells did not show a difference between the scratches in the control, miR-21 and miR-499 transfected cells (Figure 6.4a-f). The Stage III SCC4 cell line only showed a difference in migration in the miR-21 transfected cells compared to the control transfection (Figure 6.4g-k). It was more evident with the Stage III, metastatic UMSCC22B that miR-21 and miR-499 promoted migration of the cells compared to the control (Figure 6.4m-r).

Interpretation of the results still remained difficult as in several images it was difficult to distinguish between the cell boundary and the scratch (Figure 6.3q). Furthermore, in some images it was challenging to locate the exact area when the image was taken 23 hours before (Figure 6.4e, r). This compounded our ability to estimate the total area of different scratches over time. It was then decided that static image recording of these scratch assay was not suitable for measuring cell migration. We then initiated live cell imaging over an extended time course.

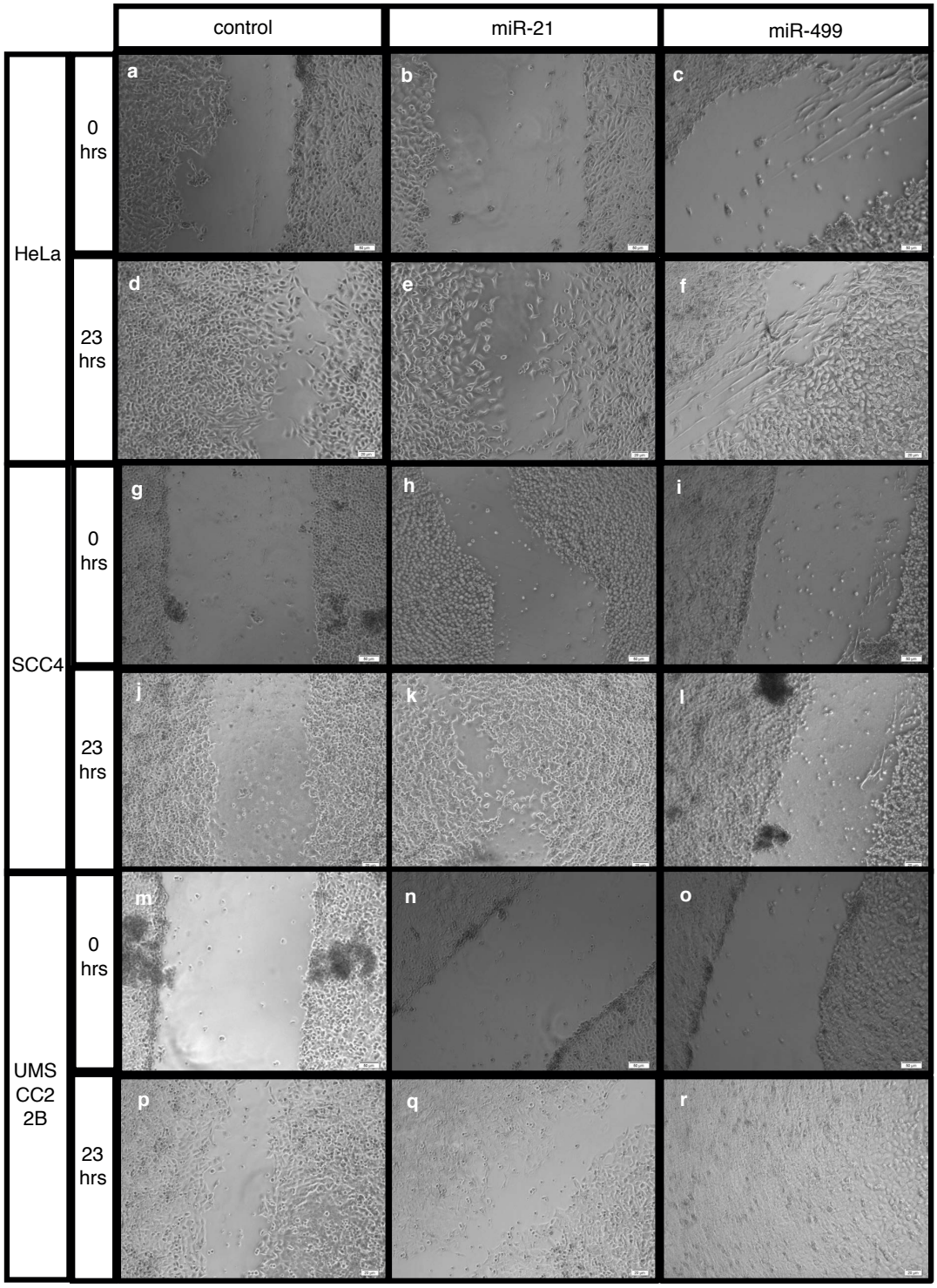

Figure 6.4. Scratch assay using still image capture. Confluent Hela, Stage III, primary SCC4 and Stage III, metastatic UMSCC22B cells were transfected with either a control, miR-21 or miR-499 miRNA mimic. At 23 hours post transfections, the cell monolayer was scratched with a tip. Images were taken at 0 and 23 hours after the scratch. The software program ImageJ was

used to determine the migration distance and cells were visualised at 4X magnification. Hela cells transfected with **(a)** control mimic. **(b)** miR-21 mimic. **(c)** miR-499 mimic at 0 hours. Hela cells transfected with **(d)** control mimic. **(e)** miR-21 mimic. **(f)** miR-499 mimic at 23 hours. SCC4 cells transfected with **(g)** control mimic. **(h)** miR-21 mimic. **(i)** miR-499 mimic at 0 hours. SCC4 cells transfected with **(j)** control mimic. **(k)** miR-21 mimic. **(l)** miR-499 mimic at 23 hours. UMSCC22B cells transfected with **(m)** control mimic. **(n)** miR-21 mimic. **(o)** miR-499 mimic at 0 hours. UMSCC22B cells transfected with **(p)** control mimic. **(q)** miR-21 mimic. **(r)** miR-499 mimic at 23 hours.

6.3.5. Live cell imaging of migrating cancer cells is more accurate and robust than still image capture

Using live cell imaging an exact coordinate of each initial scratch was recorded and the microscope could be directed to the exact spot with subsequent image captures. Analysis of the scratch was more complex and involved measuring the rate of scratch closure rather than just the width. Monitoring the scratch continuously over time provided more detail about migration of the cells rather than just a final still image. Thus live cell imaging had the additional benefit of precision and accuracy as the microscope could be manipulated by software.

Testing of the live cell imaging protocol was done with Hela cells over a period of 23 hours with an image captured every 30 minutes. The program Fiji was used for image analysis and was able to measure the area of the scratch over the total image (Figure 6.5a, b, refer to electronic data) [366]. Figure 6.4b shows an overlay of a green mask which represents the scratch area and was required for calculation of cell movement.

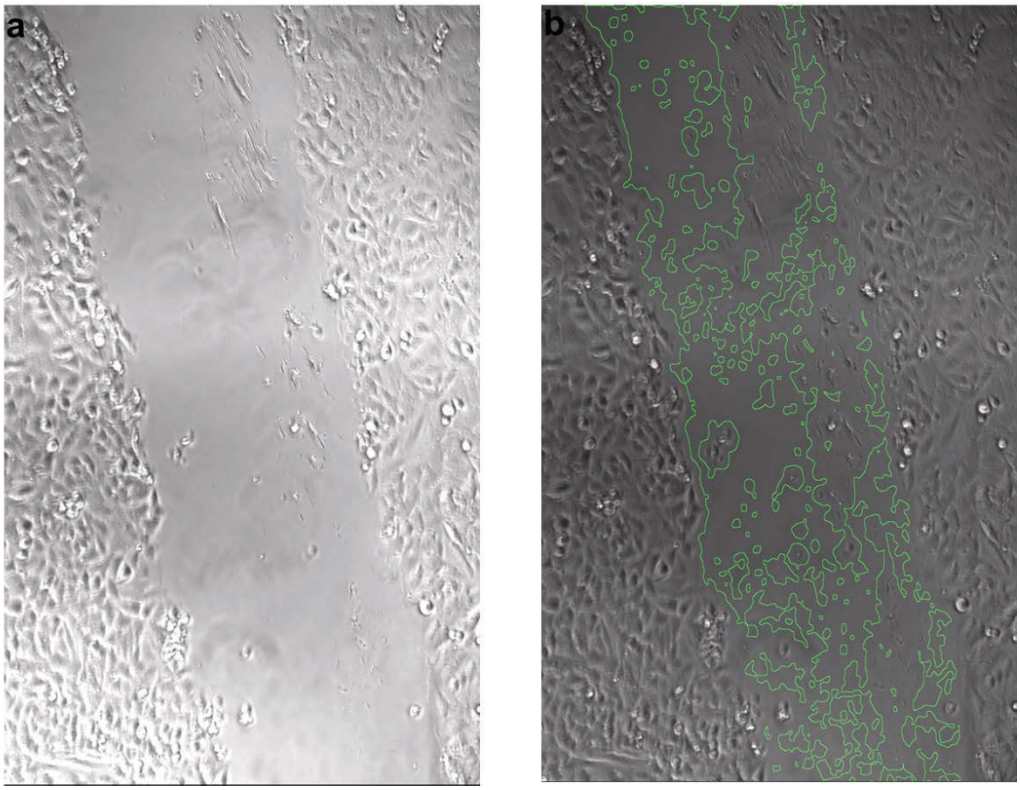

Figure 6.5. Live cell imaging analysis. Hela cells after the scratch were left in an incubated chamber set at 37°C, 5% $C0_2$ with the Nikon Ti inverted epifluorescent microscope capturing images every 30 minutes over a period of 23 hours. The rate of wound closure was then determined through Fiji program [366]. **(a)** Still image of scratched Hela cells. Cells were visualised at 10X magnification. **(b)** Still image of scratched Hela cells analysed through the program Fiji. An overlay of a green mask was placed upon the image of scratched cells to distinguish the boundary between scratch and cells. The program was able to calculate the area within the scratch and this was converted into a percentage of the scratch area over the total area of the image. This value was divided by the total time of the scratch assay (23 hours) to give the rate of migration.

The area of the scratch was plotted over time to give the rate of wound closure (Figure 6.6a, refer to the electronic data). The more negative the value, the faster the cells were migrating. When Hela cells were transfected with miR-21 and miR-499 mimics the cells were shown to migrate significantly faster compared to the control transfection (Figure 6.6b, refer to electronic data). These results proved that the live cell imagining protocol was a suitable analysis tool and that miR-21 and miR-499 appeared to have a role in promoting migration in Hela cells.

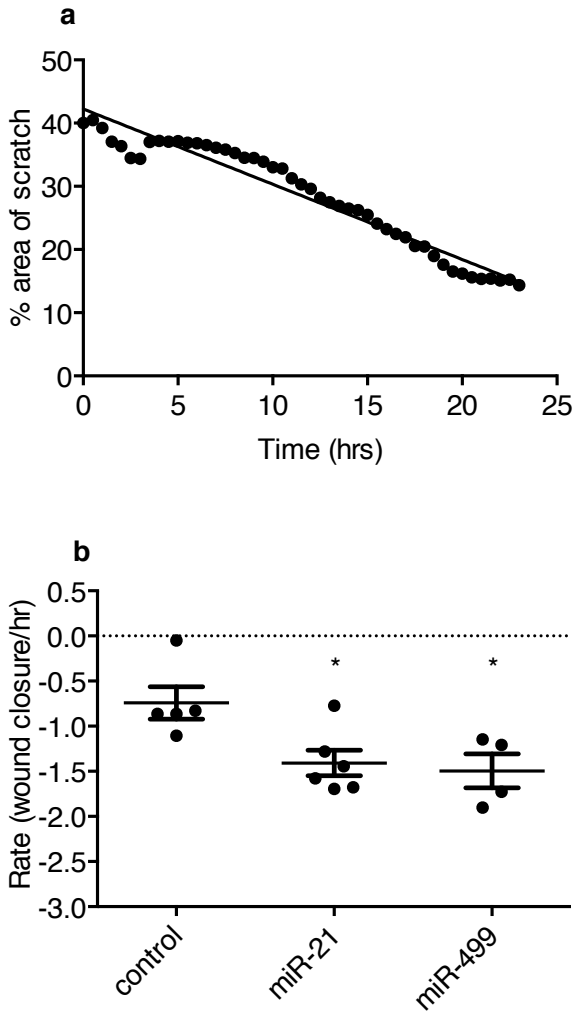

Figure 6.6. miR-21 and miR-499 promote migration in HeLa cells using live cell imaging. Hela cells were transfected with 30 nM of control, miR-21 or miR-499 and scratched with a 200 µl tip 24 hours post transfection. The cells were then left in a chamber incubated at 37°C, 5% CO_2 with the Nikon Ti inverted epifluorescent microscope capturing images every 30 minutes over a period of 23 hours. The rate of wound closure was then determined through the program Fiji. **(a)** Hela cells transfected with control mimic prior to the scratch. Graph plotting % area of the scratch over time to determine the rate of Hela wound closure over a period of 23 hours with the gradient equalling the rate. **(b)** Rate of wound closure in scratched Hela cells. (Error bars represent s.e.m. n is at least 3. *$p<0.05$, One-way anova, Dunnett test).

6.3.6. miR-21 and miR-499 promote migration in aggressive head and neck cancer cell lines

Having established the suitability of live cell imaging for measuring cell migration. We then evaluated if miR-21 and miR-499 could promote migration in HNSCC cells. Scratch assays were conducted with 30 nM of scrambled control, miR-21 and/or miR-499 mimics transfected into HNSCC cell lines over 23 hours.

SCC099, the Stage I recurrence cell line was shown to have no change in migration when miR-21, miR-499 or both miRNAs were added to the cells compared to the control transfected cells (Figure 6.7a, Table 6.3, refer to electronic data). The Stage III primary SCC4 also had no change in migration compared to the control transfected cells (Figure 6.7b, Table 6.3, refer to the electronic data). In comparison, the Stage III, metastatic UMSCC22B cells had a significant increase in migration when miR-21 was overexpressed in cells (Figure 6.7c, Table 6.3, refer to the electronic data). In the last cell line, SCC089 the Stage IV primary, showed a significant increase in migration when miR-21 and miR-499 mimics were added to cells compared to control transfected cells (Figure 6.7d, Table 6.3, refer to the electronic data). Therefore, miR-21 and miR-499 promotes migration in selective HNSCC cell lines.

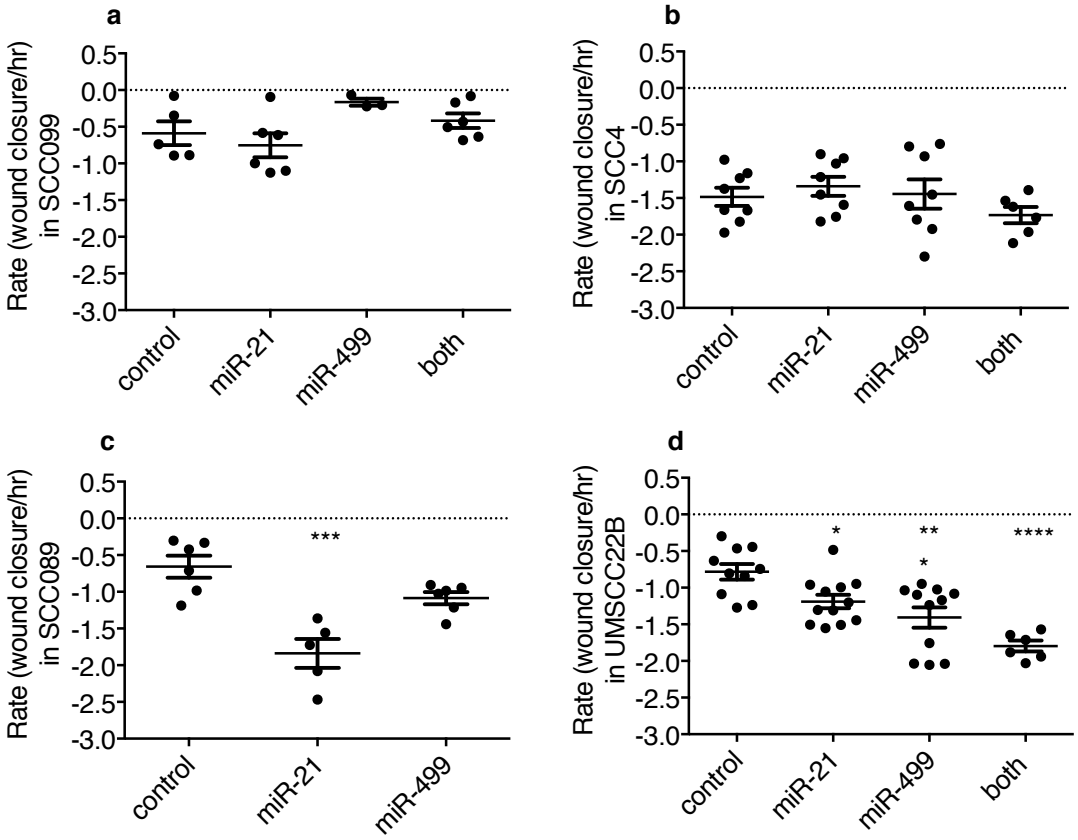

Figure 6.7. miR-21 and miR-499 promote migration in the aggressive head and neck cancer cell lines. HNSCCs were transfected with 30 nM control, miR-21, miR-499 or both miRNAs prior to the scratch and live cell imaging performed on the cells. This occurred in a humidified chamber set at 37°C, 5% $C0_2$ with the Nikon Ti inverted epifluorescent microscope capturing images every 30 minutes over a period of 23 hours. The rate of wound closure was then determined through Fiji. **(a)** Rate of wound closure in Stage I, recurrent SCC099 cells. **(b)** Rate of wound closure in Stage III, primary SCC4 cells **(c)** Rate of wound closure in Stage III, metastatic UMSCC22B cells. **(d)** Rate of wound closure in Stage IV, primary SCC089 cells. (Error bars represent s.e.m. n is at least 3. *p<0.05, ***p<0.001, ****p<0.0001, One-way anova, Dunnett test).

Table 6.3. Average rate of wound closure (percentage area of scratch/hour) of HNSCC cell lines. Cell lines examined were the Stage I primary SCC099, Stage III primary SCC4, Stage IV primary SCC089 and Stage III metastatic UMSCC22B.

Cell line	control	miR-21	miR-499	both
SCC099	-0.59	-0.75	-0.16	-0.42
SCC4	-1.48	-1.34	-1.45	-1.73
SCC089	-0.66	-1.84	-1.09	N/A
UMSCC22B	-0.78	-1.19	-1.41	-1.8

6.3.7. miR-21 and miR-499 downregulate PDCD4, SOX6 and FOXO4 RNA levels

Given that miR-21 and miR-499 overexpression lead to the promotion of migration in specific HNSCC cells, we examined possible target genes. We investigated the expression of miR-21 and miR-499 gene targets – PDCD4, SOX6 and FOXO4. These genes are involved in migration in other cancers such as breast, colorectal, hepatocellular, gastric and esophageal [29-31,293,363,374]. With this precedent they are likely to be involved in migration in HNSCC.

Expression analysis was conducted to first characterise the endogenous levels of these genes in the HNSCC cell lines. HEK293 cells were included as a negative control for a non-cancerous cell line and Hela as a positive for a cancerous cell line.

The HEK293 cell line had the highest expression of PDCD4, SOX6 and FOXO4 compared to all the cancer cell lines. (Figure 6.8a-c). Hela cells demonstrated similar expression levels for PDCD4, SOX6 and FOXO4 with the head and neck cell lines except for lower RNA levels of SOX6 (Figure 6.8a-c). The stage IV SCC089 cell line had the lowest RNA expression for PDCD4 and FOXO4 of all the cell lines (Figure 6.8a-c). The RNA expression of PDCD4, SOX6 and FOXO4 for the least aggressive cell lines stage I SCC099 and stage III SCC4 was on par with at least one other of the head and neck cancer cell lines (Figure 6.8a-c). For all three genes the metastatic Stage III UMSCC22B had the highest RNA expression out of all the cancer cell lines which was quite surprising for a metastasised cell line. It would be expected that metastatic cells would have reduced levels of tumour suppressor genes which may be involved in reversing metastasis.

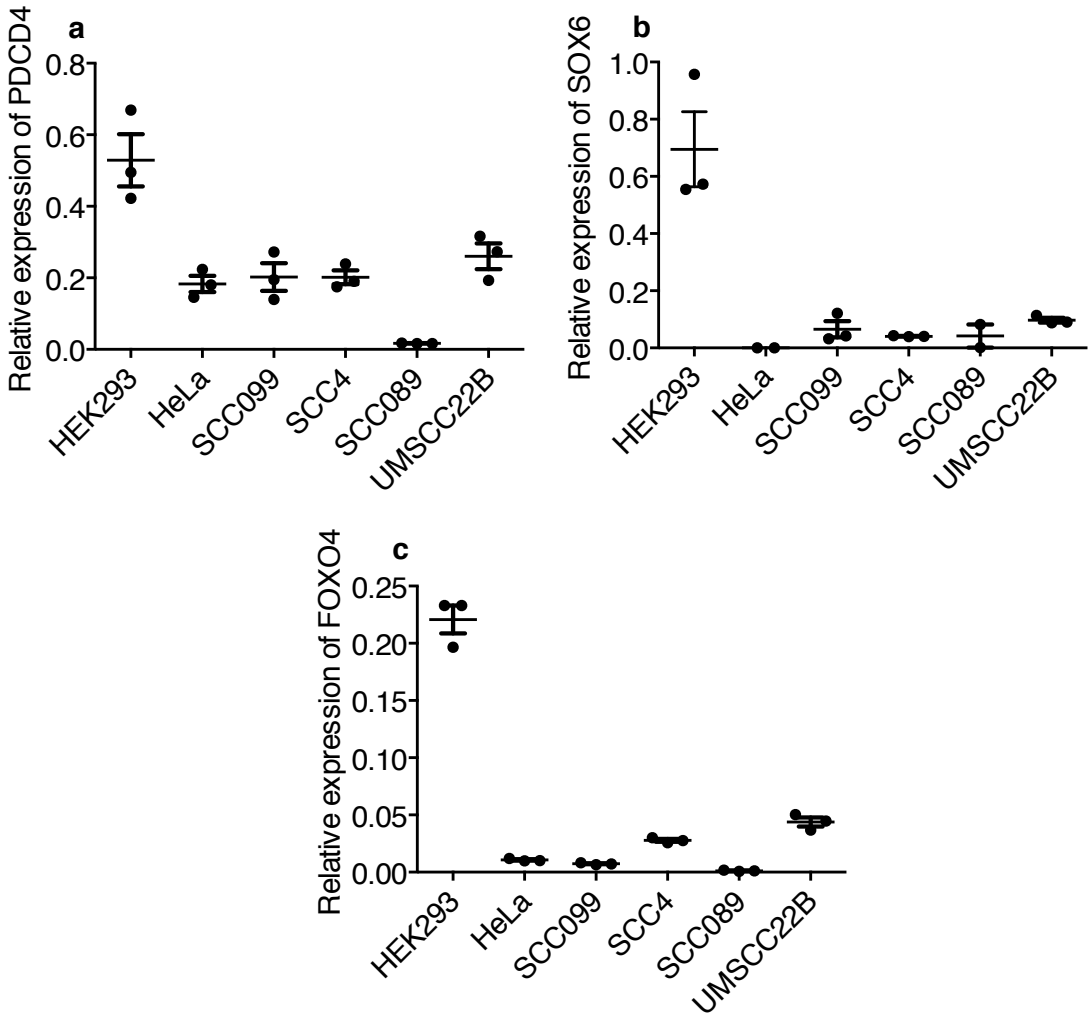

Figure 6.8. Tumour suppressor genes PDCD4, SOX6 and FOXO4 are expressed differentially in the head and neck cancer cell lines. Head and neck cells along with Hela were harvested for RNA and qPCR conducted. The expression of genes was normalised to reference gene B2M. **(a)** relative expression of PDCD4 in cells. **(b)** relative expression of SOX6 in cells. **(c)** relative expression of FOXO4 in cells. (Error bars are s.e.m. n=3).

A scratch was then conducted on miR-21 and miR-499 transfected SCC089 cells to examine wound closure and gene expression together. The SCC089 transfected cells had a higher expression of miR-21 and miR-499 compared to the control transfected cells (Figure 6.9a,b). Wound closure was measured and the cells transfected with miR-21 and miR-499 closed the scratch faster compared to the control miRNA mimic (Figure 6.9c). In these transfected cells the RNA levels of PDCD4, SOX6 and FOXO4 were downregulated when miR-21 and miR-499 were overexpressed compared to control miRNA overexpression (Figure 6.10a-c). These gene targets of miR-21 and miR-499 could be involved in pathways that normally suppress migration which are altered upon overexpression of these miRNAs.

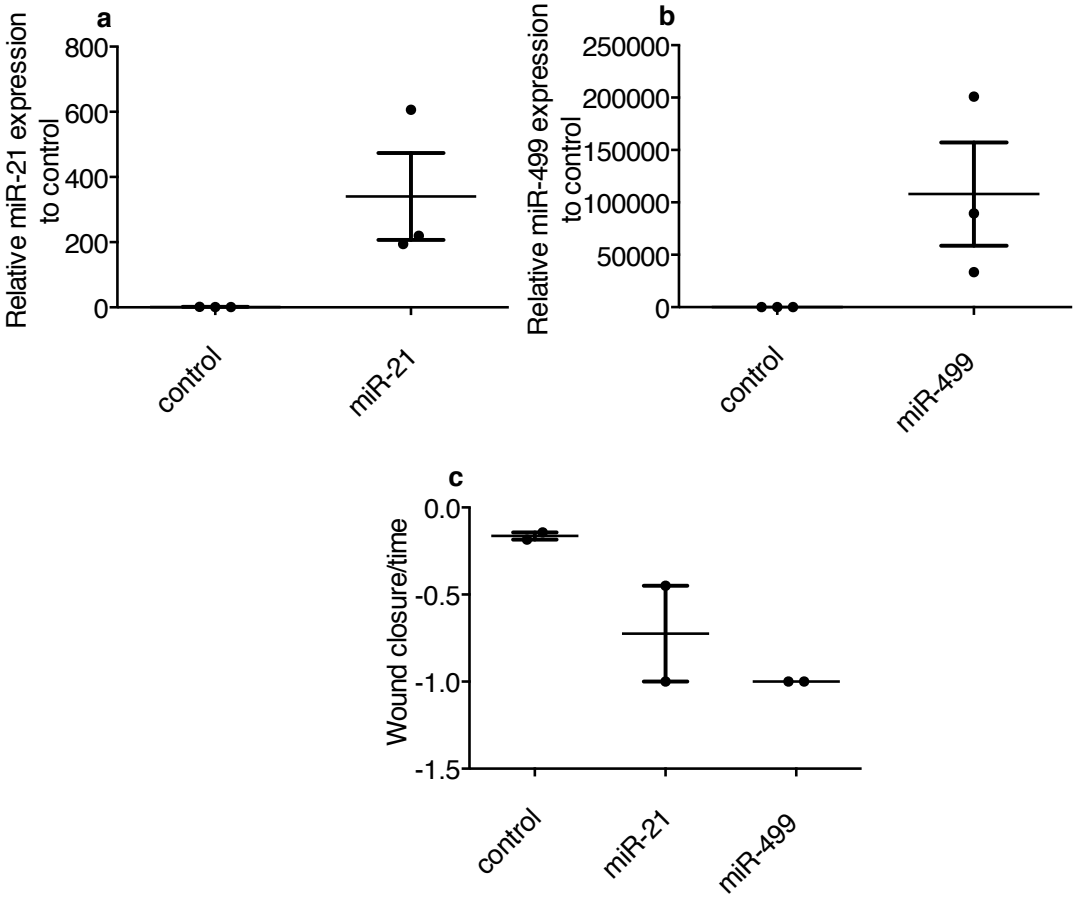

Figure 6.9. miR-21 and miR-499 promote migration in Stage IV primary SCC089 cells compared to control mimic transfected cells. SCC089 cells were transfected with 30 nM control, miR-21 or miR-499 miRNA mimics. The cells were then scratched and incubated for 23 hours. RNA was harvested from the cells and qPCR conducted. The expression of genes was normalised to reference gene RNU6B and then normalised to control to give relative expression. **(a)** relative expression of miR-21 in scratched cells. **(b)** relative expression of miR-499 in scratched cells. **(c)** Rate of wound closure of SCC089 cells over 23 hours. (Error bars are s.e.m. n is at least 2).

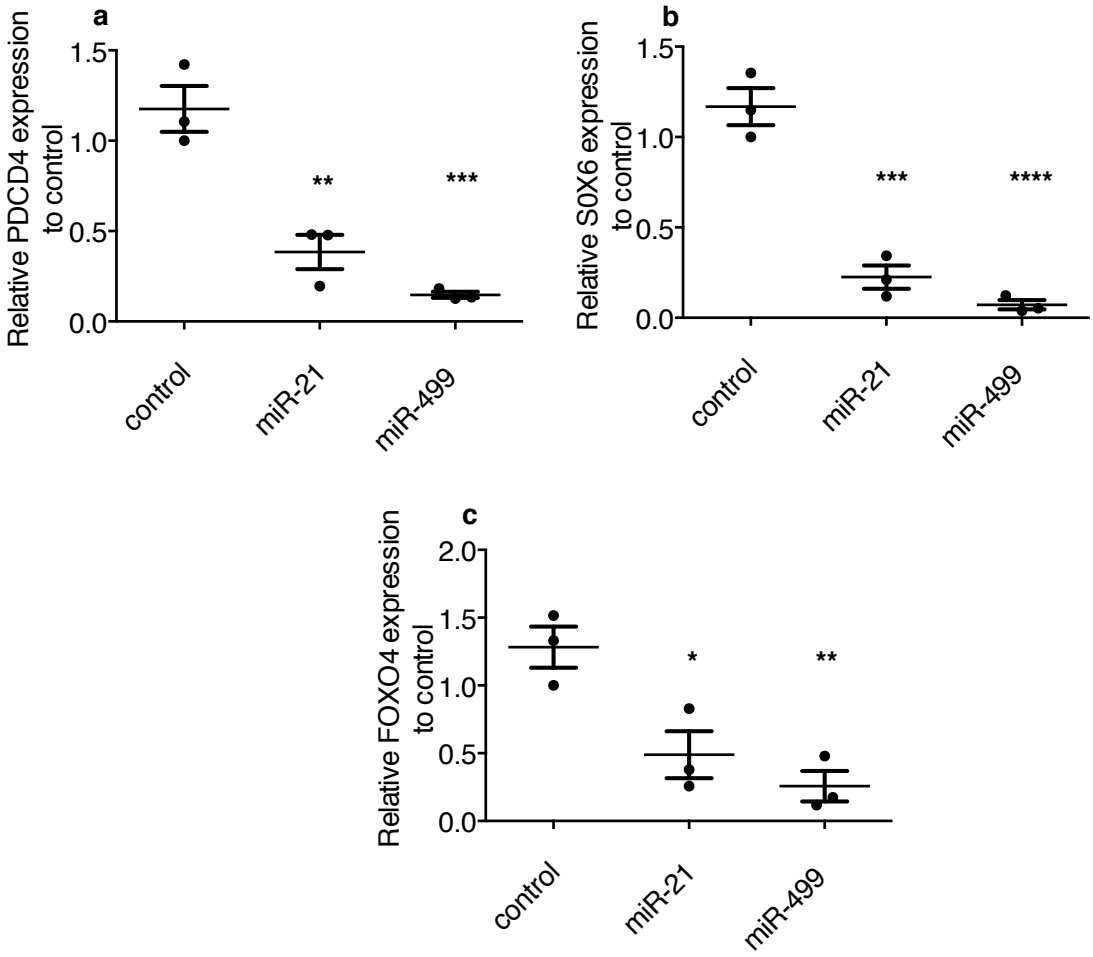

Figure 6.10. miR-21 and miR-499 target genes are downregulated in Stage IV primary SCC089 miRNA transfected cells. SCC089 cells were transfected with 30 nM of control, miR-21 or miR-499. RNA was harvested from the cells and qPCR conducted. The expression of genes was normalised to reference gene ACTB and then normalised to control to give relative expression. **(a)** levels of PDCD4 in scratched cells. **(b)** levels of SOX6 in scratched cells. **(c)** levels of FOXO4 in scratched cells (Error bars represent s.e.m. n=3. *p<0.05, **p<0.01, ***p<0.001, ****p<0.00001. One-way anova, Dunnett test).

6.4. Discussion

This chapter determined if miR-21 and miR-499 could promote migration in HNSCC cell lines. Firstly, the scratch assay was optimised and then employed with live cell imaging techniques. We showed that these two miRNAs were able to promote migration in selective HNSCC cell lines. This migration may possibly occur by downregulating a cascade of genes such as PDCD4, SOX6 and FOXO4. While these miRNAs had a role in promoting migration, they had no effect on proliferation.

Migration is a key component of cancer progression that gives cells the ability to metastasise to other tissues increasing the severity of the cancer and decreasing the chance of survival. Overexpressing miR-21 and miR-499 in the HNSCC cell lines indicated a role in migration for the more advanced tumour cell lines Stage III metastatic UMSCC22B and Stage IV SCC089.

An explanation for these observations may be that 1) there is a miRNA concentration threshold that needs to be crossed to trigger or promote migration or 2) the different HNSCC cells have different mechanisms to promote migration.

If we extend the first notion, a certain stoichiometric amount of miR-21 and miR-499 would be needed to trigger the migration pathway in any given cell. The cell lines which were susceptible to migration in the scratch assays – UMSCC22B and SCC089 would need to have higher endogenous levels of miR-21 and miR-499 compared to Stage I recurrence SCC099 and Stage III primary SCC4 (Figure 6.11). However, qPCR analysis revealed similar endogenous expression of miR-21 and miR-499 between all HNSCC cell lines (Appendix 4, Figure A6).

Therefore, it seems that miR-21 and miR-499 in selected HNSCC cells activates migration (UMSCC22B and SCC089) whereas in other cell lines

they may be involved in a different pathway (SCC099 and SCC4). Alternatively, all cell lines could have the same migration pathway however some of the cells require a higher amount of miR-21 and miR-499 to activate that pathway.

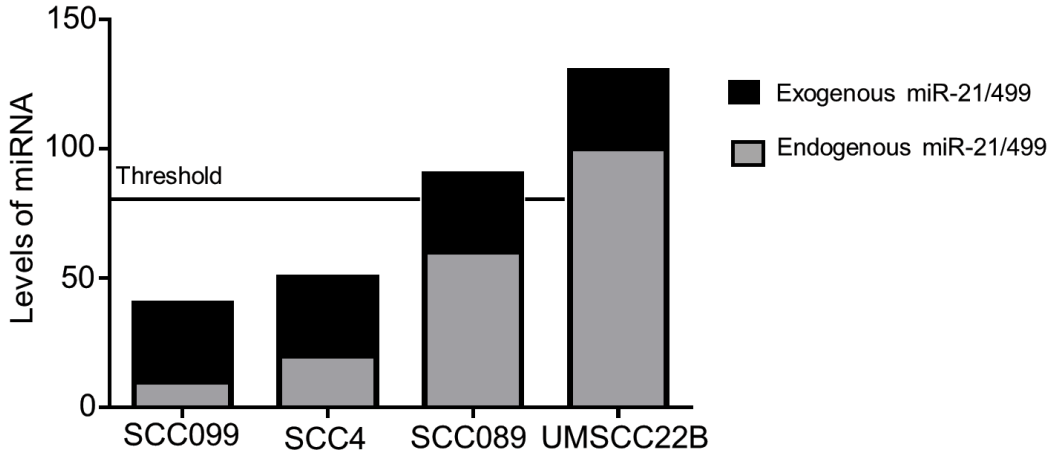

Figure 6.11. Hypothetical model on the endogenous levels of miR-21 and miR-499 in head and neck cancer cell lines analysed in the scratch. The threshold is a hypothetical miRNA concentration in the cell above which migration occurs. The level of miRNA for endogenous miR-21/miR-499 is shown in grey and the level for exogenous miR-21/miR-499 is in black.

We also observed that the miR-21 and/or miR-499 targets PDCD4, SOX6 and FOXO4 were downregulated during cell migration confirming the functionality of the miRNAs. The downregulation of these genes could potentially activate migration however to confirm this experimentally an overexpression or KD of the genes would be required.

The function of PDCD4 has been reviewed in previous chapters. SOX6 is a transcription factor involved in the process of chondrogenesis, a cell differentiation pathway leading to the formation of cartilage [375]. Depletion of SOX6 levels in mice results in skeletal abnormalities [376]. SOX6 is a member of the Sox subfamily consisting of over 20 members and is a part of the larger family of proteins which contain one or more high-mobility-group DNA binding domains [377]. During the process of chondrogenesis the three sox genes L-SOX5, SOX6 and SOX9 are co-expressed. They work together to activate chondrocyte specific genes [375,376]. The role of SOX6 in HNSCC is yet to be established.

FOXO4 is a member of the Forkhead transcription factors of which 40 have currently been identified in mammals. The members of this family are distinguished by a highly conserved, monomeric DNA-binding domain known as the Forkhead box [378]. Members of the FOXO family including FOXO4 are involved in regulating genes involved in cell proliferation, embryogenesis, glucose metabolism, atrophy, cell death, cell differentiation, DNA repair and cell cycle arrest (further reviewed in Greer and Brunet [379] and, Carlsson and Mahlapuu [380]). The FOXO family of transcription factors is regulated by the protein kinase Akt (phosphorylation) [381]. FOXO4 was initially found because it was located at a chromosomal translocation site in cancer indicating that FOXO4 could have an important function in cancer [382-384]. FOXO4 is able to abate tumour progression in a mice model [385].

PDCD4, SOX6 and FOXO4 have been shown to be regulated by miR-21 and miR-499 (Chapter 4). However, these two miRNA also target other genes

which could be responsible for migration. Studies show PTEN [386,387], RECK and TIMP3 [388] to be downregulated by either miR-21 or miR-499. Other studies specifically overexpressed the target genes of miR-21 and miR-499 (RHOB, TIAM1) in cells resulting in decreased migration [389,390]. Conversely, inhibiting the miRNA target genes PTEN and ETS1 caused increased migration in various cancer cells [391,392].

Our hypothesis that PDCD4, SOX6 and FOXO4 are involved in the migration of HNSCC cells is supported by other studies. Downregulation of PDCD4 via siRNA KD caused increased migration in breast [374], colorectal [293] and hepatocellular cancer cells [363]. Even though PDCD4 is primarily involved in translation, it has been shown that PDCD4 can suppress migration through the JNK pathway which activates cell migration [29]. PDCD4 is able to achieve this by inhibiting mitogen-activated protein kinase kinase kinase kinase 1 (MAP4K1) which then suppresses C-Jun preventing cell migration [388,393]. PDCD4 also increases the expression of E-Cadherin and TIMP2, two proteins which suppress migration [394] (Figure 6.12).

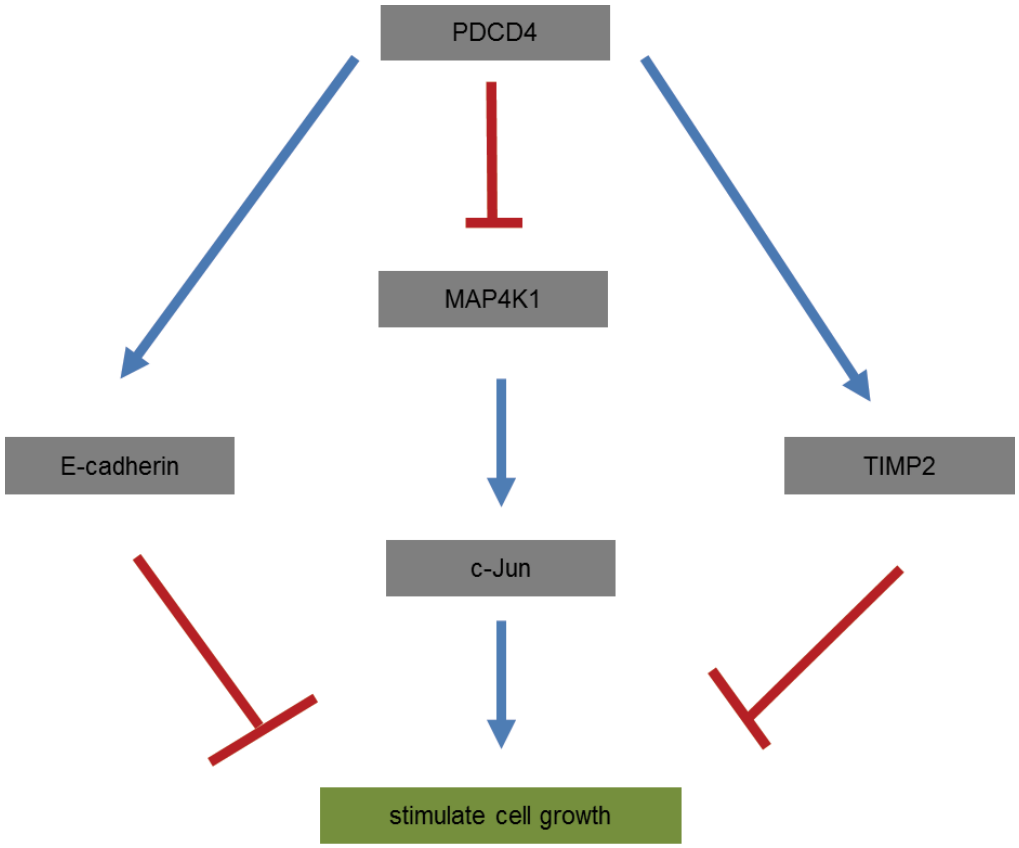

Figure 6.12. Schematic of the PDCD4 pathway that leads to suppression of migration. Dark grey boxes are genes, blue arrows show activation/stimulation and the red symbols show repression of a gene(s).

In regards to SOX6, its ectopic expression into KYSE30 and KYSE510 (Japanese human esophageal squamous cell carcinoma cell lines) caused an inhibition of migration compared to cells not containing the SOX6 overexpression vector. It was demonstrated that SOX6 stimulates G1–S cell-cycle arrest and regulates genes involved in the cell cycle [30].

In gastric cancer cells, upregulation of FOXO4 *in vitro* and *in vivo* led to a decrease in migration whereas downregulation of the gene stimulated migration [31]. This regulation was believed to occur through G1-S cell-cycle arrest. Another study found that KD of FOXO4 promoted migration of smooth muscle cells. It was thought this occurred through activation of matrix metalloproteinase 9 by FOXO4 which leads to regulation of the extracellular matrix degradation and turnover [395].

Examining the three genes regulated by miR-21 and/or miR-499 - PDCD4, SOX6 and FOXO4 revealed that this group are part of a more complicated cancer network. They are all interconnected directly and indirectly and changes in the levels of these miRNAs can easily trigger a chain reaction affecting the homeostasis of the cell.

RAS is known to stimulate the transcription factor AP-I [396] which activates miR-21 [396]. miR-21 inhibits PDCD4 and PTEN [397] and PTEN inhibits the PI-3K/PK/Akt pathway [398,399]. This pathway stimulates cell growth and inhibits apoptosis [400], suppresses FOXO4 [381] and activates SOX9 [401]. SOX9 is needed for SOX6 expression [402] which is regulated by miR-21. This network of the miRNAs and genes of interest is illustrated in Figure 6.13.

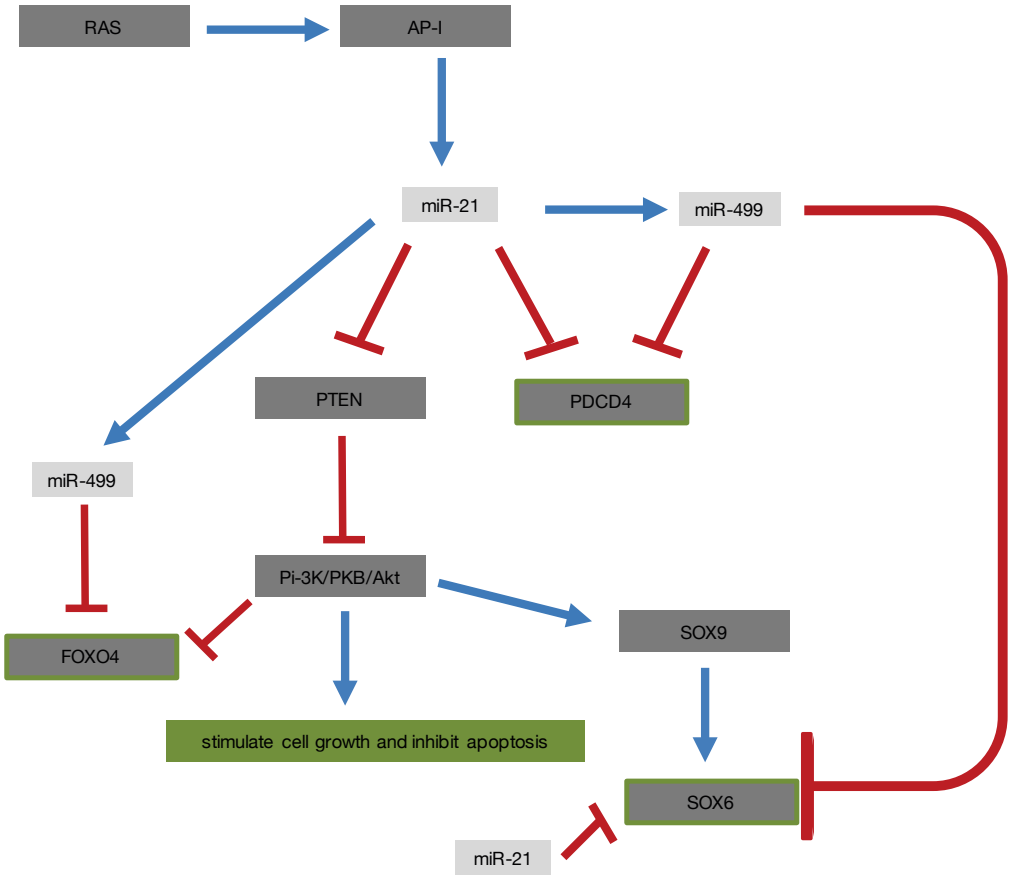

Figure 6.13. Cancer network involving the miRNAs and genes studied in Chapter 6. Dark grey boxes are genes, dark grey boxes highlighted with a green border are the three genes of interest in this study and light grey boxes miRNAs. Blue arrows show activation/stimulation and the red symbols show repression of a gene(s).

This chapter reveals the novel discovery that miR-21 and miR-499 promote migration in HNSCC. Understanding the function of miRNAs when they are aberrantly expressed in cancer will aid in design of therapeutics.

Chapter 7: General Discussion

Head and neck cancer is a global concern with increasing incident rates and poor survival rates despite improvements to technology [32,35,37-39]. Further complicating matters is that most HNSCCs are diagnosed at advanced stages [3]. This is partially due to a lack of clinical biomarkers and poor understanding of the molecular biology of this disease. A new strategy is needed to minimise the occurrences of HNSCC and limit cancer progression to advanced stages. This has resulted in a shift towards studying cancer on a molecular level as changes in the expression of various molecules are indicative of aberrations to the homeostasis of the cell. Additionally, these molecules have potential to either be biomarkers and/or therapeutic agents.

The small ncRNAs, miRNAs have proven to be useful indicators of different types of cancer [25]. They can be sensitive enough to not only be diagnostic but also prognostic and distinguish between stages of cancer and survival in patients [97,117,118]. Furthermore, miRNAs are aberrantly expressed throughout tumour development and progression [26] and thus their analysis can lead to identification and treatment of HNSCCs in the clinic.

The aim of this dissertation was to investigate miRNAs that were dysregulated in head and neck tumours, examine how they regulated their targets and the functional consequences on HNSCC cells. The specific project aims were: 1) to study the co-regulation of the tumour suppressor gene PDCD4 by miR-21 and miR-499; 2) to examine the molecular mechanism behind miR-21's regulation of miR-499; 3) to identify if miRNA-miRNA regulation was a more widespread phenomena and 4) to study the functional role of miR-21 and miR-499 in head and neck tumours.

7.1. Major findings and the future directions

7.1.1. Co-regulation of PDCD4 by miR-21 and miR-499

PDCD4 is a tumour suppressor gene that is downregulated in many tumours including head and neck [13,103,132,169,403,404]. The downregulation of PDCD4 has been linked with many oncogenic processes in the cell including cell growth, proliferation, apoptosis and cell transformation [10,167,181]. Therefore, studying the regulation of this gene can aid towards preventing the activation of cancer related pathways. It is known that the PDCD4 3´UTR is regulated by the miRNAs, miR-21 and miR-499 which are upregulated in HNSCC tumours. The PDCD4 3´UTR has a single miR-21 site and three miR-499 sites. Multiple miRNAs sites can be regulated in an interdependent manner by miRNAs [244,265,302]. Understanding cooperativity of miRNA directed regulation of a target may provide a better molecular understanding of the disease and potentially lead to novel treatments [277].

The luciferase assays with the PDCD4 3´UTR mutant vectors revealed that miR-21 downregulated the 3´UTR of PDCD4 independently of miR-499. However, miR-21 still provided a contribution to miR-499's downregulation of the 3´UTR in a cooperative manner. Interestingly, the last two miR-499 binding sites are both critical as mutations at either site abolished silencing activity. This suggested a co-dependent regulation of the 3´UTR by miR-499. The distance between the last two miR-499 sites is 66 nt, greater than the 40 nt defined in the literature for co-operative regulation [254,277]. However, because the last two miR-499 sites are regulated in a co-dependent manner the distance requirements between sites may be different. This is supported by Kloosterman et al., who revealed a co-dependent regulation of *let-7* sites on the *lin-14* gene which were separated by 57 nt [405].

Further studies are required to determine distant requirements for co-dependent regulation. This can be achieved with the last two miR-499 sites on the PDCD4 3´UTR by artificially increasing the distance between them

until regulation is lost. Studying the secondary structure of the PDCD4 3´UTR highlights the possibility of interactions between the last two miR-499 sites due to their spacial proximity. It is also curious what the purpose of the first miR-499 site on the 3´UTR could be and if it is just functionally redundant. Double mutants of the last two miR-499 sites on the PDCD4 3´UTR vector would determine if the first miR-499 site was capable of regulation at all.

It was postulated that the different modes of regulation experienced by the miRNA sites could be due to binding by different Agos. Based on the literature miRNA sites that are regulated in an independent manner (miR-21) would be bound to Ago2-RISC [265]. Experiments with Ago2 KDs revealed that miR-21 and miR-499 could still regulate the PDCD4 3´UTR efficiently even with an 80% KD of Ago2. This suggested that either only a small amount of Ago2 protein was required in the cell to still carry out its function or that another Ago was able to take over the role of Ago2. Future work would involve simultaneous multiple KDs with the other Ago family members leaving just one Ago at a time to determine if miR-21 or miR-499 could still be bound by that RISC complex. Alternatively, immunoprecipitaton with Ago2 and the other Agos would provide useful information on how much miR-21 or miR-499 was bound to the Ago to determine if there is a preferential loading.

More studies are focusing on the regulatory networks formed between miRNAs, miRNA clusters, transcription factors, genes and pathways. Examining the role and the mechanism behind multiple miRNAs regulating a single gene or set of genes can provide more information on the progression of a disease and lead to better diagnosis.

7.1.2. The overexpression of miR-21 increases miR-499 levels

The expression of one miRNA can affect the levels of another miRNA(s) and this has important implications for miRNA overexpression studies and miRNA overexpression based therapeutics. There is limited research on the mechanism behind miRNA-miRNA mediated regulation. Understanding how this regulation occurs will provide further insight into the molecular biology of cancer progression. This project identified a significant increase in miR-499 levels when miR-21 was overexpressed in cells. The mechanism behind this type of regulation was explored.

miR-21 is able to significantly increase miR-499 expression in a post-transcriptional manner. Inhibiting the synthesis of *de novo* transcripts in cells resulted in the degradation of most miRNAs including the miR-21 and miR-499 precursors within 12 hours. Whereas over the time period of 24 hours the expression of mature miR-499 did not decrease under miR-21 overexpression conditions. miR-21 is able to stabilise miR-499 expression and it is thought the mechanism behind this is through interactions with a target gene 3´UTR. Due to the low expression of miR-499 in HEK293 cells it could only be shown with miR-21 that increasing the amount of PDCD4 3´UTR in cells also increased endogenous miR-21 expression but not its precursor. The reduced rate of miR-21 decay forms the basis of the proposed mechanism.

In the literature reduced rates of miRNA decay due to interactions with target sites has been shown [19,20]. Chatterjee et al., proved that TMMP was a mechanism that occurred naturally in cells. By mutating two of the RNA targets of the *lin-4* miRNA, they found that mature *lin-4* levels was reduced but not *pre-lin*-4 [19]. This supports the idea that miRNA processing does not play a role but rather the mature miRNA is protected by interactions with its target.

To further prove this model, the PDCD4 3´UTR would have to be overexpressed in a cell line with moderate levels of miR-499 and the expression of miR-499 measured. Alternatively, HEK293 cells could be supplemented with a small dose of miR-499 and the expression of miR-499 measured as the PDCD4 3´UTR is increasingly overexpressed. Additionally, either of the miR-499 3´UTR mutants for the last two miR-499 sites could be transfected into cells with increasing concentrations and miR-499 levels measured to determine if stability of the miRNA is dependent on site availability.

This study is unique in that it has demonstrated a positive interaction between two miRNAs on their regulation of each other. Whereas studies in the literature focusing on the relationship between two or more miRNAs predominantly show that the overexpression of one miRNA results in the decrease of the other miRNA [16,17,19,406,407]. The unintentional increase of another miRNA can have serious clinical side effects or experimental bias if not taken into consideration. A microarray or panel of miRNAs should be tested when overexpressing a miRNA to determine that any resulting changes in the cell is due to the miRNA of interest. In summary miRNA-miRNA regulation is a common occurrence and a vital factor that needs to be considered in clinical trials when using a miRNA mimic.

7.1.3. Regulation of miRNAs is widespread

The regulation of miR-499 by miR-21 proved an interesting and novel discovery. This type of regulation highlights the potential of off-targeting effects when designing a therapeutic against a specific miRNA. It also suggests that the downregulation of a gene can be amplified as a secondary miRNA is activated to sustain regulation. Furthermore, the increase of one miRNA, leading to the upregulation of another miRNA can cause downstream regulation of other genes and pathways that the initial miRNA is not involved in. This allows for the widespread activation of a cascade of genes and pathways. This further complicates the molecular biology and regulatory dynamics of genes in HNSCC cells, and this study aimed to provide some insight into the nature of this type of regulation.

The first finding that miR-21 and miR-499 regulate several genes together besides PDCD4 suggests a partnership between these two miRNAs. That miR-21 stabilises miR-499 levels validates this partnership and reveals a regulatory circuitry between these miRNAs and their target genes. This additional level of regulation between the miRNAs allows for the refinement of target gene regulation and pathways. Further study into miRNA-miRNA regulation revealed that the miR-21-miR-499 regulation was not unique and in fact both miRNAs were capable of regulating multiple miRNAs. Consequently, the miRNA-miRNA regulation is a more general phenomena occurring in cells.

It was curious as to why and how miR-21 is able to selectively upregulate or downregulate specific miRNAs and not others. Examining the miRNAs that were upregulated with miR-21 overexpression presented no commonalties between them. Studying their genomic location and seed sequence proved unsuccessful as there was no trend between the most upregulated miRNAs by miR-21 overexpression. Furthermore, examining the miR-17-92 cluster which is a family of miRNAs with identical or similar seeds revealed differential regulation by miR-21 of different family members. This confirmed

that seed sequence did not play a role in miR-21's selectiveness of miRNA regulation. It would be interesting to see if miR-21 is able to stabilise the mature levels of the miRNAs upregulated in the miR-21 overexpression array when *de novo* synthesis is switched off by ActD just as it did with miR-499 (Chapter 4). This would provide insight into how miRNAs are able to differentially regulate other miRNAs.

The regulatory circuitry formed between miR-21, miR-499, PDCD4 and their other target genes could also be found with another interconnected regulatory circuitry involving miR-208. The miR-208 site is often paired up with a miR-499 site on the 3´UTR of genes (Table 7.1). The seed sequence of miR-499 is closely related to miR-208 and thus many of the genes sharing both miRNA sites have overlapping sites (Figure 7.1) [243,408].

Table 7.1. TargetScan's predictions for miR-499 and miR-208 gene targets. Highlighted are PDCD4 and eIF4G2 functionally analogous genes.

miR-499, miR-208-3p
PRKAR1A
RNF145
REEP1
H3F3B
CHD9
UBE2V2
HNRNPC
MED13
NLK
HIST1H3B
RECQL
DLD
ARGLU1
PDCD4
EIF4G2
RAB5C
SOS2
ANTXR1
ETS1
KPNA3
SOX5

miRNAs	Mature miRNA Sequence (5'-3')
miR-499	U**UAAGAC**UUGCAGUGAUGUUU
miR-208	A**UAAGACG**AGCAAAAAGCUUGU

Figure 7.1. Mature miRNA sequence of miR-499 and miR-208. Seed sequence is bolded.

The miRNA oligonucleotide array in this project revealed that when miR-499 was overexpressed, miR-208 was upregulated 8.8 fold (Refer to electronic data). Additionally, in the literature miR-208 is known to regulate miR-499 by activating Myh7b expression (the gene encoding miR-499) [138,409]. Therefore, the regulation of miR-208 and miR-499 is a positive feedback loop allowing for a more enhanced suppression of their target genes. miR-208 is not upregulated in the miR-21 overexpression array suggesting two functionally different types of regulation of miR-499 by the miRNAs. When a cardiovascular related pathway is being activated the cardiovascular miRNA miR-208 would upregulate miR-499. Whereas in a cancer pathway miR-21 would upregulate miR-499 thus allowing a differentiation of pathways and genes activated involving miR-499.

This reveals a network of miRNAs regulating other miRNAs to achieve a certain outcome. These miRNAs may be related by sequence (miR-208 and miR-499) or function (miR-21 and miR-499). Therefore further study is required to discover more miRNA-miRNA regulatory relationships and its impact on gene regulation.

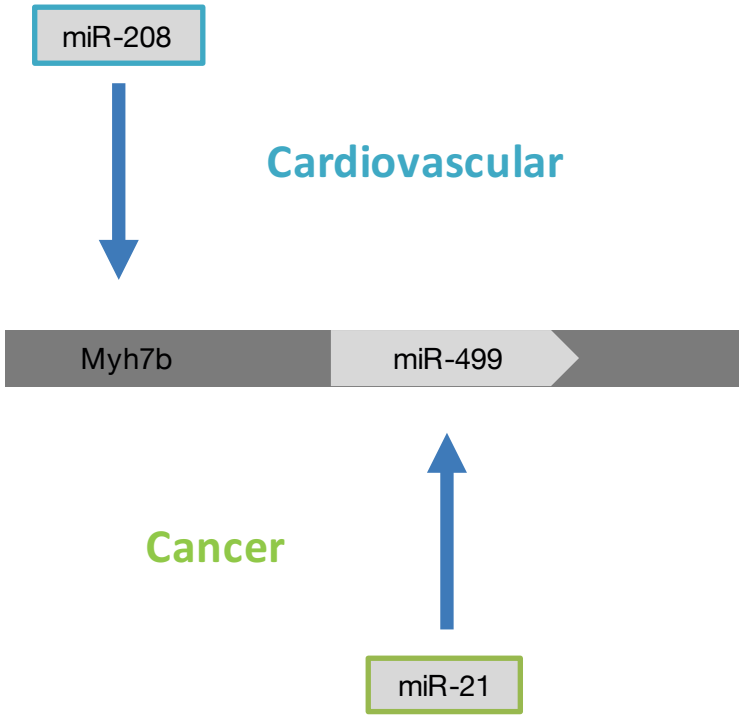

Figure 7.2. Schematic highlighting the activation of either a cancer or cardiovascular pathway depending on the miRNA. miR-499 is encoded within the Myh7b gene. miR-208 activates the Myh7b gene and miR-499 as well, whereas miR-21 activates just miR-499. Blue arrows show activation/stimulation, the dark grey box represents the gene Myh7b and light grey boxes represent miRNAs with their coloured border highlighting the pathway they are involved in.

miR-208 and miR-499 regulate PDCD4 and a functionally analogous eIF4A [410,411]. Both genes inhibit translation by forming a disruptive complex with eIF4A [410-412]. Potentially this creates a regulatory circuitry where miR-21 stimulates miR-499 and they both downregulate the tumour suppressor PDCD4. miR-499 can also stimulate miR-208 and the two of them can downregulate PDCD4 further but also the functionally similar eIF4G2 (which could otherwise presumably take over the role of PDCD4 if its expression is reduced in cells) (Figure 7.3). This highlights another layer of regulation beyond the direct miRNA-mRNA relationship.

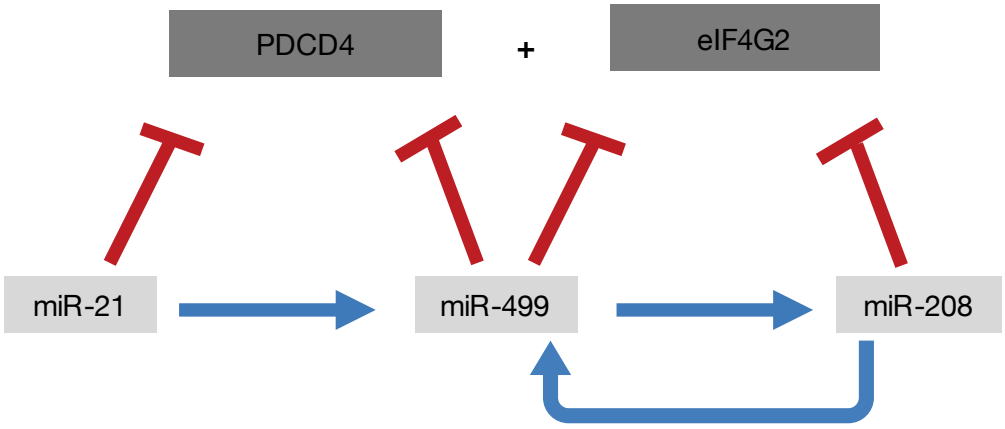

Figure 7.3. Schematic of miRNA-miRNA regulatory circuitry involved translational suppression. Blue arrows show activation/stimulation and the red blocks represent inhibition. The dark grey boxes represent genes and light grey boxes represent miRNAs.

7.1.4. miR-21 and miR-499 promote migration in HNSCC

The progression of HNSCC is accompanied by a series of molecular events in the cell with miRNAs playing a key role in orchestrating these events [26]. Identifying miRNAs that are dysregulated in cancer and then performing overexpression or KO experiments while examining a functional phenotype allows for the identification of the role of these miRNAs in cancer. Understanding how these miRNAs are involved in cancer provides the key to utilising them as therapeutic agents. Whilst the role of miR-21 has been surmised in HNSCC, miR-499 has only been shown to be involved in promoting migration in colorectal cancer cells [23,293]. Therefore, it was of interest in this study to investigate these two miRNA which are dysregulated in HNSCC and identify their role in cancer progression.

Proliferation is a key cancer pathway but miR-21 and miR-499 were shown to have no role in promoting proliferation in HNSCC cells. The scratch assay technique was developed with live cell imagining to determine if miR-21 and miR-499 were involved in migration in HNSCC cells. Live cell imaging revealed that miR-21 and miR-499 promoted migration in selected HNSCC cell lines. The miR-21 and miR-499 gene targets PDCD4, SOX6 and FOXO4 were decreased in the scratch assay and we suggest that these miRNAs through their targets may have an impact on migration. This idea is supported in previous studies which have stated their involvement [30,31,413].

To further understand how these miRNAs are involved in promoting migration in HNSCC cells. Inhibition of miR-21 and miR-499 in the head and neck cancer cell lines and then performing a scratch assay with live cell imaging would support the findings of this study if the ability of the cells to migrate was reduced. A rescue experiment with the miR-21 and miR-499 target genes PDCD4, SOX6 and FOXO4 would also determine if these genes are involved in migration. This would be achieved by joining the ORF of these genes onto an overexpression vector and then performing the assay. Overexpressing these genes in the scratched setting using HNSCC cell lines

should reduce the migratory ability of the cells if they are involved in migration. Additionally, performing the scratch on primary cells would provide additional evidence that miR-21 and miR-499 promote migration *in vivo*. Cell invasion is another aspect of cancer progression that could be examined. A cell invasion assay could be undertaken with the various HNSCC cell lines overexpressing miR-21 and miR-499 to further explore another aspect of cancer development.

In summary, miR-21 and miR-499 are overexpressed in HNSCC allowing them to promote migration and metastasis of the cells. Developing inhibitors against miR-21 and miR-499 could make useful therapeutical agents in the clinic, ultimately preventing metastasis of HNSCC cells.

7.2. Summary of the major achievements and concluding statements

The major findings from this thesis are as listed below. Firstly, the tumour suppressor gene PDCD4 was found to be co-regulated by miR-21 and miR-499 via different modes of regulation including independent, cooperative and co-dependence. Understanding the mechanism by which genes are regulated by miRNAs will be the foundation of therapeutic development.

Secondly, miR-21 positively regulates miR-499 and this adds an extra level of complexity to PDCD4 regulation. The proposed mechanism for this type of regulation is the TPPM model in which miR-21 binds to the PDCD4 3´UTR making the miR-499 sites more accessible. This in turn leads to the stability of miR-499 when it binds to the 3´UTR. Mechanistic studies such as this provide greater insight into the inner workings of the cell and are essential for understanding molecular pathways.

Thirdly, the miR-21-miR-499 regulation is not confined to just these two miRNAs and is in fact a widespread phenomenon with these two miRNAs capable of regulating multiple miRNAs. The notion that changing the expression of one miRNA can significantly affect other miRNAs has great implications for miRNA overexpression based therapeutics in the clinic. More so, studies on miRNA-miRNA regulation is lacking and greater emphasis should be placed in understanding this relationship.

Finally, miR-21 and miR-499 have been shown for the first time to both have a novel role in promoting migration in HNSCC. It is believed that this occurs by downregulating genes involved in migration such as PDCD4, SOX6 and FOXO4. Understanding the function of miRNAs in HNSCC progression will allow for the development of targeted therapeutics.

Appendix

Appendix 1. Identifying negative control for miRNA overexpression experiments using TargetScan.

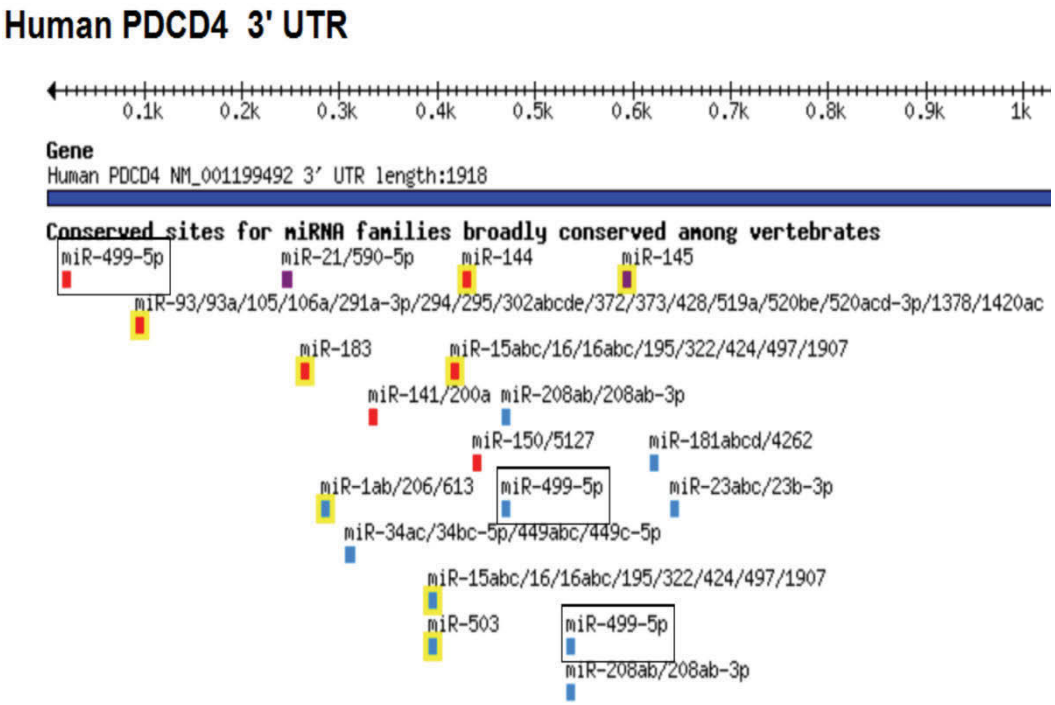

Figure A1. There are no *let-7a* sites present on the 3´UTR of PDCD4. miRNA binding sites present on the 3´UTR of PDCD4 as identified by the TargetScan algorithm.

Appendix 2. Assessing role of Ago2 in miR-21 and miR-499 mediated regulation of PDCD4 over time

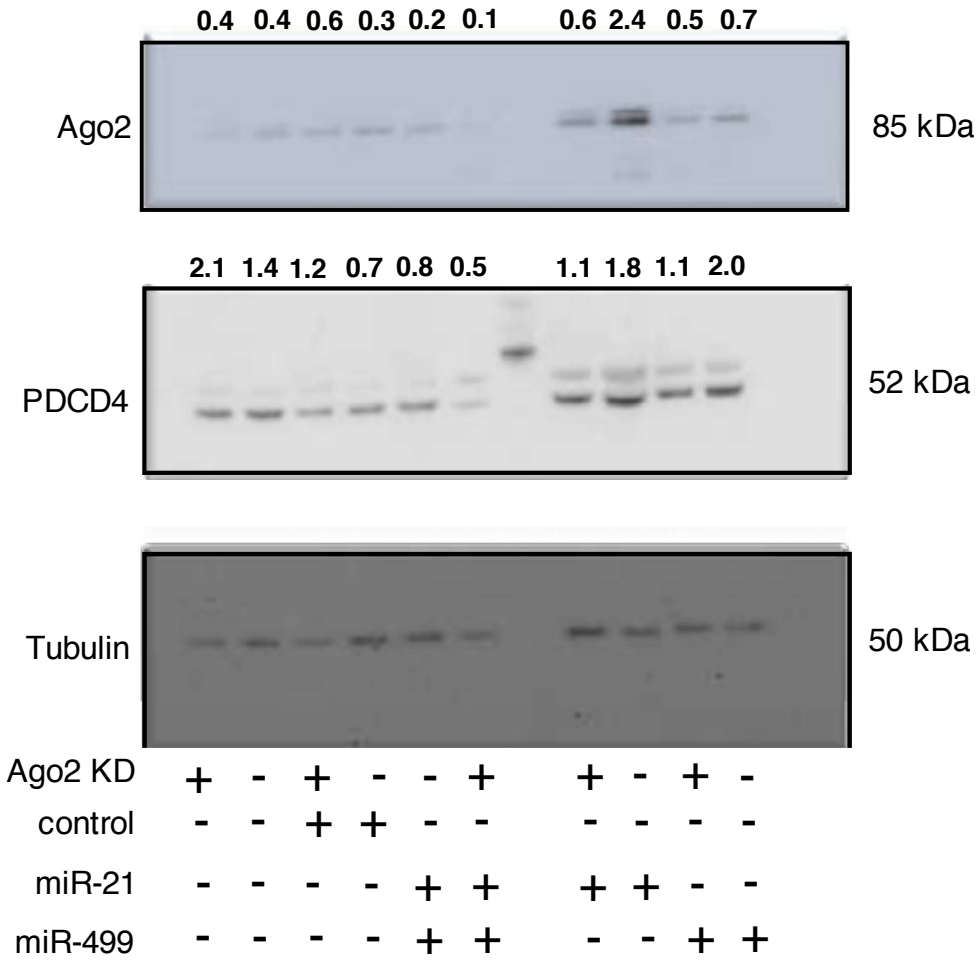

Figure A2. Protein levels of PDCD4 is reduced when Ago2 is KD at 24 hours. Inducible Ago2 shRNA cells were induced (+) or not induced (-) and transfected with control, miR-21 and miR-499 and protein harvested at 24 hours. Western blots were performed, stained with the appropriate antibody and imaged with chemilluminesce. Densitometry was performed using ImageJ with each band normalised against tubulin and the densitometry number plotted under the corresponding band. **(a)** Ago2 levels were measured on the westerns and imaged for a band at 85 kDa. **(b)** PDCD4 levels were measured on the westerns and imaged for a band at 52 kDa. **(c)** Tubulin levels were measured on the western and imaged for a band at 50 kDa.

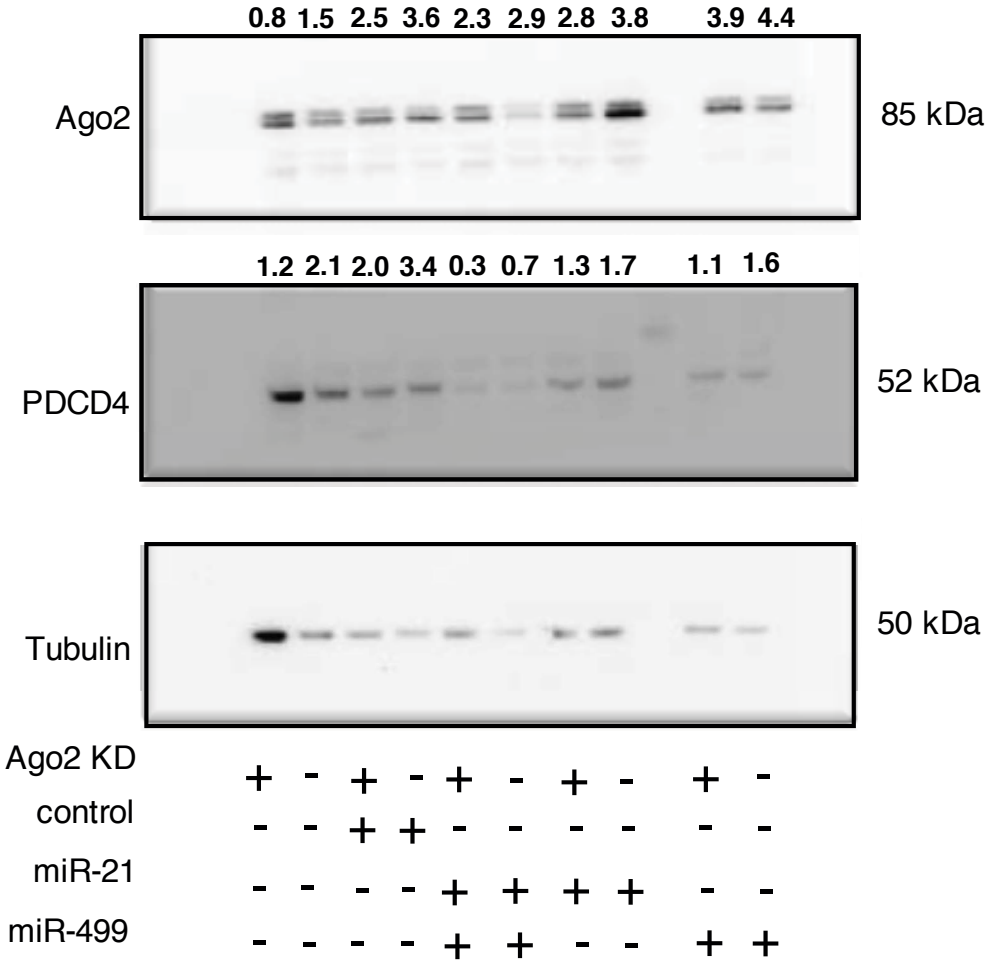

Figure A3. Protein levels of PDCD4 is reduced when Ago2 is KD at 48 hours. Inducible Ago2 shRNA cells were induced (+) or not induced (-) and transfected with control, miR-21 and miR-499 and protein harvested at 48 hours. **(a)** Ago2 levels were measured on the westerns and imaged for a band at 85 kDa. **(b)** PDCD4 levels were measured on the westerns and imaged for a band at 52 kDa. **(c)** Tubulin levels were measured on the western and imaged for a band at 50 kDa.

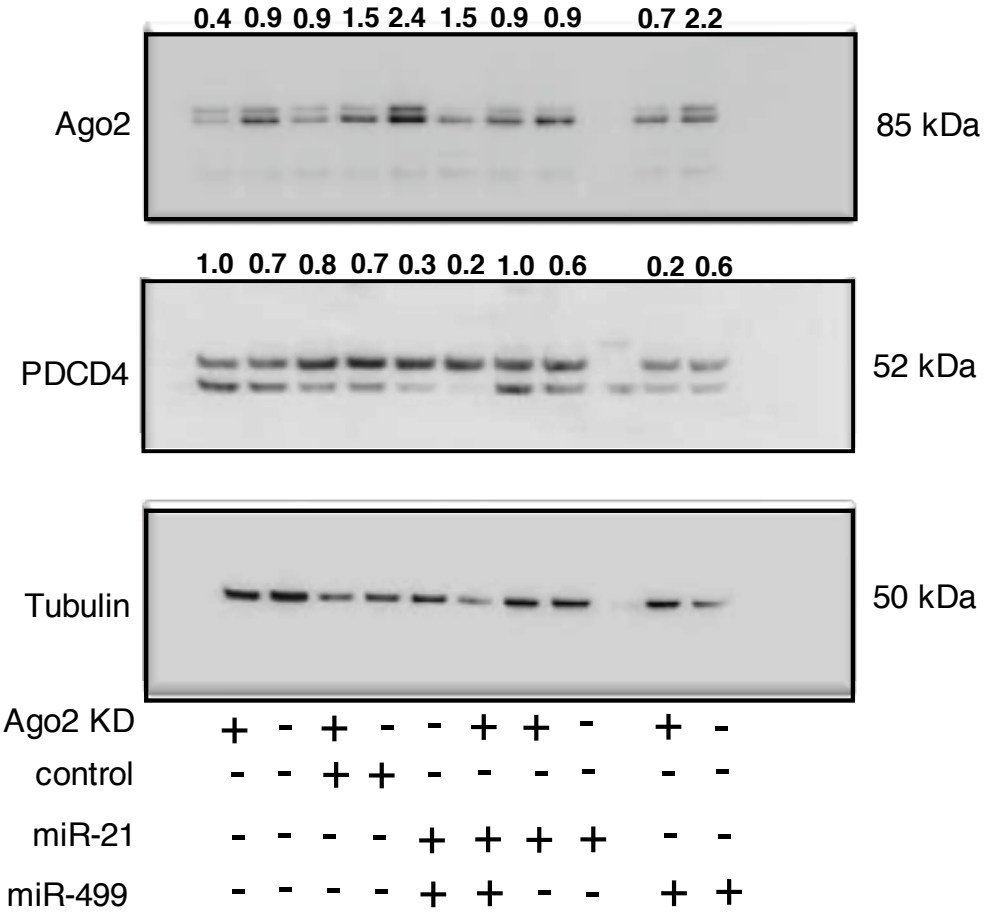

Figure A4. Protein levels of PDCD4 is reduced when Ago2 is KD at 72 hours. Inducible Ago2 shRNA cells were induced (+) or not induced (-) and transfected with control, miR-21 and miR-499 and protein harvested at 72 hours. **(a)** Ago2 levels were measured on the westerns and imaged for a band at 85 kDa. **(b)** PDCD4 levels were measured on the westerns and imaged for a band at 52 kDa. **(c)** Tubulin levels were measured on the western and imaged for a band at 50 kDa.

Appendix 3. Determining Ago1 levels when Ago2 is KD

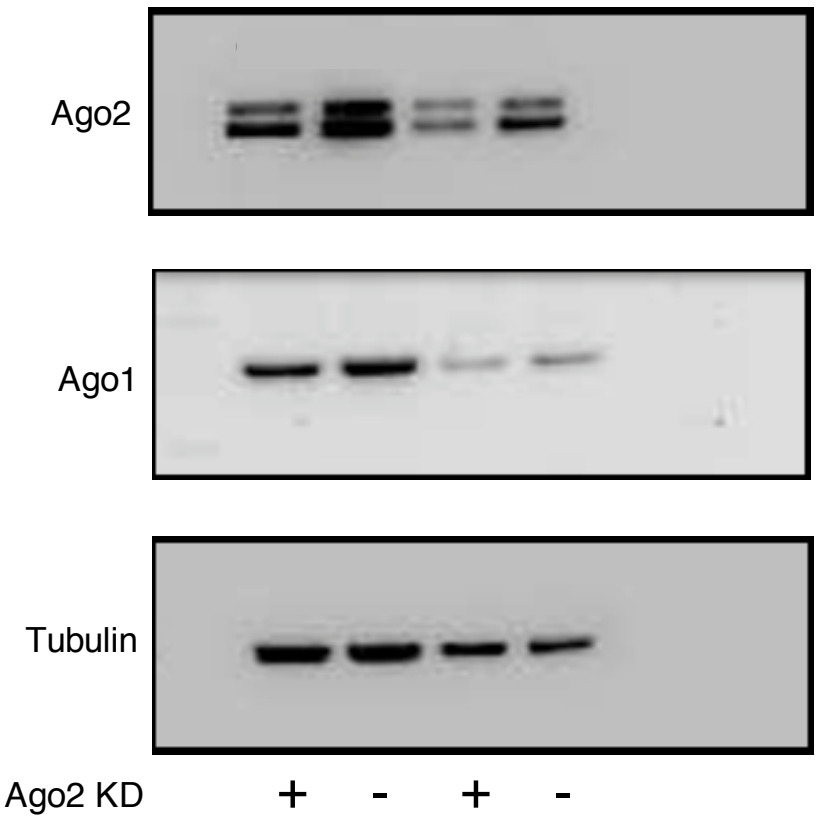

Figure A5. Protein levels of Ago1 remain unchanged when Ago2 is KD. Inducible Ago2 shRNA cells were induced (+) or not induced (-) and protein harvested at 96 hours post-induction to examine Ago2, Ago1 and tubulin protein levels.

Appendix 4. Endogenous levels of miR-21 and miR-499 in HNSCC cell lines

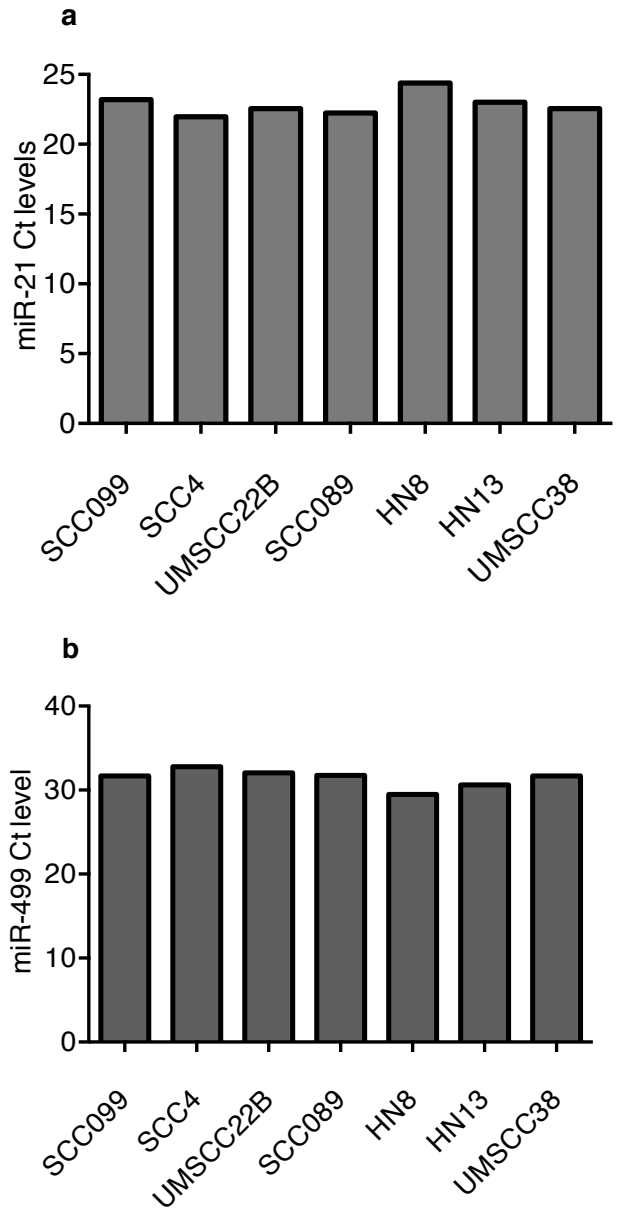

Figure A6. There are similar levels of miR-21 and miR-499 in head and neck cancer cell lines. Raw Ct levels of **(a)** miR-21 and **(b)** miR-499 in head and neck cancer cell lines SCC099, SCC4, UMSCC22B, SCC089, HN8, HN13 and UMSCC38.

References

1. Marur, S. & Forastiere, A.A. Head and Neck Cancer: Changing Epidemiology, Diagnosis, and Treatment. *Mayo Clinic Proceedings* **83**, 489-501 (2008).
2. Jemal, A., Murray, T., Ward, E., Samuels, A., Tiwari, R.C., Ghafoor, A., Feuer, E.J. & Thun, M.J. Cancer Statistics, 2005. *CA: A Cancer Journal for Clinicians* **55**, 10-30 (2005).
3. Leemans, C.R., Braakhuis, B.J. & Brakenhoff, R.H. The molecular biology of head and neck cancer. *Nature reviews. Cancer* **11**, 9-22 (2011).
4. Bhave, S.L., Teknos, T.N., Pan, Q., James, A.G. & Solove, R.J. Molecular parameters of head and neck cancer metastasis. *Critical reviews in eukaryotic gene expression* **21**, 143-153 (2011).
5. Reinhart, B.J., Slack, F.J., Basson, M., Pasquinelli, A.E., Bettinger, J.C., Rougvie, A.E., Horvitz, H.R. & Ruvkun, G. The 21-nucleotide let-7 RNA regulates developmental timing in Caenorhabditis elegans. *Nature* **403**, 901-906 (2000).
6. Tran, N., McLean, T., Zhang, X., Zhao, C.J., Thomson, J.M. & O'Brien, C. MicroRNA expression profiles in head and neck cancer cell lines. *Biochem Biophys Res Commun* **358** (2007).
7. Motoyama, K., Inoue, H., Takatsuno, Y., Tanaka, F., Mimori, K., Uetake, H., Sugihara, K. & Mori, M. Over-and under-expressed microRNAs in human colorectal cancer. *International journal of oncology* **34**, 1069 (2009).
8. Iorio, M.V., Ferracin, M., Liu, C.-G., Veronese, A., Spizzo, R., Sabbioni, S., Magri, E., Pedriali, M., Fabbri, M., Campiglio, M., Mnard, S., Palazzo, J.P., Rosenberg, A., Musiani, P., Volinia, S., Nenci, I., Calin, G.A., Querzoli, P., Negrini, M. & Croce, C.M. MicroRNA Gene Expression Deregulation in Human Breast Cancer. *Cancer Research* **65**, 7065-7070 (2005).

9. Zhang, X., Gee, H., Rose, B., Lee, C.S., Clark, J., Elliott, M., Gamble, J.R., Cairns, M.J., Harris, A., Khoury, S. & Tran, N. Regulation of the tumour suppressor PDCD4 by miR-499 and miR-21 in oropharyngeal cancers. *BMC Cancer* **16**, 1-11 (2016).
10. Jin, H., Kim, T., Hwang, S., Chang, S., Kim, H., Anderson, H., Lee, H., Lee, K., Colburn, N. & Yang, H. Aerosol delivery of urocanic acid-modified chitosan/programmed cell death 4 complex regulated apoptosis, cell cycle, and angiogenesis in lungs of K-ras null mice. *Mol Cancer Ther* **5**, 1041 - 1049 (2006).
11. Reis, P.P., Tomenson, M., Cervigne, N.K., Machado, J., Jurisica, I., Pintilie, M., Sukhai, M.A., Perez-Ordonez, B., Grenman, R., Gilbert, R.W., Gullane, P.J., Irish, J.C. & Kamel-Reid, S. Programmed cell death 4 loss increases tumor cell invasion and is regulated by miR-21 in oral squamous cell carcinoma. *Mol Cancer* **9**, 238 (2010).
12. Childs, G., Fazzari, M., Kung, G., Kawachi, N., Brandwein-Gensler, M., McLemore, M., Chen, Q., Burk, R.D., Smith, R.V., Prystowsky, M.B., Belbin, T.J. & Schlecht, N.F. Low-level expression of microRNAs let-7d and miR-205 are prognostic markers of head and neck squamous cell carcinoma. *Am J Pathol* **174**, 736-45 (2009).
13. Ramdas, L., Giri, U., Ashorn, C., Coombes, K.R., el-Naggar, A., Ang, K.K. & Story, M.D. miRNA expression profiles in head and neck squamous cell carcinoma and adjacent normal tissue. *Head & neck* **31**, 642-654 (2009).
14. Carinci, F., Lo Muzio, L., Piattelli, A., Rubini, C., Chiesa, F., Ionna, F., Palmieri, A., Maiorano, E., Pastore, A., Laino, G., Favia, G., Dolci, M. & Pezzetti, F. Potential Markers of Tongue Tumor Progression Selected by cDNA Micro Array. *International Journal of Immunopathology and Pharmacology* **18**, 513-524 (2005).
15. Hon, L. & Zhang, Z. The roles of binding site arrangement and combinatorial targeting in microRNA repression of gene expression. *Genome Biology* **8**, 1-18 (2007).

16. Forrest, A.R., Kanamori-Katayama, M., Tomaru, Y., Lassmann, T., Ninomiya, N., Takahashi, Y., de Hoon, M.J., Kubosaki, A., Kaiho, A. & Suzuki, M. Induction of microRNAs, mir-155, mir-222, mir-424 and mir-503, promotes monocytic differentiation through combinatorial regulation. *Leukemia* **24**, 460-466 (2010).
17. Hatziapostolou, M., Polytarchou, C., Aggelidou, E., Drakaki, A., Poultsides, G.A., Jaeger, S.A., Ogata, H., Karin, M., Struhl, K. & Hadzopoulou-Cladaras, M. An HNF4α-miRNA inflammatory feedback circuit regulates hepatocellular oncogenesis. *Cell* **147**, 1233-1247 (2011).
18. Kato, M., Putta, S., Wang, M., Yuan, H., Lanting, L., Nair, I., Gunn, A., Nakagawa, Y., Shimano, H. & Todorov, I. TGF-β activates Akt kinase through a microRNA-dependent amplifying circuit targeting PTEN. *Nature cell biology* **11**, 881-889 (2009).
19. Chatterjee, S., Fasler, M., Büssing, I. & Großhans, H. Target-Mediated Protection of Endogenous MicroRNAs in C. elegans. *Developmental Cell* **20**, 388-396 (2011).
20. Kuchen, S., Resch, W., Yamane, A., Kuo, N., Li, Z., Chakraborty, T., Wei, L., Laurence, A., Yasuda, T., Peng, S., Hu-Li, J., Lu, K., Dubois, W., Kitamura, Y., Charles, N., Sun, H.-w., Muljo, S., Schwartzberg, P.L., Paul, W.E., O'Shea, J., Rajewsky, K. & Casellas, R. Regulation of MicroRNA Expression and Abundance during Lymphopoiesis. *Immunity* **32**, 828-839 (2010).
21. Tuccoli, A., Poliseno, L. & Rainaldi, G. miRNAs Regulate miRNAs: Coordinated Transcriptional and Post-Transcriptional Regulation. *Cell Cycle* **5**, 2473-2476 (2006).
22. Matkovich, S.J., Hu, Y. & Dorn, G.W. Regulation of cardiac microRNAs by cardiac microRNAs. *Circulation research* **113**, 62-71 (2013).
23. Chang, S.S., Jiang, W.W., Smith, I., Poeta, L.M., Begum, S., Glazer, C., Shan, S., Westra, W., Sidransky, D. & Califano, J.A. MicroRNA alterations in head and neck squamous cell carcinoma. *International journal of cancer. Journal international du cancer* **123**, 2791-7 (2008).

24. Lu, Z., Liu, M., Stribinskis, V., Klinge, C.M., Ramos, K.S., Colburn, N.H. & Li, Y. MicroRNA-21 promotes cell transformation by targeting the programmed cell death 4 gene. *Oncogene* **27**, 4373-9 (2008).
25. Wiemer, E.A.C. The role of microRNAs in cancer: No small matter. *European Journal of Cancer* **43**, 1529-1544 (2007).
26. Wong, T.S., Liu, X.B., Wong, B.Y., Ng, R.W., Yuen, A.P. & Wei, W.I. Mature miR-184 as Potential Oncogenic microRNA of Squamous Cell Carcinoma of Tongue. *Clin Cancer Res* **14**, 2588-92 (2008).
27. Calin, G.A., Sevignani, C., Dumitru, C.D., Hyslop, T., Noch, E., Yendamuri, S., Shimizu, M., Rattan, S., Bullrich, F. & Negrini, M. Human microRNA genes are frequently located at fragile sites and genomic regions involved in cancers. *Proceedings of the National Academy of Sciences of the United States of America* **101**, 2999 (2004).
28. Richards, R.I. Fragile and unstable chromosomes in cancer: causes and consequences. *Trends in Genetics* **17**, 339-345 (2001).
29. Huang, C., Jacobson, K. & Schaller, M.D. MAP kinases and cell migration. *Journal of Cell Science* **117**, 4619-4628 (2004).
30. Qin, Y.-R., Tang, H., Xie, F., Liu, H., Zhu, Y., Ai, J., Chen, L., Li, Y., Kwong, D.L., Fu, L. & Guan, X.-Y. Characterization of Tumor-Suppressive Function of SOX6 in Human Esophageal Squamous Cell Carcinoma. *Clinical Cancer Research* **17**, 46-55 (2011).
31. Su, L., Liu, X., Chai, N., Lv, L., Wang, R., Li, X., Nie, Y., Shi, Y. & Fan, D. The transcription factor FOXO4 is down-regulated and inhibits tumor proliferation and metastasis in gastric cancer. *BMC Cancer* **14**, 1-11 (2014).
32. Mahfouz, M.E., Rodrigo, J.P., Takes, R.P., Elsheikh, M.N., Rinaldo, A., Brakenhoff, R.H. & Ferlito, A. Current potential and limitations of molecular diagnostic methods in head and neck cancer. *Eur Arch Otorhinolaryngol* **267**, 851-60 (2010).
33. McCartan, B.E., Cowan, C.G. & Healy, C.M. Regional variations in oral cancer incidence in Ireland. *Oral oncology* **41**, 677-686 (2005).

34. Mastronikolis, N.S., Fitzgerald, D., Owen, C., Neary, Z., Glaholm, J. & Watkinson, J.C. The management of squamous cell carcinoma of the neck. The Birmingham UK experience. *European Journal of Surgical Oncology (EJSO)* **31**, 461-466 (2005).

35. Gupta, S., Kong, W., Peng, Y., Miao, Q. & Mackillop, W.J. Temporal trends in the incidence and survival of cancers of the upper aerodigestive tract in Ontario and the United States. *International Journal of Cancer* **125**, 2159-2165 (2009).

36. Howlader N, Noone AM, Krapcho M, Garshell J, Miller D, Altekruse SF, Kosary CL, Yu M, Ruhl J, Tatalovich Z,Mariotto A, Lewis DR, Chen HS, Feuer EJ, Cronin KA (eds). SEER Cancer Statistics Review, 1975-2012, National Cancer Institute. Bethesda, MD, http://seer.cancer.gov/csr/1975_2012/, based on November 2014 SEER data submission, posted to the SEER web site, April 2015.

37. Australian Institute of Health and Welfare & Australasian Association of Cancer Registries 2012. Cancer in Australia: an overview, 2012. Cancer series no. 74. Cat. no. CAN 70. Canberra: AIHW. .

38. Australian Institute of Health and Welfare Pivot Table- http://www.aihw.gov.au/cancer-data/ [Accessed June 2015].

39. Australian Cancer Incidence and Mortality (ACIM) Books – All Cancers combined for Australia (ICD10 C00-C97, D45-46, D47.1, D47.3). http://www.aihw.gov.au/acim-books/ [Accessed June 2015].

40. Siegel, R., Naishadham, D. & Jemal, A. Cancer statistics, 2012. *CA: A Cancer Journal for Clinicians* **62**, 10-29 (2012).

41. Doobaree, I.U., Landis, S.H., Linklater, K.M., El-Hariry, I., Moller, H. & Tyczynski, J. Head and neck cancer in South East England between 1995–1999 and 2000–2004: An estimation of incidence and distribution by site, stage and histological type. *Oral oncology* **45**, 809-814 (2009).

42. Simard, E.P., Torre, L.A. & Jemal, A. International trends in head and neck cancer incidence rates: Differences by country, sex and anatomic site. *Oral Oncology* **50**, 387-403 (2014).

43. Shiboski, C.H., Schmidt, B.L. & Jordan, R.C.K. Tongue and tonsil carcinoma. *Cancer* **103**, 1843-1849 (2005).

44. Gillison, M.L., Koch, W.M., Capone, R.B., Spafford, M., Westra, W.H., Wu, L., Zahurak, M.L., Daniel, R.W., Viglione, M., Symer, D.E., Shah, K.V. & Sidransky, D. Evidence for a Causal Association Between Human Papillomavirus and a Subset of Head and Neck Cancers. *Journal of the National Cancer Institute* **92**, 709-720 (2000).

45. Hashibe, M., Brennan, P., Chuang, S.-c., Boccia, S., Castellsague, X., Chen, C., Curado, M.P., Dal Maso, L., Daudt, A.W., Fabianova, E., Fernandez, L., Wünsch-Filho, V., Franceschi, S., Hayes, R.B., Herrero, R., Kelsey, K., Koifman, S., La Vecchia, C., Lazarus, P., Levi, F., Lence, J.J., Mates, D., Matos, E., Menezes, A., McClean, M.D., Muscat, J., Eluf-Neto, J., Olshan, A.F., Purdue, M., Rudnai, P., Schwartz, S.M., Smith, E., Sturgis, E.M., Szeszenia-Dabrowska, N., Talamini, R., Wei, Q., Winn, D.M., Shangina, O., Pilarska, A., Zhang, Z.-F., Ferro, G., Berthiller, J. & Boffetta, P. Interaction between Tobacco and Alcohol Use and the Risk of Head and Neck Cancer: Pooled Analysis in the International Head and Neck Cancer Epidemiology Consortium. *Cancer Epidemiology Biomarkers & Prevention* **18**, 541-550 (2009).

46. Macigo, F.G., Mwaniki, D.L. & Guthua, S.W.o. Influence of dose and cessation of kiraiku, cigarettes and alcohol use on the risk of developing oral leukoplakia. *European Journal of Oral Sciences* **104**, 498-502 (1996).

47. Cheng, L., Eicher, S.A., Guo, Z., Hong, W.K., Spitz, M.R. & Wei, Q. Reduced DNA repair capacity in head and neck cancer patients. *Cancer Epidemiology Biomarkers & Prevention* **7**, 465-468 (1998).

48. Brennan, J.A., Boyle, J.O., Koch, W.M., Goodman, S.N., Hruban, R.H., Eby, Y.J., Couch, M.J., Forastiere, A.A. & Sidransky, D. Association between cigarette smoking and mutation of the p53 gene in squamous-cell carcinoma of the head and neck. *The New England Journal Of Medicine* **332**, 712-717 (1995).

49. Ahrendt, S.A., Chow, J.T., Yang, S.C., Wu, L., Zhang, M.-J., Jen, J. & Sidransky, D. Alcohol Consumption and Cigarette Smoking Increase the Frequency of p53 Mutations in Non-Small Cell Lung Cancer. *Cancer Research* **60**, 3155-3159 (2000).

50. Kutler David I., Auerbach Arleen. D., Satagopan Jaya., Giampietro Philip F., Batish Sat D., Huvos Andrew G., Goberdhan Andy BS., Shah Jatin P. & Bhuvanesh, S. HIgh incidence of head and neck squamous cell carcinoma in patients with fanconi anemia. *Arch Otolarnygol Head Neck Surg.* **129**, 106-112 (2003).

51. Pavia, M., Pileggi, C., Nobile, C.G. & Angelillo, I.F. Association between fruit and vegetable consumption and oral cancer: a meta-analysis of observational studies. *The American Journal of Clinical Nutrition* **83**, 1126-1134 (2006).

52. Larsson, L.-G., Sandström, A. & Westling, P. Relationship of Plummer-Vinson Disease to Cancer of the Upper Alimentary Tract in Sweden. *Cancer Research* **35**, 3308-3316 (1975).

53. Tyan, Y.S., Liu, S.T., Ong, W.R., Chen, M.L., Shu, C.H. & Chang, Y.S. Detection of Epstein-Barr virus and human papillomavirus in head and neck tumors. *Journal of Clinical Microbiology* **31**, 53-56 (1993).

54. HAYES, R.B., GERIN, M., RAATGEVER, J.W. & BRUYN, A.d. Wood-related Occupations, Wood Dust and Sinonasal Cancer. *American Journal of Epidemiology* **124**, 569-577 (1986).

55. Hernberg, S., Westerholm, P., Schultz-Larsen, K., Degerth, R., Kuosma, E., Englund, A., Engzell, U., Hansen, H.S. & Mutanen, P. Nasal and sinonasal cancer. Connection with occupational exposures in Denmark, Finland and Sweden. *Scandinavian journal of work, environment & health* **9**, 315-326 (1983).

56. Chien, Y.-C., Chen, J.-Y., Liu, M.-Y., Yang, H.-I., Hsu, M.-M., Chen, C.-J. & Yang, C.-S. Serologic Markers of Epstein–Barr Virus Infection and Nasopharyngeal Carcinoma in Taiwanese Men. *New England Journal of Medicine* **345**, 1877-1882 (2001).

57. Garavello, W., Bertuccio, P., Levi, F., Lucchini, F., Bosetti, C., Malvezzi, M., Negri, E. & La Vecchia, C. The oral cancer epidemic in central and eastern Europe. *International Journal of Cancer* **127**, 160-171 (2010).

58. Nair, U., Bartsch, H. & Nair, J. Alert for an epidemic of oral cancer due to use of the betel quid substitutes gutkha and pan masala: a review of agents and causative mechanisms. *Mutagenesis* **19**, 251-262 (2004).

59. Smeets, S.J., Brakenhoff, R.H., Ylstra, B., van Wieringen, W.N., van de Wiel, M.A., Leemans, C.R. & Braakhuis, B.J. Genetic classification of oral and oropharyngeal carcinomas identifies subgroups with a different prognosis. *Cell Oncol* **31**, 291-300 (2009).

60. Blackwell, K.L., Burstein, H., Pegram, M., Storniolo, A.M., Salazar, V.M., Maleski, J.E., Lin, X., Spector, N., Stein, S.H. & Berger, M.S. Determining relevant biomarkers from tissue and serum that may predict response to single agent lapatinib in trastuzumab refractory metastatic breast cancer. *J Clin Oncol (Meeting Abstracts)* **23**, 3004-(2005).

61. Saini, K.S., Loi, S., de Azambuja, E., Metzger-Filho, O., Saini, M.L., Ignatiadis, M., Dancey, J.E. & Piccart-Gebhart, M.J. Targeting the PI3K/AKT/mTOR and Raf/MEK/ERK pathways in the treatment of breast cancer. *Cancer Treatment Reviews* **39**, 935-946 (2013).

62. Ellis, M.J., Suman, V.J., Hoog, J., Lin, L., Snider, J., Prat, A., Parker, J.S., Luo, J., DeSchryver, K., Allred, D.C., Esserman, L.J., Unzeitig, G.W., Margenthaler, J., Babiera, G.V., Marcom, P.K., Guenther, J.M., Watson, M.A., Leitch, M., Hunt, K. & Olson, J.A. Randomized Phase II Neoadjuvant Comparison Between Letrozole, Anastrozole, and Exemestane for Postmenopausal Women With Estrogen Receptor–Rich Stage 2 to 3 Breast Cancer: Clinical and Biomarker Outcomes and Predictive Value of the Baseline PAM50-Based Intrinsic Subtype—ACOSOG Z1031. *Journal of Clinical Oncology* **29**, 2342-2349 (2011).

63. Taniguchi, M., Nishida, T., Hirota, S., Isozaki, K., Ito, T., Nomura, T., Matsuda, H. & Kitamura, Y. Effect of c-kit mutation on prognosis of gastrointestinal stromal tumors. *Cancer Research* **59**, 4297-4300 (1999).

64. Rubin, B.P., Singer, S., Tsao, C., Duensing, A., Lux, M.L., Ruiz, R., Hibbard, M.K., Chen, C.-J., Xiao, S. & Tuveson, D.A. KIT activation is a ubiquitous feature of gastrointestinal stromal tumors. *Cancer research* **61**, 8118-8121 (2001).

65. O'Donnell, R.K., Kupferman, M., Wei, S.J., Singhal, S., Weber, R., O'Malley, B., Jr., Cheng, Y., Putt, M., Feldman, M., Ziober, B. & Muschel, R.J. Gene expression signature predicts lymphatic metastasis in squamous cell carcinoma of the oral cavity. *Oncogene* **24**, 1244-1251 (2004).

66. Chung, C.H., Parker, J.S., Karaca, G., Wu, J., Funkhouser, W.K., Moore, D., Butterfoss, D., Xiang, D., Zanation, A., Yin, X., Shockley, W.W., Weissler, M.C., Dressler, L.G., Shores, C.G., Yarbrough, W.G. & Perou, C.M. Molecular classification of head and neck squamous cell carcinomas using patterns of gene expression. *Cancer Cell* **5**, 489-500 (2004).

67. Roepman, P., Wessels, L.F.A., Kettelarij, N., Kemmeren, P., Miles, A.J., Lijnzaad, P., Tilanus, M.G.J., Koole, R., Hordijk, G.-J., van der Vliet, P.C., Reinders, M.J.T., Slootweg, P.J. & Holstege, F.C.P. An expression profile for diagnosis of lymph node metastases from primary head and neck squamous cell carcinomas. *Nat Genet* **37**, 182-186 (2005).

68. Forastiere, A., Koch, W., Trotti, A. & Sidransky, D. Head and neck cancer. *The New England Journal Of Medicine* **345**, 1890-1900 (2001).

69. Brennan, J. & Sidransky, D. Molecular staging of head and neck squamous carcinoma. *Cancer and Metastasis Reviews* **15**, 3-10 (1996).

70. Poeta, M.L., Manola, J., Goldwasser, M.A., Forastiere, A., Benoit, N., Califano, J.A., Ridge, J.A., Goodwin, J., Kenady, D., Saunders, J.,

Westra, W., Sidransky, D. & Koch, W.M. TP53 Mutations and Survival in Squamous-Cell Carcinoma of the Head and Neck. *New England Journal of Medicine* **357**, 2552-2561 (2007).

71. Åkervall, J.A., Michalides, R.J.A.M., Mineta, H., Balm, A., Borg, Å., Dictor, M.R., Jin, Y., Loftus, B., Mertens, F. & Wennerberg, J.P. Amplification of cyclin D1 in squamous cell carcinoma of the head and neck and the prognostic value of chromosomal abnormalities and cyclin D1 overexpression. *Cancer* **79**, 380-389 (1997).
72. Namazie, A., Alavi, S., Olopade, O.I., Pauletti, G., Aghamohammadi, N., Aghamohammadi, M., Gornbein, J.A., Calcaterra, T.C., Slamon, D.J., Wang, M.B. & Srivatsan, E.S. Cyclin D1 Amplification and p16(MTS1/CDK4I) Deletion Correlate With Poor Prognosis in Head and Neck Tumors. *The Laryngoscope* **112**, 472-481 (2002).
73. Reed, A.L., Califano, J., Cairns, P., Westra, W.H., Jones, R.M., Koch, W., Ahrendt, S., Eby, Y., Sewell, D., Nawroz, H., Bartek, J. & Sidransky, D. High Frequency of p16 (CDKN2/MTS-1/INK4A) Inactivation in Head and Neck Squamous Cell Carcinoma. *Cancer Research* **56**, 3630-3633 (1996).
74. Chung, C.H., Ely, K., McGavran, L., Varella-Garcia, M., Parker, J., Parker, N., Jarrett, C., Carter, J., Murphy, B.A., Netterville, J., Burkey, B.B., Sinard, R., Cmelak, A., Levy, S., Yarbrough, W.G., Slebos, R.J.C. & Hirsch, F.R. Increased Epidermal Growth Factor Receptor Gene Copy Number Is Associated With Poor Prognosis in Head and Neck Squamous Cell Carcinomas. *Journal of Clinical Oncology* **24**, 4170-4176 (2006).
75. Forastiere, A.A., Goepfert, H., Maor, M., Pajak, T.F., Weber, R., Morrison, W., Glisson, B., Trotti, A., Ridge, J.A., Chao, C., Peters, G., Lee, D.-J., Leaf, A., Ensley, J. & Cooper, J. Concurrent Chemotherapy and Radiotherapy for Organ Preservation in Advanced Laryngeal Cancer. *New England Journal of Medicine* **349**, 2091-2098 (2003).
76. Robert, F., Ezekiel, M.P., Spencer, S.A., Meredith, R.F., Bonner, J.A., Khazaeli, M.B., Saleh, M.N., Carey, D., LoBuglio, A.F., Wheeler, R.H.,

Cooper, M.R. & Waksal, H.W. Phase I Study of Anti-Epidermal Growth Factor Receptor Antibody Cetuximab in Combination With Radiation Therapy in Patients With Advanced Head and Neck Cancer. *Journal of Clinical Oncology* **19**, 3234-3243 (2001).

77. Lee, R.C., Feinbaum, R.L. & Ambros, V. The C. elegans Heterochronic Gene *lin-4* Encodes Small RNAs with Antisense Complementarity to *lin-14*. *Cell* **75**, 843-854 (1993).
78. Hahn, M.W. & Wray, G.A. The g-value paradox. *Evolution & development* **4**, 73-75 (2002).
79. Goodstadt, L. & Ponting, C. Phylogenetic Reconstruction of Orthology, Paralogy, and Conserved Synteny for Dog and Human. *PLoS Comput Biol* **2**, e133 (2006).
80. Taft, R.J., Pheasant, M. & Mattick, J.S. The relationship between non-protein-coding DNA and eukaryotic complexity. *BioEssays* **29**, 288-299 (2007).
81. Mazumder, B., Seshadri, V. & Fox, P.L. Translational control by the 3'UTR: the ends specify the means. *Trends in Biochemical Sciences* **28**, 91-98 (2003).
82. Pesole, G., Liuni, S., Grillo, G., Licciulli, F., Mignone, F., Gissi, C. & Saccone, C. UTRdb and UTRsite: Specialized databases of sequences and functional elements of 5' and 3' untranslated regions of eukaryotic mRNAs. Update 2002. *Nucleic Acids Research* **30**, 335-340 (2002).
83. Kapranov, P., Cheng, J., Dike, S., Nix, D.A., Duttagupta, R., Willingham, A.T., Stadler, P.F., Hertel, J., Hackermüller, J., Hofacker, I.L., Bell, I., Cheung, E., Drenkow, J., Dumais, E., Patel, S., Helt, G., Ganesh, M., Ghosh, S., Piccolboni, A., Sementchenko, V., Tammana, H. & Gingeras, T.R. RNA Maps Reveal New RNA Classes and a Possible Function for Pervasive Transcription. *Science* **316**, 1484-1488 (2007).
84. Gomes, C.C. & Gomez, R.S. MicroRNA and oral cancer: future perspectives. *Oral Oncol* **44**, 910-4 (2008).

85. Consortium, T.F., Carninci, P., Kasukawa, T., Katayama, S., Gough, J., Frith, M.C., Maeda, N., Oyama, R., Ravasi, T., Lenhard, B., Wells, C., Kodzius, R., Shimokawa, K., Bajic, V.B., Brenner, S.E., Batalov, S., Forrest, A.R.R., Zavolan, M., Davis, M.J., Wilming, L.G., Aidinis, V., Allen, J.E., Ambesi-Impiombato, A., Apweiler, R., Aturaliya, R.N., Bailey, T.L., Bansal, M., Baxter, L., Beisel, K.W., Bersano, T., Bono, H., Chalk, A.M., Chiu, K.P., Choudhary, V., Christoffels, A., Clutterbuck, D.R., Crowe, M.L., Dalla, E., Dalrymple, B.P., de Bono, B., Gatta, G.D., di Bernardo, D., Down, T., Engstrom, P., Fagiolini, M., Faulkner, G., Fletcher, C.F., Fukushima, T., Furuno, M., Futaki, S., Gariboldi, M., Georgii-Hemming, P., Gingeras, T.R., Gojobori, T., Green, R.E., Gustincich, S., Harbers, M., Hayashi, Y., Hensch, T.K., Hirokawa, N., Hill, D., Huminiecki, L., Iacono, M., Ikeo, K., Iwama, A., Ishikawa, T., Jakt, M., Kanapin, A., Katoh, M., Kawasawa, Y., Kelso, J., Kitamura, H., Kitano, H., Kollias, G., Krishnan, S.P.T., Kruger, A., Kummerfeld, S.K., Kurochkin, I.V., Lareau, L.F., Lazarevic, D., Lipovich, L., Liu, J., Liuni, S., McWilliam, S., Babu, M.M., Madera, M., Marchionni, L., Matsuda, H., Matsuzawa, S., Miki, H., Mignone, F., Miyake, S., Morris, K., Mottagui-Tabar, S., Mulder, N., Nakano, N., Nakauchi, H., Ng, P., Nilsson, R., Nishiguchi, S., Nishikawa, S., Nori, F., Ohara, O., Okazaki, Y., Orlando, V., Pang, K.C., Pavan, W.J., Pavesi, G., Pesole, G., Petrovsky, N., Piazza, S., Reed, J., Reid, J.F., Ring, B.Z., Ringwald, M., Rost, B., Ruan, Y., Salzberg, S.L., Sandelin, A., Schneider, C., Schnbach, C., Sekiguchi, K., Semple, C.A.M., Seno, S., Sessa, L., Sheng, Y., Shibata, Y., Shimada, H., Shimada, K., Silva, D., Sinclair, B., Sperling, S., Stupka, E., Sugiura, K., Sultana, R., Takenaka, Y., Taki, K., Tammoja, K., Tan, S.L., Tang, S., Taylor, M.S., Tegner, J., Teichmann, S.A., Ueda, H.R., van Nimwegen, E., Verardo, R., Wei, C.L., Yagi, K., Yamanishi, H., Zabarovsky, E., Zhu, S., Zimmer, A., Hide, W., Bult, C., Grimmond, S.M., Teasdale, R.D., Liu, E.T., Brusic, V., Quackenbush, J., Wahlestedt, C., Mattick, J.S., Hume, D.A., Group, R.G.E.R., Group, G.S., Kai, C., Sasaki, D., Tomaru, Y., Fukuda,

S., Kanamori-Katayama, M., Suzuki, M., Aoki, J., Arakawa, T., Iida, J., Imamura, K., Itoh, M., Kato, T., Kawaji, H., Kawagashira, N., Kawashima, T., Kojima, M., Kondo, S., Konno, H., Nakano, K., Ninomiya, N., Nishio, T., Okada, M., Plessy, C., Shibata, K., Shiraki, T., Suzuki, S., Tagami, M., Waki, K., Watahiki, A., Okamura-Oho, Y., Suzuki, H., Kawai, J. & Hayashizaki, Y. The Transcriptional Landscape of the Mammalian Genome. *Science* **309**, 1559-1563 (2005).

86. Croce, C.M. & Calin, G.A. miRNAs, Cancer, and Stem Cell Division. *Cell* **122**, 6-7 (2005).
87. Kapranov, P., Ozsolak, F., Kim, S.W., Foissac, S., Lipson, D., Hart, C., Roels, S., Borel, C., Antonarakis, S.E., Monaghan, A.P., John, B. & Milos, P.M. New class of gene-termini-associated human RNAs suggests a novel RNA copying mechanism. *Nature* **466**, 642-646 (2010).
88. Eddy, S.R. Non-coding RNA genes and the modern RNA world. *Nat Rev Genet* **2**, 919-929 (2001).
89. Okamura, K. Diversity of animal small RNA pathways and their biological utility. *Wiley Interdisciplinary Reviews: RNA* **3**, 351-368 (2012).
90. Deng, W. & Lin, H. miwi, a Murine Homolog of piwi, Encodes a Cytoplasmic Protein Essential for Spermatogenesis. *Developmental Cell* **2**, 819-830 (2002).
91. Girard, A., Sachidanandam, R., Hannon, G.J. & Carmell, M.A. A germline-specific class of small RNAs binds mammalian Piwi proteins. *Nature* **442**, 199-202 (2006).
92. Horvitz, H.R. & Sulston, J.E. Isolation and genetic characterization of cell-lineage mutants of the nematode caenorhabditis elegans. *Genetics* **96**, 435-454 (1980).
93. Pasquinelli, A.E., Reinhart, B.J., Slack, F., Martindale, M.Q., Kuroda, M.I., Maller, B., Hayward, D.C., Ball, E.E., Degnan, B., Muller, P., Spring, J., Srinivasan, A., Fishman, M., Finnerty, J., Corbo, J., Levine, M., Leahy, P., Davidson, E. & Ruvkun, G. Conservation of the

sequence and temporal expression of let-7 heterochronic regulatory RNA. *Nature* **408**, 86-89 (2000).

94. Calin, G.A., Dumitru, C.D., Shimizu, M., Bichi, R., Zupo, S., Noch, E., Aldler, H., Rattan, S., Keating, M., Rai, K., Rassenti, L., Kipps, T., Negrini, M., Bullrich, F. & Croce, C.M. Frequent deletions and down-regulation of micro- RNA genes miR15 and miR16 at 13q14 in chronic lymphocytic leukemia. *Proceedings of the National Academy of Sciences* **99**, 15524-15529 (2002).
95. Cho, W.C.S. OncomiRs: the discovery and progress of microRNAs in cancers. (BioMed Central Ltd., 2007).
96. Cheng, A.M., Byrom, M.W., Shelton, J. & Ford, L.P. Antisense inhibition of human miRNAs and indications for an involvement of miRNA in cell growth and apoptosis. *Nucleic Acids Research* **33**, 1290-1297 (2005).
97. Volinia, S., Calin, G.A., Liu, C.-G., Ambs, S., Cimmino, A., Petrocca, F., Visone, R., Iorio, M., Roldo, C., Ferracin, M., Prueitt, R.L., Yanaihara, N., Lanza, G., Scarpa, A., Vecchione, A., Negrini, M., Harris, C.C. & Croce, C.M. A microRNA expression signature of human solid tumors defines cancer gene targets. *Proceedings of the National Academy of Sciences of the United States of America* **103**, 2257-2261 (2006).
98. Hui, A.B., Lenarduzzi, M., Krushel, T., Waldron, L., Pintilie, M., Shi, W., Perez-Ordonez, B., Jurisica, I., O'Sullivan, B., Waldron, J., Gullane, P., Cummings, B. & Liu, F.F. Comprehensive MicroRNA profiling for head and neck squamous cell carcinomas. *Clin Cancer Res* **16**, 1129-39 (2010).
99. Calin, G.A. & Croce, C.M. MicroRNA signatures in human cancers. *Nat Rev Cancer* **6**, 857-866 (2006).
100. Lee, E.J., Gusev, Y., Jiang, J., Nuovo, G.J., Lerner, M.R., Frankel, W.L., Morgan, D.L., Postier, R.G., Brackett, D.J. & Schmittgen, T.D. Expression profiling identifies microRNA signature in pancreatic cancer. *International Journal of Cancer* **120**, 1046-1054 (2007).

101. Roldo, C., Missiaglia, E., Hagan, J.P., Falconi, M., Capelli, P., Bersani, S., Calin, G.A., Volinia, S., Liu, C.-G., Scarpa, A. & Croce, C.M. MicroRNA Expression Abnormalities in Pancreatic Endocrine and Acinar Tumors Are Associated With Distinctive Pathologic Features and Clinical Behavior. *Journal of Clinical Oncology* **24**, 4677-4684 (2006).

102. Chan, J.A., Krichevsky, A.M. & Kosik, K.S. MicroRNA-21 Is an Antiapoptotic Factor in Human Glioblastoma Cells. *Cancer Research* **65**, 6029-6033 (2005).

103. Asangani, I.A., Rasheed, S.A.K., Nikolova, D.A., Leupold, J.H., Colburn, N.H., Post, S. & Allgayer, H. MicroRNA-21 (miR-21) post-transcriptionally downregulates tumor suppressor Pdcd4 and stimulates invasion, intravasation and metastasis in colorectal cancer. *Oncogene* **27**, 2128-2136 (2007).

104. Meng, F., Henson, R., Lang, M., Wehbe, H., Maheshwari, S., Mendell, J.T., Jiang, J., Schmittgen, T.D. & Patel, T. Involvement of Human Micro-RNA in Growth and Response to Chemotherapy in Human Cholangiocarcinoma Cell Lines. *Gastroenterology* **130**, 2113-2129 (2006).

105. Kalluri, R. & Weinberg, R.A. The basics of epithelial-mesenchymal transition. *The Journal of Clinical Investigation* **119**, 1420-1428 (2009).

106. Acloque, H., Adams, M.S., Fishwick, K., Bronner-Fraser, M. & Nieto, M.A. Epithelial-mesenchymal transitions: the importance of changing cell state in development and disease. *The Journal of Clinical Investigation* **119**, 1438-1449 (2009).

107. Kalluri, R. & Neilson, E.G. Epithelial-mesenchymal transition and its implications for fibrosis. *Journal of Clinical Investigation* **112**, 1776-1784 (2003).

108. Preston-Martin, S., Pike, M.C., Ross, R.K. & Henderson, B.E. Epidemiologic evidence for the increased cell proliferation model of carcinogenesis. *Environmental Health Perspectives* **101**, 137-138 (1993).

109. Hayashita, Y., Osada, H., Tatematsu, Y., Yamada, H., Yanagisawa, K., Tomida, S., Yatabe, Y., Kawahara, K., Sekido, Y. & Takahashi, T. A Polycistronic MicroRNA Cluster, miR-17-92, Is Overexpressed in Human Lung Cancers and Enhances Cell Proliferation. *Cancer Research* **65**, 9628-9632 (2005).

110. Johnson, C.D., Esquela-Kerscher, A., Stefani, G., Byrom, M., Kelnar, K., Ovcharenko, D., Wilson, M., Wang, X., Shelton, J., Shingara, J., Chin, L., Brown, D. & Slack, F.J. The let-7 MicroRNA Represses Cell Proliferation Pathways in Human Cells. *Cancer Research* **67**, 7713-7722 (2007).

111. Pauli, B.U. & Knudson, W. Tumor invasion: A consequence of destructive and compositional matrix alterations. *Human Pathology* **19**, 628-639 (1988).

112. Zhang, J.-g., Wang, J.-j., Zhao, F., Liu, Q., Jiang, K. & Yang, G.-h. MicroRNA-21 (miR-21) represses tumor suppressor PTEN and promotes growth and invasion in non-small cell lung cancer (NSCLC). *Clinica Chimica Acta* **411**, 846-852 (2010).

113. Burk, U., Schubert, J., Wellner, U., Schmalhofer, O., Vincan, E., Spaderna, S. & Brabletz, T. *A reciprocal repression between ZEB1 and members of the miR‐200 family promotes EMT and invasion in cancer cells*, 582-589 (2008).

114. Pollard, T.D. & Borisy, G.G. Cellular Motility Driven by Assembly and Disassembly of Actin Filaments. *Cell* **112**, 453-465 (2003).

115. Wang, H.-J., Ruan, H.-J., He, X.-J., Ma, Y.-Y., Jiang, X.-T., Xia, Y.-J., Ye, Z.-Y. & Tao, H.-Q. MicroRNA-101 is down-regulated in gastric cancer and involved in cell migration and invasion. *European Journal of Cancer* **46**, 2295-2303 (2010).

116. Tian, Y., Luo, A., Cai, Y., Su, Q., Ding, F., Chen, H. & Liu, Z. MicroRNA-10b Promotes Migration and Invasion through KLF4 in Human Esophageal Cancer Cell Lines. *Journal of Biological Chemistry* **285**, 7986-7994 (2010).

117. Lu, J., Getz, G., Miska, E.A., Alvarez-Saavedra, E., Lamb, J., Peck, D., Sweet-Cordero, A., Ebert, B.L., Mak, R.H., Ferrando, A.A., Downing, J.R., Jacks, T., Horvitz, H.R. & Golub, T.R. MicroRNA expression profiles classify human cancers. *Nature* **435**, 834-838 (2005).

118. Cummins, J.M. & Velculescu, V.E. Implications of micro-RNA profiling for cancer diagnosis. *Oncogene* **25**, 6220-6227 (2006).

119. Yanaihara, N., Caplen, N., Bowman, E., Seike, M., Kumamoto, K., Yi, M., Stephens, R.M., Okamoto, A., Yokota, J., Tanaka, T., Calin, G.A., Liu, C.-G., Croce, C.M. & Harris, C.C. Unique microRNA molecular profiles in lung cancer diagnosis and prognosis. *Cancer Cell* **9**, 189-198 (2006).

120. Calin, G.A., Ferracin, M., Cimmino, A., Di Leva, G., Shimizu, M., Wojcik, S.E., Iorio, M.V., Visone, R., Sever, N.I., Fabbri, M., Iuliano, R., Palumbo, T., Pichiorri, F., Roldo, C., Garzon, R., Sevignani, C., Rassenti, L., Alder, H., Volinia, S., Liu, C.-g., Kipps, T.J., Negrini, M. & Croce, C.M. A MicroRNA Signature Associated with Prognosis and Progression in Chronic Lymphocytic Leukemia. *New England Journal of Medicine* **353**, 1793-1801 (2005).

121. Krutzfeldt, J., Rajewsky, N., Braich, R., Rajeev, K.G., Tuschl, T., Manoharan, M. & Stoffel, M. Silencing of microRNAs in vivo with /ˆantagomirs/'. *Nature* **438**, 685-689 (2005).

122. He, H., Jazdzewski, K., Li, W., Liyanarachchi, S., Nagy, R., Volinia, S., Calin, G.A., Liu, C.-g., Franssila, K., Suster, S., Kloos, R.T., Croce, C.M. & de la Chapelle, A. The role of microRNA genes in papillary thyroid carcinoma. *Proceedings of the National Academy of Sciences of the United States of America* **102**, 19075-19080 (2005).

123. Avissar, M., Christensen, B.C., Kelsey, K.T. & Marsit, C.J. MicroRNA expression ratio is predictive of head and neck squamous cell carcinoma. *Clinical Cancer Research* **15**, 2850-2855 (2009).

124. Tran, N., McLean, T., Zhang, X., Zhao, C.J., Thomson, J.M., O,ÄôBrien, C. & Rose, B. MicroRNA expression profiles in head and

neck cancer cell lines. *Biochemical and biophysical research communications* **358**, 12-17 (2007).

125. Hermsen, M., Alonso Guervós, M., Meijer, G., Baak, J., van Diest, P., Alvarez Marcos, C. & Sampedro, A. New chromosomal regions with high-level amplifications in squamous cell carcinomas of the larynx and pharynx, identified by comparative genomic hybridization. *The Journal of Pathology* **194**, 177-182 (2001).
126. Speicher, M.R., Howe, C., Crotty, P., du Manoir, S., Costa, J. & Ward, D.C. Comparative Genomic Hybridization Detects Novel Deletions and Amplifications in Head and Neck Squamous Cell Carcinomas. *Cancer Research* **55**, 1010-1013 (1995).
127. Krichevsky, A.M. & Gabriely, G. miR-21: a small multi-faceted RNA. *Journal of Cellular and Molecular Medicine* **13**, 39-53 (2009).
128. Si, M.L., Zhu, S., Wu, H., Lu, Z., Wu, F. & Mo, Y.Y. miR-21-mediated tumor growth. *Oncogene* **26**, 2799-2803 (2006).
129. Satzger, I., Mattern, A., Kuettler, U., Weinspach, D., Niebuhr, M., Kapp, A. & Gutzmer, R. microRNA-21 is upregulated in malignant melanoma and influences apoptosis of melanocytic cells. *Experimental Dermatology* **21**, 509-514 (2012).
130. Kulda, V., Pesta, M., Topolcan, O., Liska, V., Treska, V., Sutnar, A., Rupert, K., Ludvikova, M., Babuska, V., Holubec Jr, L. & Cerny, R. Relevance of miR-21 and miR-143 expression in tissue samples of colorectal carcinoma and its liver metastases. *Cancer Genetics and Cytogenetics* **200**, 154-160 (2010).
131. Zhang, Z., Li, Z., Gao, C., Chen, P., Chen, J., Liu, W., Xiao, S. & Lu, H. miR-21 plays a pivotal role in gastric cancer pathogenesis and progression. *Lab Invest* **88**, 1358-1366 (2008).
132. Frankel, L., Christoffersen, N., Jacobsen, A., Lindow, M., Krogh, A. & Lund, A. Programmed cell death 4 (PDCD4) is an important functional target of the microRNA miR-21 in breast cancer cells. *J Biol Chem* **283**, 1026 - 1033 (2008).

133. Zaman, M.S., Shahryari, V., Deng, G., Thamminana, S., Saini, S., Majid, S., Chang, I., Hirata, H., Ueno, K., Yamamura, S., Singh, K., Tanaka, Y., Tabatabai, Z.L. & Dahiya, R. Up-Regulation of MicroRNA-21 Correlates with Lower Kidney Cancer Survival. *PLoS ONE* **7**, e31060 (2012).

134. Scapoli, L., Palmieri, A., Muzio, L.L., Pezzetti, F., Rubini, C., Girardi, A., Farinella, F., Mazzotta, M. & Carinci, F. MicroRNA Expression Profiling of Oral Carcinoma Identifies New Markers of Tumor Progression. *International Journal of Immunopathology and Pharmacology* **23**, 1229-1234 (2010).

135. Avissar, M., McClean, M.D., Kelsey, K.T. & Marsit, C.J. MicroRNA expression in head and neck cancer associates with alcohol consumption and survival. *Carcinogenesis* **30**, 2059-2063 (2009).

136. Adachi, T., Nakanishi, M., Otsuka, Y., Nishimura, K., Hirokawa, G., Goto, Y., Nonogi, H. & Iwai, N. Plasma MicroRNA 499 as a Biomarker of Acute Myocardial Infarction. *Clinical Chemistry* **56**, 1183-1185 (2010).

137. Wilson, K.D., Hu, S., Venkatasubrahmanyam, S., Fu, J.-D., Sun, N., Abilez, O.J., Baugh, J.J.A., Jia, F., Ghosh, Z., Li, R.A., Butte, A.J. & Wu, J.C. Dynamic MicroRNA Expression Programs During Cardiac Differentiation of Human Embryonic Stem Cells: Role for miR-499. *Circulation: Cardiovascular Genetics* **3**, 426-435 (2010).

138. Wang, J.-X., Jiao, J.-Q., Li, Q., Long, B., Wang, K., Liu, J.-P., Li, Y.-R. & Li, P.-F. miR-499 regulates mitochondrial dynamics by targeting calcineurin and dynamin-related protein-1. *Nat Med* **17**, 71-78 (2011).

139. Iwai, N. & Naraba, H. Polymorphisms in human pre-miRNAs. *Biochemical and Biophysical Research Communications* **331**, 1439-1444 (2005).

140. George, G., Gangwar, R., Mandal, R., Sankhwar, S. & Mittal, R. Genetic variation in microRNA genes and prostate cancer risk in North Indian population. *Molecular Biology Reports* **38**, 1609-1615 (2011).

141. Okubo, M., Tahara, T., Shibata, T., Yamashita, H., Nakamura, M., Yoshioka, D., Yonemura, J., Ishizuka, T., Arisawa, T. & Hirata, I. Association Between Common Genetic Variants in Pre-microRNAs and Gastric Cancer Risk in Japanese Population. *Helicobacter* **15**, 524-531 (2010).

142. Zhou, B., Wang, K., Wang, Y., Xi, M., Zhang, Z., Song, Y. & Zhang, L. Common genetic polymorphisms in pre-microRNAs and risk of cervical squamous cell carcinoma. *Molecular Carcinogenesis* **50**, 499-505 (2011).

143. Hu, Z., Liang, J., Wang, Z., Tian, T., Zhou, X., Chen, J., Miao, R., Wang, Y., Wang, X. & Shen, H. Common genetic variants in pre-microRNAs were associated with increased risk of breast cancer in Chinese women. *Hum Mutat* **30**, 79-84 (2009).

144. Catucci, I., Yang, R., Verderio, P., Pizzamiglio, S., Heesen, L., Hemminki, K., Sutter, C., Wappenschmidt, B., Dick, M., Arnold, N., Bugert, P., Niederacher, D., Meindl, A., Schmutzler, R.K., Bartram, C.C., Ficarazzi, F., Tizzoni, L., Zaffaroni, D., Manoukian, S., Barile, M., Pierotti, M.A., Radice, P., Burwinkel, B. & Peterlongo, P. Evaluation of SNPs in miR-146a, miR196a2 and miR-499 as low-penetrance alleles in German and Italian familial breast cancer cases. *Human Mutation* **31**, E1052-E1057 (2010).

145. Srivastava, K., Srivastava, A. & Mittal, B. Common genetic variants in pre-microRNAs and risk of gallbladder cancer in North Indian population. *J Hum Genet* **55**, 495-499 (2010).

146. Tian, T., Shu, Y., Chen, J., Hu, Z., Xu, L., Jin, G., Liang, J., Liu, P., Zhou, X., Miao, R., Ma, H., Chen, Y. & Shen, H. A Functional Genetic Variant in microRNA-196a2 Is Associated with Increased Susceptibility of Lung Cancer in Chinese. *Cancer Epidemiology Biomarkers & Prevention* **18**, 1183-1187 (2009).

147. Vinci, S., Gelmini, S., Pratesi, N., Conti, S., Malentacchi, F., Simi, L., Pazzagli, M. & Orlando, C. Genetic variants in miR-146a, miR-149, miR-196a2, miR-499 and their influence on relative expression in lung

cancers. in *Clinical Chemistry and Laboratory Medicine* Vol. 49 2073 (2011).

148. Zhou, J., Lv, R., Song, X., Li, D., Hu, X., Ying, B., Wei, Y. & Wang, L. Association Between Two Genetic Variants in miRNA and Primary Liver Cancer Risk in the Chinese Population. *DNA and Cell Biology* **31**, 524-530 (2011).
149. Chu, Y.-H., Tzeng, S.-L., Lin, C.-W., Chien, M.-H., Chen, M.-K. & Yang, S.-F. Impacts of MicroRNA Gene Polymorphisms on the Susceptibility of Environmental Factors Leading to Carcinogenesis in Oral Cancer. *PLoS ONE* **7**, e39777 (2012).
150. Liu, Z., Li, G., Wei, S., Niu, J., El-Naggar, A.K., Sturgis, E.M. & Wei, Q. Genetic variants in selected pre-microRNA genes and the risk of squamous cell carcinoma of the head and neck. *Cancer* **116**, 4753-4760 (2010).
151. Qiu, M.-T., Hu, J.-W., Ding, X.-X., Yang, X., Zhang, Z., Yin, R. & Xu, L. Hsa-miR-499 rs3746444 Polymorphism Contributes to Cancer Risk: A Meta-Analysis of 12 Studies. *PLoS ONE* **7**, e50887 (2012).
152. Matsuoka, S., Edwards, M.C., Bai, C., Parker, S., Zhang, P., Baldini, A., Harper, J.W. & Elledge, S.J. p57KIP2, a structurally distinct member of the p21CIP1 Cdk inhibitor family, is a candidate tumor suppressor gene. *Genes & development* **9**, 650-662 (1995).
153. Luo, Y., Hurwitz, J. & Massagué, J. Cell-cycle inhibition by independent CDK and PCNA binding domains in p21Cip1. (1995).
154. Lin, S.-C., Liu, C.-J., Lin, J.-A., Chiang, W.-F., Hung, P.-S. & Chang, K.-W. miR-24 up-regulation in oral carcinoma: Positive association from clinical and in vitro analysis. *Oral Oncology* **46**, 204-208 (2010).
155. Tsai, Y.-S., Lin, C.-S., Chiang, S.-L., Lee, C.-H., Lee, K.-W. & Ko, Y.-C. Areca Nut Induces miR-23a and Inhibits Repair of DNA Double-Strand Breaks by Targeting FANCG. *Toxicological Sciences* **123**, 480-490 (2011).

156. Yang, Y., Kuang, Y., De Oca, R.M., Hays, T., Moreau, L., Lu, N., Seed, B. & D'Andrea, A.D. Targeted disruption of the murine Fanconi anemia gene,Fancg/Xrcc9. *Blood* **98**, 3435-3440 (2001).

157. Joenje, H., Ten Foe, J.L., Oostra, A., Van Berkel, C., Rooimans, M., Schroeder-Kurth, T., Wegner, R., Gille, J., Buchwald, M. & Arwert, F. Classification of Fanconi anemia patients by complementation analysis: evidence for a fifth genetic subtype. *Blood* **86**, 2156-2160 (1995).

158. Kupfer, G.M., Näf, D., Suliman, A., Pulsipher, M. & D'Andrea, A.D. The Fanconi anaemia proteins, FAA and FAC interact to form a nuclear complex. *Nature genetics* **17**, 487-490 (1997).

159. Hui, A.B., Lenarduzzi, M., Krushel, T., Waldron, L., Pintilie, M. & Shi, W. Comprehensive MicroRNA profiling for head and neck squamous cell carcinomas. *Clin Cancer Res* **16** (2010).

160. Petrocca, F., Vecchione, A. & Croce, C.M. Emerging role of miR-106b-25/miR-17-92 clusters in the control of transforming growth factor β signaling. *Cancer research* **68**, 8191-8194 (2008).

161. Koff, A., Ohtsuki, M., Polyak, K., Roberts, J. & Massague, J. Negative regulation of G1 in mammalian cells: inhibition of cyclin E-dependent kinase by TGF-beta. *Science* **260**, 536-539 (1993).

162. Kingsley, D.M. The TGF-beta superfamily: new members, new receptors, and new genetic tests of function in different organisms. *Genes & development* **8**, 133-146 (1994).

163. Sheedy, F.J., Palsson-McDermott, E., Hennessy, E.J., Martin, C., O'Leary, J.J., Ruan, Q., Johnson, D.S., Chen, Y. & O'Neill, L.A.J. Negative regulation of TLR4 via targeting of the proinflammatory tumor suppressor PDCD4 by the microRNA miR-21. *Nat Immunol* **11**, 141-147 (2010).

164. Mathonnet, G., Fabian, M.R., Svitkin, Y.V., Parsyan, A., Huck, L., Murata, T., Biffo, S., Merrick, W.C., Darzynkiewicz, E., Pillai, R.S., Filipowicz, W., Duchaine, T.F. & Sonenberg, N. MicroRNA Inhibition of

Translation Initiation in Vitro by Targeting the Cap-Binding Complex eIF4F. *Science* **317**, 1764-1767 (2007).

165. Yang, H.-S., Jansen, A.P., Komar, A.A., Zheng, X., Merrick, W.C., Costes, S., Lockett, S.J., Sonenberg, N. & Colburn, N.H. The Transformation Suppressor Pdcd4 Is a Novel Eukaryotic Translation Initiation Factor 4A Binding Protein That Inhibits Translation. *Molecular and Cellular Biology* **23**, 26-37 (2003).
166. Svitkin, Y.V., Pause, A., Haghighat, A., Pyronnet, S., Witherell, G., Belsham, G.J. & Sonenberg, N. The requirement for eukaryotic initiation factor 4A (eIF4A) in translation is in direct proportion to the degree of mRNA 5' secondary structure. *RNA* **7**, 382-394 (2001).
167. Jansen, A.P., Camalier, C.E. & Colburn, N.H. Epidermal Expression of the Translation Inhibitor Programmed Cell Death 4 Suppresses Tumorigenesis. *Cancer Research* **65**, 6034-6041 (2005).
168. Loh, P.G., Yang, H.-S., Walsh, M.A., Wang, Q., Wang, X., Cheng, Z., Liu, D. & Song, H. Structural basis for translational inhibition by the tumour suppressor Pdcd4. *The EMBO Journal* **28**, 274-285 (2009).
169. Chen, Y., Knosel, T., Kristiansen, G., Pietas, A., Garber, M., Matsuhashi, S., Ozaki, I. & Petersen, I. Loss of PDCD4 expression in human lung cancer correlates with tumour progression and prognosis. *J Pathol* **200**, 640 - 646 (2003).
170. Wang, X., Tang, S., Le, S.-Y., Lu, R., Rader, J.S., Meyers, C. & Zheng, Z.-M. Aberrant Expression of Oncogenic and Tumor-Suppressive MicroRNAs in Cervical Cancer Is Required for Cancer Cell Growth. *PLoS ONE* **3**, e2557 (2008).
171. Huang, J., Zhao, L., Xing, L. & Chen, D. MicroRNA-204 Regulates Runx2 Protein Expression and Mesenchymal Progenitor Cell Differentiation. *STEM CELLS* **28**, 357-364 (2010).
172. Tay, Y., Zhang, J., Thomson, A.M., Lim, B. & Rigoutsos, I. MicroRNAs to Nanog, Oct4 and Sox2 coding regions modulate embryonic stem cell differentiation. *Nature* **455**, 1124-1128 (2008).

173. Brennecke, J., Hipfner, D.R., Stark, A., Russell, R.B. & Cohen, S.M. bantam Encodes a Developmentally Regulated microRNA that Controls Cell Proliferation and Regulates the Proapoptotic Gene hid in Drosophila. *Cell* **113**, 25-36 (2003).

174. Yamakuchi, M., Ferlito, M. & Lowenstein, C.J. miR-34a repression of SIRT1 regulates apoptosis. *Proceedings of the National Academy of Sciences* **105**, 13421-13426 (2008).

175. Esau, C., Davis, S., Murray, S.F., Yu, X.X., Pandey, S.K., Pear, M., Watts, L., Booten, S.L., Graham, M., McKay, R., Subramaniam, A., Propp, S., Lollo, B.A., Freier, S., Bennett, C.F., Bhanot, S. & Monia, B.P. miR-122 regulation of lipid metabolism revealed by in vivo antisense targeting. *Cell Metabolism* **3**, 87-98 (2006).

176. Gao, P., Tchernyshyov, I., Chang, T.-C., Lee, Y.-S., Kita, K., Ochi, T., Zeller, K.I., De Marzo, A.M., Van Eyk, J.E., Mendell, J.T. & Dang, C.V. c-Myc suppression of miR-23a/b enhances mitochondrial glutaminase expression and glutamine metabolism. *Nature* **458**, 762-765 (2009).

177. Ramkissoon, S.H., Mainwaring, L.A., Ogasawara, Y., Keyvanfar, K., Philip McCoy Jr, J., Sloand, E.M., Kajigaya, S. & Young, N.S. Hematopoietic-specific microRNA expression in human cells. *Leukemia Research* **30**, 643-647 (2006).

178. Chen, C.-Z., Li, L., Lodish, H.F. & Bartel, D.P. MicroRNAs Modulate Hematopoietic Lineage Differentiation. *Science* **303**, 83-86 (2004).

179. Olive, V., Bennett, M.J., Walker, J.C., Ma, C., Jiang, I., Cordon-Cardo, C., Li, Q.-J., Lowe, S.W., Hannon, G.J. & He, L. miR-19 is a key oncogenic component of mir-17-92. *Genes & Development* **23**, 2839-2849 (2009).

180. Voorhoeve, P.M., le Sage, C., Schrier, M., Gillis, A.J.M., Stoop, H., Nagel, R., Liu, Y.-P., van Duijse, J., Drost, J., Griekspoor, A., Zlotorynski, E., Yabuta, N., De Vita, G., Nojima, H., Looijenga, L.H.J. & Agami, R. A Genetic Screen Implicates miRNA-372 and miRNA-373 As Oncogenes in Testicular Germ Cell Tumors. *Cell* **124**, 1169-1181 (2006).

181. Lu, M., Zhang, Q., Deng, M., Miao, J., Guo, Y., Gao, W. & Cui, Q. An Analysis of Human MicroRNA and Disease Associations. *PLoS ONE* **3**, e3420 (2008).

182. Babak, T., Zhang, W., Morris, Q., Blencowe, B.J. & Hughes, T.R. Probing microRNAs with microarrays: Tissue specificity and functional inference. *RNA* **10**, 1813-1819 (2004).

183. Cheng, Y., Zhu, P., Yang, J., Liu, X., Dong, S., Wang, X., Chun, B., Zhuang, J. & Zhang, C. *Ischaemic preconditioning-regulated miR-21 protects heart against ischaemia/reperfusion injury via anti-apoptosis through its target PDCD4*, 431-439 (2010).

184. Care, A., Catalucci, D., Felicetti, F., Bonci, D., Addario, A., Gallo, P., Bang, M.-L., Segnalini, P., Gu, Y., Dalton, N.D., Elia, L., Latronico, M.V.G., Hoydal, M., Autore, C., Russo, M.A., Dorn, G.W., Ellingsen, O., Ruiz-Lozano, P., Peterson, K.L., Croce, C.M., Peschle, C. & Condorelli, G. MicroRNA-133 controls cardiac hypertrophy. *Nat Med* **13**, 613-618 (2007).

185. Hashemi, M., Eskandari-Nasab, E., Zakeri, Z., Atabaki, M., Bahari, G., Jahantigh, M., Taheri, M. & Ghavami, S. Association of pre-miRNA-146a rs2910164 and pre-miRNA-499 rs3746444 polymorphisms and susceptibility to rheumatoid arthritis. *Molecular medicine reports* **7**, 287-291 (2013).

186. Stagakis, E., Bertsias, G., Verginis, P., Nakou, M., Hatziapostolou, M., Kritikos, H., Iliopoulos, D. & Boumpas, D.T. Identification of novel microRNA signatures linked to human lupus disease activity and pathogenesis: miR-21 regulates aberrant T cell responses through regulation of PDCD4 expression. *Annals of the Rheumatic Diseases* **70**, 1496-1506 (2011).

187. Esteller, M. Non-coding RNAs in human disease. *Nat Rev Genet* **12**, 861-874 (2011).

188. Cao, X., Yeo, G., Muotri, A.R., Kuwabara, T. & Gage, F.H. Noncoding RNAs in the mammalian central nervous system. *Annual Review of Neuroscience* **29**, 77-103 (2006).

189. Jeon, Y.J., Kim, O.J., Kim, S.Y., Oh, S.H., Oh, D., Kim, O.J., Shin, B.S. & Kim, N.K. Association of the miR-146a, miR-149, miR-196a2, and miR-499 Polymorphisms With Ischemic Stroke and Silent Brain Infarction Risk. *Arteriosclerosis, Thrombosis, and Vascular Biology* **33**, 420-430 (2013).

190. Friedman, R.C., Farh, K.K.-H., Burge, C.B. & Bartel, D.P. Most mammalian mRNAs are conserved targets of microRNAs. *Genome Research* **19**, 92-105 (2009).

191. Kutanzi, K., Yurchenko, O., Beland, F., Checkhun, V.F. & Pogribny, I. MicroRNA-mediated drug resistance in breast cancer. *Clinical Epigenetics* **2**, 171-185 (2011).

192. Mayr, C. & Bartel, D.P. Widespread Shortening of 3′ UTRs by Alternative Cleavage and Polyadenylation Activates Oncogenes in Cancer Cells. *Cell* **138**, 673-684 (2009).

193. Kumar, M.S., Lu, J., Mercer, K.L., Golub, T.R. & Jacks, T. Impaired microRNA processing enhances cellular transformation and tumorigenesis. *Nat Genet* **39**, 673-677 (2007).

194. Mukherji, S., Ebert, M.S., Zheng, G.X., Tsang, J.S., Sharp, P.A. & van Oudenaarden, A. MicroRNAs can generate thresholds in target gene expression. *Nature genetics* **43**, 854-859 (2011).

195. Tay, Y., Kats, L., Salmena, L., Weiss, D., Tan, Shen M., Ala, U., Karreth, F., Poliseno, L., Provero, P., Di Cunto, F., Lieberman, J., Rigoutsos, I. & Pandolfi, Pier P. Coding-Independent Regulation of the Tumor Suppressor PTEN by Competing Endogenous mRNAs. *Cell* **147**, 344-357 (2011).

196. Taft, R.J., Simons, C., Nahkuri, S., Oey, H., Korbie, D.J., Mercer, T.R., Holst, J., Ritchie, W., Wong, J.J.L., Rasko, J.E.J., Rokhsar, D.S., Degnan, B.M. & Mattick, J.S. Nuclear-localized tiny RNAs are associated with transcription initiation and splice sites in metazoans. *Nat Struct Mol Biol* **17**, 1030-1034 (2010).

197. Lagos-Quintana, M., Rauhut, R., Lendeckel, W. & Tuschl, T. Identification of Novel Genes Coding for Small Expressed RNAs. *Science* **294**, 853-858 (2001).

198. Lau, N.C., Lim, L.P., Weinstein, E.G. & Bartel, D.P. An Abundant Class of Tiny RNAs with Probable Regulatory Roles in Caenorhabditis elegans. *Science* **294**, 858-862 (2001).

199. Lee, Y., Kim, M., Han, J., Yeom, K.-H., Lee, S., Baek, S.H. & Kim, V.N. MicroRNA genes are transcribed by RNA polymerase II. *EMBO J* **23**, 4051-4060 (2004).

200. Lee, Y., Jeon, K., Lee, J.-T., Kim, S. & Kim, V.N. MicroRNA maturation: stepwise processing and subcellular localization. *EMBO J* **21**, 4663-4670 (2002).

201. Cai, X., Hagehorn, C.H. & Cullen, B.R. Human microRNAs are processed from capped, polyadenylated transcripts that can also function as mRNAs. *RNA* **10**, 1957-1966 (2004).

202. Denli, A.M., Tops, B.B.J., Plasterk, R.H.A., Ketting, R.F. & Hannon, G.J. Processing of primary microRNAs by the Microprocessor complex. *Nature* **432**, 231-235 (2004).

203. Yi, R., Qin, Y., Macara, I.G. & Cullen, B.R. Exportin-5 mediates the nuclear export of pre-microRNAs and short hairpin RNAs. *Genes & Development* **17**, 3011-3016 (2003).

204. Hutvagner, G., McLachlan, J., Pasquinelli, A.E., Balint, E., Tuschl, T. & Zamore, P.D. A Cellular Function for the RNA-Interference Enzyme Dicer in the Maturation of the let-7 Small Temporal RNA. *Science* **293**, 834-838 (2001).

205. Chendrimada, T.P., Gregory, R.I., Kumaraswamy, E., Norman, J., Cooch, N., Nishikura, K. & Shiekhattar, R. TRBP recruits the Dicer complex to Ago2 for microRNA processing and gene silencing. *Nature* **436**, 740-744 (2005).

206. Schwarz, D.S., Hutvágner, G., Du, T., Xu, Z., Aronin, N. & Zamore, P.D. Asymmetry in the Assembly of the RNAi Enzyme Complex. *Cell* **115**, 199-208 (2003).

207. Zhou, H., Huang, X., Cui, H., Luo, X., Tang, Y., Chen, S., Wu, L. & Shen, N. miR-155 and its star-form partner miR-155* cooperatively regulate type I interferon production by human plasmacytoid dendritic cells. *Blood* **116**, 5885-5894 (2010).

208. Yang, J.-S., Phillips, M.D., Betel, D., Mu, P., Ventura, A., Siepel, A.C., Chen, K.C. & Lai, E.C. Widespread regulatory activity of vertebrate microRNA* species. *Rna* **17**, 312-326 (2011).

209. Kawamata, T. & Tomari, Y. Making RISC. *Trends in Biochemical Sciences* **35**, 368-376 (2010).

210. Khvorova, A., Reynolds, A. & Jayasena, S.D. Functional siRNAs and miRNAs Exhibit Strand Bias. *Cell* **115**, 209-216 (2003).

211. Hammond, S.M., Bernstein, E., Beach, D. & Hannon, G.J. An RNA-directed nuclease mediates post-transcriptional gene silencing in Drosophila cells. *Nature* **404**, 293-296 (2000).

212. Liu, J., Carmell, M.A., Rivas, F.V., Marsden, C.G., Thomson, J.M., Song, J.-J., Hammond, S.M., Joshua-Tor, L. & Hannon, G.J. Argonaute2 Is the Catalytic Engine of Mammalian RNAi. *Science* **305**, 1437-1441 (2004).

213. Hutvagner, G. & Simard, M.J. Argonaute proteins: key players in RNA silencing. *Nature Reviews. Molecular Cell Biology* **9**, 22-32 (2008).

214. Song, J.-J., Smith, S.K., Hannon, G.J. & Joshua-Tor, L. Crystal Structure of Argonaute and Its Implications for RISC Slicer Activity. *Science* **305**, 1434-1437 (2004).

215. Morita, S., Horii, T., Kimura, M., Goto, Y., Ochiya, T. & Hatada, I. One Argonaute family member, Eif2c2 (Ago2), is essential for development and appears not to be involved in DNA methylation. *Genomics* **89**, 687-696 (2007).

216. Kim, D.H., Villeneuve, L.M., Morris, K.V. & Rossi, J.J. Argonaute-1 directs siRNA-mediated transcriptional gene silencing in human cells. *Nature structural & molecular biology* **13**, 793-797 (2006).

217. Chen, Z., Lai, T.-C., Jan, Y.-H., Lin, F.-M., Wang, W.-C., Xiao, H., Wang, Y.-T., Sun, W., Cui, X. & Li, Y.-S. Hypoxia-responsive miRNAs

target argonaute 1 to promote angiogenesis. *The Journal of clinical investigation* **123**, 1057-1067 (2013).

218. Winter, J. & Diederichs, S. Argonaute-3 activates the let-7a passenger strand microRNA. *RNA biology* **10**, 1631-1643 (2013).
219. Modzelewski, Andrew J., Holmes, Rebecca J., Hilz, S., Grimson, A. & Cohen, Paula E. AGO4 Regulates Entry into Meiosis and Influences Silencing of Sex Chromosomes in the Male Mouse Germline. *Developmental Cell* **23**, 251-264 (2012).
220. Kim, Y. & Kim, V.N. MicroRNA Factory: RISC Assembly from Precursor MicroRNAs. *Molecular cell* **46**, 384-386 (2012).
221. Kobayashi, H. & Tomari, Y. RISC assembly: Coordination between small RNAs and Argonaute proteins. *Biochimica et Biophysica Acta (BBA)-Gene Regulatory Mechanisms* **1859**, 71-81 (2016).
222. Schirle, N.T. & MacRae, I.J. The crystal structure of human Argonaute2. *Science* **336**, 1037-1040 (2012).
223. Nakanishi, K., Weinberg, D.E., Bartel, D.P. & Patel, D.J. Structure of yeast Argonaute with guide RNA. *Nature* **486**, 368-374 (2012).
224. Elkayam, E., Kuhn, C.-D., Tocilj, A., Haase, A.D., Greene, E.M., Hannon, G.J. & Joshua-Tor, L. The structure of human argonaute-2 in complex with miR-20a. *Cell* **150**, 100-110 (2012).
225. Liu, X., Jin, D.-Y., McManus, Michael T. & Mourelatos, Z. Precursor MicroRNA-Programmed Silencing Complex Assembly Pathways in Mammals. *Molecular cell* **46**, 507-517 (2012).
226. Kanellopoulou, C., Muljo, S.A., Kung, A.L., Ganesan, S., Drapkin, R., Jenuwein, T., Livingston, D.M. & Rajewsky, K. Dicer-deficient mouse embryonic stem cells are defective in differentiation and centromeric silencing. *Genes & Development* **19**, 489-501 (2005).
227. Martinez, J., Patkaniowska, A., Urlaub, H., Lührmann, R. & Tuschl, T. Single-Stranded Antisense siRNAs Guide Target RNA Cleavage in RNAi. *Cell* **110**, 563-574 (2002).
228. Murchison, E.P., Partridge, J.F., Tam, O.H., Cheloufi, S. & Hannon, G.J. Characterization of Dicer-deficient murine embryonic stem cells.

Proceedings of the National Academy of Sciences of the United States of America **102**, 12135-12140 (2005).

229. Betancur, J.G. & Tomari, Y. Dicer is dispensable for asymmetric RISC loading in mammals. *Rna* **18**, 24-30 (2012).
230. Kim, Y., Yeo, J., Lee, J.H., Cho, J., Seo, D., Kim, J.-S. & Kim, V.N. Deletion of human tarbp2 reveals cellular microRNA targets and cell-cycle function of TRBP. *Cell reports* **9**, 1061-1074 (2014).
231. Parker, J.S., Roe, S.M. & Barford, D. Structural insights into mRNA recognition from a PIWI domain–siRNA guide complex. *Nature* **434**, 663-666 (2005).
232. Kwak, P.B. & Tomari, Y. The N domain of Argonaute drives duplex unwinding during RISC assembly. *Nature structural & molecular biology* **19**, 145-151 (2012).
233. Ma, J.-B., Yuan, Y.-R., Meister, G., Pei, Y., Tuschl, T. & Patel, D.J. Structural basis for 5′ -end-specific recognition of guide RNA by the A. fulgidus Piwi protein. *Nature* **434**, 666-670 (2005).
234. Gu, S., Jin, L., Huang, Y., Zhang, F. & Kay, M.A. Slicing-independent RISC activation requires the argonaute PAZ domain. *Current Biology* **22**, 1536-1542 (2012).
235. Lytle, J.R., Yario, T.A. & Steitz, J.A. Target mRNAs are repressed as efficiently by microRNA-binding sites in the 5′ UTR as in the 3′ UTR. *Proceedings of the National Academy of Sciences* **104**, 9667-9672 (2007).
236. Lee, I., Ajay, S.S., Yook, J.I., Kim, H.S., Hong, S.H., Kim, N.H., Dhanasekaran, S.M., Chinnaiyan, A.M. & Athey, B.D. New class of microRNA targets containing simultaneous 5′ -UTR and 3′ -UTR interaction sites. *Genome research* **19**, 1175-1183 (2009).
237. Li, Y.-P., Gottwein, J.M., Scheel, T.K., Jensen, T.B. & Bukh, J. MicroRNA-122 antagonism against hepatitis C virus genotypes 1–6 and reduced efficacy by host RNA insertion or mutations in the HCV 5′ UTR. *Proceedings of the National Academy of Sciences* **108**, 4991-4996 (2011).

238. Brennecke, J., Stark, A., Russell, R.B. & Cohen, S.M. Principles of MicroRNA–Target Recognition. *PLoS Biol* **3**, e85 (2005).

239. Lewis, B.P., Shih, I., Jones-Rhoades, M.W., Bartel, D.P. & Burge, C.B. Prediction of mammalian microRNA targets. *Cell* **115**, 787-798 (2003).

240. Chandradoss, S.D., Schirle, N.T., Szczepaniak, M., MacRae, I.J. & Joo, C. A dynamic search process underlies microRNA targeting. *Cell* **162**, 96-107 (2015).

241. Zeng, Y., Yi, R. & Cullen, B.R. MicroRNAs and small interfering RNAs can inhibit mRNA expression by similar mechanisms. *Proceedings of the National Academy of Sciences* **100**, 9779-9784 (2003).

242. van den Berg, A., Mols, J. & Han, J. RISC-target interaction: cleavage and translational suppression. *Biochimica et Biophysica Acta (BBA)-Gene Regulatory Mechanisms* **1779**, 668-677 (2008).

243. Lewis, B.P., Burge, C.B. & Bartel, D.P. Conserved seed pairing, often flanked by adenosines, indicates that thousands of human genes are microRNA targets. *Cell* **120**, 15-20 (2005).

244. Grimson, A., Farh, K., Johnston, W., Garrett-Engele, P., Lim, L. & Bartel, D. MicroRNA targeting specificity in mammals: determinants beyond seed pairing. *Mol Cell* **27**, 91 - 105 (2007).

245. Dome, J.S. & Coppes, M.J. Recent advances in Wilms tumor genetics. *Current Opinion in Pediatrics* **14**, 5-11 (2002).

246. Carmell, M.A., Xuan, Z., Zhang, M.Q. & Hannon, G.J. The Argonaute family: tentacles that reach into RNAi, developmental control, stem cell maintenance, and tumorigenesis. *Genes & Development* **16**, 2733-2742 (2002).

247. Karube, Y., Tanaka, H., Osada, H., Tomida, S., Tatematsu, Y., Yanagisawa, K., Yatabe, Y., Takamizawa, J., Miyoshi, S., Mitsudomi, T. & Takahashi, T. Reduced expression of Dicer associated with poor prognosis in lung cancer patients. *Cancer Science* **96**, 111-115 (2005).

248. Chiosea, S., Jelezcova, E., Chandran, U., Acquafondata, M., McHale, T., Sobol, R.W. & Dhir, R. Up-Regulation of Dicer, a Component of the

MicroRNA Machinery, in Prostate Adenocarcinoma. *The American journal of pathology* **169**, 1812-1820 (2006).

249. Zhang, L., Huang, J., Yang, N., Greshock, J., Megraw, M.S., Giannakakis, A., Liang, S., Naylor, T.L., Barchetti, A., Ward, M.R., Yao, G., Medina, A., O, O'Brien-Jenkins, A., Katsaros, D., Hatzigeorgiou, A., Gimotty, P.A., Weber, B.L. & Coukos, G. microRNAs exhibit high frequency genomic alterations in human cancer. *Proceedings of the National Academy of Sciences* **103**, 9136-9141 (2006).
250. Doench, J.G., Petersen, C.P. & Sharp, P.A. siRNAs can function as miRNAs. *Genes & Development* **17**, 438-442 (2003).
251. Su, N., Wang, Y., Qian, M. & Deng, M. Combinatorial regulation of transcription factors and microRNAs. *BMC systems biology* **4**, 1 (2010).
252. Lee, R.C., Feinbaum, R.L. & Ambros, V. The C. elegans heterochronic gene lin-4 encodes small RNAs with antisense complementarity to lin-14. *Cell* **75**, 843-854 (1993).
253. Bartel, D.P. MicroRNAs: Genomics, Biogenesis, Mechanism, and Function. *Cell* **116**, 281-297 (2004).
254. Grimson, A., Farh, K.K.-H., Johnston, W.K., Garrett-Engele, P., Lim, L.P. & Bartel, D.P. MicroRNA Targeting Specificity in Mammals: Determinants beyond Seed Pairing. *Molecular Cell* **27**, 91-105 (2007).
255. Lim, L.P., Lau, N.C., Garrett-Engele, P., Grimson, A., Schelter, J.M., Castle, J., Bartel, D.P., Linsley, P.S. & Johnson, J.M. Microarray analysis shows that some microRNAs downregulate large numbers of target mRNAs. *Nature* **433**, 769-773 (2005).
256. John, B., Enright, A.J., Aravin, A., Tuschl, T., Sander, C. & Marks, D.S. Human MicroRNA Targets. *PLoS Biol* **2**, e363 (2004).
257. Stark, A., Brennecke, J., Bushati, N., Russell, R.B. & Cohen, S.M. Animal MicroRNAs Confer Robustness to Gene Expression and Have a Significant Impact on 3′ UTR Evolution. *Cell* **123**, 1133-1146 (2005).
258. Lai, X., Schmitz, U., Gupta, S.K., Bhattacharya, A., Kunz, M., Wolkenhauer, O. & Vera, J. Computational analysis of target hub gene

repression regulated by multiple and cooperative miRNAs. *Nucleic Acids Research* **40**, 8818-8834 (2012).

259. Chi, S.W., Zang, J.B., Mele, A. & Darnell, R.B. Argonaute HITS-CLIP decodes microRNA-mRNA interaction maps. *Nature* **460**, 479-486 (2009).
260. Hafner, M., Landthaler, M., Burger, L., Khorshid, M., Hausser, J., Berninger, P., Rothballer, A., Ascano Jr, M., Jungkamp, A.-C., Munschauer, M., Ulrich, A., Wardle, G.S., Dewell, S., Zavolan, M. & Tuschl, T. Transcriptome-wide Identification of RNA-Binding Protein and MicroRNA Target Sites by PAR-CLIP. *Cell* **141**, 129-141 (2010).
261. König, J., Zarnack, K., Rot, G., Curk, T., Kayikci, M., Zupan, B., Turner, D.J., Luscombe, N.M. & Ule, J. iCLIP reveals the function of hnRNP particles in splicing at individual nucleotide resolution. *Nature structural & molecular biology* **17**, 909-915 (2010).
262. Lal, A., Thomas, M.P., Altschuler, G., Navarro, F., O'Day, E., Li, X.L., Concepcion, C., Han, Y.-C., Thiery, J., Rajani, D.K., Deutsch, A., Hofmann, O., Ventura, A., Hide, W. & Lieberman, J. Capture of MicroRNA–Bound mRNAs Identifies the Tumor Suppressor miR-34a as a Regulator of Growth Factor Signaling. *PLoS Genet* **7**, e1002363 (2011).
263. Banerjee, D. & Slack, F. Control of developmental timing by small temporal RNAs: a paradigm for RNA-mediated regulation of gene expression. *BioEssays* **24**, 119-129 (2002).
264. Pillai, R.S., Bhattacharyya, S.N., Artus, C.G., Zoller, T., Cougot, N., Basyuk, E., Bertrand, E. & Filipowicz, W. Inhibition of Translational Initiation by Let-7 MicroRNA in Human Cells. *Science* **309**, 1573-1576 (2005).
265. Broderick, J.A., Salomon, W.E., Ryder, S.P., Aronin, N. & Zamore, P.D. Argonaute protein identity and pairing geometry determine cooperativity in mammalian RNA silencing. *RNA* **17**, 1858-1869 (2011).
266. Krek, A., Grun, D., Poy, M.N., Wolf, R., Rosenberg, L., Epstein, E.J., MacMenamin, P., da Piedade, I., Gunsalus, K.C., Stoffel, M. &

Rajewsky, N. Combinatorial microRNA target predictions. *Nat Genet* **37**, 495-500 (2005).

267. Wu, S., Huang, S., Ding, J., Zhao, Y., Liang, L., Liu, T., Zhan, R. & He, X. Multiple microRNAs modulate p21Cip1/Waf1 expression by directly targeting its 3[prime] untranslated region. *Oncogene* **29**, 2302-2308 (2010).
268. Sætrom, P., Heale, B.S.E., Snøve, O., Aagaard, L., Alluin, J. & Rossi, J.J. Distance constraints between microRNA target sites dictate efficacy and cooperativity. *Nucleic Acids Research* **35**, 2333-2342 (2007).
269. Doench, J.G. & Sharp, P.A. Specificity of microRNA target selection in translational repression. *Genes & Development* **18**, 504-511 (2004).
270. Hua, Z., Lv, Q., Ye, W., Wong, C.-K.A., Cai, G., Gu, D., Ji, Y., Zhao, C., Wang, J., Yang, B.B. & Zhang, Y. MiRNA-Directed Regulation of VEGF and Other Angiogenic Factors under Hypoxia. *PLoS ONE* **1**, e116 (2006).
271. Bamford, S., Dawson, E., Forbes, S., Clements, J., Pettett, R., Dogan, A., Flanagan, A., Teague, J., Futreal, P.A., Stratton, M.R. & Wooster, R. The COSMIC (Catalogue of Somatic Mutations in Cancer) database and website. *Br J Cancer* **91**, 355-358 (2004).
272. Lewis, J. & Bartlett, A. Inscribing a discipline: tensions in the field of bioinformatics. *New Genetics and Society* **32**, 243-263 (2013).
273. Nielsen, C.B., Shomron, N., Sandberg, R., Hornstein, E., Kitzman, J. & Burge, C.B. Determinants of targeting by endogenous and exogenous microRNAs and siRNAs. *RNA* **13**, 1894-1910 (2007).
274. Tsang, J.S., Ebert, M.S. & van Oudenaarden, A. Genome-wide Dissection of MicroRNA Functions and Cotargeting Networks Using Gene Set Signatures. *Molecular Cell* **38**, 140-153 (2010).
275. Xu, J., Li, Y., Li, X., Li, C., Shao, T., Bai, J., Chen, H. & Li, X. Dissection of the potential characteristic of miRNA-miRNA functional synergistic regulations. *Mol Biosyst* **9**, 217-24 (2013).

276. Na, Y.-J. & Kim, J.H. Understanding cooperativity of microRNAs via microRNA association networks. *BMC Genomics* **14**, S17-S17 (2013).

277. Rinck, A., Preusse, M., Laggerbauer, B., Lickert, H., Engelhardt, S. & Theis, F.J. The human transcriptome is enriched for miRNA-binding sites located in cooperativity-permitting distance. *RNA Biology* **10**, 1125-1135 (2013).

278. Kloosterman, W.P., Wienholds, E., Ketting, R.F. & Plasterk, R.H.A. Substrate requirements for let-7 function in the developing zebrafish embryo. *Nucleic Acids Research* **32**, 6284-6291 (2004).

279. Jopling, C.L., Schütz, S. & Sarnow, P. Position-Dependent Function for a Tandem MicroRNA miR-122-Binding Site Located in the Hepatitis C Virus RNA Genome. *Cell Host & Microbe* **4**, 77-85 (2008).

280. Jopling, C.L., Yi, M., Lancaster, A.M., Lemon, S.M. & Sarnow, P. Modulation of Hepatitis C Virus RNA Abundance by a Liver-Specific MicroRNA. *Science* **309**, 1577-1581 (2005).

281. Nachmani, D., Lankry, D., Wolf, D.G. & Mandelboim, O. The human cytomegalovirus microRNA miR-UL112 acts synergistically with a cellular microRNA to escape immune elimination. *Nature immunology* **11**, 806-813 (2010).

282. Saito, T. & Sætrom, P. MicroRNAs – targeting and target prediction. *New Biotechnology* **27**, 243-249 (2010).

283. Haley, B. & Zamore, P.D. Kinetic analysis of the RNAi enzyme complex. *Nat Struct Mol Biol* **11**, 599-606 (2004).

284. Gu, S., Jin, L., Zhang, F., Sarnow, P. & Kay, M.A. The biological basis for microRNA target restriction to the 3' untranslated region in mammalian mRNAs. *Nature structural & molecular biology* **16**, 144-150 (2009).

285. Duursma, A.M., Kedde, M., Schrier, M., le Sage, C. & Agami, R. miR-148 targets human DNMT3b protein coding region. *RNA* **14**, 872-877 (2008).

286. Elcheva, I., Goswami, S., Noubissi, F.K. & Spiegelman, V.S. CRD-BP Protects the Coding Region of βTrCP1 mRNA from miR-183-Mediated Degradation. *Molecular Cell* **35**, 240-246 (2009).

287. Forman, J.J., Legesse-Miller, A. & Coller, H.A. A search for conserved sequences in coding regions reveals that the let-7 microRNA targets Dicer within its coding sequence. *Proceedings of the National Academy of Sciences* **105**, 14879-14884 (2008).

288. Jin, H. & Wang, C. MicroRNA-9 functions as an oncogene and targets PDCD4 gene in cervical cancer. *International Journal of Clinical and Experimental Pathology* **9**, 2726-2734 (2016).

289. Wang, Y.Q., Guo, R.D., Guo, R.M., Sheng, W. & Yin, L.R. MicroRNA-182 promotes cell growth, invasion, and chemoresistance by targeting programmed cell death 4 (PDCD4) in human ovarian carcinomas. *J Cell Biochem* **114**, 1464-73 (2013).

290. Li, J., Fu, H., Xu, C., Tie, Y., Xing, R., Zhu, J., Qin, Y., Sun, Z. & Zheng, X. miR-183 inhibits TGF-beta1-induced apoptosis by downregulation of PDCD4 expression in human hepatocellular carcinoma cells. *BMC Cancer* **10**, 354 (2010).

291. Wang, W., Zhao, L., Wei, X., Wang, L., Liu, S., Yang, Y., Wang, F., Sun, G., Zhang, J., Ma, Y., Zhao, Y. & Yu, J. MicroRNA-320a promotes 5-FU resistance in human pancreatic cancer cells. *Sci Rep* **6**, 27641 (2016).

292. Fu, W.F., Chen, W.B., Dai, L., Yang, G.P., Jiang, Z.Y., Pan, L., Zhao, J. & Chen, G. Inhibition of miR-141 reverses cisplatin resistance in non-small cell lung cancer cells via upregulation of programmed cell death protein 4. *Eur Rev Med Pharmacol Sci* **20**, 2565-72 (2016).

293. Liu, X., Zhang, Z., Sun, L., Chai, N., Tang, S., Jin, J., Hu, H., Nie, Y., Wang, X., Wu, K., Jin, H. & Fan, D. microRNA-499-5p promotes cellular invasion and tumor metastasis in colorectal cancer by targeting FOXO4 and PDCD4. *Carcinogenesis* (2011).

294. Technologies, L. RNAiMAX Reverse Transfections Lipofectamine. in *Life Technologies Protocols* Vol. 2012 (2006).

295. Schmittgen, T.D. & Livak, K.J. Analyzing real-time PCR data by the comparative C(T) method. *Nat Protoc* **3**, 1101-8 (2008).

296. Garcia, M., Jemal, A., Ward, E., Center, M., Hao, Y., Siegel, R. . Global Cancer Facts & Figures. *American Cancer Society Atlanta, GA.* (2007).

297. Zakowicz, H., Yang, H., Stark, C., Wlodawer, A., Laronde-Leblanc, N. & Colburn, N. Mutational analysis of the DEAD-box RNA helicase eIF4AII characterizes its interaction with transformation suppressor Pdcd4 and eIF4GI. *RNA* **11**, 261 - 274 (2005).

298. Meng, H., Wang, K., Chen, X., Guan, X., Hu, L., Xiong, G., Li, J. & Bai, Y. MicroRNA-330-3p functions as an oncogene in human esophageal cancer by targeting programmed cell death 4. *American Journal of Cancer Research* **5**(2015).

299. Li, H.A.O., Xu, H., Shen, H. & Li, H.A.O. microRNA-106a modulates cisplatin sensitivity by targeting PDCD4 in human ovarian cancer cells. *Oncology Letters* **7**, 183-188 (2014).

300. Wang, Y.-Q., Guo, R.-D., Guo, R.-M., Sheng, W. & Yin, L.-R. MicroRNA-182 promotes cell growth, invasion, and chemoresistance by targeting programmed cell death 4 (PDCD4) in human ovarian carcinomas. *Journal of Cellular Biochemistry* **114**, 1464-1473 (2013).

301. Li, J., Fu, H., Xu, C., Tie, Y., Xing, R., Zhu, J., Qin, Y., Sun, Z. & Zheng, X. miR-183 inhibits TGF-β1-induced apoptosis by downregulation of PDCD4 expression in human hepatocellular carcinoma cells. *BMC Cancer* **10**, 1-10 (2010).

302. Krek, A., Grun, D., Poy, M., Wolf, R., Rosenberg, L., Epstein, E., MacMenamin, P., da Piedade, I., Gunsalus, K., Stoffel, M. & Rajewsky, N. Combinatorial microRNA target predictions. *Nat Genet* **37**, 495 - 500 (2005).

303. Girish, V. & Vijayalakshmi, A. Affordable image analysis using NIH Image/ImageJ. *Indian J Cancer* **41**, 47 (2004).

304. Schmitter, D., Filkowski, J., Sewer, A., Pillai, R.S., Oakeley, E.J., Zavolan, M., Svoboda, P. & Filipowicz, W. Effects of Dicer and

Argonaute down-regulation on mRNA levels in human HEK293 cells. *Nucleic acids research* **34**, 4801-4815 (2006).

305. Lafkas, G.N. Massachusetts Institute of Technology (2011).
306. Jopling, C.L., Sch¸tz, S. & Sarnow, P. Position-Dependent Function for a Tandem MicroRNA miR-122-Binding Site Located in the Hepatitis C Virus RNA Genome. *Cell host & microbe* **4**, 77-85 (2008).
307. Lewis, M.A., Quint, E., Glazier, A.M., Fuchs, H., De Angelis, M.H., Langford, C., van Dongen, S., Abreu-Goodger, C., Piipari, M., Redshaw, N., Dalmay, T., Moreno-Pelayo, M.A., Enright, A.J. & Steel, K.P. An ENU-induced mutation of miR-96 associated with progressive hearing loss in mice. *Nat Genet* **41**, 614-618 (2009).
308. GeneArt. Vol. 2015 (Invitrogen).
309. Weiss, J.N. The Hill equation revisited: uses and misuses. *The FASEB Journal* **11**, 835-41 (1997).
310. Pro, I. WaveMetrics. *Inc.: Lake Oswego, OR* (1996).
311. Yusupova, G.Z., Yusupov, M.M., Cate, J.H.D. & Noller, H.F. The Path of Messenger RNA through the Ribosome. *Cell* **106**, 233-241 (2001).
312. Maroney, P.A., Yu, Y., Fisher, J. & Nilsen, T.W. Evidence that microRNAs are associated with translating messenger RNAs in human cells. *Nature* **200**, 6 (2006).
313. Nottrott, S., Simard, M.J. & Richter, J.D. Human let-7a miRNA blocks protein production on actively translating polyribosomes. *Nature structural & molecular biology* **13**, 1108-1114 (2006).
314. Petersen, C.P., Bordeleau, M.-E., Pelletier, J. & Sharp, P.A. Short RNAs repress translation after initiation in mammalian cells. *Molecular cell* **21**, 533-542 (2006).
315. Humphreys, D.T., Westman, B.J., Martin, D.I. & Preiss, T. MicroRNAs control translation initiation by inhibiting eukaryotic initiation factor 4E/cap and poly(a) tail function. *Proc Natl Acad Sci U S A* **102**(2005).
316. Nilsen, T.W. Mechanisms of microRNA-mediated gene regulation in animal cells. *TRENDS in Genetics* **23**, 243-249 (2007).

317. Kertesz, M., Iovino, N., Unnerstall, U., Gaul, U. & Segal, E. The role of site accessibility in microRNA target recognition. *Nat Genet* **39**(2007).

318. Reuter, J.S. & Mathews, D.H. RNAstructure: software for RNA secondary structure prediction and analysis. *BMC Bioinformatics* **11**, 1-9 (2010).

319. Wang, D., Zhang, Z., O'Loughlin, E., Lee, T., Houel, S., O'Carroll, D., Tarakhovsky, A., Ahn, N.G. & Yi, R. Quantitative functions of Argonaute proteins in mammalian development. *Genes & development* **26**, 693-704 (2012).

320. Jones, T.R. & Cole, M.D. Rapid cytoplasmic turnover of c-myc mRNA: requirement of the 3'untranslated sequences. *Molecular and Cellular Biology* **7**, 4513-4521 (1987).

321. Shalgi, R., Lieber, D., Oren, M. & Pilpel, Y. Global and Local Architecture of the Mammalian microRNA–Transcription Factor Regulatory Network. *PLoS Comput Biol* **3**, e131 (2007).

322. Yang, J.-H., Li, J.-H., Jiang, S., Zhou, H. & Qu, L.-H. ChIPBase: a database for decoding the transcriptional regulation of long non-coding RNA and microRNA genes from ChIP-Seq data. *Nucleic Acids Research* **41**, D177-D187 (2013).

323. Yeom, K.-H., Lee, Y., Han, J., Suh, M.R. & Kim, V.N. Characterization of DGCR8/Pasha, the essential cofactor for Drosha in primary miRNA processing. *Nucleic Acids Research* **34**, 4622-4629 (2006).

324. Viswanathan, S.R., Daley, G.Q. & Gregory, R.I. Selective blockade of microRNA processing by Lin-28. *Science (New York, N.Y.)* **320**, 97-100 (2008).

325. Baccarini, A., Chauhan, H., Gardner, T.J., Jayaprakash, A.D., Sachidanandam, R. & Brown, B.D. Kinetic analysis reveals the fate of a microRNA following target regulation in mammalian cells. *Current biology* **21**, 369-376 (2011).

326. Dweep, H. & Gretz, N. miRWalk2.0: a comprehensive atlas of microRNA-target interactions. *Nat Meth* **12**, 697-697 (2015).

327. Griffiths-Jones, S., Grocock, R.J., Van Dongen, S., Bateman, A. & Enright, A.J. miRBase: microRNA sequences, targets and gene nomenclature. *Nucleic acids research* **34**, D140-D144 (2006).
328. Lai, E.C., Wiel, C. & Rubin, G.M. Complementary miRNA pairs suggest a regulatory role for miRNA:miRNA duplexes. *RNA* **10**, 171-175 (2004).
329. Shalgi, R., Lieber, D., Oren, M. & Pilpel, Y. Global and local architecture of the mammalian microRNA-transcription factor regulatory network. *PLoS Comput Biol* **3**, e131 (2007).
330. Guo, A.-Y., Sun, J., Jia, P. & Zhao, Z. A novel microRNA and transcription factor mediated regulatory network in schizophrenia. *BMC systems biology* **4**, 10 (2010).
331. Hobert, O. Gene regulation by transcription factors and microRNAs. *Science* **319**, 1785-1786 (2008).
332. Re, A., Corá, D., Taverna, D. & Caselle, M. Genome-wide survey of microRNA–transcription factor feed-forward regulatory circuits in human. *Molecular BioSystems* **5**, 854-867 (2009).
333. Fazi, F., Rosa, A., Fatica, A., Gelmetti, V., De Marchis, M.L., Nervi, C. & Bozzoni, I. A minicircuitry comprised of microRNA-223 and transcription factors NFI-A and C/EBPα regulates human granulopoiesis. *Cell* **123**, 819-831 (2005).
334. Weinstein, J.N., Myers, T.G., O'Connor, P.M., Friend, S.H., Fornace, A.J., Kohn, K.W., Fojo, T., Bates, S.E., Rubinstein, L.V. & Anderson, N.L. An information-intensive approach to the molecular pharmacology of cancer. *Science* **275**, 343-349 (1997).
335. Cho, S., Jang, I., Jun, Y., Yoon, S., Ko, M., Kwon, Y., Choi, I., Chang, H., Ryu, D., Lee, B., Kim, V.N., Kim, W. & Lee, S. miRGator v3.0: a microRNA portal for deep sequencing, expression profiling and mRNA targeting. *Nucleic Acids Research* **41**, D252-D257 (2013).
336. Griffiths-Jones, S., Grocock, R., van Dongen, S., Bateman, A. & Enright, A. miRBase: microRNA sequences, targets and gene nomenclature. *Nucleic Acids Res* **34**, D140 - 144 (2006).

337. Raymond, F., Carbonneau, J., Boucher, N., Robitaille, L., Boisvert, S., Wu, W.-K., De Serres, G., Boivin, G. & Corbeil, J. Comparison of Automated Microarray Detection with Real-Time PCR Assays for Detection of Respiratory Viruses in Specimens Obtained from Children. *Journal of Clinical Microbiology* **47**, 743-750 (2009).

338. Allanach, K., Mengel, M., Einecke, G., Sis, B., Hidalgo, L.G., Mueller, T. & Halloran, P.F. Comparing Microarray Versus RT-PCR Assessment of Renal Allograft Biopsies: Similar Performance Despite Different Dynamic Ranges. *American Journal of Transplantation* **8**, 1006-1015 (2008).

339. Huang, C.-X., Zhu, Y., Duan, G.-L., Yao, J.-F., Li, Z.-Y., Li, D. & Wang, Q.-Q. Screening for MiRNAs related to laryngeal squamous carcinoma stem cell radiation. *Asian Pacific Journal of Cancer Prevention* **14**, 4533-4537 (2013).

340. Wu, T.-Y., Zhang, T.-H., Qu, L.-M., Feng, J.-P., Tian, L.-L., Zhang, B.-H., Li, D.-D., Sun, Y.-N. & Liu, M. MiR-19a is correlated with prognosis and apoptosis of laryngeal squamous cell carcinoma by regulating TIMP-2 expression. *Int J Clin Exp Pathol* **7**, 56-63 (2014).

341. Harris, T., Jimenez, L., Kawachi, N., Fan, J.-B., Chen, J., Belbin, T., Ramnauth, A., Loudig, O., Keller, C.E. & Smith, R. Low-level expression of miR-375 correlates with poor outcome and metastasis while altering the invasive properties of head and neck squamous cell carcinomas. *The American journal of pathology* **180**, 917-928 (2012).

342. Lajer, C., Nielsen, F., Friis-Hansen, L., Norrild, B., Borup, R., Garnaes, E., Rossing, M., Specht, L., Therkildsen, M. & Nauntofte, B. Different miRNA signatures of oral and pharyngeal squamous cell carcinomas: a prospective translational study. *British journal of cancer* **104**, 830-840 (2011).

343. Severino, P., Brüggemann, H., Andreghetto, F.M., Camps, C., Klingbeil, M.d.F.G., de Pereira, W.O., Soares, R.M., Moyses, R., Wünsch-Filho, V. & Mathor, M.B. MicroRNA expression profile in head and neck cancer: HOX-cluster embedded microRNA-196a and

microRNA-10b dysregulation implicated in cell proliferation. *BMC cancer* **13**, 1 (2013).

344. Liu, Z., Li, G., Wei, S., Niu, J., El-Naggar, A.K. & Sturgis, E.M. Genetic variants in selected pre-microRNA genes and the risk of squamous cell carcinoma of the head and neck. *Cancer* **116**(2010).
345. Lu, Y.-C., Chen, Y.-J., Wang, H.-M., Tsai, C.-Y., Chen, W.-H., Huang, Y.-C., Fan, K.-H., Tsai, C.-N., Huang, S.-F. & Kang, C.-J. Oncogenic function and early detection potential of miRNA-10b in oral cancer as identified by microRNA profiling. *Cancer prevention research* **5**, 665-674 (2012).
346. Hebert, C., Norris, K., Scheper, M.A., Nikitakis, N. & Sauk, J.J. High mobility group A2 is a target for miRNA-98 in head and neck squamous cell carcinoma. *Molecular cancer* **6**, 5 (2007).
347. Lin, T., Zhou, F., Zhou, H., Pan, X., Sun, Z. & Peng, G. MicroRNA-378g enhanced radiosensitivity of NPC cells partially by targeting protein tyrosine phosphatase SHP-1. *International journal of radiation biology* **91**, 859-866 (2015).
348. Tran, N., O'Brien, C.J., Clark, J. & Rose, B. Potential role of micro-RNAs in head and neck tumorigenesis. *Head Neck* **32**(2010).
349. Xiao, C., Srinivasan, L., Calado, D.P., Patterson, H.C., Zhang, B., Wang, J., Henderson, J.M., Kutok, J.L. & Rajewsky, K. Lymphoproliferative disease and autoimmunity in mice with increased miR-17-92 expression in lymphocytes. *Nat Immunol* **9**, 405-414 (2008).
350. Yan, H.l., Xue, G., Mei, Q., Wang, Y.z., Ding, F.x., Liu, M.F., Lu, M.H., Tang, Y., Yu, H.y. & Sun, S.h. Repression of the miR‐17‐92 cluster by p53 has an important function in hypoxia‐induced apoptosis. *The EMBO journal* **28**, 2719-2732 (2009).
351. Li, X., Di, B., Song, Q. & Shen, Y. *Metastasis of Head and Neck Squamous Cell Carcinoma*, (INTECH Open Access Publisher, 2012).
352. Gilbert, H. & Kagan, A.R. Recurrence patterns in squamous cell carcinoma of the oral cavity, pharynx, and larynx. *Journal of surgical oncology* **6**, 357-380 (1974).

353. Leemans, C.R., Tiwari, R., Nauta, J., Van der Waal, I. & Snow, G.B. Regional lymph node involvement and its significance in the development of distant metastases in head and neck carcinoma. *Cancer* **71**, 452-456 (1993).

354. Vikram, B., Strong, E.W., Shah, J.P. & Spiro, R. Failure at distant sites following multimodality treatment for advanced head and neck cancer. *Head & neck surgery* **6**, 730-733 (1984).

355. Price, K.A. & Cohen, E.E. Current treatment options for metastatic head and neck cancer. *Current treatment options in oncology* **13**, 35-46 (2012).

356. Kotwall, C., Sako, K., Razack, M.S., Rao, U., Bakamjian, V. & Shedd, D.P. Metastatic patterns in squamous cell cancer of the head and neck. *The American Journal of Surgery* **154**, 439-442 (1987).

357. Morton, R., Rugman, F., Dorman, E., Stoney, P., Wilson, J., McCormick, M., Veevers, A. & Stell, P. Cisplatinum and bleomycin for advanced or recurrent squamous cell carcinoma of the head and neck: a randomised factorial phase III controlled trial. *Cancer chemotherapy and pharmacology* **15**, 283-289 (1985).

358. Seiwert, T.Y., Jagadeeswaran, R., Faoro, L., Janamanchi, V., Nallasura, V., El Dinali, M., Yala, S., Kanteti, R., Cohen, E.E. & Lingen, M.W. The MET receptor tyrosine kinase is a potential novel therapeutic target for head and neck squamous cell carcinoma. *Cancer research* **69**, 3021-3031 (2009).

359. Nohata, N., Hanazawa, T., Kinoshita, T., Inamine, A., Kikkawa, N., Itesako, T., Yoshino, H., Enokida, H., Nakagawa, M. & Okamoto, Y. Tumour-suppressive microRNA-874 contributes to cell proliferation through targeting of histone deacetylase 1 in head and neck squamous cell carcinoma. *British journal of cancer* **108**, 1648-1658 (2013).

360. Kinoshita, T., Nohata, N., Fuse, M., Hanazawa, T., Kikkawa, N., Fujimura, L., Watanabe-Takano, H., Yamada, Y., Yoshino, H. & Enokida, H. Tumor suppressive microRNA-133a regulates novel

targets: moesin contributes to cancer cell proliferation and invasion in head and neck squamous cell carcinoma. *Biochemical and biophysical research communications* **418**, 378-383 (2012).

361. Howard, J., Cheng, H., Perez, J., Ratner, E., Fertig, E., Considine, M., Ochs, M., Slebos, R., Weidhaas, J. & Chung, C. miRNA array analysis determines miR-205 is overexpressed in head and neck squamous cell carcinoma and enhances cellular proliferation. *J. Cancer Res. Ther* **1**, 153-162 (2013).
362. Yao, Q., Xu, H., Zhang, Q.-Q., Zhou, H. & Qu, L.-H. MicroRNA-21 promotes cell proliferation and down-regulates the expression of programmed cell death 4 (PDCD4) in HeLa cervical carcinoma cells. *Biochemical and biophysical research communications* **388**, 539-542 (2009).
363. Zhu, Q., Wang, Z., Hu, Y., Li, J., Li, X., Zhou, L. & Huang, Y. miR-21 promotes migration and invasion by the miR-21-PDCD4-AP-1 feedback loop in human hepatocellular carcinoma. *Oncology reports* **27**, 1660-1668 (2012).
364. Si, M., Zhu, S., Wu, H., Lu, Z., Wu, F. & Mo, Y. miR-21-mediated tumor growth. *Oncogene* **26**, 2799-2803 (2007).
365. Hu, Z., Chen, X., Zhao, Y., Tian, T., Jin, G., Shu, Y., Chen, Y., Xu, L., Zen, K. & Zhang, C. Serum MicroRNA signatures identified in a genome-wide serum MicroRNA expression profiling predict survival of non–small-cell lung cancer. *Journal of Clinical Oncology* **28**, 1721-1726 (2010).
366. Schindelin, J., Arganda-Carreras, I., Frise, E., Kaynig, V., Longair, M., Pietzsch, T., Preibisch, S., Rueden, C., Saalfeld, S. & Schmid, B. Fiji: an open-source platform for biological-image analysis. *Nature methods* **9**, 676-682 (2012).
367. White, J.S., Weissfeld, J.L., Ragin, C.C., Rossie, K.M., Martin, C.L. & Shuster, M. The influence of clinical and demographic risk factors on the establishment of head and neck squamous cell carcinoma cell lines. *Oral Oncol* **43**(2007).

368. Grénman, R., Carey, T.E., McClatchey, K.D., Wagner, J.G., Pekkola‐Heino, K., Schwartz, D.R., Wolf, G.T., Lacivita, L.P., Ho, L. & Baker, S.R. In vitro radiation resistance among cell lines established from patients with squamous cell carcinoma of the head and neck. *Cancer* **67**, 2741-2747 (1991).

369. Korpal, M., Lee, E.S., Hu, G. & Kang, Y. The miR-200 family inhibits epithelial-mesenchymal transition and cancer cell migration by direct targeting of E-cadherin transcriptional repressors ZEB1 and ZEB2. *Journal of Biological Chemistry* **283**, 14910-14914 (2008).

370. Ma, L., Teruya-Feldstein, J. & Weinberg, R.A. Tumour invasion and metastasis initiated by microRNA-10b in breast cancer. *Nature* **449**, 682-688 (2007).

371. Dews, M., Homayouni, A., Yu, D., Murphy, D., Sevignani, C., Wentzel, E., Furth, E.E., Lee, W.M., Enders, G.H. & Mendell, J.T. Augmentation of tumor angiogenesis by a Myc-activated microRNA cluster. *Nature genetics* **38**, 1060-1065 (2006).

372. Yamakuchi, M., Lotterman, C.D., Bao, C., Hruban, R.H., Karim, B., Mendell, J.T., Huso, D. & Lowenstein, C.J. P53-induced microRNA-107 inhibits HIF-1 and tumor angiogenesis. *Proceedings of the National Academy of Sciences* **107**, 6334-6339 (2010).

373. Liang, C.-C., Park, A.Y. & Guan, J.-L. In vitro scratch assay: a convenient and inexpensive method for analysis of cell migration in vitro. *Nature protocols* **2**, 329-333 (2007).

374. Santhanam, A.N., Baker, A.R., Hegamyer, G., Kirschmann, D.A. & Colburn, N.H. Pdcd4 repression of lysyl oxidase inhibits hypoxia-induced breast cancer cell invasion. *Oncogene* **29**, 3921-3932 (2010).

375. Lefebvre, V., Behringer, R. & De Crombrugghe, B. L-Sox5, Sox6 and Sox9 control essential steps of the chondrocyte differentiation pathway. *Osteoarthritis and Cartilage* **9**, S69-S75 (2001).

376. Smits, P., Li, P., Mandel, J., Zhang, Z., Deng, J.M., Behringer, R.R., de Crombrugghe, B. & Lefebvre, V. The transcription factors L-Sox5 and

Sox6 are essential for cartilage formation. *Developmental cell* **1**, 277-290 (2001).

377. Denny, P., Swift, S., Connor, F. & Ashworth, A. An SRY-related gene expressed during spermatogenesis in the mouse encodes a sequence-specific DNA-binding protein. *The EMBO journal* **11**, 3705 (1992).
378. Weigel, D. & Jäckle, H. The fork head domain: a novel DNA binding motif of eukaryotic transcription factors? *Cell* **63**, 455-456 (1990).
379. Greer, E.L. & Brunet, A. FOXO transcription factors at the interface between longevity and tumor suppression. *Oncogene* **24**, 7410-7425 (2005).
380. Carlsson, P. & Mahlapuu, M. Forkhead transcription factors: key players in development and metabolism. *Developmental biology* **250**, 1-23 (2002).
381. Cantley, L.C. The phosphoinositide 3-kinase pathway. *Science* **296**, 1655-1657 (2002).
382. Parry, P., Wei, Y. & Evans, G. Cloning and characterization of the t (X; II) breakpoint from a leukemic cell line identify a new member of the forkhead gene family. *Genes, Chromosomes and Cancer* **11**, 79-84 (1994).
383. Corral, J., Forster, A., Thompson, S., Lampert, F., Kaneko, Y., Slater, R., Kroes, W., Van der Schoot, C., Ludwig, W. & Karpas, A. Acute leukemias of different lineages have similar MLL gene fusions encoding related chimeric proteins resulting from chromosomal translocation. *Proceedings of the National Academy of Sciences* **90**, 8538-8542 (1993).
384. Borkhardt, A., Repp, R., Haas, O.A., Leis, T., Harbott, J., Kreuder, J., Hammermann, J., Henn, T. & Lampert, F. Cloning and characterization of AFX, the gene that fuses to MLL in acute leukemias with at (X; 11)(q13; q23). *Oncogene* **14**, 195-202 (1997).
385. Yang, H., Zhao, R., Yang, H.-Y. & Lee, M.-H. Constitutively active FOXO4 inhibits Akt activity, regulates p27 Kip1 stability, and

suppresses HER2-mediated tumorigenicity. *Oncogene* **24**, 1924-1935 (2005).

386. Lou, Y., Yang, X., Wang, F., Cui, Z. & Huang, Y. MicroRNA-21 promotes the cell proliferation, invasion and migration abilities in ovarian epithelial carcinomas through inhibiting the expression of PTEN protein. *International journal of molecular medicine* **26**, 819-827 (2010).
387. Zhang, B.G., Li, J.F., Yu, B.Q., Zhu, Z.G., Liu, B.Y. & Yan, M. microRNA-21 promotes tumor proliferation and invasion in gastric cancer by targeting PTEN. *Oncology reports* **27**, 1019-1026 (2012).
388. Gabriely, G., Wurdinger, T., Kesari, S., Esau, C.C., Burchard, J., Linsley, P.S. & Krichevsky, A.M. MicroRNA 21 promotes glioma invasion by targeting matrix metalloproteinase regulators. *Molecular and cellular biology* **28**, 5369-5380 (2008).
389. Connolly, E.C., Van Doorslaer, K., Rogler, L.E. & Rogler, C.E. Overexpression of miR-21 Promotes an In vitro Metastatic Phenotype by Targeting the Tumor Suppressor RHOB. *Molecular Cancer Research* **8**, 691-700 (2010).
390. Cottonham, C.L., Kaneko, S. & Xu, L. miR-21 and miR-31 Converge on TIAM1 to Regulate Migration and Invasion of Colon Carcinoma Cells. *Journal of Biological Chemistry* **285**, 35293-35302 (2010).
391. Liu, Z.-L., Wang, H., Liu, J. & Wang, Z.-X. MicroRNA-21 (miR-21) expression promotes growth, metastasis, and chemo-or radioresistance in non-small cell lung cancer cells by targeting PTEN. *Molecular and cellular biochemistry* **372**, 35-45 (2013).
392. Wei, W., Hu, Z., Fu, H., Tie, Y., Zhang, H., Wu, Y. & Zheng, X. MicroRNA-1 and microRNA-499 downregulate the expression of the ets1 proto-oncogene in HepG2 cells. *Oncology reports* **28**, 701-706 (2012).
393. Yang, H.-S., Matthews, C.P., Clair, T., Wang, Q., Baker, A.R., Li, C.-C.H., Tan, T.-H. & Colburn, N.H. Tumorigenesis Suppressor Pdcd4 Down-Regulates Mitogen-Activated Protein Kinase Kinase Kinase

Kinase 1 Expression To Suppress Colon Carcinoma Cell Invasion. *Molecular and Cellular Biology* **26**, 1297-1306 (2006).

394. Grunder, E., D'Ambrosio, R., Fiaschetti, G., Abela, L., Arcaro, A., Zuzak, T., Ohgaki, H., Lv, S.-Q., Shalaby, T. & Grotzer, M. MicroRNA-21 suppression impedes medulloblastoma cell migration. *European Journal of Cancer* **47**, 2479-2490 (2011).
395. Li, H., Liang, J., Castrillon, D.H., DePinho, R.A., Olson, E.N. & Liu, Z.-P. FoxO4 regulates tumor necrosis factor alpha-directed smooth muscle cell migration by activating matrix metalloproteinase 9 gene transcription. *Molecular and cellular biology* **27**, 2676-2686 (2007).
396. Talotta, F., Cimmino, A., Matarazzo, M., Casalino, L., De Vita, G., D'Esposito, M., Di Lauro, R. & Verde, P. An autoregulatory loop mediated by miR-21 and PDCD4 controls the AP-1 activity in RAS transformation. *Oncogene* **28**, 73-84 (2009).
397. Sheedy, F.J., Palsson-McDermott, E., Hennessy, E.J., Martin, C., O'Leary, J.J., Ruan, Q., Johnson, D.S., Chen, Y. & O'Neill, L.A. Negative regulation of TLR4 via targeting of the proinflammatory tumor suppressor PDCD4 by the microRNA miR-21. *Nature immunology* **11**, 141-147 (2010).
398. Cantley, L.C. & Neel, B.G. New insights into tumor suppression: PTEN suppresses tumor formation by restraining the phosphoinositide 3-kinase/AKT pathway. *Proceedings of the National Academy of Sciences* **96**, 4240-4245 (1999).
399. Vanhaesebroeck, B. & Alessi, D.R. The PI3K–PDK1 connection: more than just a road to PKB. *Biochemical Journal* **346**, 561-576 (2000).
400. Lawlor, M.A. & Alessi, D.R. PKB/Akt a key mediator of cell proliferation, survival and insulin responses? *Journal of cell science* **114**, 2903-2910 (2001).
401. Cheng, C.-C., Uchiyama, Y., Hiyama, A., Gajghate, S., Shapiro, I.M. & Risbud, M.V. PI3K/AKT regulates aggrecan gene expression by modulating Sox9 expression and activity in nucleus pulposus cells of

the intervertebral disc. *Journal of Cellular Physiology* **221**, 668-676 (2009).

402. Akiyama, H., Chaboissier, M.-C., Martin, J.F., Schedl, A. & de Crombrugghe, B. The transcription factor Sox9 has essential roles in successive steps of the chondrocyte differentiation pathway and is required for expression of Sox5 and Sox6. *Genes & Development* **16**, 2813-2828 (2002).
403. Childs, G., Fazzari, M., Kung, G., Kawachi, N., Brandwein-Gensler, M. & McLemore, M. Low-level expression of microRNAs let-7d and miR-205 are prognostic markers of head and neck squamous cell carcinoma. *Am J Pathol* **174**(2009).
404. Carinci, F., Lo Muzio, L., Piattelli, A., Rubini, C., Chiesa, F. & Ionna, F. Potential markers of tongue tumor progression selected by cDNA microarray. *Int J Immunopathol Pharmacol* **18**(2005).
405. Kloosterman, W.P., Wienholds, E., de Bruijn, E., Kauppinen, S. & Plasterk, R.H.A. In situ detection of miRNAs in animal embryos using LNA-modified oligonucleotide probes. *Nat Meth* **3**, 27-29 (2006).
406. Chen, P.-S., Su, J.-L., Cha, S.-T., Tarn, W.-Y., Wang, M.-Y., Hsu, H.-C., Lin, M.-T., Chu, C.-Y., Hua, K.-T. & Chen, C.-N. miR-107 promotes tumor progression by targeting the let-7 microRNA in mice and humans. *The Journal of clinical investigation* **121**(2011).
407. Tang, R., Li, L., Zhu, D., Hou, D., Cao, T., Gu, H., Zhang, J., Chen, J., Zhang, C.-Y. & Zen, K. Mouse miRNA-709 directly regulates miRNA-15a/16-1 biogenesis at the posttranscriptional level in the nucleus: evidence for a microRNA hierarchy system. *Cell research* **22**, 504-515 (2012).
408. Bohuslav Ostadal, N.S.D. *Cardiac Adaptations: Molecular Mechanisms*, 466 (Springer Science and Business Media, 2012).
409. van Rooij, E., Quiat, D., Johnson, B.A., Sutherland, L.B., Qi, X., Richardson, J.A., Kelm Jr, R.J. & Olson, E.N. A Family of microRNAs Encoded by Myosin Genes Governs Myosin Expression and Muscle Performance. *Developmental Cell* **17**, 662-673 (2009).

410. Imataka, H., Olsen, H.S. & Sonenberg, N. A new translational regulator with homology to eukaryotic translation initiation factor 4G. *The EMBO Journal* **16**, 817-825 (1997).

411. Takahashi, K., Maruyama, M., Tokuzawa, Y., Murakami, M., Oda, Y., Yoshikane, N., Makabe, K.W., Ichisaka, T. & Yamanaka, S. Evolutionarily conserved non-AUG translation initiation in NAT1/p97/DAP5 (EIF4G2). *Genomics* **85**, 360-371 (2005).

412. Suzuki, C., Garces, R.G., Edmonds, K.A., Hiller, S., Hyberts, S.G., Marintchev, A. & Wagner, G. PDCD4 inhibits translation initiation by binding to eIF4A using both its MA3 domains. *Proceedings of the National Academy of Sciences* **105**, 3274-3279 (2008).

413. Zhang, S., Li, J., Jiang, Y., Xu, Y. & Qin, C. Programmed cell death 4 (PDCD4) suppresses metastastic potential of human hepatocellular carcinoma cells. *Journal of Experimental & Clinical Cancer Research* **28**, 1 (2009).